

FAST RELIEF, FUTURE CONSEQUENCES: ASSESSING THE IMPACT OF OVER-
THE-COUNTER PAIN MEDICATIONS ON MALE REPRODUCTIVE HEALTH

by

KRISTA MAYE CROW

(Under the Direction of Charles A. Easley IV)

ABSTRACT

Over the past five decades, semen parameters, including sperm counts, have rapidly declined in men worldwide. Although this decline remains largely unexplained, exposure to lifestyle factors, such as medication usage, could provide a possible explanation. Reproductive aged men are using more medications than in previous years. Additionally, men are waiting longer to father children than previously, which has been associated with greater medication use. Together, these factors have increased the number of over-the-counter medications men take in their reproductive years.

Some scientific evidence suggests that medications, even the common non-steroidal anti-inflammatory drugs (NSAIDs), can negatively impact male reproductive health. Even though NSAIDs account for more than half of all analgesic usage worldwide, the mechanisms by which these drugs impact male fertility remain largely uncharacterized. Animal studies provide valuable information; however, applications to humans are sometimes limited by the differences in drug metabolism and pharmacokinetics, warranting more human-like models to further our understanding. Using an established stem cell-based model of human spermatogenesis, we evaluated two NSAIDs, naproxen

and ibuprofen, under long-term conditions at physiologically relevant concentrations. Here, we demonstrate that long-term naproxen and ibuprofen exposure have marginal effects *in vitro*. Expanding upon this study to include the somatic niche, we assessed the impact of both NSAIDs on non-human primate (NHP) primary Sertoli cells and the functionality of the blood-testis barrier (BTB), a specialized structure formed from junctions between adjacent Sertoli cells that regulates the entry of nutritional substances, vital molecules (e.g., hormones), and toxicants (e.g., drugs, environmental toxicants) into the adluminal compartment where spermiogenesis takes place. Our study revealed that serum levels of naproxen and ibuprofen exposure compromises the function of the BTB by perturbing the Sertoli cell tight junctions. Together, these models provide a unique opportunity to experimentally study drug toxicity on the seminiferous tubule epithelium while also providing the ability to assess mechanisms in a cost-effective manner. The results of these studies highlight the potential for these common medications to affect male fertility *in vitro* and potentially associate NSAID usage as a contributing factor in the decline of sperm counts.

INDEX WORDS: Non-steroidal anti-inflammatory drugs, ibuprofen, naproxen, reproductive toxicology, stem cells, spermatogenesis, blood-testis barrier, Sertoli cells

FAST RELIEF, FUTURE CONSEQUENCES: ASSESSING THE IMPACT OF OVER-
THE-COUNTER PAIN MEDICATIONS ON MALE REPRODUCTIVE HEALTH

by

KRISTA MAYE CROW

B.S., Robert Morris University, 2016

A Dissertation Submitted to the Graduate Faculty of The University of Georgia in Partial
Fulfillment of the Requirements for the Degree

DOCTOR OF PHILOSOPHY

ATHENS, GEORGIA

2023

© 2023

Krista Maye Crow

All Rights Reserved

FAST RELIEF, FUTURE CONSEQUENCES: ASSESSING THE IMPACT OF OVER-
THE-COUNTER PAIN MEDICATIONS ON MALE REPRODUCTIVE HEALTH

by

KRISTA MAYE CROW

Major Professor:	Charles A. Easley IV
Committee:	Erin K. Lipp
	Franklin D. West
	Anne Marie Zimeri

Electronic Version Approved:

Ron Walcott
Vice Provost for Graduate Education and Dean of the Graduate School
The University of Georgia
May 2023

ACKNOWLEDGEMENTS

My deepest thank you to my advisor, Dr. Chas Easley. Thank you for your guidance, patience, and advice throughout my graduate school career. From all the challenges and pivots along the way, your support and wisdom helped me become the scientist I am today. Thank you for believing in me. To my outstanding committee members, Dr. Erin Lipp, Dr. Frank West, and Dr. Anne Marie Zimeri, thank you for your continuous support, being wonderful scientists and role models, and challenging me to be the best scientist and person. I could not have asked for a better group of people to help me through this challenging yet rewarding period of growth and development.

To the past and present Easley lab family, Dr. In Ki Cho, Beth, Clayton, Ian, Kylie, Elisabeth, and Krissy, thank you for your unwavering support, endless laughs, and memories. I will always cherish our hallway lunches, rides on the cart to get packages, and fun times in and out of the lab, especially at trivia. A special thank you to Dr. In Ki Cho for always keeping me grounded, reminding me of the bigger picture, and for continuous words of encouragement. Thank you, Beth, for being an amazing friend and coworker and always going above and beyond to help the lab in extraordinary ways; I am incredibly blessed that our time in the lab brought us together. Thank you, Dr. Alyse Steves, for your mentorship, patience, kindness, and teachings about stem cell culture and reproductive toxicology. Thank you, Jackie, for being a wonderful, caring, warm-spirited friend and coworker. Thank you to the talented undergraduate researchers Julia and Jamie; working alongside you was such an honor. To Katherine, thank you for ridding the

graduate school roller coaster with me, celebrating the victories, supporting me through the lows, staying with me in the lab until the very early morning hours, being a wonderful board mate on the EHS GSA Executive Board, and for always being a friend. Thank you to everyone in the EHS department for your continuous support and friendship.

Thank you to the University of Georgia's fantastic histology experts, Nicole Young, Craig Dixon, and Jennifer Kempf, and flow cytometry expert, Julie Nelson, who helped with critical parts of my experiments. Thank you, Dr. Anthony Chan, for your assistance with the viral transductions, providing the fluorescent reporter constructs and the non-human primate testicular tissue while at Yerkes National Primate Center. A special thank you to Dr. Ana Planinić, Professor Davor Ježek, Nagham Younis, Dr. Kyle Orwig, Dr. Gerald Schatten, Dr. Calvin Simerly, and Dr. Carlos Castro for allowing me to visit your labs, teaching me about male factor infertility, and your mentorship.

I am grateful for all my friends that I have in Athens and back in Pittsburgh, for cheerfully supporting me during my academic journey. A loving thanks to my parents, Kirk and Marie Symosko, my sister Sheri and her husband Tim Egger, my in-laws, Brian and Tracy Crow, and my brother-in-law Zac Crow, for always inspiring me to do my best, believing in me no matter what, and loving me unconditionally. A special thank you to Mike Creech for always being a listening ear, reminding me about the important things in life, and being a friend. I am also thankful for my anxiety-reducing, cheerful canine champion, Maverick. Lastly, I endlessly thank my husband, CJ, for being a constant source of patience, infinite love, laughter, and strength, during all the challenges and triumphs of graduate school and life. Thank you for always supporting my personal and professional aspirations.

TABLE OF CONTENTS

	Page
ACKNOWLEDGEMENTS	iv
LIST OF TABLES	xi
LIST OF FIGURES	xiii
CHAPTER	
1 DESCRIPTION OF DISSERTATION STRUCTURE	1
2 INTRODUCTION (LITERATURE REVIEW)	3
2.1 ABSTRACT	4
2.2 GLOBAL CRISIS	5
2.3 MEDICATION USAGE IN MALE INFERTILITY DIAGNOSIS IS OFTEN INADEQUATELY ADDRESSED AND INVESTIGATED, AND OFTEN TIMES UNDERAPPRECIATED.....	7
2.4 WINDOWS OF SUSCEPTIBILITY AND MALE REPRODUCTIVE PHYSIOLOGY.....	9
2.5 THE BENEFITS AND CHALLENGES ASSOCIATED WITH STUDYING THE EFFECTS OF PHARMACEUTICALS ON THE MALE REPRODUCTIVE TRACT	11
2.6 USING STEM CELL MODELS TO STUDY TOXICOLOGY AND HUMAN REPRODUCTION	14

2.7 NSAID THERAPY CAN CAUSE DISRUPTIONS TO THE MALE REPRODUCTIVE SYSTEM.....	19
2.8 STUDYING THE EFFECTS OF COMMON MEDICATIONS USING AN IN VITRO HUMAN SPERMATOGENESIS MODEL.....	23
2.9 USING AN IN VITRO SYSTEM TO STUDY THE BLOOD-TESTIS BARRIER DYNAMICS	25
2.10 STUDYING THE EFFECTS OF COMMON MEDICATIONS USING AN IN VITRO SERTOLI CELL-BASED MODEL TO STUDY THE BLOOD-TESTIS BARRIER.....	31
3 INVESTIGATING THE EFFECTS OF NSAIDS ON HUMAN SPERMATOGENESIS USING A STEM CELL BASED MODEL	35
3.1 INTRODUCTION	35
3.2 PURPOSE OF THE STUDY	41
3.3 STUDY INNOVATION	41
3.4 RESULTS: LONG-TERM NAPROXEN EXPOSURE ALTERS THE MITOCHONDRIAL MEMBRANE POLARIZATION IN IN VITRO SPERMATOGENIC CULTURES, BUT CHRONIC IBUPROFEN EXPOSURE DOES NOT IMPACT THE MITOCHONDRIAL MEMBRANE POTENTIAL	42
3.4 RESULTS: LONG-TERM NAPROXEN EXPOSURE ALTERS THE CELL VIABILITY IN ONE CELL LINE DIFFERENTIATED IN IN VITRO SPERMATOGENIC CONDITIONS, BUT CHRONIC	

IBUPROFEN EXPOSURE DOES NOT IMPACT THE CELL VIABILITY	53
3.4 RESULTS: LONG-TERM NAPROXEN EXPOSURE ALTERS THE CELL CYCLE IN ONE CELL LINE DIFFERENTIATED IN IN VITRO SPERMATOGENIC CULTURES, BUT CHRONIC IBUPROFEN EXPOSURE DOES NOT IMPACT THE CELL CYCLE.....	63
3.5 DISCUSSION.....	78
3.6 MATERIALS AND METHODS	79
4 IBUPROFEN AND NAPROXEN EXPOSURE ALTERS THE FUNCTION OF THE NON-HUMAN PRIMATE BLOOD-TESTIS BARRIER	84
4.1 ABSTRACT	85
4.2 INTRODUCTION	86
4.3 RESULTS: SHORT-TERM NSAID TREATMENT ALTERS THE TESTICULAR BARRIER FUNCTION WITHOUT AFFECTING THE VIABILITY OF IN VITRO PRIMARY SERTOLI CELLS	88
4.3 SHORT-TERM NSAID TREATMENT ALTERS THE EXPRESSION OF GENES INVOLVED IN THE BLOOD-TESTIS BARRIER FUNCTION.....	96
4.3 IBUPROFEN EXPOSURE ENRICHES GENES IN DISEASES ASSOCIATED WITH MALE FACTOR INFERTILITY USING THE HUMAN PHENOTYPE ONTOLOGY DATABASE	99
4.3 RESULTS: HUMAN TESTICULAR TISSUE EXPRESSES NSAID INHIBITING ENZYMES IN VIVO	121

4.4 DISCUSSION.....	131
4.5 MATERIALS AND METHODS	138
4.6 AUTHOR CONTRIBUTIONS	149
4.7 COMPETING INTERESTS.....	149
4.8 ACKNOWLEDGMENTS	149
5 TESTIBOW: A GENETIC MULTICOLOR PLATFORM FOR LABELING AND ANALYSING IN VITRO HUMAN SPERMATOGENICN CELL POPULATIONS.....	151
5.1 INTRODUCTION	151
5.2 STUDY INNOVATION	158
5.3 RESULTS: TESTIBOW 1.0: A FLUORESCENT REPORTER SYSTEM COUPLED WITH OUR IN VITRO MODEL OF HUMAN SPERMATOGENESIS	158
5.3 RESULTS: TESTIBOW 2.0: A POLYCISTRONIC FLUORESCENT REPORTER SYSTEM COUPLED WITH OUR IN VITRO MODEL OF HUMAN SPERMATOGENESIS	166
5.4 OUTCOMES AND CHALLENGES ASSOCIATED WITH TESTIBOW1.0 AND TESTIBOW 2.0.....	176
5.5 CURRENTLY IN PRODUCTION: TESTIBOW 3.0.....	178
5.6 SUMMARY AND FUTURE DIRECTIONS	195
5.7 MATERIALS AND METHODS	196
6 CONCLUDING REMARKS	205
REFERENCES.....	208

APPENDICES

A APPENDIX A	253
B APPENDIX B.....	358

LIST OF TABLES

	Page
Table 4.1: Ibuprofen-induced non-human primate primary Sertoli cell gene enrichment using the Human phenotype ontology database.	115
Table 4.2: Naproxen-induced non-human primate primary Sertoli cell gene enrichment using the Human phenotype ontology database.	116
Table 4.3: Normalized RNA-seq results of genes from non-human primate primary Sertoli cells involved in the cyclooxygenase pathway (<i>PTGS1</i> , <i>PTGS2</i> , <i>PTGIS</i> , <i>PTGES</i> , <i>PTGIR</i> , <i>PTGER4</i> , <i>PTGDR</i> , <i>PTGER3</i> , <i>PTGER2</i> , <i>PTGDS</i> , <i>PTGES3</i> , <i>PTGR3</i> , <i>PTGR2</i> , and <i>PTGR1</i>), Sertoli cell function (<i>AR</i> , <i>SOX9</i> , and <i>GATA4</i>), tight junctions (<i>CLDN 3,4,8</i> , and <i>11</i>), and inflammation response (<i>NFE2L2</i> and <i>GDF15</i>), representing the log fold change and p-adjusted value (padj).	117
Table 4.4: Clinical patient data.	129
Table 5.1: CRISPR gRNA sequences.	187
Table 5.2: TALEN mRNA.	188
Table 6.1: 400 μ M naproxen significant differentially expressed genes.	254
Table 6.2: 40 μ M naproxen significant differentially expressed genes.	269
Table 6.3: 4 μ M naproxen significant differentially expressed genes.	270
Table 6.4: 100 μ M ibuprofen significant differentially expressed genes.	271
Table 6.5: 10 μ M ibuprofen significant differentially expressed genes.	352
Table 6.6: 1 μ M ibuprofen significant differentially expressed genes.	354

Table 6.7: Oligonucleotide primer sequences.	356
Table 6.8: Antibodies used for immunocytochemistry and immunohistochemistry.	357
Table 7.1: Testibow oligonucleotide primers.	359
Table 7.2: Antibodies used for Testibow immunocytochemistry experiments	360

LIST OF FIGURES

	Page
Figure 3.1: Flow cytometry plots for long-term naproxen-treated spermatogenic cells derived from human male ESCs for mitochondrial membrane potential data.	45
Figure 3.2: Long-term naproxen exposure alters the mitochondrial membrane polarization and increases cell death of spermatogenic cells derived from human male ESCs.....	47
Figure 3.3: Flow cytometry plots for long-term ibuprofen-treated spermatogenic cells derived from human male ESCs for mitochondrial membrane potential data.	49
Figure 3.4: Long-term ibuprofen exposure does not alter the mitochondrial membrane polarization of spermatogenic cells derived from human male ESCs.	51
Figure 3.5: Flow cytometry plots for long-term naproxen-treated spermatogenic cells derived from human male ESCs for cell viability data.	55
Figure 3.6: Long-term naproxen exposure decreases the cell viability of spermatogenic cells derived from human male ESCs.	57
Figure 3.7: Flow cytometry plots for long-term ibuprofen-treated spermatogenic cells derived from human male ESCs for cell viability data.	59
Figure 3.8: Long-term ibuprofen exposure does not alter the cell viability of spermatogenic cells derived from human male ESCs.	61
Figure 3.9: Flow cytometry plots for long-term naproxen-treated spermatogenic cells derived from human male ESCs for cell cycle data.	66

Figure 3.10: Long-term naproxen exposure impacts the cell cycle in spermatogenic cells derived from human male ESCs.	68
Figure 3.11: Long-term naproxen exposure does not impact the viability of haploid cells differentiated in spermatogenic conditions derived from human male ESCs.	70
Figure 3.12: Flow cytometry plots for long-term ibuprofen-treated spermatogenic cells derived from human male ESCs for cell cycle data.	72
Figure 3.13: Long-term ibuprofen exposure does not impact the cell cycle in spermatogenic cells derived from human male ESCs.	74
Figure 3.14: Long-term ibuprofen exposure impacts the viability of haploid cells differentiated in spermatogenic conditions derived from human male ESCs.	76
Figure 4.1: Short-term NSAID treatment does not induce apoptosis or alter mitochondrial membrane potential of non-human primate primary Sertoli cells in vitro.	90
Figure 4.2: Short-term NSAID treatment alters the Transepithelial Electrical Resistance (TER) of non-human primate primary Sertoli cells in vitro.	92
Figure 4.3: Short-term NSAID treatment does not alter the barrier permeability of non-human primate primary Sertoli cells in vitro.	94
Figure 4.4: Ribonucleic acid sequencing analysis of non-human primate primary Sertoli cells exposed to naproxen in vitro.	101
Figure 4.5: Ribonucleic acid sequencing analysis of non-human primate primary Sertoli cells exposed to ibuprofen in vitro.	103
Figure 4.6: Heatmap of genes involved in cell junction regulation from non-human primate primary Sertoli cells exposed to naproxen and ibuprofen in vitro.	105

Figure 4.7: Heatmap of genes involved in inflammatory response from non-human primate primary Sertoli cells exposed to naproxen in vitro.	107
Figure 4.8: Heatmap of genes involved in cell junction regulation and inflammatory response gene sets from non-human primate primary Sertoli cells exposed to ibuprofen in vitro.	109
Figure 4.9: Validation of RNA-seq data by RT-qPCR.	111
Figure 4.10: Predicted network interactions between proteins from non-human primate primary Sertoli cells exposed to naproxen and ibuprofen in vitro.	113
Figure 4.11: Sertoli cells in human testicular tissue express NSAID inhibiting enzyme, COX-1.	123
Figure 4.12: Sertoli cells in human testicular tissue express NSAID inhibiting enzyme, COX-2.	125
Figure 4.13: Human testicular tissue express NSAID inhibiting enzyme, COX-2.	127
Figure 4.14: Non-human primate primary Sertoli cells validated in vitro using qPCR and fluorescence microscopy.	136
Figure 5.1: Diagram of the fluorescent reporter system, Testibow 1.0.	162
Figure 5.2: Characterization of human male ESCs transduced with the spermatogenic fluorescent reporters.	164
Figure 5.3: A polycistronic vector for the in vitro fluorescent reporter system.	168
Figure 5.4: Diagram of the polycistronic fluorescent reporter system, Testibow 2.0. ...	170
Figure 5.5: PCR validation of human male ESCs transduced with Testibow 2.0.	172
Figure 5.6: Functionality of Testibow 2.0.	174
Figure 5.7: Diagram of the fluorescent reporter system, Testibow 3.0.	183

Figure 5.8: Donor DNA synthesis.	185
Figure 5.9: Antibiotic kill curve of BJ cells.	189
Figure 5.10: Stable pool generation.	191
Figure 5.11: Stable pool generation.	193

CHAPTER 1

DESCRIPTION OF DISSERTATION STRUCTURE

Serving to fulfill the requirements set in the University of Georgia's Theses and Dissertations Student Guide to Preparation and Processing (revised in November 2021) for using regular and journal articles as chapters, this introductory chapter serves to inform the reader of the structure of this dissertation. The regular chapters included in this dissertation are Chapters 1, 3 and 5. The manuscript chapters are Chapter 2 and 4 and will be submitted to scholarly scientific journals.

Chapter 2, "Introduction (Literature Review) will be prepared and submitted for publication in the near future to the journal of *Fertility & Sterility Reviews*. Changes are expected to be made in this preparation process including changing the title, removing unnecessary information, and creation of figures. At the time of writing this chapter (February 20, 2023), Chapter 4, "Ibuprofen and naproxen exposure alters the function of the non-human primate blood-testis barrier" will be submitted for publication in the journal, *Journal of Clinical Investigations Insight*. In order to incorporate this chapter into this dissertation, changes were made to include the supplemental figures and tables. The long tables describing the differentially expressed genes and the supplemental methods tables are included in Appendix A, to prevent breaking up the chapter. During the manuscript preparation process, changes are expected to be made including removing any unnecessary information, alterations to the titles, and revising the figures for conciseness.

Excluding this current chapter, Chapters 3 and 5 are written as normal chapters. Chapter 3, “Investigating the Effects of NSAIDs on Human Spermatogenesis using a Stem Cell Based Model” was designed to collect preliminary data regarding the reproductive toxicity of NSAIDs on human spermatogenesis and laid the foundation for Chapter 4. Chapter 5, “Testibow: A Genetic Multicolor Platform for Labeling and Analyzing in vitro Human Spermatogenic Cell Populations” will be prepared and submitted for publication at a later date. Changes are expected to be made during this preparation process including removal of unnecessary information, changing the title, and revising the figures for succinctness.

Overall, Chapters 2 and 4 of this dissertation will be further edited and submitted for publication at a later date, Chapter 3 served as preliminary data and general reasoning for Chapter 4, and Chapter 5 of this dissertation will be further edited and submitted for publication in the future.

CHAPTER 2

INTRODUCTION (LITERATURE REVIEW) ¹

¹ Krista M. Symosko Crow and Charles A. Easley IV. To be submitted to *F&S Reviews*.

2.1 ABSTRACT

Numerous studies have reported that semen parameters, including sperm counts, among men around the world are declining at a rapid pace. Chemical exposures and lifestyle factors present in our environment pose a threat to reproductive function in humans. In addition to the rapid reduction in male fertility, the increased usage of medications by reproductive-aged men is of great concern. Over the last several years, the connection between medication usage during pregnancy and genital malformations in newborn boys has been frequently addressed in the literature. However, the impact of medications, particularly those available over-the-counter, on the adult male reproductive tract has been inadequately addressed, even though some evidence suggests that drugs can negatively impact male fertility. Despite the existing evidence in the literature, over-the-counter medication usage is often inadequately addressed during the evaluation of male infertility, even though the information may be clinically relevant.

Over-the-counter analgesics, such as non-steroidal anti-inflammatory drugs (NSAIDs), are the most frequently used products worldwide by men. NSAIDs such as ibuprofen and naproxen are commonly used to relieve pain, fever, and inflammation. Until recently, few human studies have evaluated their impacts on the male reproductive system. The relationship between medication usage in adult men and the reproductive health consequences is often challenging to study in humans, mainly because the majority of studies have been small and observational, with differences in doses and endpoints. Animal studies have been used to help explain this relationship; however, there are

distinct species-specific differences in pharmacokinetics and reproductive biology, stressing the need for more human-relevant models. Therefore, we used a comprehensive approach to understand how common analgesics can impact sperm production. Stem cells have the unique ability to differentiate into any cell within the body and, thus, provide a unique opportunity to study the effect of environmental exposures on human reproductive health. Recently, a stem cell-based human spermatogenesis model was developed that mimics several critical stages of human sperm production and successfully demonstrated that known reproductive toxicants can be studied using this differentiation model. Here, we describe one study that used this model to study the effects of two NSAIDs, ibuprofen and naproxen, on *in vitro* human spermatogenesis. Additionally, to test whether NSAIDs alter the function of the Blood-testis barrier, an important structure formed by Sertoli cells that play a critical role in spermatogenic differentiation, we used a system most relevant to humans, non-human primate (NHP), rhesus macaque primary Sertoli cells. Using this *in vitro* barrier model containing NHP Sertoli cells, we describe the impacts of NSAIDs on the function of the Blood-testis barrier and Sertoli cells. In combination with the evidence in the literature, our comprehensive studies provide a holistic understanding of how common medications can impact male fertility.

2.2 GLOBAL CRISIS

As humans, we often take things for granted, and our fertility is no exception. As Dr. Shanna Swan, a leading environmental and reproductive health researcher, said, "...many people take it as a given that they'll be able to have babies when the time is right..." [1], and now, couples worldwide are facing the harsh reality that our fertility is in trouble. Not only do these couples who experience reproductive trouble or infertility

have to accept that they may or may not have their own biological children, but they also face emotional challenges [2-5] and financial hardships [6-8]. In the mid-1990s, researchers started to express their concern about the environment's impact on reproductive health. Carlsen et al. reported a decline in semen quality, including sperm counts, from the late 1930s to the early 1990s [9]. But it was not until 2017 that the declining sperm counts in Western countries, including North America, Europe, and Australia, were put on the radar. In this meta-analysis, the researchers described that semen parameters, including sperm counts, have declined by almost 60% in men living in Western countries between 1973 and 2013 [10]. However, in 2022, researchers reported that this decline in sperm counts is occurring at an accelerated pace and now includes men living in South America, Asia, and Africa [11]. This steep decline in sperm counts worldwide is a significant public health concern.

Although genetic mutations are associated with male infertility, evidence from the literature suggests several environmental exposures, including flame retardants [12] and medical interventions can reduce fertility in men (reviewed in [13, 14]). Also, certain lifestyles, such as high stress, cigarette smoking, alcohol consumption, and illegal drug use, can negatively impact male fertility (reviewed in [15]). Several advances in experimental and Assisted Reproductive Technologies (ART) have assisted sub-fertile or infertile couples with their family planning needs (reviewed in [16]). However, we must simultaneously examine how our environment and lifestyles affect our fertility and educate the public and healthcare providers about prevention efforts.

2.3 MEDICATION USAGE IN MALE INFERTILITY DIAGNOSIS IS OFTEN INADEQUATELY ADDRESSED AND INVESTIGATED, AND OFTEN TIMES UNDERAPPRECIATED

Across the United States (U.S.), men in their reproductive years are using more medications than previously, with nearly 70% of men between the ages of 18-44 taking prescriptions or over-the-counter (OTC) medications [17]. Additionally, men are waiting longer to have their first child, with nearly 25% of men in developed countries having their first child after the age of 40 [18-21]. As such, the increasing paternal age is associated with greater medication usage.

Male reproductive health is generally underappreciated during medical evaluations, even though poor reproductive health is associated with poor overall health. For example, low semen quality and infertility are biomarkers for poor general health, which both are associated with shorter lifespans [22-28]. Despite this connection, many healthcare practitioners fail to consider a man's family planning needs when prescribing or suggesting OTC medications [29]. This overlook is incredibly important since drugs have been shown to negatively affect male reproductive health by acting through hormones, directly on the gonads, or altering sperm and sexual function [29]. Men reporting to an infertility clinic in Germany reported taking an average of two medications, with more than half of these medications having a reported adverse side effect on male reproduction [30]. In a separate study, 165 men with chronic conditions and no medical explanation for their infertility took medications believed to impair fertility [31]. When 73 patients switched to a less toxic drug, semen quality drastically improved, and conception occurred in 85% of couples, suggesting some medications can

negatively impact male reproduction. Despite these connections, only some reproductive health specialists are aware that certain drugs can negatively impact the reproductive system in men [17], emphasizing the need to consider a patient's medication usage during the evaluation of male infertility.

There are a few reasons that this translation from the lab bench to the clinic regarding the impact of medications on male fertility is occurring slowly. One challenge is that the evaluation of drugs has insufficient requirements for the inclusion of reproductive toxicity in men [29]. In 2011, the U.S. Food and Drug Administration (FDA) required the evaluation of male reproductive toxicity screening in premarketing studies [32]. These studies include toxicity assessments related to damage to the male reproductive hormones, changes in endocrine function, compromised semen parameters, abnormal mating behavior, and an overall decline in fertility [33]. Yet, most medications in current use were approved before this required testing, and thus, the FDA-required labels may be inconsistent with our current knowledge [34]. These pre-approved medications, such as OTC non-steroidal anti-inflammatory drugs (NSAIDs), could pose significant risks to male fertility.

Second, there is an absence of literature describing the association between drugs and male infertility. This is partly due to more research on women and during pregnancy [29]. In other cases, this is due to challenges associated with studying the impact and determining the mechanism by which medications negatively affect male fertility. Thus, there are a limited number of resources available for practitioners to counsel their male patients on potential medication-related adverse effects on their fertility [17, 29]. This could result in men being treated with drugs that can impair their fertility and

improper counseling on adverse fertility effects [29]. Therefore, the primary focus of this dissertation is to explore how OTC medications, like NSAIDs, can alter male reproductive health and contribute to the decline in sperm production. We will also describe innovations in an *in vitro* model that can be used to elucidate the mechanisms associated with pharmaceuticals and altered male reproductive health.

2.4 WINDOWS OF SUSCEPTIBILITY AND MALE REPRODUCTIVE PHYSIOLOGY

2.4.1 Windows of Susceptibility

During development, there are several windows of susceptibility where pharmaceuticals could damage the developing male gametes, negatively influencing fertility. One such window occurs early in development where disruptions during this time have been shown to contribute to the development of congenital disorders such as cryptorchidism (failure of one or both testicles to descend into the scrotum) and hypospadias (the opening of the urethra is not located at the tip of the penis), dysregulation of spermatogenesis, poor semen quality, and testicular cancer [35, 36]. Each of these disorders has been shown to negatively impact a man's fertility which could arise from fetal origin [36]. While several genetic defects have been associated with testicular dysgenesis [37, 38], medication usage could also be a contributing factor.

There are several other windows of susceptibility in which medications can influence male germ cell development. These windows occur during postnatal development and include mini-puberty (the first few months of life), peri-puberty (shortly before puberty), and puberty. Each window is dependent upon proper hormone regulation. If a medication interferes with androgen function at any of these stages, there

could be defects in spermatogenesis, leading to sub-fertility or infertility in adults ([39], reviewed in [40]). In addition, since men are using more medications, these medications could disrupt somatic cell function (Leydig, Sertoli, and Peritubular cells) or directly alter spermatogenesis.

2.4.2 Male reproductive physiology

The male reproductive system is regulated by the hypothalamic-pituitary-gonadal (HPG) axis (reviewed in [40]). After puberty, the hypothalamus produces and secretes gonadotropin-releasing hormone (GnRH), which travels to the anterior pituitary gland to produce follicle stimulating hormone (FSH) and luteinizing hormone (LH). These two hormones travel to the testis to act upon the somatic cells. Luteinizing hormone acts upon the Leydig cells to stimulate the production and secretion of testosterone. Meanwhile, FSH works in conjunction with testosterone on the Sertoli cells to facilitate spermatogenesis and spermiogenesis. This feedback loop tightly regulates testosterone, LH, and FSH signaling in the testis throughout the adult life. Thus, any medication that interferes with the hormonal balance can cause major alterations to sperm production and negatively impact male fertility.

Spermatogenesis is a complex, cyclical, well-organized process occurring throughout the reproductive life of an organism [41]. Male gametes are produced from the spermatogonial stem cells (SSCs) through several mitotic and meiotic cell divisions. Located outside the Blood-testis barrier (BTB), the SSCs divide to maintain the SSC pool or produce progenitor cells committed to precede through spermatogenesis. The progenitor cells divide mitotically as they become differentiated SSCs before undergoing meiosis. These differentiated SSCs undergo mitosis to produce primary spermatocytes,

which will then enter meiosis. From here, the cells will undergo two meiotic divisions to produce secondary spermatocytes and round spermatids. The round spermatids undergo morphological transformations into mature spermatozoa, including nuclear condensation and tail and acrosome formation through spermiogenesis (reviewed in [40]). Overall, male reproductive function is a highly sensitive process, and exposure to medications at anyone of these stages can result in adverse health effects ranging from impaired male hormone production, alterations in spermatogenesis and spermiogenesis, changes in semen parameters, or infertility [35] (reviewed in [40]).

2.5 THE BENEFITS AND CHALLENGES ASSOCIATED WITH STUDYING THE EFFECTS OF PHARMACEUTICALS ON THE MALE REPRODUCTIVE TRACT

Most of our knowledge about the effects of medications on adult male reproductive health and human sperm production has been derived from animal models [35, 42-45]. Rodents, such as mice and rats, are the most used *in vivo* models to study reproductive toxicology. Using rodents in biomedical research has economic advantages since they are relatively small and require minimal resources and space [46]. Also, rodents have a short gestation period, produce large numbers of offspring, and rapidly develop to adulthood [46], making them great models to study the reproductive system. Despite these advantages, species-specific differences regarding their reproductive physiology prevent the accurate assessment of how certain toxicants and medications can affect human male fertility.

First, there are kinetic and biological differences among mammals. For example, mice have the smallest SSC pool (0.3%) relative to the total number of spermatogenic

cells produced, followed by non-human primates having a larger SSC pool (4%) relative to the total number of their spermatogenic cells produced, and then humans with a significantly larger SSC pool at 22% [47]. Following division, the committed but undifferentiated cells undergo several transit-amplifying mitotic divisions yielding a higher number of differentiated SSCs prior to meiosis [47, 48]. This number of amplifying divisions dictates the number of sperm produced. There are twelve of these divisions in mice, eight in non-human primates, and five in humans [47]. These divisions result in 40 million sperm per gram of testis parenchyma produced per day in mice, 41 million sperm produced in a non-human primate, and only 4.4 million sperm produced in humans.

Not only are there differences in the type of differentiating cells, but also the length of spermatogenesis. In mice, spermatogenesis takes about 35 days, while in humans, it takes about 64 [49-54]. Third, there are differences in pharmacokinetics, including the route of administration, absorption, distribution, and concentration of the drug in the male reproductive tract [17]. Because the dosages used in the experimental species are often quite high to elicit a toxic response, the application to humans is sometimes limited. Furthermore, endpoints such as sperm concentration, motility, and morphology following medication administration can be inaccurate and not necessarily correlate with any effects on fecundity [29] since these factors are variable even in normal, fertile men [17]. Finally, these studies typically assess morphological and structural defects and hormone level analysis to evaluate the potential of reproductive toxicity [17, 55]. Because of the limitations inherent to these studies, understanding the subcellular medication-induced effects are rarely studied. These species differences could

result in distinct species-specific sensitivities to medications, making it difficult to generalize the medication-induced effects across species [29]. While informative, these models have inherent flaws that make it challenging to translate the medication-induced effects into humans and for the data to be used in the clinic.

On the other hand, human health can be directly studied using pharmaceutical and observational trials. For studying the effect of medications on fertility outcomes, clinical trials should be large, randomized, double-blinded, and placebo- and confounding variable-controlled; however, these gold standard studies have not been published for most medications, specifically for NSAIDs [17]. Most existing studies included too few men, making it difficult to conclude the effects of the medications; thus, valuable information from properly powered observational studies can be more applicable in the clinic [17]. It is important to note that there is also individual variation in medication response, possibly due to differences in demographic factors, drug interactions, environmental exposures, and genetic predispositions [17]. These factors could result in some individuals having more severe adverse effects than others.

Further, drugs of the same class may have different effects, limiting the applicability of data across a single class [17]. Together, these factors emphasize the need for a benchtop model to robustly study the effects of medications in an unbiased way. Stem cell-based *in vitro* models represent one platform to assess the reproductive toxicity of medications. The results from these studies could be used by the healthcare providers to minimize adverse drug effects and medication-induced infertility.

2.6 USING STEM CELL MODELS TO STUDY TOXICOLOGY AND HUMAN REPRODUCTION

Traditionally, toxicology studies have used mammalian model organisms to understand how humans respond to environmental exposures. Animal models have added great value to our knowledge of medicine and the development of pharmaceuticals. However, differences in physiology and pharmacokinetics between humans and animals, as mentioned above, have raised questions about how well animal models predict human toxicity. These questions are usually addressed as uncertainty factors in health risk assessments when determining a safe exposure level for humans [56].

In recent years, there has been an increasing push to find alternative models to animal testing when possible. This support has come from national governing agencies, such as the U.S. FDA, U.S. Environmental Protection Agency (EPA), and the Principal of Three Rs. Both the FDA and EPA have prioritized efforts to reduce animal testing by encouraging laboratories and universities to develop and use alternative methods and strategies. In 2019, the EPA announced that it would reduce its request for and the funding of animal studies by 30% by 2025, with the goal to eliminate it by 2035 [57]. The FDA announced a similar program to develop alternative testing methods but without a set timeline. The Principals of Three Rs (Replacement, Reduction, and Refinement) refer to substituting protocols that use animals with those that do not, reducing the number of animals used to obtain precise information, and refining the procedures applied to animals to reduce severity [58]. Although human health can also be studied for toxicological effects using clinical trials and cohorts unintentionally exposed to environmental toxicants, alternative methods, such as stem cell-based models, hold

great promise to screen the toxicological effects of pharmaceuticals rapidly, unbiasedly, and efficiently on human health.

Through the last several decades, research has utilized the capabilities of stem cell-based models to study human biology. Given their pluripotent feature, stem cell differentiation protocols have allowed researchers to study human development, organ systems, diseases, and toxicant effects *in vitro* in almost every adult organism cell type [59]. Recently, one of the most promising applications of stem cells is their use in the drug discovery pipeline. Researchers across academia, biotechnology, and pharmaceutical companies have used stem cells to screen compounds on a large and reproducible scale, identify novel molecular targets for potential drug candidates, and as a cost- and time-effective approach to identify the off-target effects of medications.

In the U.S., researchers can purchase pluripotent stem cells approved by the National Institutes of Health from the WiCell Research Institute located in Madison, Wisconsin [60]. Since the derivation of the first human embryonic stem cell line (ESC) in the late 1990s [61], WiCell has over 1500 cell lines in its catalog for researchers to use around the world [60]. These cell lines include human ESCs and induced pluripotent stem cell lines (iPSCs) with various diseases (e.g., Alzheimer's disease, Cardiomyopathy, and Fragile X syndrome) and genetic mutations. This ease of access allows researchers to use the same validated cell lines, promoting scientific consistency [56]. Further, given the relatively low cost, researchers can conduct toxicological and pharmacological testing on different genetic backgrounds to identify sensitive populations, all while minimizing confounding variables [56]. Similarly, the use of patient-derived iPSCs has the potential to test drug therapies for safety and efficacy prior to patient testing [56]. Overall,

stemcells are valuable tools that can be used in the drug discovery process and have the potential to uncover dangerous side effects of medications before they enter clinical trials or the market.

In addition, stem cells provide an excellent model for studying (1) processes related to reproduction, (2) reproductive toxicity, and (3) restoring fertility. Recently, Easley and colleagues [62, 63] demonstrated that human ESCs and iPSCs could be differentiated in *in vitro* conditions into advanced spermatogenic-like cell types, including undifferentiated and differentiated spermatogonial stem cell-like cells, primary and secondary spermatocyte-like cells, and spermatid-like cells, representing all of the major cell types observed during human spermatogenesis. A few years later, Easley and colleagues [59] demonstrated that this model could recapitulate the clinical phenotypes of two known reproductive toxicants, 2-bromopropane and 1,2-dibromo-3-chloropropane. Since these original publications, this model has been used to test the reproductive toxicity of hexabromocyclododecane, tetrabromobisphenol A [12], perfluorinated alkyl substances (PFAS) [64], polybrominated biphenyl-153 [65], cannabis extract [66], NSAIDs (Chapter 3), pesticides, opioids, and tobacco smoke extract (unpublished).

Given the general ease of adding environmental chemicals and pharmaceuticals to the cell culture media, this model is especially important for studying the impacts of pharmaceuticals on spermatogenesis rather than just analyzing the effects on hormone levels or human spermatozoa, as in the studies mentioned earlier. Additionally, due to the location of the SSCs outside of the BTB, which are exposed to xenobiotics in the bloodstream, this model is suited for studying the changes that occur throughout spermatogenesis. Overall, these factors suggest that this model is ideally suited for

studying the processes related to male gametogenesis and examining the mechanism behind how medications can lead to impaired fertility or, at worst, infertility [59].

Beyond the use of the human *in vitro* spermatogenesis model, stem cell protocols have been developed to advance the study of human reproduction further. Recently, Easley's *in vitro* spermatogenesis model has also been used to generate non-human primate (NHP) haploid spermatid-like cells that can fertilize NHP oocytes and produce blastocysts [63], providing an opportunity for infertile men to have their own biological children through the use of patient-specific *in vitro* derived spermatids. This *in vitro* model is also being adapted to generate a high-throughput and high-content platform to identify potential male contraceptives and characterize potential male reproductive toxicants (Chapter 5).

Each year, millions of women use some form of hormonal contraceptive. Generally, these medications are considered safe and effective; however, many women experience adverse side effects that lead to either voluntary or medically required termination. In these cases, women have few reliable options to assist in their family planning needs. Recently, there has been renewed interest in the development of contraceptives for men. Male forms of oral contraception have largely been ineffective, mostly because there is a lack of a human spermatogenesis platform for screening potential contraceptives. Therefore, Chapter 5 of this dissertation sought to utilize Easley's novel *in vitro* human spermatogenesis model to generate a fluorescent reporter system that can be used to identify possible male contraceptives [62].

In this study, we have generated two fluorescent reporter systems, Testibow 1.0 and Testibow 2.0, coupled with our *in vitro* spermatogenesis model, which fluorescently

labels spermatogenic cells throughout their development. This system utilizes fluorescence-based imaging to identify and characterize potential drug targets that successfully block spermatogenesis but permits full restoration following treatment cessation. To date, we have been successful in generating individual, stable human ESC lines expressing designated spermatogenic promoters and fluorescent proteins in each of these systems. We have proven these combinations function in the *in vitro* spermatogenesis model through live-cell imaging analyses. These results were then validated through immunocytochemistry experiments to determine if each fluorescent reporter was consistent with the endogenous gene expression. However, we have encountered several challenges that limit these platforms' ability to be used rapidly and efficiently. Currently, we are developing Testibow 3.0 using genome editing technology to generate the fluorescence reporter system. Overall, this novel fluorescent reporter platform has the potential to not only be used to identify male contraceptives but could also be used to examine the mechanism of action of how NSAIDs and other environmental toxicants disrupt human spermatogenesis while also further validating this model to use as a screening tool for therapeutics prior to clinical trials.

Through the introduction of biomaterials and microfluidics, three-dimensional culture systems have allowed mechanistic studies into the interactions between the male germ cells and the somatic niche (reviewed in [67]) and the study of early pregnancy and normal female reproduction [68, 69]. Further, these more advanced and complex microfluidic culture systems, such as EVATAR™, a female reproductive tract system complete with a 28-day menstrual cycle [70], can be paired with stem cell-based systems for an even more advanced study of human reproductive toxicants and pharmaceuticals.

These tools can be used in toxicological studies to examine how the xenobiotic in question interacts with human cell types. These models are particularly important for studying endocrine-disrupting chemicals and medications which can interfere with normal hormone production and signaling. The results from these studies can be studied on their own or compared with those from animal and epidemiological studies, like in the study by Greeson and colleagues [65], to provide valuable information for risk assessment [56]. These combined models can be used to further our understanding of the complex effects of environmental exposures and medications that can negatively affect human reproduction. Additionally, these three-dimensional culture systems have the potential to be paired with patient-specific iPSCs to restore fertility in both men and women where current treatment options fail to address their infertility [16].

2.7 NSAID THERAPY CAN CAUSE DISRUPTIONS TO THE MALE REPRODUCTIVE SYSTEM

2.7.1 NSAID therapy-induced alterations to the reproductive system

It has been well established that maternal medication use during pregnancy can impact offspring health, including acetaminophen/ paracetamol (Tylenol®) and NSAIDs such as ibuprofen (Motrin®/Advil®) and acetylsalicylic acid (Aspirin). Maternal use of mild analgesics during pregnancy increased the prevalence of cryptorchidism [71-75], the most common reproductive abnormality in newborn boys [72, 73]. Two additional studies published similar associations more than ten years later [25, 71]. These studies reported exposure to acetaminophen, ibuprofen, and acetylsalicylic acid during the second trimester increased the risk of cryptorchidism. The mothers who took more than one of these analgesics simultaneously for more than two weeks had the highest risk of

giving birth to a newborn son with cryptorchidism. Similarly, women who consumed ibuprofen and acetylsalicylic acid during pregnancy had an increased risk of giving birth to a newborn son with hypospadias [72, 76, 77]. While it is still unknown when timing and what doses are the most critical, these studies provide evidence that maternal use of NSAIDs during pregnancy can disrupt gonadal development and may compromise the child's fertility in the future.

In the adult male, medications can have pre-, testicular, and post-testicular effects, including alterations to the HPG axis, direct effects on spermatogenesis and spermiogenesis, impairment of sperm function, or a decrease in sexual function (e.g., erections, ejaculation, and libido) [29]. Pre-testicular disturbances affect the HPG axis, usually at the androgen receptors, by altering the activity of the endogenous androgens or by interfering with the feedback loops, leading to alterations in androgen function and production and impairing spermatogenesis and fertility (reviewed in [17]). Testicular disturbances occur near the seminiferous tubules and can directly affect the Leydig, Sertoli, and germ cells, leading to impairments in spermatogenesis, sperm maturation, and fertility ([34], reviewed in [17]). Post-testicular disturbances occur once the sperm leaves the seminiferous tubules. These disturbances can result in impaired ejaculatory reflex or altered seminal plasma, both of which could modify sperm function during conception (reviewed in [17]). Overall, drugs have the potential to alter male fertility at all stages of sperm development, and the effects are becoming increasingly concerning.

2.7.2 NSAIDs and endocrine disruption

Most studies have focused on medications acting as endocrine disrupting compounds. For example, researchers determined that ibuprofen can profoundly

influence the biochemical and enzymatic processes causing hormonal disruption in aquatic species [78, 79]. In adult male zebrafish, exposure to ibuprofen for 14 days decreased plasma testosterone levels, while exposure to both ibuprofen and naproxen down regulated the transcription of follicle stimulating hormone receptor (*FSHR*), luteinizing hormone receptor (*LHR*), and testosterone producing enzymes Cytochrome P450 17A1 (*CYP17A1*) and 17 β -Hydroxysteroid dehydrogenase (*17 β -HSD*) in the testis, suggesting NSAIDs may modulate hormone production and alter sperm production [80]. Thus, NSAIDs pose a serious threat to aquatic species' reproductive capabilities, which may indicate other animals may have similar alterations in their reproductive health.

2.7.2 NSAIDs and alterations in rodent reproductive function

Several studies have shown the harmful effects of analgesics, mainly aspirin and acetaminophen, on adult rodent male reproductive systems [81-84]. These studies showed alterations in hormone production, pyknotic changes in Sertoli cells, increase in the incidence of physical characteristics associated with male infertility (e.g., testicular hypoplasia, reduced anogenital distance, reduced number of spermatogenic cells, and decreased diameter of the seminiferous tubules) [83, 85-87]. Further, chronic administration of ibuprofen and naproxen to adult male mice and rats decreased testosterone levels [88], lowered sperm counts, and altered motility [89]. Although the overall effects of NSAIDs on rodent reproduction appear minimal, these studies warrant further trials in men (reviewed in [17]).

2.7.3 NSAIDs and adverse effects on human adult reproduction

To date, only a small number of studies have evaluated the effect of NSAIDs on adult male reproductive health. Acetaminophen, often grouped with NSAIDs based on its

pain-relieving quality, has been studied the most frequently and has relatively severe effects (reviewed in [17]). These studies revealed men with high levels of urinary acetaminophen had reduced sperm motility, altered sperm morphology, increased sperm DNA fragmentation, and an increased time to pregnancy [90, 91]. Other classes of NSAIDs have been shown to alter male reproduction. Indomethacin, a prescription-only NSAID used to treat arthritis, but not naproxen increased prolactin levels (important for maintaining testosterone levels) in 20 healthy adult men [92]. Additionally, fourteen days of indomethacin and oxaprozin (prescription-only NSAIDs used to treat osteoarthritis and rheumatoid arthritis) administration did not affect LH, FSH, testosterone, or semen parameters in adult men [93], suggesting an overall minimal effect on male hormone levels. Interestingly, naproxen often appears on the list of medications that causes delayed or retrograde ejaculation [94]. This was only reported in one case study but has propagated through the literature for the last 40 years and warrants further investigation. However, a recent study on the effects of ibuprofen on male fertility brought renown attention to the effects of popular OTC medications on male fertility. This study revealed that ibuprofen alters the hormonal profiles in healthy adult men following 14 days of administration [95]. While ibuprofen did not alter testosterone levels, the LH and free testosterone/ LH ratio levels increased and decreased, respectively. Further, ibuprofen decreased anti-Müllerian hormone (AMH), a peptide hormone secreted by the Sertoli cells. Together, ibuprofen produces a state of compensated hypogonadism, a condition often diagnosed in older men and consists of compromised Leydig cell function, but testosterone levels can be normally sustained by increased LH levels [96]. Because

ibuprofen displays broad endocrine disruption properties, fluctuations in reproductive hormones could result in infertility [97].

Overall, the effects of NSAID therapy on male reproductive function appears to be minimal. But, because of the increased use among reproductive-aged men and the rapidly declining semen parameters in men across the globe, there is a pressing need to determine whether these popular medications are a contributing factor. Using a comprehensive approach, the remaining sections of this dissertation review our findings regarding the direct testicular toxicity of ibuprofen and naproxen on male germ cells and the somatic niche.

2.8 STUDYING THE EFFECTS OF COMMON MEDICATIONS USING AN IN VITRO HUMAN SPERMATOGENESIS MODEL

The *in vitro* model developed by Easley and colleagues [62] provides a unique platform for directly assessing the effects of pharmaceuticals on the male reproductive tract. As previously discussed, medications can alter male reproductive health by acting as endocrine disrupting chemicals and exerting toxicity through the HPG axis, directly affecting spermatogenesis or having post-testicular effects. While there is evidence that NSAIDs can affect different aspects of male reproductive function, very little information is available about the mechanisms behind NSAID-induced reproductive disturbances and the direct effects on human spermatogenesis.

Chapter 3 studies NSAIDs, a class of pharmaceuticals increasingly used by reproductive-aged men worldwide to treat inflammation and pain. The safety of ibuprofen and naproxen in humans has been studied since their first introduction. While generally safe, post-marketing surveillance and phase IV studies are still important to

investigate their unique adverse effects on human reproduction [98]. One example in this context is the direct effects of ibuprofen and naproxen on human spermatogenesis. Therefore, this study aimed to better understand the direct effects of naproxen and ibuprofen on human spermatogenesis, without the presence of the somatic cells, at clinically relevant concentrations.

In this study, human ESCs were exposed to serum levels of naproxen and ibuprofen for ten days as they differentiated into spermatogenic lineages. The subcellular toxicological effects that could lead to impaired spermatogenesis were assessed after the long-term exposure. These evaluations on the spermatogenic-like cells included cell viability, mitochondrial membrane potential, cell cycle progression, and haploid cell production in a dose-dependent manner. Unlike long-term ibuprofen exposure, the *in vitro* derived spermatogenic cells may be more susceptible to naproxen-induced toxicity by directly altering the mitochondrial membrane potential and cell viability. Although the results appear to be cell-line specific, given the results of this study, the overall impacts of naproxen and ibuprofen treatment appear to have minimal effects on *in vitro* human spermatogenesis.

Previous studies observed decreased sperm counts in rats and mice chronically treated (35 days) with naproxen and ibuprofen, respectively [89, 99]. It is possible that significant differences in both exposures could emerge with longer treatments or at higher doses. This study indicates that it would be beneficial for future studies to focus on other cellular response mechanisms, such as oxidative damage and lipid peroxidation (reviewed in [98]), for determining NSAID-induced alterations to the *in vitro* spermatogenic-like cells.

Overall, this study, combined with previously published studies, illustrates how this *in vitro* human spermatogenesis model can be used to study the reproductive toxicity of various environmental chemicals and pharmaceuticals, which would be unethical to study in humans. With its relative ease and relevance to the clinic, this stem cell model is an important tool for expanding our knowledge about the effects of medications on male reproductive health. In the future, more medications can be tested using this model, including drug mixtures. This model could be combined with cells of the somatic niche to further our understanding of the systemic effects and adverse reactions that could influence spermatogenesis. Additionally, these experiments could be incorporated into the drug discovery process and provide a new standard for how pharmaceutical compounds are assessed in a cost-effective manner.

2.9 USING AN IN VITRO SYSTEM TO STUDY THE BLOOD-TESTIS BARRIER DYNAMICS

2.9.1 Introduction to the Blood-testis barrier and its function

The original concept of the BTB was first described in the early 1900s when dyes were injected into animals, and the testis and the brain were not stained [100-102]. However, it was not for another 67 years that the function of the BTB was fully appreciated. Scientists determined that dyes which were able to penetrate the seminiferous tubules in prepubertal rats were unable to in adult rats and that the fluid components in the mammalian testis differed (rete testis, seminiferous tubules, blood plasma, and testicular lymph) depending upon the site of collection [103-106]. Several years later, scientists further defined the structure of the BTB in the mammalian testis

using electron microscopy to include the presence of tight junctions between adjacent Sertoli cells [107-110].

The somatic Sertoli cells, also known as ‘nurse cells,’ assist in the proliferation, differentiation, and maturation of male germ cells. The Sertoli cells form the BTB, a specialized, dynamic structure that divides the seminiferous epithelium into the apical (adluminal) and basal compartments (reviewed in [111]). In the testis, the BTB has multiple functions that are essential to support spermatogenesis. First, the BTB regulates the entry of specific nutritional substances (e.g., amino acids), vital molecules (e.g., hormones), and toxicants (e.g., medications and environmental exposures) into the adluminal compartment, where spermiogenesis and spermiation occur [112]. This is because the blood vessels, capillaries, and lymphatic vessels are located in the interstitium between the seminiferous tubules and do not penetrate the tubules. This results in the BTB having to regulate the transcellular (through the intracellular transport pathway) and the paracellular (between adjacent Sertoli cells) transport of these substances across the barrier into the apical compartment [112]. Second, the BTB creates an immunological barrier by suppressing an immunological response to autoantigens residing in the germ cells undergoing meiosis [113, 114]. This BTB function contributes to the immune-privilege status of the testis to avoid the production of anti-sperm antibodies, which would lead to infertility [115]. Additionally, the Sertoli cells contribute to maintaining the immune-privileged state of the testis by secreting immunosuppressive molecules to block an immune response to the autoantigens in the differentiating germ cells [116-121]. Although these biomolecules are unknown, they are speculated to consist of cytokines and prostaglandins [114, 122, 123]. Thus, it is possible that NSAIDs could

alter the immunosuppressive properties of the Sertoli cells through the action of prostaglandins, which NSAIDs inhibit the production of. Finally, the BTB is crucial to maintaining cell polarity in the seminiferous epithelium. Besides the localization of the Sertoli cell nuclei near the basal compartment, the BTB segregates the cellular events that occur during spermatogenesis by providing a physical separation between cells undergoing spermatogenic renewal, proliferation, and differentiation. The SSCs, undifferentiated and differentiated spermatogonia, and preleptotene spermatocytes are located in the basal compartment, and the zygotene, pachytene, and diplotene spermatocytes, secondary spermatocytes, spermatids, and spermatozoa are located in the adluminal compartment [112].

2.9.2 Blood-testis barrier structure

Unlike other barriers, the BTB is constituted of four different cell junctions, including tight junctions, desmosomes, gap junctions, and ectoplasmic specializations [106, 124-126]. Briefly, the tight junctions are responsible for preventing solutes and large molecules between the paracellular space while restricting the flow of proteins and lipids between the basolateral and apical compartments [127]. The ectoplasmic specializations are testis-specific adhesion junctions and are found between the Sertoli cells (defined as the basal ectoplasmic specializations) and between the Sertoli cells and elongating spermatids (apical ectoplasmic specializations) [128, 129]. The desmosomes are cell-cell intermediate filament-based anchoring junctions found at the Sertoli-spermatid interface and at the BTB between adjacent Sertoli cells [130-136]. Lastly, the gap junctions are cell-cell channels that allow the flow of metabolites, ions, and molecules smaller than 1 kDa in size (reviewed in [127, 129, 134, 137]). These junctional

proteins coexist together to form one of the tightest blood-tissue barriers in the human body [106, 108, 112, 126, 138-140].

Despite this feature, the BTB undergoes restructuring to facilitate the movement of the preleptotene spermatocytes from the basal to the apical compartment as they differentiate into leptotene and zygotene spermatocytes [141-143]. This junctional coordination regulates the temporal opening and closing of the BTB to facilitate the movement of the preleptotene spermatocytes into the adluminal compartment [144]. Thus, any perturbations from medications or environmental toxicants that induce testicular injury through interactions with the BTB can result in subsequent damage to the developing germ cells and cause male infertility [112].

2.9.3 Using an in vitro Sertoli cell model to study BTB dynamics

In the United States, researchers can purchase human primary Sertoli cells through iXCells Biotechnologies located in San Diego, California [145]. iXCells has over 75 human primary cells in their catalog for academic, biotechnology, and pharmaceutical researchers to use around the globe [146]. These cell lines include primary human cells derived from numerous tissues, including the skin, liver, and kidney, with various diseases (e.g., Type 1/2 Diabetes, Osteoarthritis, and Rheumatoid Arthritis) [147]. This ease of access allows researchers to use the same validated and functional cell lines to monitor how environmental exposures alter the BTB before additional time, money, and resources are used to study these effects in human populations. However, immortal cell lines, such as the mouse Sertoli cell line, MSC-1, have been used instead of primary cells since they are more cost-effective, easier to use, and provide reproducible results [148]. While these cells were similar morphologically and possessed several biochemical

markers as the primary mouse Sertoli cells, the immortal cells lacked immune function (reviewed in [148]). Thus, experiments that used immortal Sertoli cells should be repeated using primary Sertoli cells to ensure accurate conclusions.

Sertoli cells can be cultured *in vitro* to form an epithelial barrier that closely resembles the *in vivo* BTB functionally and structurally [149, 150]. For example, when Sertoli cells are seeded at a high density on an extracellular matrix, like Matrigel®, they become polarized [149, 150] and form a functional tight junction permeability barrier with visible ultrastructures such as tight junctions, basal ectoplasmic specializations, gap junctions, and desmosomes between the adjacent Sertoli cells [149, 151, 152]. This model system has been used to study the mechanisms of how gap junctions [153] and desmosomes [154] interact with the basal ectoplasmic specializations and tight junctions to help to maintain the integrity of the BTB. Moreover, this model system has even been used to examine the effect of environmental toxicants, such as cadmium, on the BTB function [155-158], and, thus, could further our biological understanding of how environmental exposures and medications cause testicular dysfunction.

There are two pathways through which medications and extracellular molecules can move across an epithelial barrier to exert their pharmacological effects (1) paracellularly, which is moving through intercellular junctions between adjacent cells, and (2) transcellularly, which is through the cells [159]. The paracellular pathway involves molecules' passive diffusion, which is regulated by tight junctions [159]. In contrast, the transcellular pathway is mediated by specific transporters located on the apical or basolateral plasma membrane [160, 161]. Lipophilic drugs generally cross barriers transcellularly, and hydrophilic drugs cross the membrane paracellularly

(reviewed in [162]). Since NSAIDs can cross several human blood-tissue barriers, this model is especially important for determining if NSAIDs could interfere with BTB integrity and function.

Techniques to assess the formation of the tight junctions and the ability of molecules to pass across the epithelial barrier are imperative for quantifying barrier tissue function following xenobiotic exposure. As such, the formation of tight junctions can be assessed by quantifying the transepithelial electrical resistance [163] and measuring the flux of different-sized fluorescent tracers to inform us of how medications and other xenobiotics impact the transepithelial transport [159]. In short, the Sertoli cells are cultured on a semipermeable membrane. The tight junction barrier function is measured using two electrodes, one placed in an apical chamber and the other placed in the basal chamber. Then, the resistance to the flow of current across the Sertoli cell epithelium is calculated to yield the transepithelial electrical resistance [164, 165], providing a simple method to assess the integrity of the *in vitro* BTB. For the paracellular flux assays, the upper chamber media gets replaced with the probes of interest, and over an allotted time course, media is withdrawn from the lower chamber. Afterward, the aliquots are measured with a fluorescence microplate reader, and the resulting data can be used to measure the absolute amounts of flux and the diffusion rate [166]. Given the relatively low cost of both assays, these tools can be used in toxicological studies to examine how different chemicals and medications can alter barrier tissue dynamics. Models such as Sertoli cells cultured *in vitro* provide valuable information for (1) determining how toxicants can cross the BTB, enter the adluminal compartment, and wreak havoc on

meiosis and the differentiation of germ cells into haploid spermatids and (2) managing toxicant-induced infertility in humans due to Sertoli cell damage [167].

2.10 STUDYING THE EFFECTS OF COMMON MEDICATIONS USING AN IN VITRO SERTOLI CELL-BASED MODEL TO STUDY THE BLOOD-TESTIS BARRIER

Rodent Sertoli cells (mouse and rat) cultured *in vitro* that mimic the BTB *in vivo* are valuable tools for studying environmental toxicant induced Sertoli cell dysfunction. These *in vitro* models have been used to test the toxicity of Bisphenol A [168], cadmium [169], and Perfluorooctane sulfonate [170]. Some of these findings have even been reproduced *in vivo*, showing the capabilities of these *in vitro* models to illustrate how environmental exposures can perturb Sertoli cell function and BTB integrity [171-174]. This *in vitro* model has also been shown to work with NHP primary Sertoli cells exposed to NSAIDs (Chapter 4), alcohol, and per- and polyfluoroalkyl substances (unpublished). Given the general ease of adding the environmental exposures directly into the cell culture media to mimic *in vivo* exposure to the Sertoli cells, there are an infinite number of opportunities to study chemicals and medications for BTB alterations. This *in vitro* NHP Sertoli cell model removes the reliance on rodent Sertoli cells, providing a more relevant model to study environmental exposures and toxicant-mediated Sertoli cell dysfunction [175]. Further, mechanistic studies can be used to determine the cellular targets (such as at the BTB) can lead to new treatments for managing infertility.

Chapter 4 continues the reproductive study on two mild analgesics, naproxen, and ibuprofen. Recently, ibuprofen exposure to healthy adult men was shown to decrease the stimulatory action of FSH and decrease the levels of AMH, indicating that the function of

the Sertoli cells was impaired [95]. Using an *ex vivo* adult human testis model, expression of AMH and INHBB genes also decreased, further suggesting Sertoli cell impairment. Nonetheless, no in-depth studies have analyzed the effect of naproxen or ibuprofen on the junctional formation or barrier permeability. Therefore, this study aimed to better understand how NSAID exposure may impact the Sertoli cell BTB function and integrity at clinically relevant concentrations.

In this study, *in vitro* NHP primary Sertoli cells were exposed to serum levels of naproxen and ibuprofen for five days to develop tight junctions and simulate the BTB. The subcellular effects that could lead to impaired Sertoli cell BTB dysfunction were assessed after exposure. These evaluations on the NHP primary Sertoli cells included toxicological assays such as cell viability and mitochondrial membrane potential, Sertoli cell functional assays like transepithelial electrical resistance and paracellular flux, and gene expression analysis in a dose-dependent manner. The results from this combined approach revealed (1) short-term NSAID treatment does not induce apoptosis or alter the mitochondrial membrane potential, suggesting NSAID treatment does not alter the overall health of the NHP primary Sertoli cells, and (2) both naproxen and ibuprofen treatment increased the transepithelial electrical resistance, reflecting an overall strengthening in the integrity of the Sertoli cell tight junctions. However, neither naproxen nor ibuprofen affected the passing of 0.62 kDa or 10 kDa-sized molecules, suggesting that ibuprofen and naproxen exposure compromises the integrity of the Sertoli cell tight junctions through a mechanism within the Sertoli cells which allows the selective paracellular flux of different-sized molecules in the presence of strengthened tight junctions.

An mRNA sequencing experiment was then performed on the *in vitro* NHP primary Sertoli cells exposed to naproxen and ibuprofen to better understand the connection between NSAID use and the compromised Sertoli cell junction integrity. The highest concentrations of naproxen and ibuprofen had the largest change in gene expression compared to their respective controls. Gene set enrichment analysis for both naproxen and ibuprofen revealed an enrichment of genes involved in apical junctions. In addition, we observed an enrichment of genes by ibuprofen involved in an inflammatory response, androgen response, and cell junction regulation. But we only observed an enrichment of genes involved in an inflammatory response in the NHP primary Sertoli cells exposed to naproxen. These results suggest that these two drugs alter the function of Sertoli cells through different pathways, both of which could result in sub-fertility or infertility.

Since both naproxen and ibuprofen altered the expression of genes important for proper Sertoli cell and BTB function, we examined whether genes enriched in our NSAID-exposed NHP Sertoli cells were associated with phenotypes related to male factor infertility, such as cryptorchidism. We observed that the middle and highest dose of ibuprofen enriched genes in phenotypes such as cryptorchidism, functional abnormality of male internal genitalia, and aplasia/hypoplasia of the testes. Interestingly, naproxen treatment did not enrich genes in diseases associated with male factor infertility. Together, these results suggest that naproxen and ibuprofen perturb Sertoli cell function utilizing different pathways and that NSAID therapy may cause a lack of mechanical and immunoprotective support to the germ cells. These changes could indirectly disrupt male germ cell development and compromise fertility.

This study illustrates how *in vitro* NHP primary Sertoli cells can be used to study the impacts of pharmaceuticals and environmental toxicants on BTB dynamics in ways that are impracticable to study in humans. Given the relative ease and relevance to human male reproduction, this model is a highly reproducible and convenient approach to investigating the molecular mechanisms associated with xenobiotic-induced Sertoli cell injury. In the future, this model could be combined with male germ cells to provide new insights into the interactions between the Sertoli cells and developing germ cells. These studies could examine how compounds disrupt the spatiotemporal expression of proteins that regulate the transport of germ cells across the BTB and provide an in-depth analysis of cell adhesion. This model would advance the field of toxicology and drug discovery in a cost-effective, reliable manner that allows mechanistic studies and experiments to monitor how medications and environmental toxicants alter testicular function, resulting in sub-fertility or infertility. As such, this *in vitro* model could theoretically show how human exposure to common medications can disrupt male reproductive health before clinical trials.

CHAPTER 3

INVESTIGATING THE EFFECTS OF NSAIDS ON HUMAN SPERMATOGENESIS USING A STEM CELL-BASED MODEL

3.1 INTRODUCTION

Globally, an estimated 50 to 80 million reproductive-aged couples are affected by infertility [176, 177], with male factor infertility accounting for nearly half of all infertility cases [178]. In the United States alone, 10-12% of men are diagnosed with infertility each year [178-181]. Evidence suggests that semen parameters, including sperm counts, have rapidly declined in men living in North America, Europe, and Australia over the last 50 years [10]. However, new data revealed that this decline in sperm has become significantly steeper since 2000 [11]. Between 1973-2011, there was a greater than 1% decline in sperm counts [10]. From 2000-2018, the percentage of sperm count decline per year doubled, increasing from just over 1% post-1972 to 2.6%, suggesting this trend is occurring at an accelerated pace [11]. Further, this decline in semen parameters extends from men living in Western countries to those in South and Central America, Asia, and Africa [11]. Recognized as a significant public health concern across the world, understanding the causes of this rapid decline in sperm counts is paramount.

3.1.1 Sales and Use of Analgesics

Human and animal health has dramatically improved since the development of analgesics to treat episodic and chronic healthcare problems. Over the last 20 years,

analgesics, such as NSAIDs, have been increasingly used and are now the most used over-the-counter (OTC) medications in North America and around the globe [182, 183]. More than 30 million people use NSAIDs daily, accounting for nearly 60% of the United States (U.S.) OTC analgesic market [184, 185]. Two non-steroidal anti-inflammatory drugs (NSAIDs), ibuprofen and naproxen, also known in the U.S. as Motrin[®]/Advil[®] and Aleve[®], respectively, are among the top 12 most commonly used medications by men ages 18-44 years [186]. These drugs are frequently used to relieve pain, fever, and inflammation caused by headaches, toothaches, and back pain, amongst other minor ailments [34, 186, 187]. NSAIDs can be purchased as non-prescription strength/OTC at various retail stores, making them easily accessible to the general public. Over the next eight years, the global NSAID market is projected to increase by almost \$12 billion, partly due to the higher availability of oral NSAID products and increasing demand [188]. Hence, these readily available medications could pose a serious health effect to male fertility.

NSAID use is increasingly common as men enter or are in their 30s and those who are physically active or blue-collar workers [189-191]. Their heavy usage among this population could pose significant complications to their fertility. Further, as men are waiting longer to start a family, the increased likelihood of consuming more NSAIDs over their lifetime and during their family planning process could contribute to the decline in male fertility. Despite the widespread usage and overall assumption that these medications are safe [17], there is still a significant lack of understanding about the adverse health effects on the human male reproductive system.

3.1.2 NSAID Characteristics and Metabolism

More than 5,000 years ago, the principle of NSAID therapy was first introduced when willow bark was used to treat musculoskeletal pain [192, 193]. However, it was not until the mid-1800s that the active ingredient in willow bark, known as salicin, was isolated. By the late 1800s, salicylic acid was mass-produced, and within a few years, aspirin (acetylsalicylic acid) was developed [192, 193]. However, it was not for another 70 years before the first non-aspirin NSAIDs, ibuprofen and indomethacin, were developed [192, 193]. Shortly after, many new classes of NSAIDs were developed, including naproxen [192, 193].

In 1971, NSAIDs were demonstrated to inhibit the production of prostaglandins by blocking the substrate, arachidonic acid, from binding to the cyclooxygenase (COX) active site [194]. Upon release from membrane phospholipids, arachidonic acid is catalyzed by the COX pathway to form Prostaglandin-G₂ (PGG₂), which is immediately converted to Prostaglandin-H₂ (PGH₂). PGH₂ undergoes further enzymatic reactions to form prostanoids, such as thromboxanes (produced by platelets and involved in blood clot formation), prostacyclin (involved in vasodilation, inhibition of platelet activation, and an inflammatory mediator), and prostaglandins (involved in the maintenance of homeostasis and inflammatory processes) (reviewed in [195-198]). Today, it is widely accepted that the inhibition of the COX pathway accounts for the antipyretic (fever reducing), analgesic (pain-relieving), and anti-inflammatory properties of NSAIDs [194, 199-202].

Both naproxen and ibuprofen are non-selective COX inhibitors, meaning each drug inhibits cyclooxygenases- 1 (COX-1) and -2 (COX-2) enzymes. Generally, COX-1

is constitutively expressed in most cell types and catalyzes the production of prostaglandins involved in maintaining homeostasis [203]. In comparison, COX-2 can be induced by cytokines, inflammatory mediators, and mitogenic factors and has a role in cellular replication and differentiation and the mediation of pain, inflammation, and fever [194, 195, 204, 205].

Prostaglandins and their receptors are found throughout the male reproductive tract, including in the seminal plasma, where they were initially discovered [17]. Evidence suggests that prostaglandins appear to be associated with sperm quality [93, 206, 207], where men with low fertility and oligozoospermia had lower seminal prostaglandins, suggesting that prostaglandins are important for normal fertility [208]. In the testis, COX-1, COX-2, Prostaglandin F₂ α (PGF₂ α), and Prostaglandin-D₂ (PGD₂) are known to be involved in the production of testosterone by the Leydig cells [209]; however, the role of COX and prostaglandins in the Sertoli cells and the spermatogenic process is relatively scarce [203]. In brief, COX-2 and Prostaglandin-E₂ (PGE₂) were identified in spermatogenic cells in rats [210], but their function within this process is unknown. While recent investigations described the expression and function COX and prostaglandins in testicular pathophysiology, information regarding their roles within the male genital tract are still relatively limited.

Both naproxen and ibuprofen are classified as NSAIDs and are similar in many ways. NSAIDs are relatively lipid-soluble, weak acids, and generally have high bioavailability following oral administration [211]. Due to their chemical properties, naproxen and ibuprofen are well absorbed from the gastrointestinal tract and have high bioavailability at 95% and 80%, respectively [211]. Both are highly bound to plasma

proteins at therapeutic concentrations, limiting their distribution. Naproxen and ibuprofen are metabolized in the liver and excreted in the urine, with naproxen also being eliminated in feces [211, 212].

Ibuprofen is considered more short-acting, with a fast onset of action, and better for treating acute pain. In contrast, naproxen is considered long-acting, with a slower onset of action, and better for treating chronic conditions [213]. Since ibuprofen has a half-life of two hours, this drug usually needs to be administered every six to eight hours [211]. In comparison, naproxen has a longer half-life at 12-17 hours and needs to be administered once or twice daily [214-216]. In 24 hours, the recommended maximum dosage for adults and children over the age of 12 is 1200 mg for ibuprofen and 1000 mg for naproxen [213]. It is recommended to take each NSAID at the lowest effective dose for the shortest amount of time to reduce the risk of side effects since OTC users are not generally monitored for adverse drug reactions by a healthcare provider [217].

3.1.3 Analgesics in the environment

Due to the widespread use of analgesics, an unintended consequence has been the introduction of these compounds and their metabolites into aquatic environments. Medications have been identified in effluents from production facilities, hospitals, private homes, and veterinary facilities, leading to contamination of surface and groundwater [218], and eventually drinking water (reviewed in [219]); therefore, posing a significant threat to human health around the world [220]. Additionally, pharmaceuticals may reach the sewer system through improper disposal of unused drugs flushed down the toilet entering the sewer system and then wastewater treatment plants. Their presence in surface and groundwater usually results from the excretion of these drugs in their native

form or as metabolites, passing into the sewer system and eventually reaching wastewater treatment facilities [78, 79]. For example, influent wastewater containing both ibuprofen and naproxen, have been documented. Ibuprofen concentrations have been recorded to reach 5.78 – 1673 mg/L, and naproxen concentrations have reached 7.6 – 33.9 mg/L [79, 221]. Similarly, NSAIDs are consistently at the top of the list of pharmaceuticals identified in effluents from wastewater treatment facilities and are considered environmental contaminants in terms of their frequency and concentration due to their incomplete removal [182]. Although at low concentrations, humans can be inadvertently exposed to NSAIDs, which may negatively affect reproductive health.

Several studies have suggested how environmental and lifestyle factors can impair male fertility, including therapeutic drugs [12, 13, 222-224]. Any medication that harms the Sertoli or Leydig cells, or spermatogonia can negatively affect spermatogenesis and sperm maturation, adversely affecting fertility [34]. However, there is still a significant lack of understanding of the adverse effects of NSAIDs on the human male reproductive system despite their increased usage and presence in the environment.

In brief, indomethacin, but not naproxen, increased prolactin levels in 20 healthy adult men [92]. Neither indomethacin or oxaprozin treatment affect gonadotropins, testosterone, or semen parameters in adult men [93]. On the other hand, ibuprofen alters hormonal profiles in adult reproductive aged men [96]. Furthermore, men with high levels of urinary acetaminophen had more severe effects on sperm and adult male fertility [90, 91]. Because acetaminophen has shown to affect adult male fertility, some practitioners are recommending men to discontinue acetaminophen during conception [17]. With the exception to acetaminophen, the effects of NSAIDs on male reproductive

health appear to be negligible, but only a few studies have assessed the effects on human male reproduction. Thus, there is a pressing need to determine whether these popular medications affect human spermatogenesis and male fertility. Therefore, this study is only going to focus on naproxen and ibuprofen, two NSAIDs that are highly taken by reproductive aged men, to assess their direct effects on human spermatogenesis.

3.2 PURPOSE OF THE STUDY

Despite the growing body of knowledge about the increased uses of naproxen and ibuprofen, and potential reproductive harm, this study aimed to evaluate the direct effects of naproxen and ibuprofen on human spermatogenesis, which has not been assessed to date.

3.3 STUDY INNOVATION

In our lab, we have developed an *in vitro* model of human spermatogenesis to further our understanding of how environmental exposures, including pharmaceuticals, impact male fertility [62]. Human male embryonic stem cells (ESCs) and human induced pluripotent stem cells (iPSCs) can be directly differentiated into spermatogonial stem cell-like cells, primary and secondary spermatocyte-like cells, and spermatid-like cells using our *in vitro* model, which closely resembles human spermatogenesis *in vivo* [62]. We have successfully recapitulated the clinical phenotypes of 1,2-dibromo-3-chloropropane (DBCP) and 2-bromopropane (2-BP), two known human reproductive toxicants [59]. Also, we determined how PBB153, a brominated flame retardant, alters DNA methylation in our *in vitro*-derived spermatids, leading to alterations in the expression of genes critical to proper human development [65]. This model allows us to evaluate naproxen and ibuprofen's impact on spermatogenesis mechanistically.

Therefore, this study aimed to assess the subcellular effects that could lead to impaired spermatogenesis, including cell viability of spermatogenic-like lineages, mitochondrial membrane potential, cell cycle progression, and haploid cell production following long-term exposure to plasma levels of ibuprofen and naproxen.

3.4 RESULTS: LONG-TERM NAPROXEN EXPOSURE ALTERS THE MITOCHONDRIAL MEMBRANE POLARIZATION IN IN VITRO SPERMATOGENIC CULTURES, BUT CHRONIC IBUPROFEN EXPOSURE DOES NOT IMPACT THE MITOCHONDRIAL MEMBRANE POTENTIAL

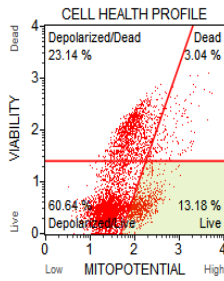
The mitochondria are one of the most important cellular organelles with functions including the generation of ATP for cellular energy, maintenance of calcium homeostasis, cell signaling, regulation of cell cycle progression, and containing key regulators of cell death processes such as apoptosis [225-230]. Since cellular energy is produced during mitochondrial respiration and is stored as an electrochemical gradient across the mitochondrial membrane, a loss of this transmembrane potential can be observed during the early stages of apoptosis [231]. As such, changes in the mitochondria are highly sensitive indicators of cell health and stress. Several clinically approved drugs have been removed from the market as a result of causing impaired mitochondrial function [232]. Therefore, understanding how naproxen and ibuprofen affect mitochondrial activity can help us predict the possible exposure-related toxic effects [233]. Ibuprofen and naproxen have been shown to alter the mitochondrial function or impair oxidative phosphorylation in yeast, A549 (lung carcinoma epithelial cells), and COS-7 (African green monkey kidney fibroblast-like cells) and rat liver cells [234-237]

in vitro and *in vivo*; however, the mitochondrial effects on human sperm cells are minimal.

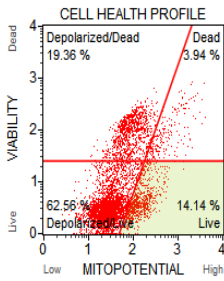
Here, we examined whether plasma levels of naproxen and ibuprofen negatively affect the mitochondrial membrane potential in our *in vitro* human spermatogenesis model using a cationic, lipophilic dye to detect changes in the mitochondrial membrane potential and 7-aminoactinomycin D (7-AAD) as an indicator of cell health supplied by the Muse® MitoPotential Kit to assess the mitochondrial membrane depolarization. Our differentiation protocol produces a mixed population of spermatogonial stem cell-like cells, primary and secondary spermatocyte-like cells, and haploid spermatid-like cells. Starting on Day 1 of the spermatogenic differentiation, the cells were treated with naproxen or ibuprofen at concentrations reflecting plasma levels in healthy adult men ranging from 10^{-4} to 10^{-5} M [95, 238, 239] to mimic long-term usage. Differentiating spermatogonial stem cell-like cells were exposed to naproxen at concentrations of 4 μ M, 40 μ M, or 400 μ M [238] or ibuprofen at concentrations of 1 μ M, 10 μ M, or 100 μ M [95]. Both naproxen and ibuprofen treatment groups were analyzed compared to the water- and 0.1% ethanol vehicle controls, respectively. We generated flow cytometry plots showing the percentage of live, live/depolarized, dead/ depolarized, and dead in our *in vitro* cultures exposed to naproxen and ibuprofen, respectively (Figures 3.1 and 3.3) using three genetically distinct National Institutes of Health-approved human male cell lines. Long-term naproxen exposure significantly decreased the mitochondrial membrane potential at the 400 μ M exposure in the WA01 and WA23 human ESCs differentiated *in vitro*, with a similar but insignificant trend in the WA14 cell line (Figure 3.2 B). Further, there was a significant decrease in the percentage of live cells at the 400 μ M exposure

(Figure 3.2 A) and a significant increase in the depolarized/ live cells at the 400 μ M exposure in the WA23 huma ESCs differentiated *in vitro*; however, the WA01 and WA14 had a similar but nonsignificant trend (Figure 3.2 C). Lastly, 40 μ M and 400 μ M naproxen increased the percentage of dead cells in the WA01, and WA23 human ESCs differentiated *in vitro* (Figure 3.2 D). In contrast, long-term ibuprofen exposure did not alter the mitochondrial membrane potential of the human ESCs differentiated in *in vitro* spermatogenic conditions (Figure 3.4 A-C). However, 10 μ M ibuprofen exposure increased the percentage of dead cells in the WA01 ESCs differentiated *in vitro* (Figure 3.4 D).

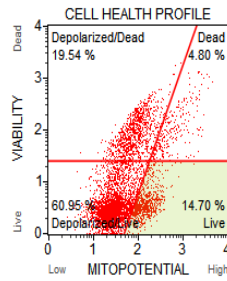
A WA01



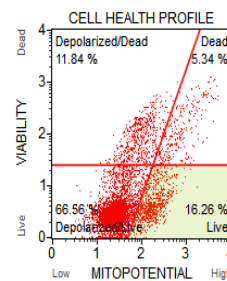
Water Control



Naproxen 40 μM

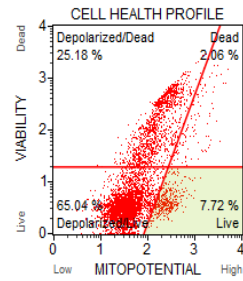


Naproxen 4 μM

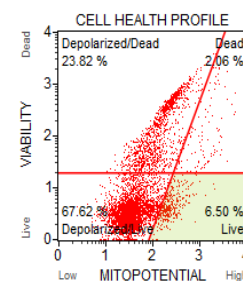


Naproxen 400 μM

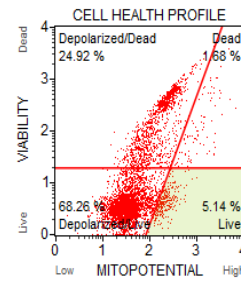
B WA14



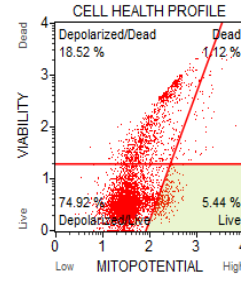
Water Control



Naproxen 40 μM

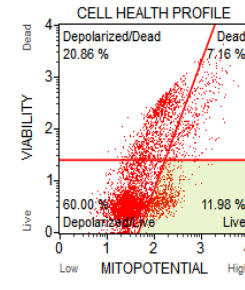


Naproxen 4 μM

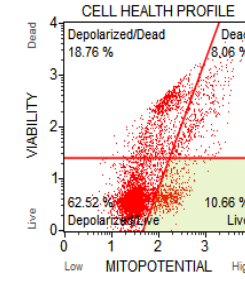


Naproxen 400 μM

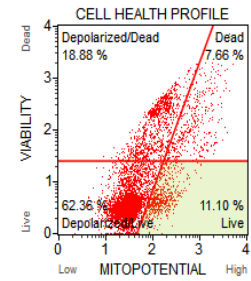
C WA23



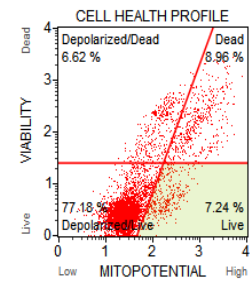
Water Control



Naproxen 40 μM



Naproxen 4 μM

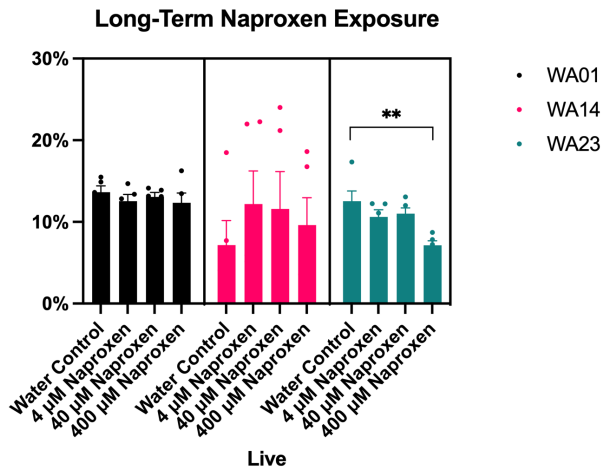


Naproxen 400 μM

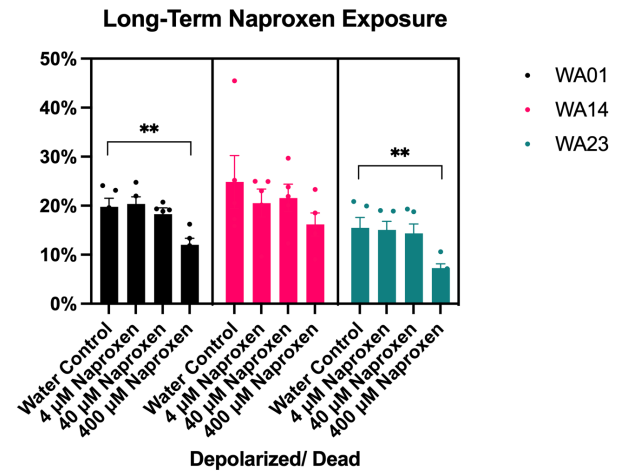
Figure 3.1. Flow cytometry plots for long-term naproxen-treated spermatogenic cells derived from human male ESCs for mitochondrial membrane potential data.

Flow cytometry analyses for indicating the percent live cells, percent depolarized/ live cells, percent depolarized/dead cells, and percent dead cells. The lower right quadrant represents the viable cells, the lower left quadrant represents the depolarized/live cells, the upper left quadrant represents the depolarized/ dead cells, and the upper right quadrant represents the dead cells.

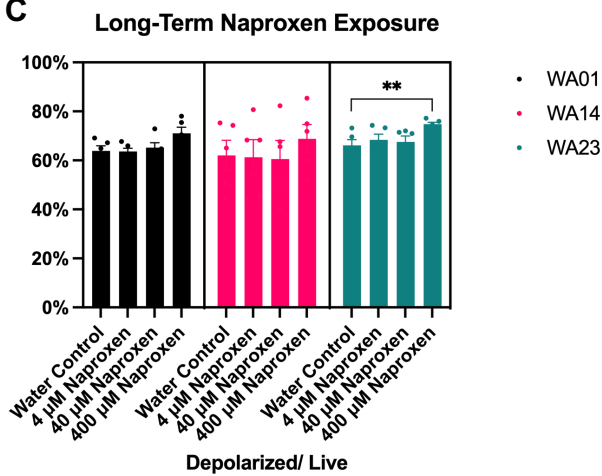
A



B



C



D

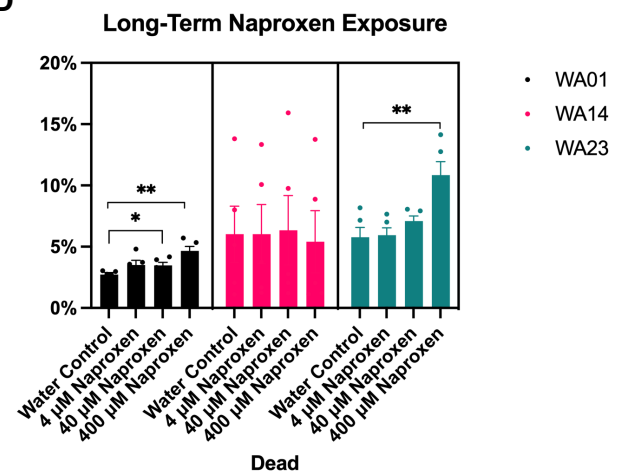
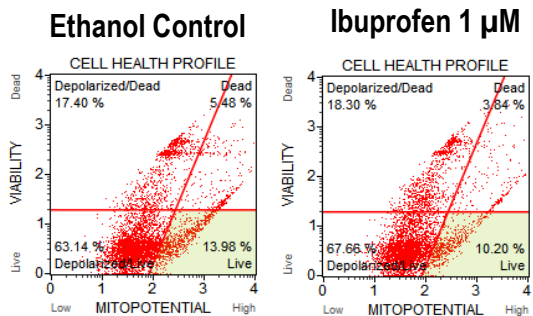
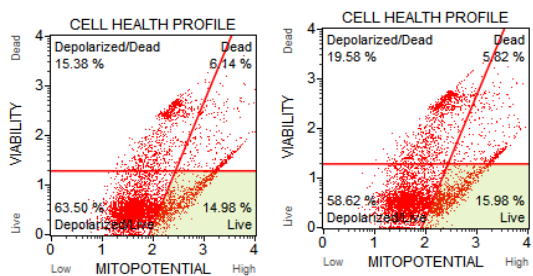


Figure 3.2. Long-term naproxen exposure alters the mitochondrial membrane polarization and increases cell death of spermatogenic cells derived from human male ESCs. Graphical representation showing that exposure to 400 μ M naproxen from Day 1 to Day 10 alters the mitochondrial membrane potential and viability in WA23 human ESCs, and the mitochondrial membrane potential in WA01 human ESCs differentiated in *in vitro* spermatogenic conditions in comparison to water-only vehicle control. A total of 5,000 events were acquired, with five replications ($n = 5$) performed for each drug treatment. Significant alterations in the mitochondrial membrane potential were determined by using a two-tailed Student's *t*-test, where * is $p < 0.05$, ** is $p < 0.01$, and *** is $p < 0.001$. Each bar represents the mean \pm SEM.

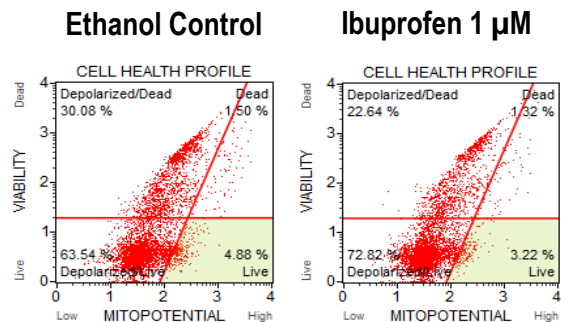
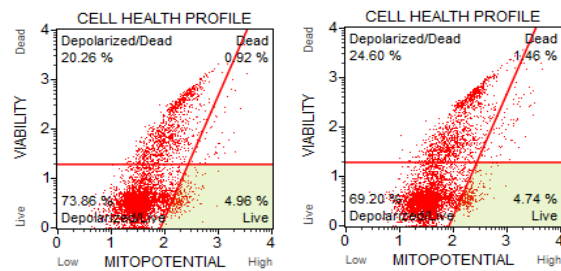
A WA01



Ibuprofen 10 μ M

Ibuprofen 100 μ M

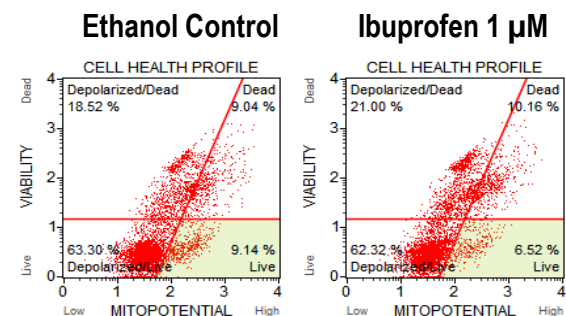
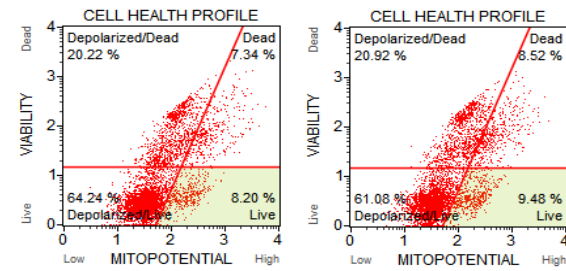
B WA14



Ibuprofen 10 μ M

Ibuprofen 100 μ M

C WA23



Ibuprofen 10 μ M

Ibuprofen 100 μ M

Figure 3.3. Flow cytometry plots for long-term ibuprofen-treated spermatogenic cells derived from human male ESCs for mitochondrial membrane potential data.

Flow cytometry analyses for indicating the percent live cells, percent depolarized/ live cells, percent depolarized/dead cells, and percent dead cells. The lower right quadrant represents the viable cells, the lower left quadrant represents the depolarized/live cells, the upper left quadrant represents the depolarized/ dead cells, and the upper right quadrant represents the dead cells.

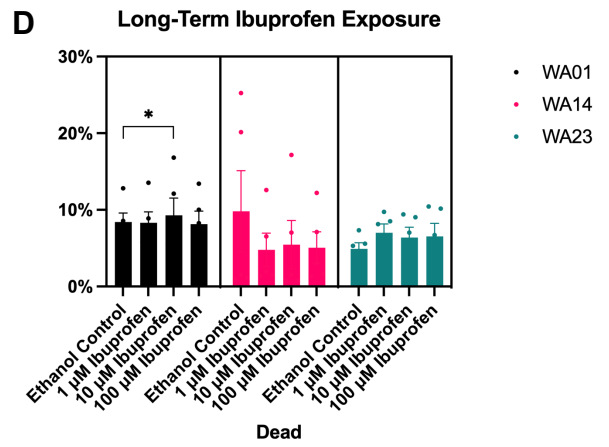
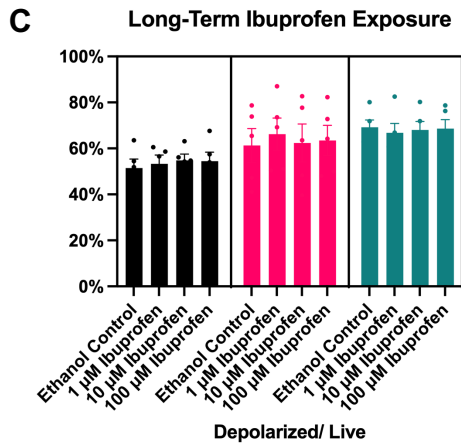
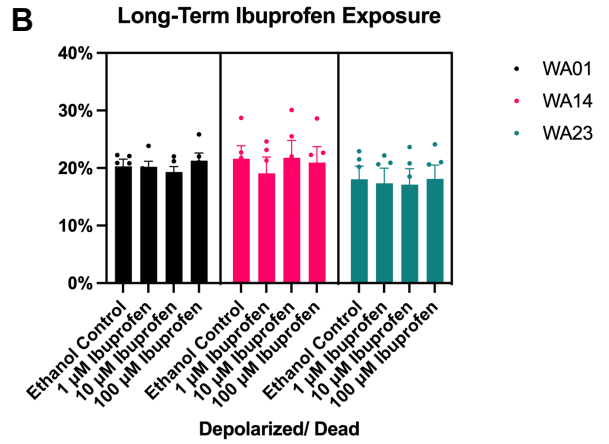
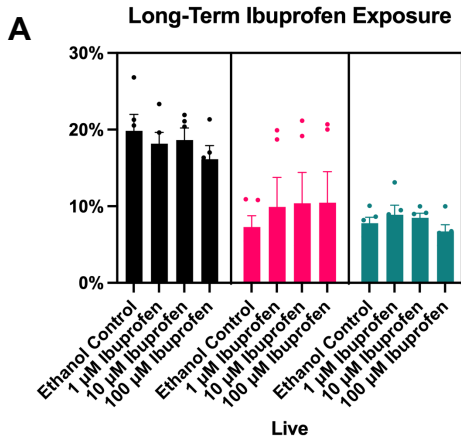


Figure 3.4. Long-term ibuprofen exposure does not alter the mitochondrial membrane polarization of spermatogenic cells derived from human male ESCs.

Graphical representation showing that exposure to 1 μM , 10 μM , or 100 μM ibuprofen from Day 1 to Day 10 does not alter the mitochondrial membrane potential of WA01, WA14, or WA23 human ESCs differentiated in *in vitro* spermatogenic conditions in comparison to the 0.1% ethanol-only vehicle control. Graphical representation shows that exposure to 10 μM ibuprofen alters the viability of WA01 human ESCs differentiated in *in vitro* spermatogenic conditions compared to a 0.1% ethanol-only vehicle control. A total of 5,000 events were acquired, with five replications ($n = 5$) performed for each drug treatment. Significant alterations in the mitochondrial membrane potential were determined by using a two-tailed Student's *t*-test, where * is $p < 0.05$, ** is $p < 0.01$, and *** is $p < 0.001$. Each bar represents the mean \pm SEM.

3.4 RESULTS: LONG-TERM NAPROXEN EXPOSURE ALTERS THE CELL VIABILITY IN ONE CELL LINE DIFFERENTIATED IN IN VITRO SPERMATOGENIC CONDITIONS, BUT CHRONIC IBUPROFEN EXPOSURE DOES NOT IMPACT THE CELL VIABILITY

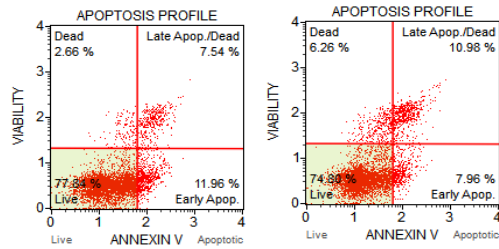
Several environmental toxicants have been shown to decrease the viability of spermatogenic cells [12, 59, 240]; however, information regarding the effects of NSAIDs on the viability of sperm cells is somewhat limited [99, 241]. For example, male rats treated chronically with approximately oral human equivalent doses of naproxen caused lower epididymal sperm counts [89]. In one study, mice given intraperitoneal injections of 0.02-0.06x human equivalent doses of ibuprofen had normal parameters of epididymal sperm [242]. Although, no studies have evaluated naproxen or ibuprofen's effect on human spermatogenic cells thus far.

Here, we examined whether plasma levels of naproxen and ibuprofen affect the cell viability of human spermatogenic cells using our *in vitro* human spermatogenesis model [12, 59, 62, 64, 65]. We assessed cell viability in this model using Annexin V to detect apoptotic cells and 7-AAD as an indicator of cell health supplied by the Muse[®] Annexin V & Dead Cell Kit (Luminex) to assess cell viability. We generated flow cytometry analyses reporting the percentage of live, early apoptotic, late apoptotic, and dead cells in our *in vitro* spermatogenic cells treated with naproxen and ibuprofen, respectively (Figure 3.5 and 3.7).

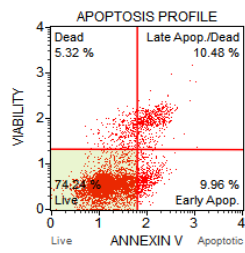
Similar to the mitochondrial membrane potential results, long-term naproxen exposure significantly decreased the cell viability at the 40 μ M naproxen exposure in the WA23 human ESCs differentiated *in vitro* (Figure 3.6 A), with the 400 μ M naproxen

exposure approaching significance ($p < 0.08$). Further, there was a significant increase in the percentage of late apoptotic cells at the 4 μM , 40 μM , and 400 μM exposures in the WA23 human ESCs and at the 4 μM exposure in the WA01 human ESCs differentiated *in vitro* (Figure 3.6 C). In comparison, long-term ibuprofen exposure did not alter the cell viability of human male ESCs differentiated in the *in vitro* spermatogenic conditions (Figure 3.8 A-D). However, in both NSAIDs, apoptosis was more pronounced than necrosis.

A WA01

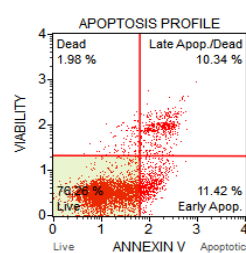


Water Control



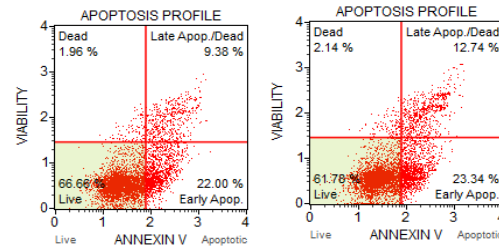
Naproxen 40 μM

Naproxen 4 μM

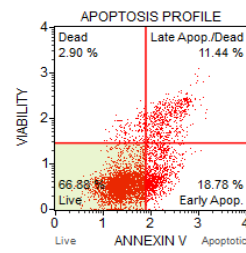


Naproxen 400 μM

B WA14

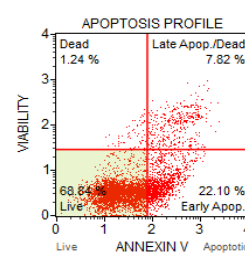


Water Control



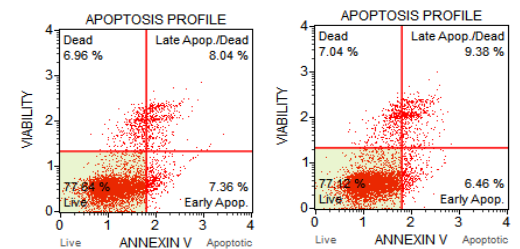
Naproxen 40 μM

Naproxen 4 μM

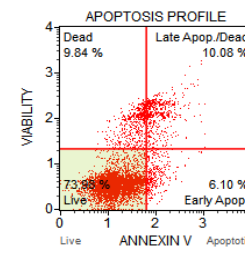


Naproxen 400 μM

C WA23

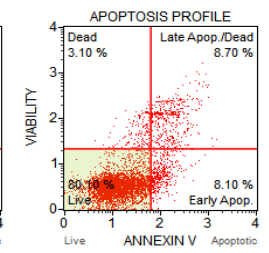


Water Control



Naproxen 40 μM

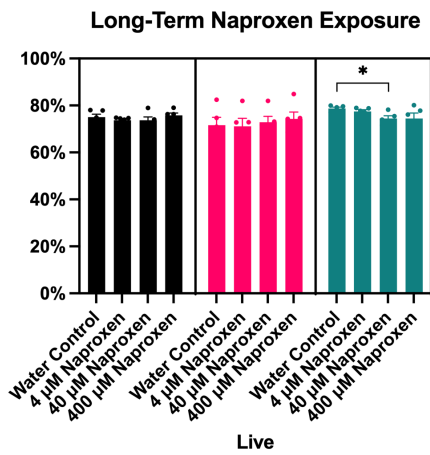
Naproxen 4 μM



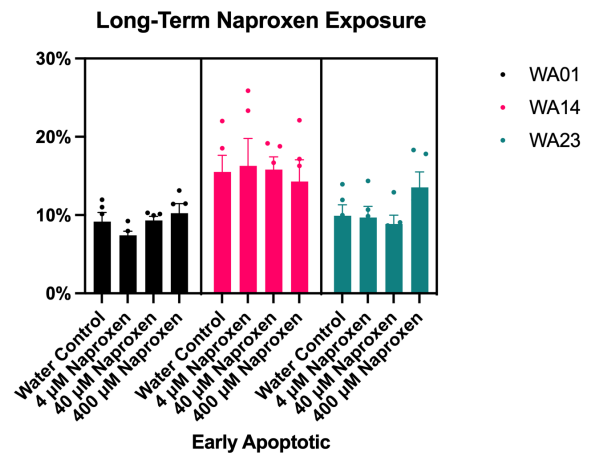
Naproxen 400 μM

Figure 3.5. Flow cytometry plots for long-term naproxen-treated spermatogenic cells derived from human male ESCs for cell viability data. Flow cytometry analyses for indicating the percent live cells, percent early apoptotic, percent late apoptotic, and percent dead cells. The lower left quadrant represents the live/viable cells, the lower right quadrant represents the early apoptotic cells, the upper right quadrant represents the late apoptotic/ dead cells, and the upper left quadrant represents the dead/ necrotic cells.

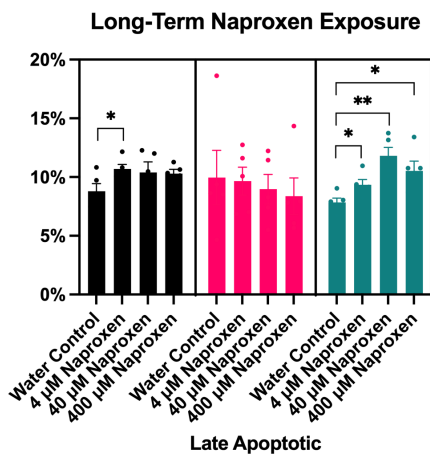
A



B



C



D

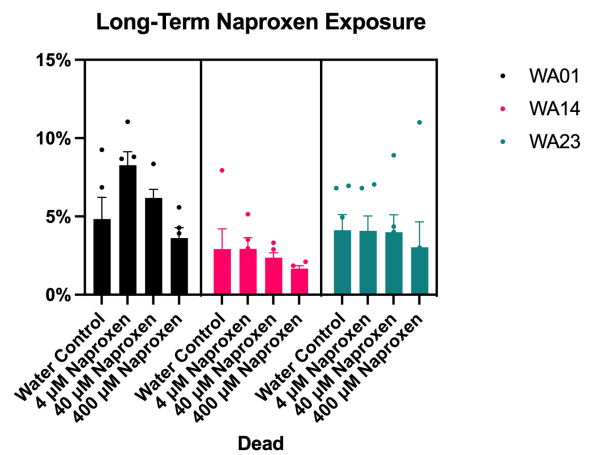
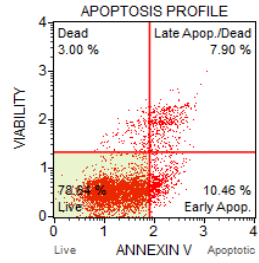
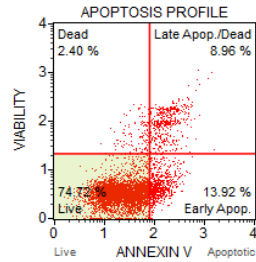


Figure 3.6. Long-term naproxen exposure decreases the cell viability of spermatogenic cells derived from human male ESCs. Graphical representation shows that exposure to 40 μ M naproxen from Day 1 to Day 10 alters the viability in WA23 human ESCs differentiated in *in vitro* spermatogenic conditions compared to the water-only vehicle control. A total of 5,000 events were acquired, with five replications ($n = 5$) performed for each drug treatment. Significant alterations in the mitochondrial membrane potential were determined by using a two-tailed Student's *t*-test, where * is $p < 0.05$, ** is $p < 0.01$, and *** is $p < 0.001$. Each bar represents the mean \pm SEM.

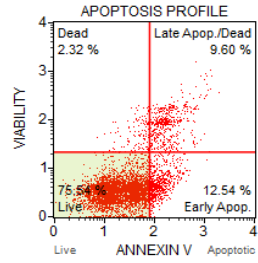
A WA01



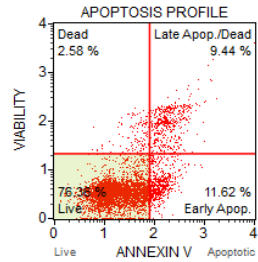
Ethanol Control



Ibuprofen 10 µM

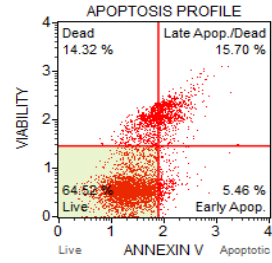


Ibuprofen 100 µM

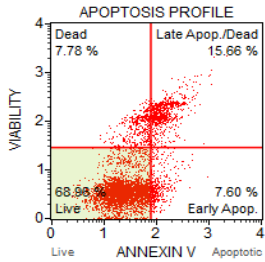


Ibuprofen 100 µM

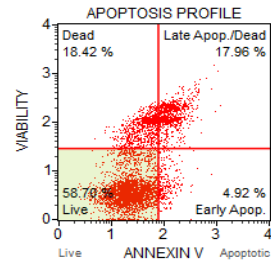
B WA14



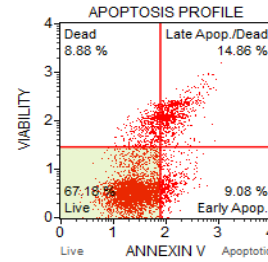
Ethanol Control



Ibuprofen 10 µM

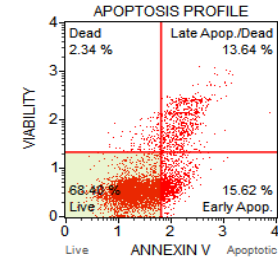


Ibuprofen 1 µM

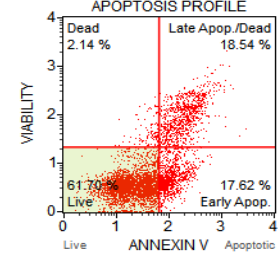


Ibuprofen 100 µM

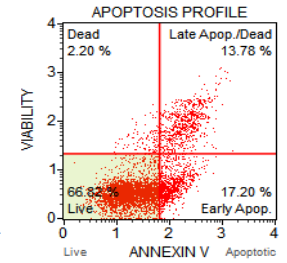
C WA23



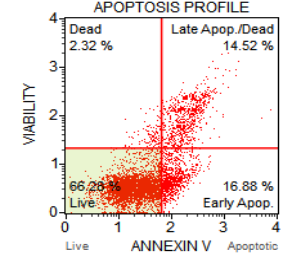
Ethanol Control



Ibuprofen 10 µM



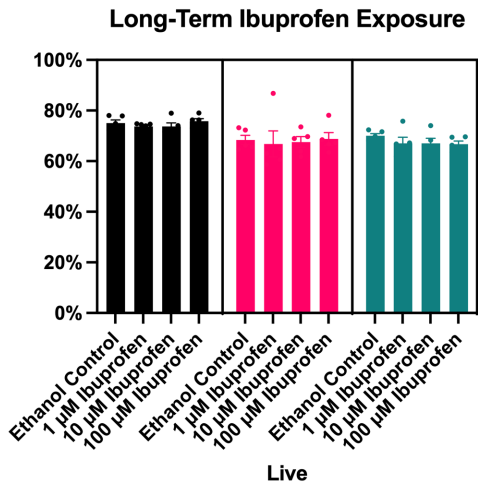
Ibuprofen 1 µM



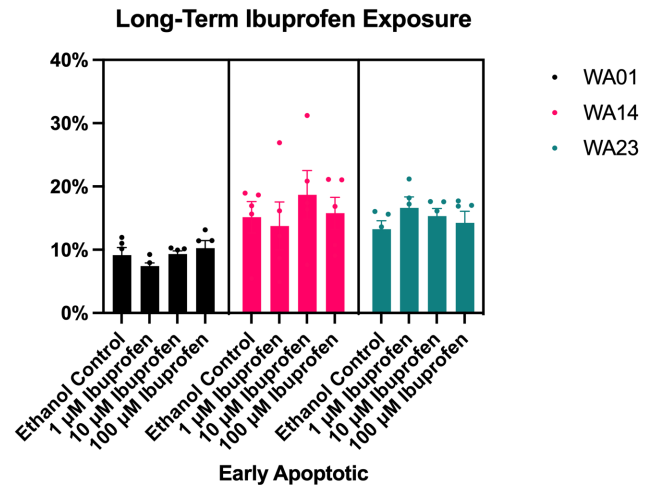
Ibuprofen 100 µM

Figure 3.7. Flow cytometry plots for long-term ibuprofen-treated spermatogenic cells derived from human male ESCs for cell viability data. Flow cytometry analyses for indicating the percent live cells, percent early apoptotic, percent late apoptotic, and percent dead cells. The lower left quadrant represents the live/viable cells, the lower right quadrant represents the early apoptotic cells, the upper right quadrant represents the late apoptotic/ dead cells, and the upper left quadrant represents the dead/ necrotic cells.

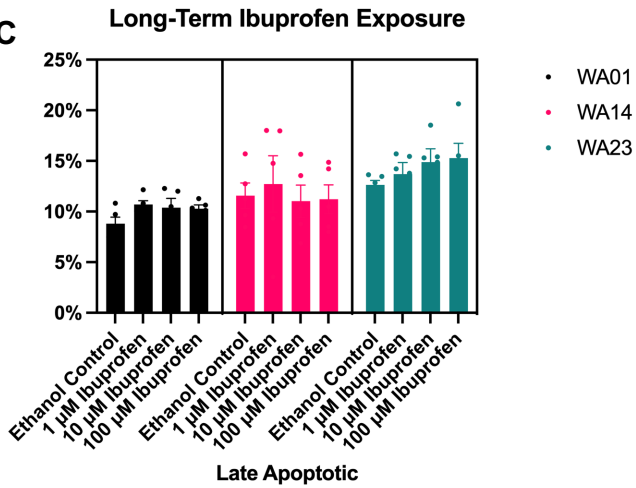
A



B



C



D

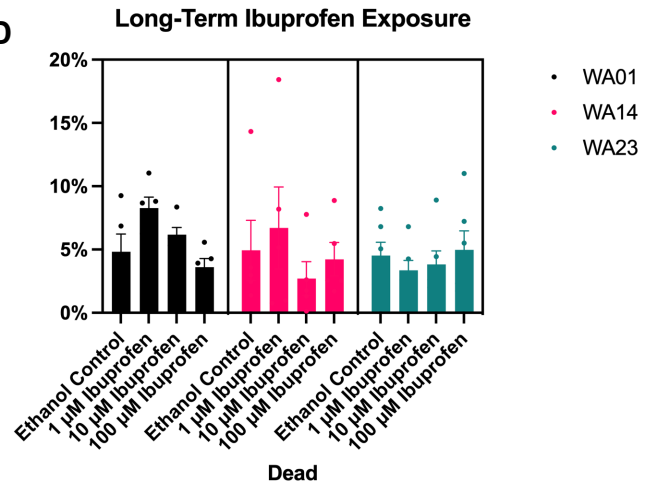


Figure 3.8. Long-term ibuprofen exposure does not alter the cell viability of spermatogenic cells derived from human male ESCs. Graphical representation showing that exposure to 1 μM , 10 μM , or 100 μM ibuprofen from Day 1 to Day 10 does not alter the viability of WA01, WA14, or WA23 human ESCs differentiated in *in vitro* spermatogenic conditions in comparison to a 0.1% ethanol-only vehicle control. A total of 5,000 events were acquired, with five replications ($n = 5$) performed for each drug treatment. Significant alterations in the mitochondrial membrane potential were determined by using a two-tailed Student's *t*-test, where * is $p < 0.05$, ** is $p < 0.01$, and *** is $p < 0.001$. Each bar represents the mean \pm SEM.

3.4 RESULTS: LONG-TERM NAPROXEN EXPOSURE ALTERS THE CELL CYCLE IN ONE CELL LINE DIFFERENTIATED IN IN VITRO SPERMATOGENIC CULTURES, BUT CHRONIC IBUPROFEN EXPOSURE DOES NOT IMPACT THE CELL CYCLE

Spermatogenic cells maintain genomic integrity through cell cycle checkpoints, which determine whether cells will remain in a state of arrest at the checkpoint or proceed through the cell cycle [243]. Deleterious effects during DNA replication, chromosomal segregation, or other forms of DNA mutations can lead to cell death or cancer [244]. Environmental exposures that disrupt these processes can alter the cell cycle, providing vital information regarding cell health. However, information regarding the effects of naproxen and ibuprofen on the cell cycle during human spermatogenesis is limited.

Ibuprofen induced cell cycle arrest at the S phase of BV-2 cells (mouse microglial cell line) [243], and cell proliferation of human glioblastoma cells was altered through ibuprofen-induced G0/G1 cell cycle arrest [245]. Additionally, ibuprofen and naproxen prevented new neuronal cell cycle events from occurring in a transgenic mouse model of Alzheimer's disease [246]. Here, we examined whether plasma levels of naproxen and ibuprofen affect the cell cycle of human spermatogenic cells using our *in vitro* human spermatogenesis model [12, 59, 62, 64, 65]. We assessed the cell cycle of spermatogenic cells in our model using propidium iodide to detect cells at different cell cycle stages based on DNA content supplied by the Muse[®] Cell Cycle Kit (Luminex). We generated flow cytometry analyses reporting the percentage of haploid cells and cells in the G0/G1

phase, S phase, and G2/M phase in our *in vitro* spermatogenic cells treated with naproxen and ibuprofen, respectively (Figure 3.9 and 3.12).

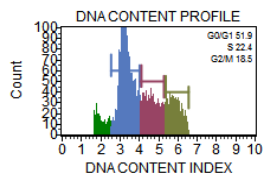
Here we report that long-term naproxen exposure significantly increased the percentage of cells in the G0/G1 phase of the cell cycle (Figure 3.10 A) with a significant simultaneous decrease of cells in the S phase (Figure 3.10 B) in WA01 human ESCs differentiated in *in vitro* spermatogenic conditions exposed to 400 μ M naproxen. There were similar trends in the G0/G1, S, and G2/M phases of the WA14 and WA23 human cell lines, but these results were not significant. In contrast, long-term ibuprofen exposure did not alter the cell cycle of human ESCs differentiated in *in vitro* spermatogenic conditions (Figure 3.13 A-C); however, we did observe an increased percentage of cells in the S phase with a subsequent reduction of the percentage of cells in G2/M phase, but these results were not significant.

Since spermatogenesis results in the production of haploid spermatids, and both naproxen and ibuprofen have been shown to have mixed results on animal sperm counts (reviewed in [17]), we wanted to assess the impacts of both NSAIDs on our *in vitro*-derived haploid spermatid-like cells. Here we report that long-term naproxen exposure significantly increased the percentage of haploid spermatids in the WA23 human ESCs differentiated in *in vitro* spermatogenic conditions exposed to 400 μ M naproxen (Figure 3.11). It is important to note that this increase in haploid cells seen in the naproxen-exposed cells was not likely due to an increase in meiosis leading to the generation of more haploid spermatids. Instead, the increased percentage of haploid cells likely increased due to spermatogonia or primary spermatocytes undergoing cell death, resulting in more haploid cells present in our mixed spermatogenic cell cultures [12];

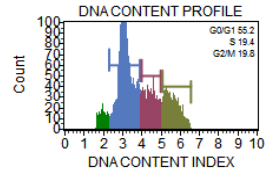
however, further experiments are needed to determine what cell population may be a direct target of naproxen exposure. Interestingly, long-term ibuprofen exposure significantly decreased the percentage of haploid spermatids in the WA23 human ESCs differentiated in *in vitro* spermatogenic conditions exposed to 10 μ M ibuprofen (Figure 3.14). These results suggest that the spermatids, a highly sensitive cell population from our mixed spermatogenic cells may be sensitive to NSAID toxicity; however, additional studies are needed to explore this phenotype further.

Overall, these analyses show that human spermatogenic cells may be more susceptible to naproxen-induced toxicity than to ibuprofen by directly altering the mitochondrial membrane potential and affecting cell viability. Although the toxic results appear to be cell lineage-specific, with the WA23s being the more susceptible to damage, the overall results appear minimal. Thus, it would be beneficial for future studies to determine if naproxen or ibuprofen alters the expression of spermatogenic-related genes and subcellular processes, if these toxicity-related phenotypes can be rescued, and if different NSAID classes have the same effects on *in vitro* human spermatogenesis.

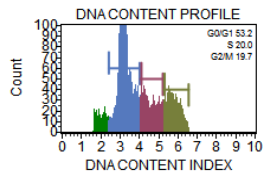
A WA01



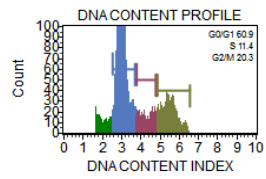
Water Control



Naproxen 4 µM

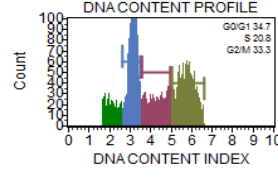


Naproxen 40 µM

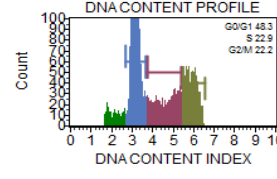


Naproxen 400 µM

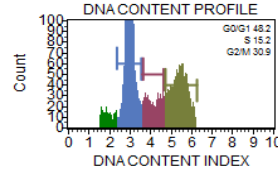
B WA14



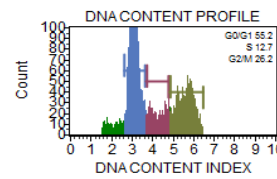
Water Control



Naproxen 4 µM

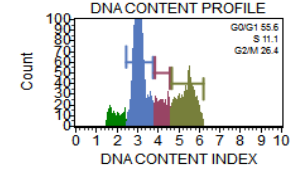


Naproxen 40 µM

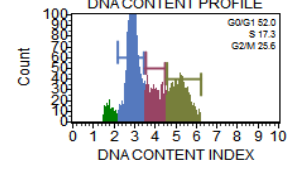


Naproxen 400 µM

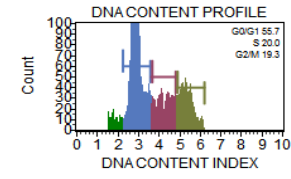
C WA23



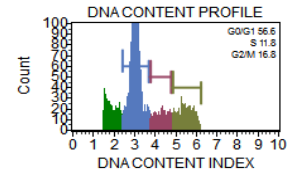
Water Control



Naproxen 4 µM



Naproxen 40 µM



Naproxen 400 µM

Figure 3.9. Flow cytometry plots for long-term naproxen-treated spermatogenic cells derived from human male ESCs for cell cycle data. Flow cytometry analyses of the cell cycle profiles following long-term naproxen exposure. These plots indicate the percent of cells in the G0/G1 phase, the percent of cells in the S phase, and the percent of cells in the G2/M phase. The green peak corresponds to the haploid phase, the blue peak corresponds G0/G1 phase, the purple peak corresponds to the S phase, and the beige peak corresponds to the G2/M phase.

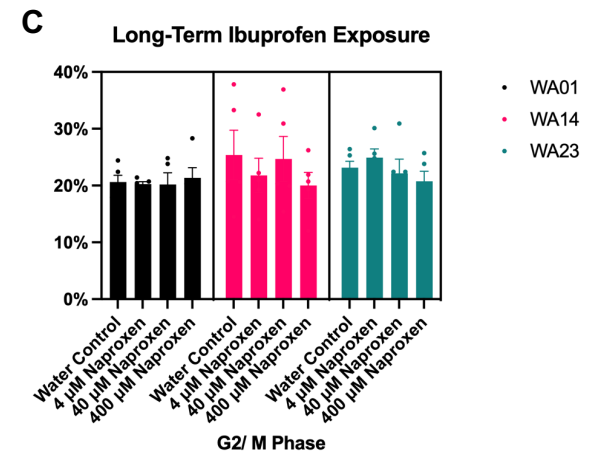
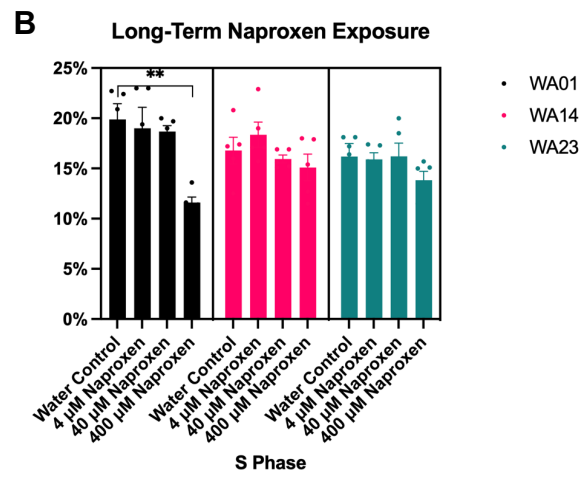
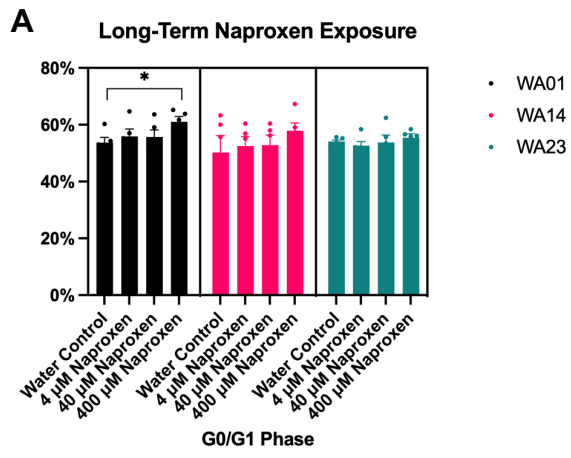


Figure 3.10. Long-term naproxen exposure impacts the cell cycle in spermatogenic cells derived from human male ESCs. Graphical representation shows that exposure to 400 μ M naproxen from Day 1 to Day 10 alters the cell cycle profiles of actively dividing WA01 human ESCs differentiated in *in vitro* spermatogenic conditions compared to the water-only vehicle control. A total of 5,000 events were acquired, with five replications ($n = 5$) performed for each drug treatment. Significant alterations in the mitochondrial membrane potential were determined by using a two-tailed Student's *t*-test, where * is $p < 0.05$, ** is $p < 0.01$, and *** is $p < 0.001$. Each bar represents the mean \pm SEM.

Long-Term Naproxen Exposure

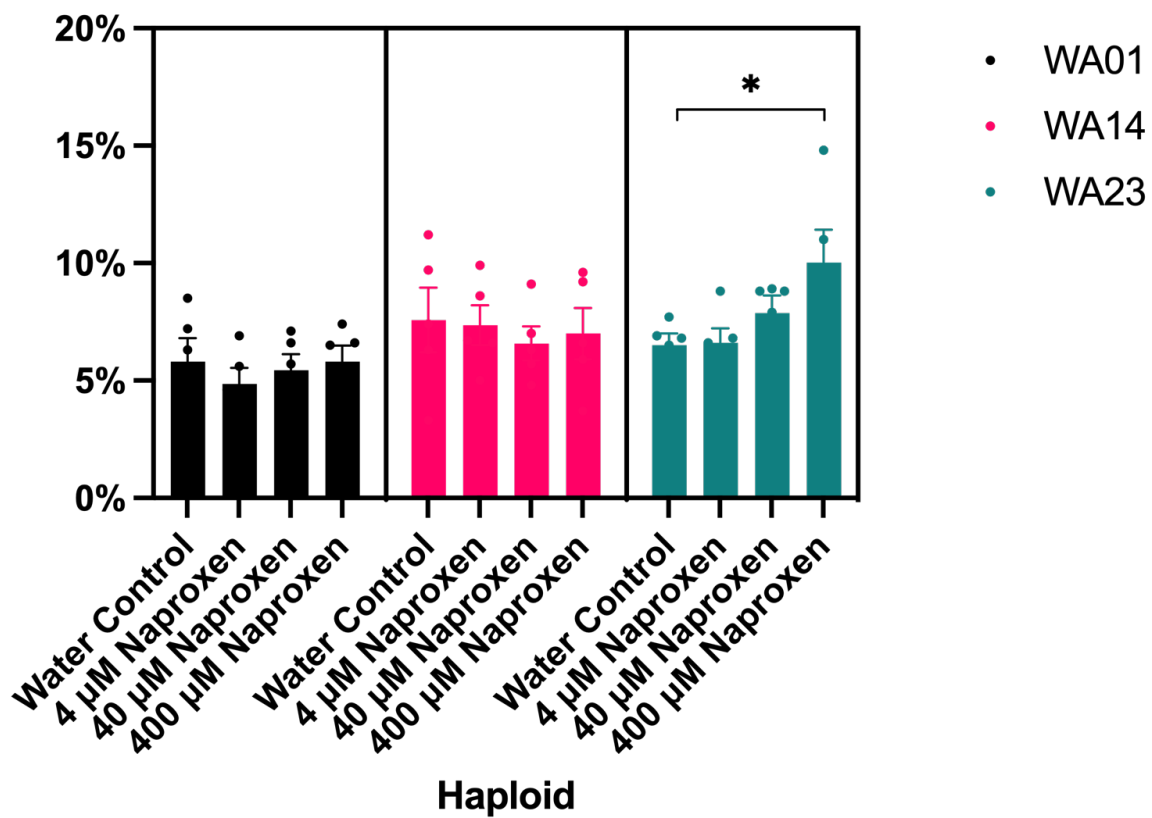
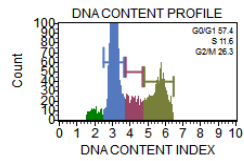


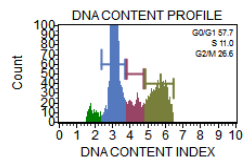
Figure 3.11. Long-term naproxen exposure does not impact the viability of haploid cells differentiated in spermatogenic conditions derived from human male ESCs.

Graphical representation shows that 400 μ M naproxen increases the percentage of haploid cells in the WA23 human ESCs differentiated in *in vitro* spermatogenic conditions compared to the water-only vehicle control. A total of 5,000 events were acquired, with five replications ($n = 5$) performed for each drug treatment. Significant alterations in the mitochondrial membrane potential were determined by using a two-tailed Student's *t*-test, where * is $p < 0.05$, ** is $p < 0.01$, and *** is $p < 0.001$. Each bar represents the mean \pm SEM.

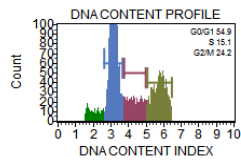
A WA01



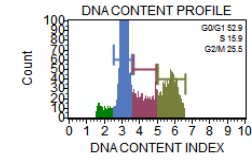
Ethanol Control



Ibuprofen 10 μM

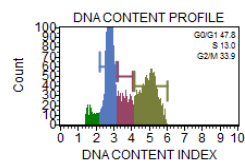


Ibuprofen 1 μM

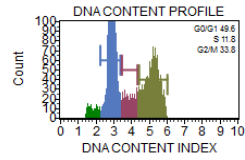


Ibuprofen 100 μM

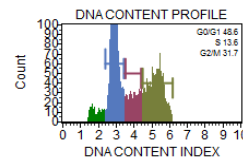
B WA14



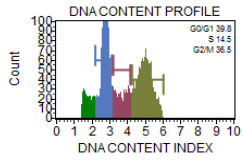
Ethanol Control



Ibuprofen 10 μM

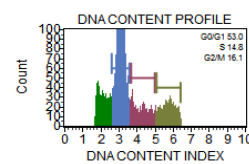


Ibuprofen 1 μM

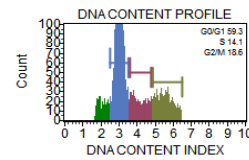


Ibuprofen 100 μM

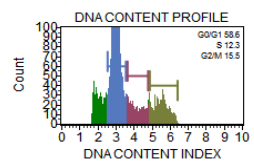
C WA23



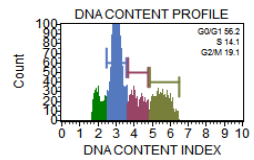
Ethanol Control



Ibuprofen 10 μM



Ibuprofen 1 μM



Ibuprofen 100 μM

Figure 3.12. Flow cytometry plots for long-term ibuprofen-treated spermatogenic cells derived from human male ESCs for cell cycle data. Flow cytometry analyses of the cell cycle profiles following long-term ibuprofen exposure. These plots indicate the percent of cells in the G₀/G₁ phase, the percent of cells in the S phase, and the percent of cells in the G₂/M phase. The green peak corresponds to the haploid phase, the blue peak corresponds G₀/G₁ phase, the purple peak corresponds to the S phase, and the beige peak corresponds to the G₂/M phase.

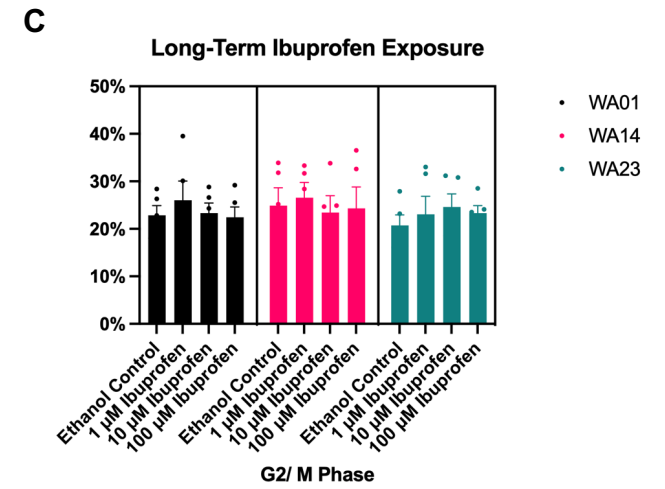
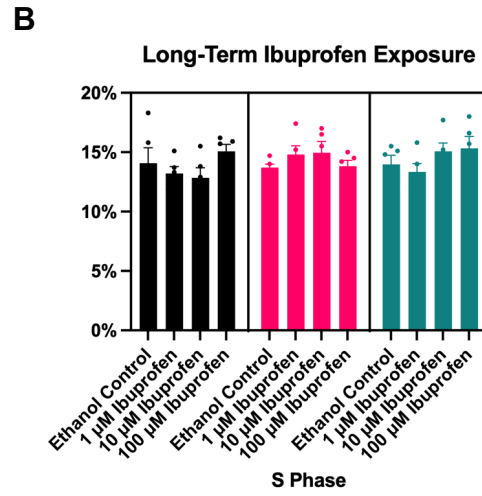
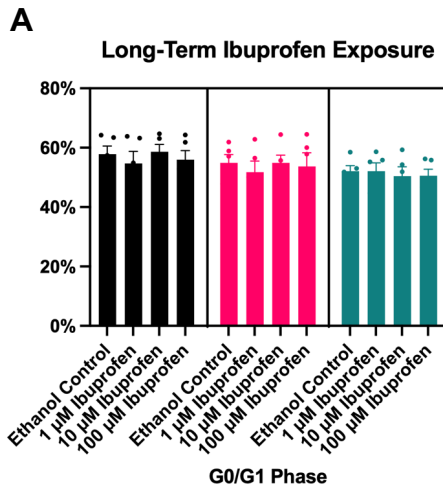


Figure 3.13. Long-term ibuprofen exposure does not impact the cell cycle in spermatogenic cells derived from human male ESCs. Graphical representation showing that exposure to 1 μM , 10 μM , or 100 μM ibuprofen from Day 1 to Day 10 does not alter the cell cycle profiles of actively dividing WA01, WA14, or WA23 human ESCs differentiated in *in vitro* spermatogenic conditions in comparison to the 0.1% ethanol-only vehicle control. A total of 5,000 events were acquired, with five replications ($n = 5$) performed for each drug treatment. Significant alterations in the mitochondrial membrane potential were determined by using a two-tailed Student's *t*-test, where * is $p < 0.05$, ** is $p < 0.01$, and *** is $p < 0.001$. Each bar represents the mean \pm SEM.

Long-Term Ibuprofen Exposure

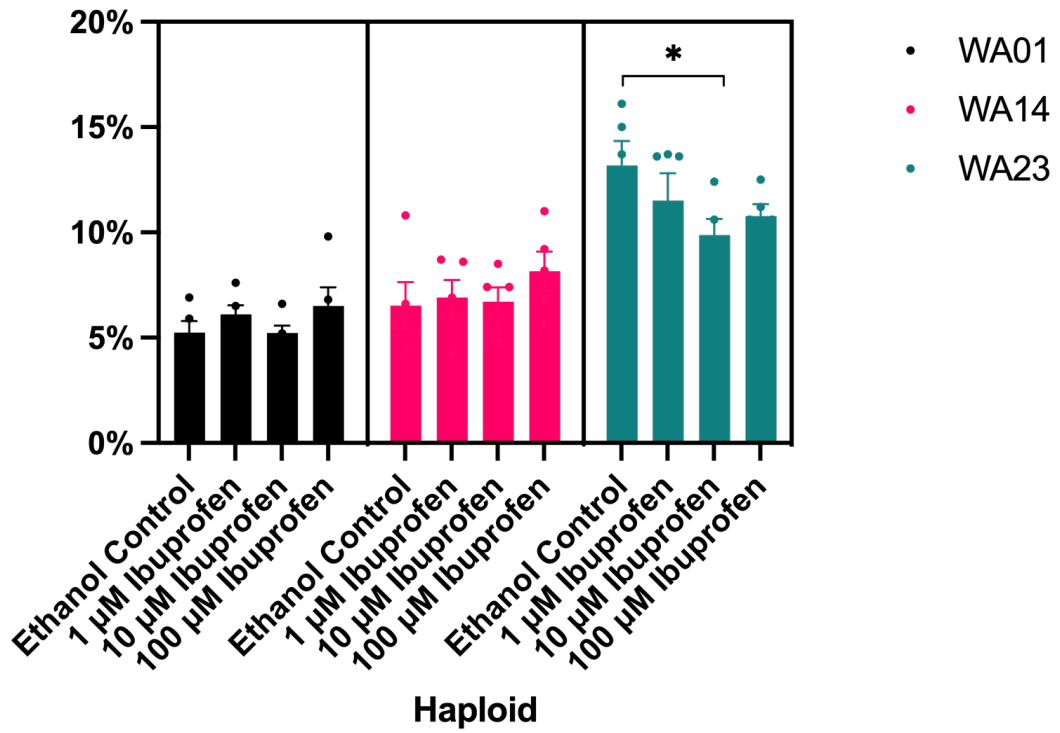


Figure 3.14. Long-term ibuprofen exposure impacts the viability of haploid cells differentiated in spermatogenic conditions derived from human male ESCs.

Graphical representation shows that 10 μ M ibuprofen decreases the percentage of haploid cells in WA23 human ESCs differentiated in *in vitro* spermatogenic conditions compared to a 0.1% ethanol-only vehicle control. A total of 5,000 events were acquired, with five replications ($n = 5$) performed for each drug treatment. Significant alterations in the mitochondrial membrane potential were determined by using a two-tailed Student's *t*-test, where * is $p < 0.05$, ** is $p < 0.01$, and *** is $p < 0.001$. Each bar represents the mean \pm SEM.

3.5 DISCUSSION

Despite the widespread and increasing usage of NSAIDs among reproductive-aged men, and that these drugs and their metabolites are released into the environment and often detected in wastewater, surface water, and drinking water, although at a much lower concentration than the therapeutic dose [219, 247-253] exposing the general population to an uncontrolled low dose, limited studies exist on the potential adult male human reproductive health effects (reviewed in [17]). In studies assessing the impacts of NSAIDs on human male fertility, some classes of NSAIDs have been associated with alterations in male hormones [92, 254, 255]. However, no direct effects on human spermatogenesis have been assessed.

Here, we investigated the direct impacts of naproxen and ibuprofen on human *in vitro* spermatogenic cell lineages. Although cell line-specific, we report that naproxen exposure impacts the viability of *in vitro* human spermatogenic cells at the lowest concentration of 4 μM during the ten days of treatment, with further alterations in the mitochondrial membrane potential to support this observation. Accordingly, there is an increase in the percentage of cells in the G0/G1 phase with a corresponding decrease in the S phase of the cell cycle, possibly indicating that 400 μM naproxen causes the cells to arrest. Therefore, naproxen exposure may alter cell survival, metabolism, and growth, as seen in other cell lines such as human urinary bladder cancer and rat osteoblasts [256, 257]. This finding suggests that, although unlikely, males who chronically take naproxen could experience a decrease in their sperm production; however, further studies are needed to link naproxen therapy with infertility.

Interestingly, ibuprofen had more subtle effects on the human *in vitro* spermatogenic cell lineages. We report here that although cell line specific, ibuprofen generally increases the percentage of cells undergoing apoptosis and subtly increases the percentage of cells in the G2/M phase. These results reveal that naproxen and ibuprofen may have different mechanisms of toxicity. Overall, the results from these experiments indicate that different genetic backgrounds may have different responses to the same NSAIDs, highlighting the complexity of how genetics plays a role in toxicity.

In conclusion, the results from this study using our *in vitro* human stem cell-based model of spermatogenesis suggest that naproxen and ibuprofen therapy have minimal effects on human spermatogenesis. Although this study did not evaluate steroidogenesis and the viability of the somatic cells (e.g., Leydig and Sertoli cells), our results highlight the need for more information regarding how naproxen, ibuprofen, and other classes of NSAIDs may directly alter human spermatogenesis and male fertility. As semen parameters continue to decline in men across the world, future studies are highly recommended to determine the potential impact of NSAIDs on male fertility, especially as the general public is exposed to these medications daily and more men are using these drugs than ever before.

3.6 MATERIALS AND METHODS

Cell culture, Spermatogenic differentiation of ESCs, and NSAID treatment

Cell Culture: National Institutes of Health-approved WA01 (H1, WiCell), WA14 (H14, WiCell), and WA23 (H23, WiCell) male, human embryonic stem cell lines (ESCs) were cultured and maintained in mTeSR Plus media (STEMCELL Technologies) on Matrigel® (Corning® Life Sciences) as previously described [12, 62, 64, 65]. Briefly, the

cells were cultured in 10 cm dishes and refed with mTeSR™ plus every other day for five to seven days. The hESCs were passaged using either Dispase in DMEM/F12 (STEMCELL Technologies) or ReLeSR™ (STEMCELL Technologies) when the cell density reached approximately 80% confluency and plated onto Matrigel® (Corning® Life Sciences) coated plates [12, 62, 64, 65]. Routine karyotyping was performed every four to six months through WiCell's karyotyping core service to ensure proper chromosomal content and lack of translocation. The Easley lab performed routine mycoplasma contamination every six months to ensure the cell lines were free from contamination.

Spermatogenic differentiation of ESCs: Direct differentiation into spermatogenic lineages was performed as previously described [12, 59, 62, 64, 65]. Briefly, differentiating cells were maintained on mitomycin C-inactivated mouse STO-feeder cells and maintained in mouse spermatogonial stem cell (SSC) medium containing the following: MEMalpha + L-glutamine (ThermoFisher), 0.2% Bovine Serum Albumin (MilliporeSigma), 0.2 mg/mL ascorbic acid (MilliporeSigma), 0.2% Chemically Defined Lipid Mixture (Millipore Sigma), 5 µg/mL insulin (MilliporeSigma), 10 µg/mL (MilliporeSigma), 50 µM β-mercaptoethanol (MilliporeSigma), 30 nM sodium selenite (MilliporeSigma), 10 mM HEPES (Gibco), 0.5x Penicillin/Streptomycin (Gibco), 20 ng/mL glial-derived neurotrophic factor (GDNF, Peprotech), and 1 ng/mL human basic fibroblast growth factor (hbFGF, Peprotech) for 10 days. The SSC media was gassed with a blood gas mixture consisting of 5% carbon dioxide, 5% oxygen, and balanced with 90% nitrogen for 30 seconds, and inverted several times to mix following initial media preparation. Approximately 250,000 STOs cultured in Fibroblast medium were added to

each well 24 hours before passaging. After changing to the SSC medium, media changes occurred every other day for ten days.

NSAID treatment: Since the testicular concentrations of NSAIDs in adult men are unknown, we estimated the amount of exposure to the testis using previously established pharmacokinetic data. The cells were treated with naproxen (MilliporeSigma) or ibuprofen (MilliporeSigma) at concentrations reflecting plasma levels in healthy adult men ranging from 10^{-4} to 10^{-5} M [95, 238]. Differentiating spermatogonial stem cell-like cells were exposed to naproxen at concentrations of 4 μ M, 40 μ M, or 400 μ M [238] or ibuprofen at concentrations of 1 μ M, 10 μ M, or 100 μ M [95]. The cells were maintained in SSC media with naproxen dissolved in water and ibuprofen dissolved in 0.1% ethanol or water- or ethanol-only vehicle controls, and a 1:1,000 dilution of bFGF and GDNF beginning on Day 1 of the differentiation to mimic long-term usage. A minimal volume of ethanol was used, which was unlikely to cause cell death and have negligible effects on spermatogenic differentiation and products. A 100 mM ibuprofen and 400 mM chemical stock were prepared, stored at room temperature, and protected from light. On Day 10, the cells were briefly rinsed with 1X DPBS without calcium or magnesium (ThermoFisher), collected using TrypLE™ Express (ThermoFisher), and analyzed according to the protocols described below.

Cell viability and apoptosis

By utilizing the Muse® Annexin V and Dead Cell Assay Kit (Luminex), cell viability was assessed for cells treated with naproxen or ibuprofen by measuring the percentage of apoptotic cells in the cultures by staining unfixed cells with Annexin V and 7-AAD as per manufacturer's instructions in preparation for flow cytometry. Each

sample was analyzed on the Muse[®] benchtop flow cytometer (MilliporeSigma) and analyzed at 5,000 events for five replications ($n = 5$) per analgesic concentration and water- or ethanol-only control.

Mitochondrial membrane potential

The mitochondrial membrane potential was assessed using the Muse[®] MitoPotential Kit (Luminex) to stain unfixed cells exposed to naproxen or ibuprofen with the supplied dye and 7-AAD as per the manufacturer's instructions to prepare the samples for flow cytometry. Each sample was analyzed on the Muse[®] benchtop flow cytometer (MilliporeSigma) and analyzed at 5,000 events for five replications ($n = 5$) per analgesic concentration and water- or ethanol-only control.

Cell cycle progression and haploid cell production

The Muse[®] Cell Cycle Assay Kit (Luminex) was utilized to assess cell cycle progression and haploid spermatid production for cells treated with naproxen or ibuprofen by generating cell cycle plots containing G0/G1, S phase, G2/M, and haploid cell peaks through staining ethanol-fixed cells with propidium iodide as per manufacturer's instructions in preparation for flow cytometry. Each sample was run on the Muse[®] benchtop flow cytometer (MilliporeSigma) and analyzed at 5,000 events for five replications ($n = 5$) per analgesic concentration and water- or ethanol-only control.

Statistical analysis

The statistical analyses for cell viability, mitochondrial membrane potential, and cell cycle were performed in GraphPad Prism software (version 9). Significant differences in samples compared to water-only control for naproxen or ethanol-only control for ibuprofen were determined using a Student's t-test, where * is $p < 0.05$, ** is

$p < 0.01$, and *** is $p < 0.0001$ to determine which treatment group was statistically different from the control. The data were expressed as the mean \pm SEM.

CHAPTER 4

IBUPROFEN AND NAPROXEN EXPOSURE ALTERS THE FUNCTION OF
THE NON-HUMAN PRIMATE BLOOD-TESTIS BARRIER ²

² Krista M. Symosko Crow, In Ki Cho, R. Clayton Edenfield, Kristen F. Easley, Ana Planinić, Nagham Younis, Elizabeth Waters, James S. McClellan, Amanda Colvin Zielen, Kylie Tager, Carlos Castro, Calvin Simerly, Gerald Schatten, Kyle Orwig, Davor Ježek, Michael Koval, Charles A. Easley IV. To be submitted to *JCI Insights*.

4.1 ABSTRACT

Semen parameters, including sperm counts, have rapidly declined in men across the globe over the last five decades. Although this decline has remained largely unexplained, environmental exposures, such as the increasing usage of non-steroidal anti-inflammatory drugs (NSAIDs), could provide one possible explanation. Recent studies have linked NSAID usage with declining male fertility, but the mechanisms by which these analgesics impact male fertility, including the Blood-testis barrier, remain largely uncharacterized. It is well known that NSAID therapy causes severe complications to the gastrointestinal mucosa following oral administration. However, it is unknown whether NSAID usage alters other tissue barriers such as the Blood-testis barrier. In the male reproductive tract, the Blood-testis barrier is a specialized structure that divides the seminiferous epithelium into the apical (adluminal) and basal compartments. This barrier structure (1) regulates the entry of nutritional substances, vital molecules, and toxicants into the adluminal section where spermiogenesis takes place, (2) separates the cells undergoing spermatogenic renewal, proliferation, and differentiation and those that are undergoing meiosis and maturation, and (3) creates an immunological barrier by blocking an immune response from occurring during spermatogenesis and shielding the developing spermatids from anti-sperm antibodies. If the blood-tissue barrier function is compromised, the patient could become infertile. Utilizing non-human primate primary Sertoli cells, we show that short-term naproxen and ibuprofen treatment increased the transepithelial electrical resistance, reflecting a strengthening of the Sertoli cell junctions.

Furthermore, RNA-sequencing revealed naproxen and ibuprofen treatment altered the expression of genes that contribute to maintaining the Blood-testis barrier and apical junction genes important for proper Blood-testis barrier function. Genes that were significant differentially expressed following ibuprofen exposure were enriched in human phenotypic abnormalities associated with male factor infertility. Together, these results suggest that short-term naproxen and ibuprofen treatment compromises the function of the Blood-testis barrier by disrupting the integrity of the Sertoli cell junctions. These disruptive Blood-testis-barrier effects highlight the potential of NSAID involvement in male factor infertility.

4.2 INTRODUCTION

Over the last several decades, numerous studies reported an increased number of male infertility cases, sparking a global crisis [10]. While genetic and several environmental factors are associated with impaired fertility, the increasing usage of medications may disrupt sperm production, leading to temporary or persistent infertility [34]. Over-the-counter (OTC) analgesics, such as ibuprofen and naproxen, are among the most frequently used pharmaceutical compounds worldwide [182]. Increasing evidence from recent years shows heavier usage of common non-steroidal anti-inflammatory drugs (NSAIDs) by reproductive-aged men [17, 34]. According to a 2016 survey on NSAID usage, 90% of reproductive-aged (≥ 18) men in the United States have reported using ibuprofen for one week, and 11% of these users exceeded the daily limit [258], making NSAID therapy especially relevant for future fathers. Additionally, NSAID use is particularly interesting because evidence shows OTC pain-reliever usage increases with age, especially by men entering or in their 30s [189]. However, information about the

reproductive toxicity of these regularly consumed NSAIDs is lacking, even though the data may be clinically relevant.

Given the increased usage of NSAIDs around the globe, evidence from recent years shows that NSAID usage can generate negative endocrine and reproductive effects in both human and animal model systems [89, 95, 239, 259-261]. Nonetheless, no in-depth studies have analyzed the impact of two mild analgesics, naproxen, and ibuprofen, on the human Blood-testis barrier (BTB). Produced by Sertoli cells, often called “nurse cells,” this barrier regulates the entry of nutritional substances, vital molecules, and harmful toxicants into the apical compartment where post-meiotic germ cell development occurs. This specialized structure also plays a crucial role in the differentiation of spermatogonia into spermatids (reviewed in [112]).

Therefore, in this study, we focused on how plasma levels of naproxen and ibuprofen affect the function of the BTB. Because of the inherent challenges in identifying the reproductive toxicity potential of drugs in the adult human, we performed a unique combination of approaches using non-human primate (NHP) primary Sertoli cells: (1) an *in vitro* BTB model, (2) standard reproductive toxicity assays, and (3) whole transcriptome mRNA-sequencing. These results revealed that naproxen and ibuprofen may impede male fertility by compromising the integrity of the Sertoli cell junctions by modifying the expression of junctional proteins.

4.3 RESULTS: SHORT-TERM NSAID TREATMENT ALTERS THE TESTICULAR BARRIER FUNCTION WITHOUT AFFECTING THE VIABILITY OF IN VITRO PRIMARY SERTOLI CELLS

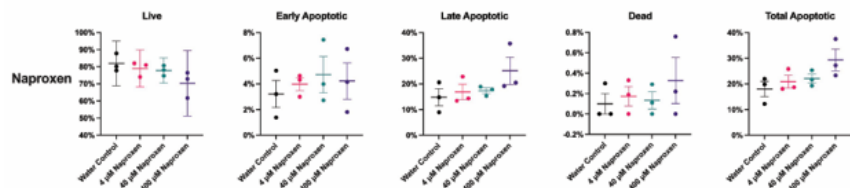
This study aimed to determine the effect of short-term NSAID treatment, such as naproxen and ibuprofen, on the function of NHP primary Sertoli cells *in vitro*. Recently, evidence suggested that these two NSAIDs are among the top 12 most used medications worldwide [186, 262]. However, studies examining the impact of NSAIDs on semen parameters have generally been inconclusive, making it more challenging to understand the overall effects on male fertility [17, 98, 263, 264]. To determine whether either NSAIDs had a deleterious effect on Sertoli cell viability (Figure 4.1 A-B) or altered the mitochondrial potential (Figure 4.1 C-D), we examined confluent monolayers of NHP primary Sertoli cells treated with plasma serum levels of naproxen or ibuprofen for three consecutive days. Neither naproxen nor ibuprofen exposure affected the cell viability or caused mitochondrial dysfunction (Figure 4.1).

Next, we examined the effects of short-term naproxen and ibuprofen on the barrier function of primary NHP Sertoli cells cultured on Transwell semi-permeable supports by measuring the transepithelial electrical resistance (TER), or the instantaneous transcellular permeability to ions which occurs on a microsecond time scale, and the paracellular flux of various sized solutes which occurs over a time scale of minutes to several hours [166, 265]. We determined that both naproxen and ibuprofen exposure altered the testicular epithelial barrier function by TER (Figure 4.2 A and B). The Sertoli cells showed an increase in TER on Day 2 following 400 μ M naproxen treatment and a dose-dependent increase on Day 3 ($n = 12$; Figure 4.2 A). Treatment with 10 μ M

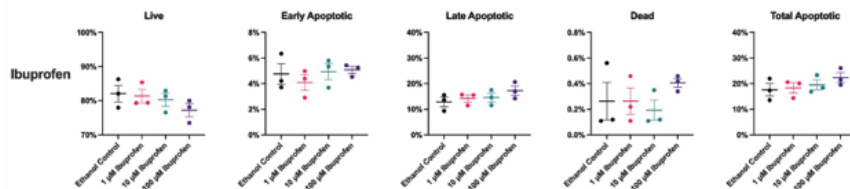
ibuprofen resulted in a decrease in TER on Day 2 but an increase in TER on Day 3 ($n = 12$; Figure 4.2 B). Interestingly, neither naproxen nor ibuprofen exposure altered the paracellular diffusion of the two macromolecule fluorescent probes of differing sizes (Figure 4.3). Given the effects on barrier function, we focused our additional studies on gene expression analysis.

**NHP Sertoli Cell
Three Day NSAID Exposure
Annexin V**

A

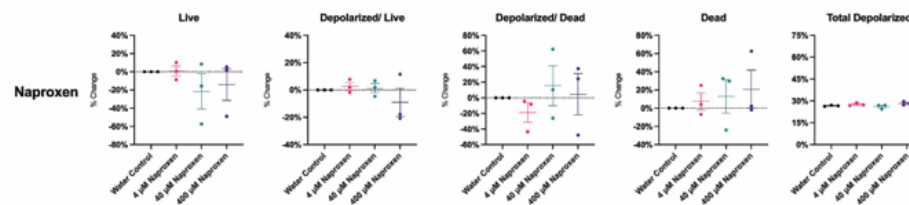


B



**NHP Sertoli Cell
Three Day NSAID Exposure
Mitochondrial Membrane Potential**

C



D

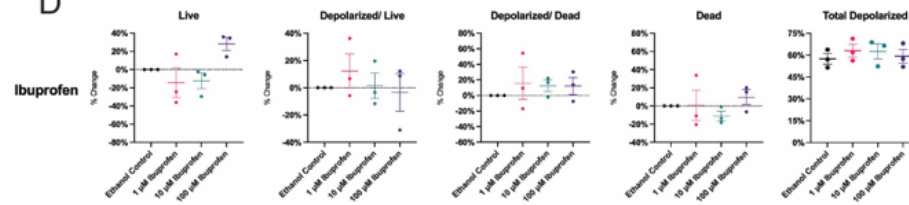


Figure 4.1. Short-term NSAID treatment does not induce apoptosis or alter mitochondrial membrane potential of non-human primate primary Sertoli cells in vitro. Short-term NSAID treatment does not alter viability or mitochondrial membrane potential of non-human primate primary Sertoli cells. The Sertoli cells were treated for three consecutive days with 4 μ M, 40 μ M, and 400 μ M naproxen and 1 μ M, 10 μ M, and 100 μ M ibuprofen prior to the Annexin V (**A-B**) and Mitochondrial membrane potential assays (**C-D**). (**A-B**) Graphical representation showing that exposure to naproxen (**A**) or ibuprofen (**B**) does not induce apoptosis in the non-human primate primary Sertoli cells. (**C-D**) Graphical representation showing that exposure to naproxen (**C**) or ibuprofen (**D**) does not significantly decrease the mitochondrial membrane potential in the non-human primate primary Sertoli cells. A total of 1,000 events were acquired with three replications ($n = 3$) performed for each drug treatment per assay. Significant alterations in cell viability and mitochondrial membrane potential were determined by a two-tailed Student's t-test, where * is $p < 0.05$, ** is $p < 0.01$, and *** is $p < 0.001$. Each bar represents the mean \pm SEM.

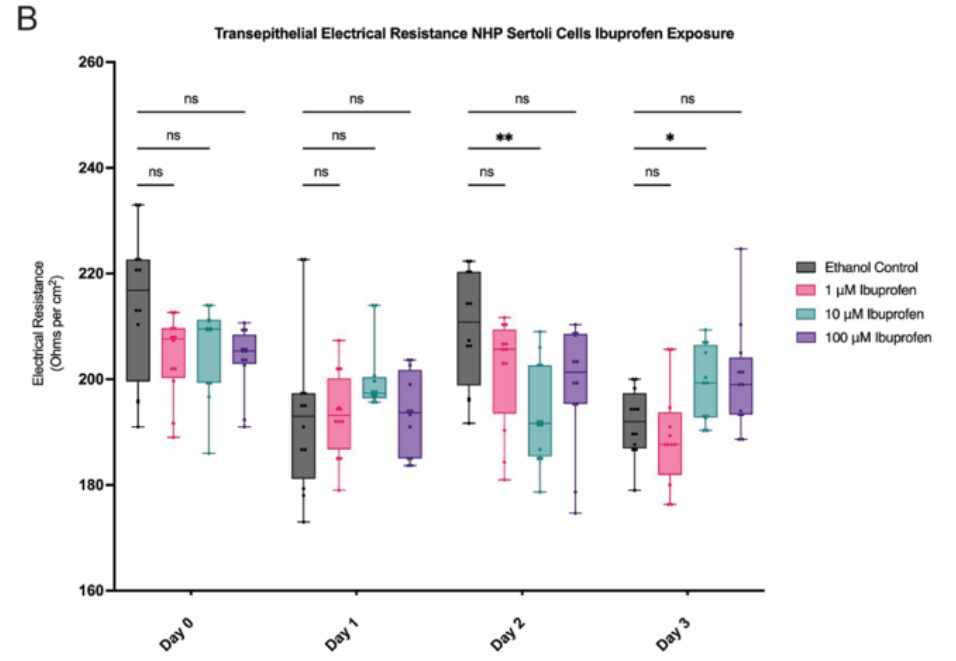
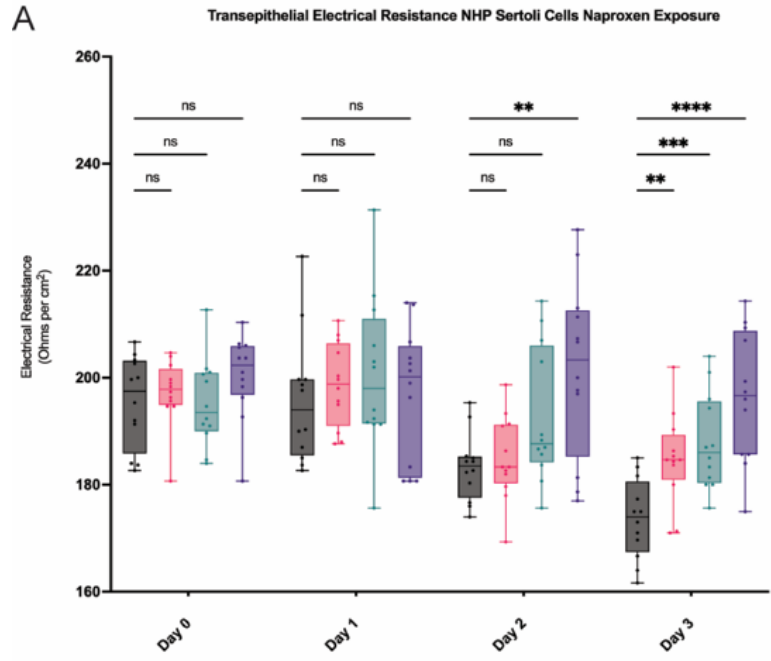


Figure 4.2. Short-term NSAID treatment alters the Transepithelial Electrical Resistance (TER) of non-human primate primary Sertoli cells in vitro. In order to measure the integrity of the Blood-testis barrier and the Sertoli cell tight junctions, transepithelial electrical resistance (TER) was measured. Short-term treatment with naproxen (**A**) and ibuprofen (**B**) at serum levels significantly increased the TER, reflecting a strengthening of the integrity of the Sertoli cell tight junctions. Twelve ($n = 12$) replicates for TER were performed for each condition. Significant alterations in TER were determined by a 2-way ANOVA with Dunnett's multiple comparisons test, where ns is not significant, * is $p < 0.05$, ** is $p < 0.01$, and *** is $p < 0.001$. Data represent the minimum and maximum values.

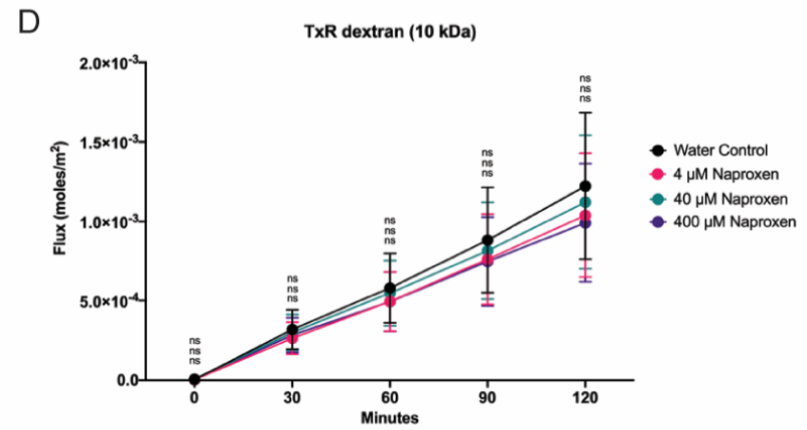
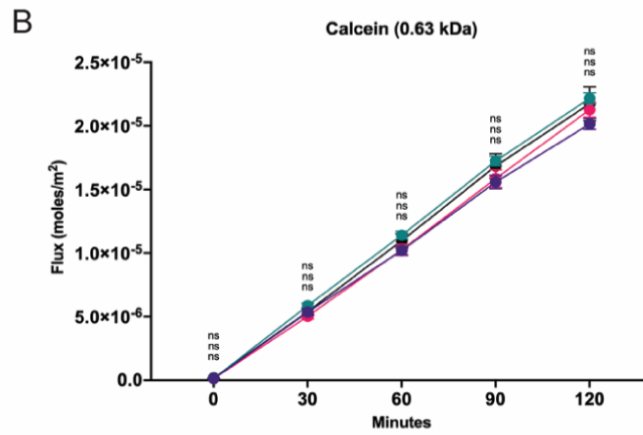
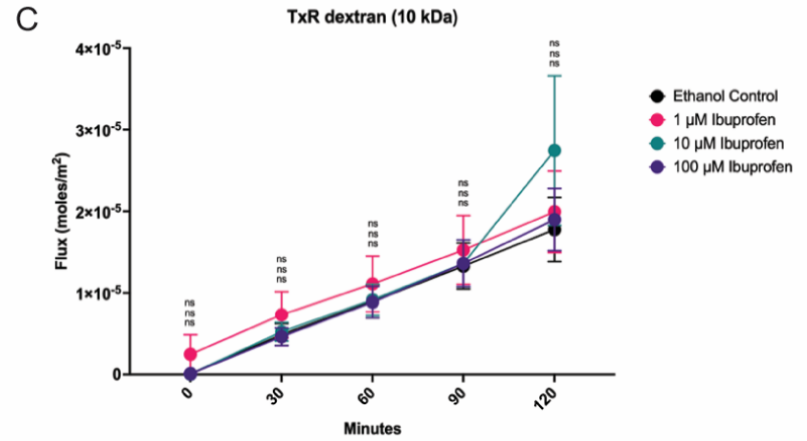
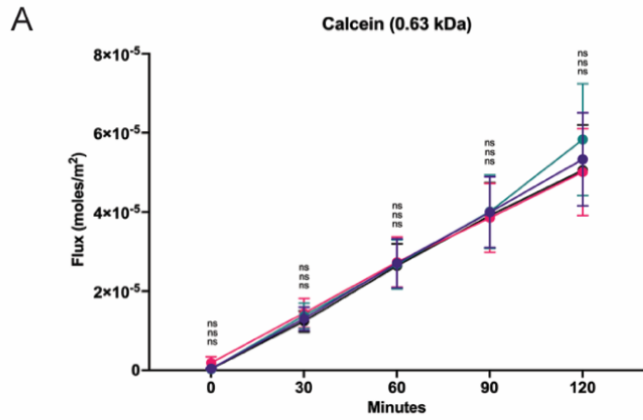


Figure 4.3. Short-term NSAID treatment does not alter the barrier permeability of non-human primate primary Sertoli cells in vitro. In order to measure the integrity of the Blood-testis barrier and the Sertoli cell tight junctions, barrier permeability was measured. **(A-D)** Short-term treatment with ibuprofen **(A, C)** and naproxen **(B, D)** did not affect the passing of calcein (0.62 kDa) or of the larger, dextran (10 kDa) molecule through the paracellular space. Eight ($n = 8$) replicates for the paracellular flux assays were performed for each condition. Significant alterations in barrier permeability were determined by a 2-way ANOVA with Dunnett's multiple comparisons test, where ns is not significant, * is $p < 0.05$, ** is $p < 0.01$, and *** is $p < 0.001$. Each point represents the mean

4.3 RESULTS: SHORT-TERM NSAID TREATMENT ALTERS THE EXPRESSION OF GENES INVOLVED IN THE BLOOD-TESTIS BARRIER FUNCTION

The BTB functions to 1) create a specialized environment that is necessary for the growth and differentiation of developing germ cells, 2) regulate the passage of vital molecules and prevent toxicant entry into the apical compartment, and 3) serve as an immunological barrier [266, 267]. Additionally, because the spermatogonia, preleptotene, and leptotene spermatocytes reside in the basal compartment, the BTB must periodically open to accommodate the passaging of these germ cells into the apical compartment for further maturation (reviewed in [123]). To date, NSAID therapy has been shown to affect other biological responses and induce cytotoxic effects by interacting with cellular membranes and altering their biomechanical properties [268], such as in the gastric mucosal barrier. Thus, we hypothesized that these functional changes in Sertoli cells would be driven by the altered expression of genes.

Using our *in vitro* barrier model system, we treated our NHP primary Sertoli cells in plasma serum levels of naproxen and ibuprofen and water- and 0.1% ethanol-only vehicle controls, respectively, isolated total RNA and performed mRNA-sequencing analyses. Both the principal component and Poisson distance plot analyses showed that 400 μM naproxen-exposed Sertoli cells are distinctly different from the 4 μM and 40 μM naproxen and water control samples (Figure 4.4 A-B). The 400 μM naproxen dose had the most significant effects, resulting in the most alterations in gene expression when compared to the water vehicle control, 4 μM , and 40 μM naproxen doses (Figure 4.4 C; Tables 6.1). Compared to the control, the 4 μM naproxen sample had 6 significant

differentially expressed genes, 4 genes which were up regulated and 2 genes which were down regulated (Figure 4.4 D), the 40 μM naproxen sample had 9 significant differentially expressed genes, 6 genes which were up regulated and 3 genes which were down-regulated (Figure 4.4 E), and the 400 μM naproxen sample had 158 significant differentially expressed genes, 53 genes which were up regulated and 105 genes which were down regulated (Figure 4.4 F), highlighting a concentration-dependent impact on gene expression. Interestingly, at 4 μM and 40 μM naproxen exposures, the gene expression profile of the Sertoli cells appeared to be similar to the water control (Figure 4.4 C).

Similar to naproxen, both the principal component and Poisson distance plot analyses showed that 100 μM ibuprofen-exposed Sertoli cells are distinctly different from the 1 μM and 10 μM ibuprofen and 0.1% ethanol control samples (Figure 4.5 A-B). The 100 μM ibuprofen dose had the most significant effects, resulting in dramatic alterations in gene expression when compared to the 0.1% ethanol control and 1 μM and 10 μM ibuprofen doses (Figure 4.5 C; Tables 6.4). Compared to the control, the 1 μM ibuprofen sample had 14 significant differentially expressed genes, 6 genes that were up regulated and 8 genes that were down regulation (Figure 4.5 D), the 10 μM ibuprofen sample had 13 significant differentially expressed genes, 4 genes which were upregulated and 9 genes which were down regulated (Figure 4.5 E), and the 100 μM ibuprofen sample had 1,567 significant differentially expressed genes, 801 genes up regulated and 766 genes down regulated (Figure 4.5 F). Interestingly, at 1 μM and 10 μM ibuprofen, the gene expression profile of the Sertoli cells appeared to be very similar to the 0.1% ethanol control (Figure 4.5 C).

Further, gene set enrichment analyses revealed several common themes among the differentially expressed genes for both naproxen and ibuprofen compared to their respective controls. We observed an enrichment of genes in our primary NHP Sertoli cells exposed to naproxen and ibuprofen for genes involved in apical junctions (M5915; Figure 4.6 A-B). A recent study revealed that the Sertoli cell tight junction barrier function can be perturbed through alterations in the production of collagen and matrix metalloprotease-9 (*MMP-9*) [269]. Here we show that although naproxen exposure did not alter the expression of collagen genes, 100 μ M ibuprofen significantly decreased the expression of several collagen genes (*COL12A1*, *COL1A1*, *COL4A2*, *COL4A4*, *COL5A2*, *COL8A1*, and *COL8A1*; Table 6.4). Both 400 μ M naproxen and 100 μ M ibuprofen altered the expression of *MMP-9* (Tables 6.1, 6.4), suggesting the Sertoli cell integrity could be compromised following NSAID therapy. Furthermore, we found both 400 μ M naproxen (*LAMA4* & *LMNB1*; Table 1) and 100 μ M ibuprofen (*LAMA2*, *LAMA3*, *LAMA4*, *LAMC1*; Table 6.4) treatments altered the expression of several laminins, which are critical in maintaining the integrity of the BTB barrier and Sertoli cell tight junctions [270].

In addition to an enrichment of genes involved in Sertoli cell tight junction barrier dynamics, we observed an enrichment of genes by ibuprofen involved in inflammatory response (M5932), androgen response (M5908), and cell junction regulation (PI3K/AKT/mTOR signaling, M5923; transforming growth factor (TGF- β) signaling, M5896; and WNT/ β -catenin signaling, M5895; [271] Figure 4.8). Interestingly, we only observed an enrichment of inflammatory response genes in our primary NHP Sertoli cells exposed to naproxen (Figure 4.7), suggesting these two drugs may alter Sertoli cell

function via different pathways. Additionally, we confirmed the mRNA-sequencing results with RT-qPCR of selected genes involved in Sertoli cell and BTB function, and inflammation response (Figure 4.9).

Among genes with a fold change of > 1.5 in either direction, STRING analysis identified *Cit* (which was down regulated by naproxen; Figure 4.10 A, Table 6.1) as a central node in the protein interaction network and a key regulator of adherens junction integrity [272]. Unlike naproxen, STRING analysis of genes enriched in primary Sertoli cells exposed to ibuprofen identified a complex network of pathways and target proteins in the protein interaction network such as *ADAMTS5* (which was up regulated by ibuprofen; Figure 4.10 B, Table 6.4) and a key regulator of adherens junction integrity and inflammation [273], as well as *AR*, *VCL*, and *MMP-9* (which were up regulated by ibuprofen) and *LAMA2* and *LAMA4* (which were down regulated by ibuprofen), all of which assist in maintaining the integrity of the BTB [274]. Together, these results suggest that alterations in the expression of genes that contribute to maintaining the BTB can alter junction dynamics in the testis.

4.3 RESULTS: IBUPROFEN EXPOSURE ENRICHES GENES IN DISEASES ASSOCIATED WITH MALE FACTOR INFERTILITY USING THE HUMAN PHENOTYPE ONTOLOGY DATABASE

We performed human phenotype ontology (HPO) analyses of genes that were significant differentially expressed in our primary NHP Sertoli cells exposed to naproxen and ibuprofen for phenotypes associated with male factor infertility. Using the HPO database, we found that 10 μ M and 100 μ M ibuprofen enriched genes in diseases associated with male factor infertility, including cryptorchidism (HP:0000028),

functional abnormality of male internal genitalia (HP:0000025), aplasia/hypoplasia of the testes (HP:0010468), and infertility (HP:0000789) (Table 4.1). Interestingly, naproxen treatment was not associated with male factor infertility phenotypes (Table 4.2). Collectively, the results from the gene set enrichment analysis show that although naproxen and ibuprofen may perturb Sertoli cell function through altering the gene expression of genes involved in different pathways, NSAID therapy may lead to a lack of mechanical, metabolic, and immunoprotective support of the germ cells by the Sertoli cells [17] and that such changes could indirectly disrupt sperm maturation and compromise male fertility.

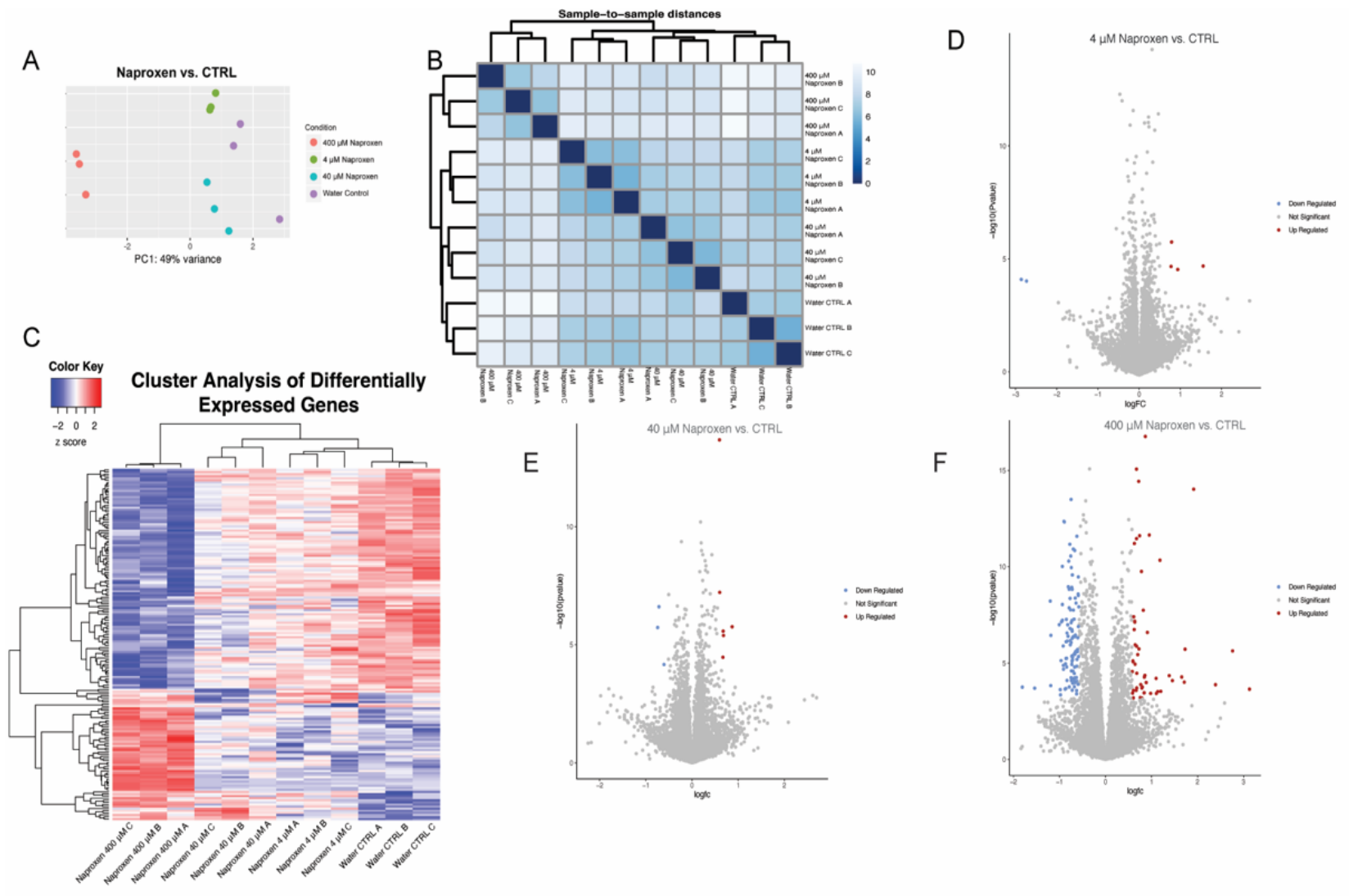


Figure 4.4. Ribonucleic acid sequencing analysis of non-human primate primary Sertoli cells exposed to naproxen in vitro. (A) Principal component analysis plot of three biological replicates after exposure to 4 μ M, 40 μ M, and 400 μ M naproxen compared to the water vehicle control. (B) Poisson distance plot showing dissimilarities among the samples based on the transcriptome profiles after exposure to 4 μ M, 40 μ M, and 400 μ M naproxen compared to the water vehicle control. (C) Hierarchical clustering of differentially expressed genes in non-human primate primary Sertoli cells exposed to 4 μ M, 40 μ M, and 400 μ M naproxen compared to the water vehicle control. (D-F) Volcano plots depicting differentially expressed genes that show \pm 1.5-fold change and p-adjusted values less than 0.01. (D) 6 genes in the 4 μ M exposure sample, 4 genes up regulated (red) and 2 genes down regulated (blue), (E) 9 genes in the 40 μ M exposure sample, 6 genes up regulated (red) and 3 genes down regulated (blue), and (F) 158 genes in the 400 μ M exposure sample, 53 genes up regulated (red) and 105 genes down regulated (blue). The heatmap (C) represents normalized gene expression by limma, normalized by each row.

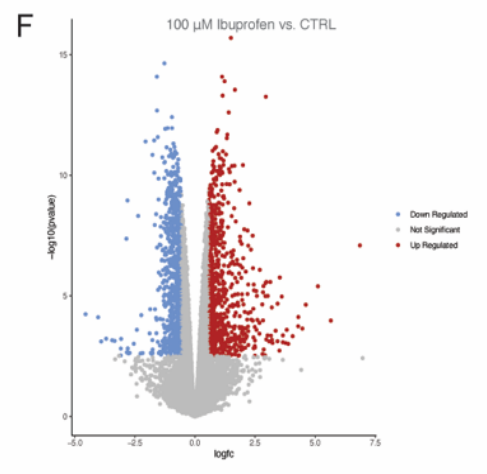
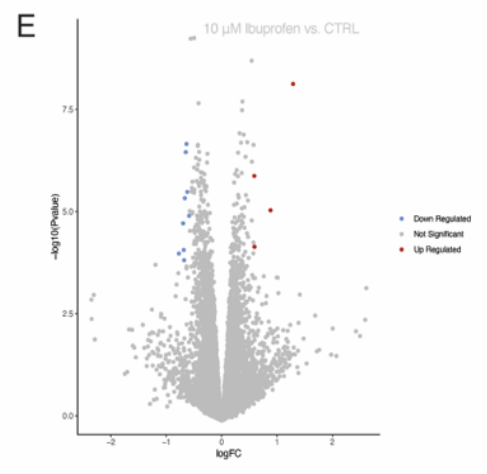
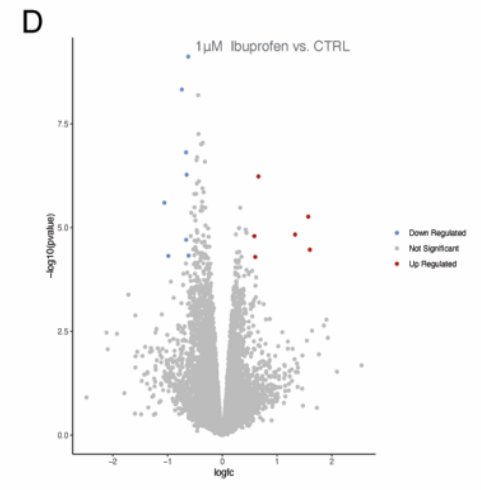
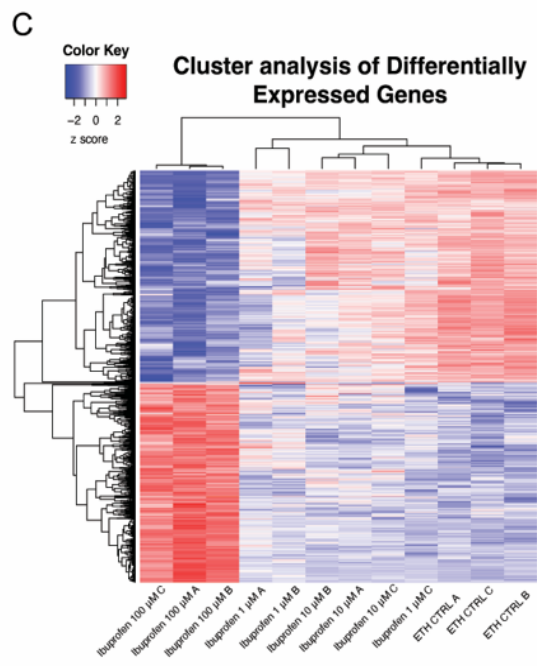
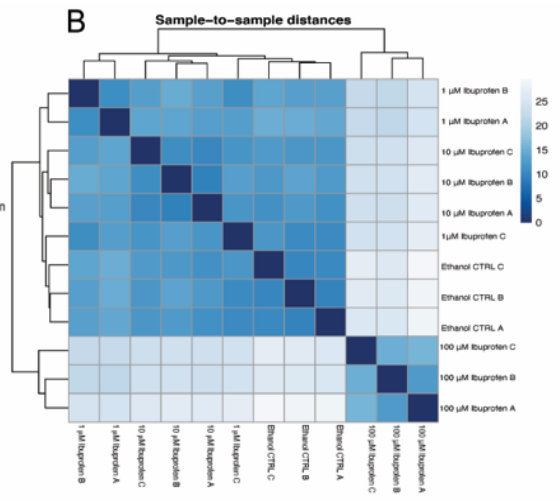
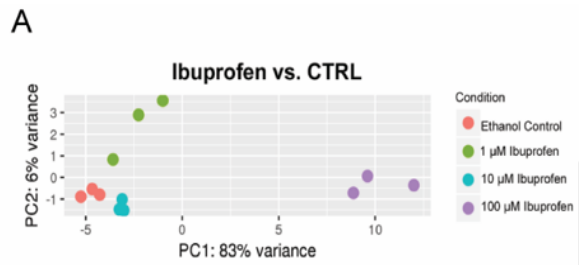


Figure 4.5. Ribonucleic acid sequencing analysis of non-human primate primary Sertoli cells exposed to ibuprofen in vitro. (A) Principal component analysis plot of three biological replicates after exposure to 1 μ M, 10 μ M, and 100 μ M ibuprofen compared to the 0.1% ethanol vehicle control. (B) Poisson distance plot showing dissimilarities among the samples based on the transcriptome profiles after exposure to 1 μ M, 10 μ M, and 100 μ M ibuprofen compared to the 0.1% ethanol vehicle control. (C) Hierarchical clustering of differentially expressed genes in non-human primate primary Sertoli cells exposed to 1 μ M, 10 μ M, and 100 μ M ibuprofen compared to 0.1% ethanol vehicle control. (D-F) Volcano plots depicting differentially expressed genes that show \pm 1.5-fold change and p-adjusted values less than 0.01. (D) 14 genes in the 1 μ M exposure sample, 6 genes up regulated (red) and 8 genes down regulated (blue), (E) 13 genes in the 10 μ M exposure sample, 4 genes up regulated (red) and 9 genes down regulated (blue), and (F) 1,567 genes in the 100 μ M exposure sample, 801 genes up regulated (red) and 766 genes down regulated (blue). The heatmap (C) represents normalized gene expression by limma, normalized by each row.

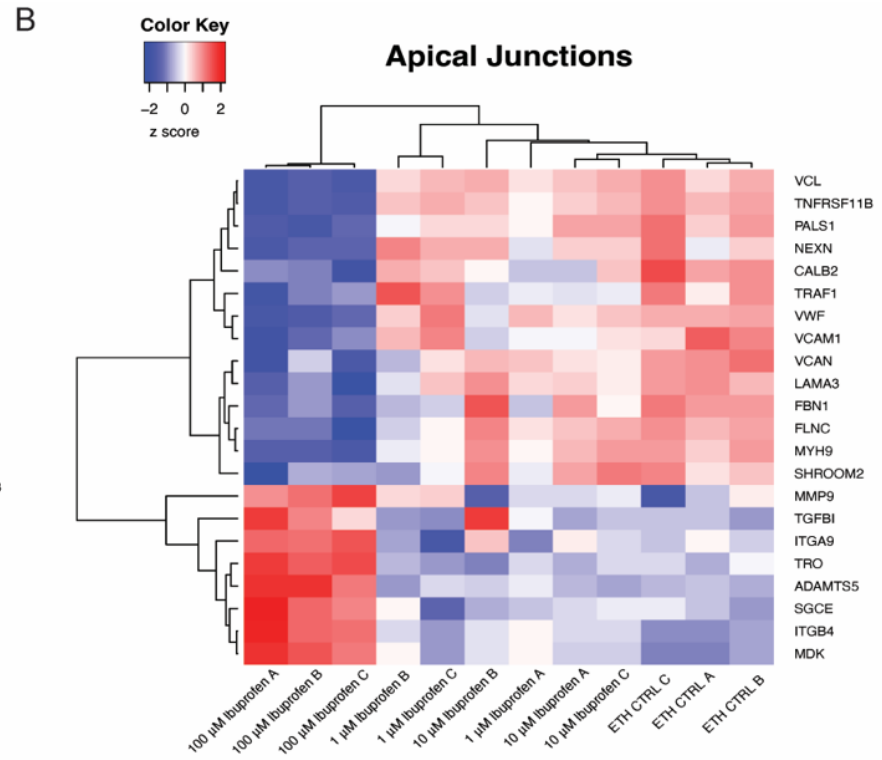
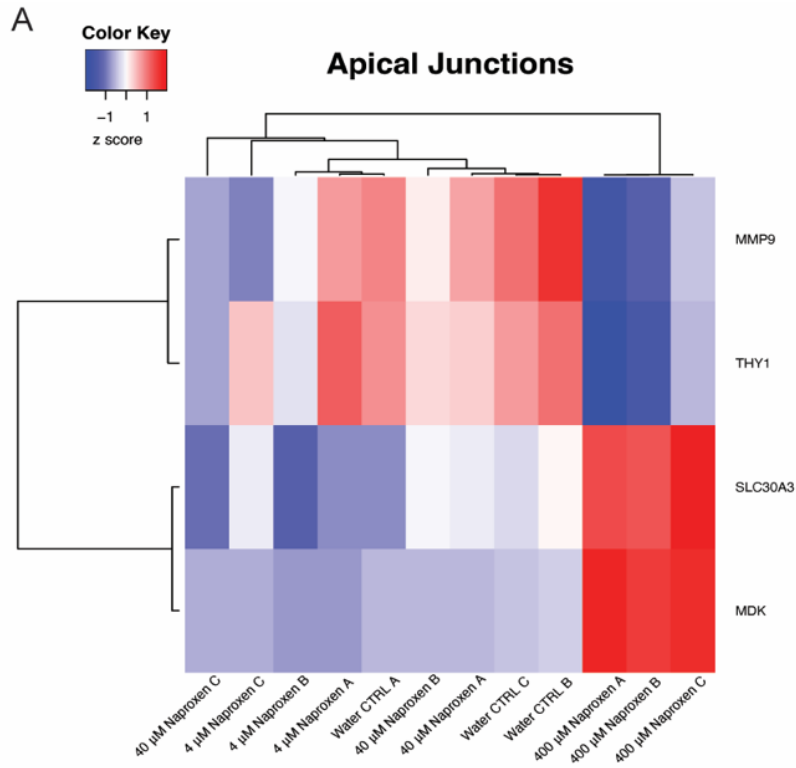


Figure 4.6. Heatmap of genes involved in cell junction regulation from non-human primate primary Sertoli cells exposed to naproxen and ibuprofen in vitro. (A)

Heatmap of genes significantly enriched in the apical junction's gene set (M5915) from the gene set enrichment analysis of the non-human primate primary Sertoli cells after exposure to 4 μ M, 40 μ M, and 400 μ M naproxen compared to the water vehicle control.

(B) Heatmap of genes significantly enriched in the apical junction's gene set (M5915) from the gene set enrichment analysis of the non-human primate primary Sertoli cells after exposure to 1 μ M, 10 μ M, and 100 μ M ibuprofen.

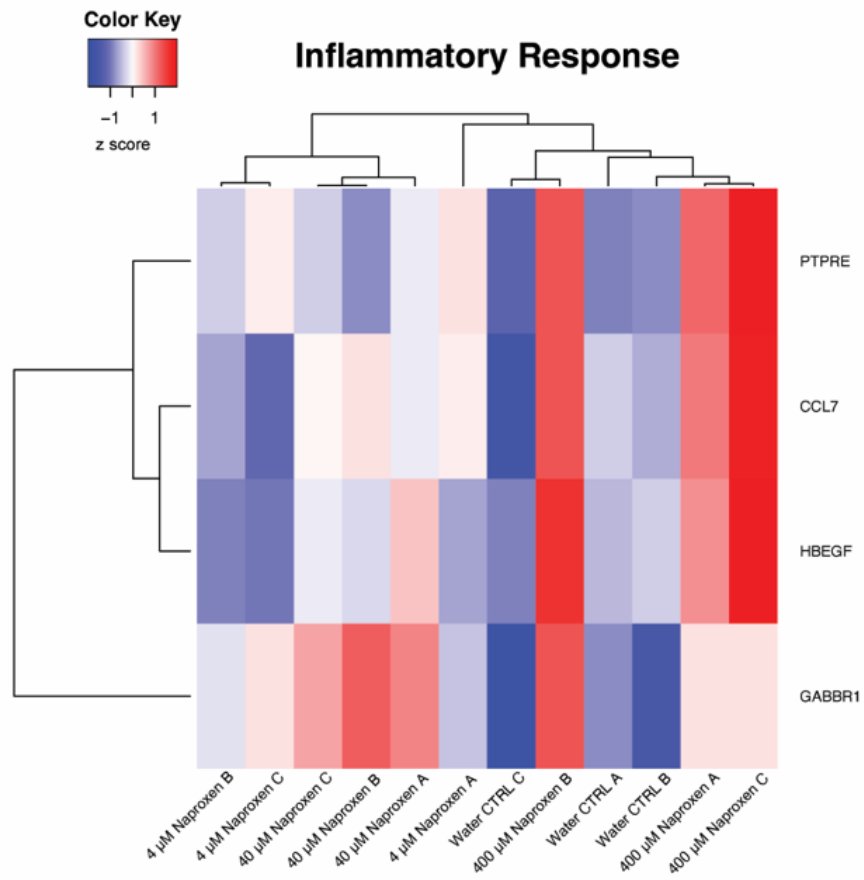


Figure 4.7. Heatmap of genes involved in inflammatory response from non-human primate primary Sertoli cells exposed to naproxen in vitro. Heatmap of genes significantly enriched using the Hallmark database, inflammatory response gene set (M5932), from the gene set enrichment analysis of the non-human primate primary Sertoli cells after exposure to 4 μ M, 40 μ M, and 400 μ M naproxen compared to the water vehicle control. The heatmap represents normalized gene expression by limma, normalized by each row.

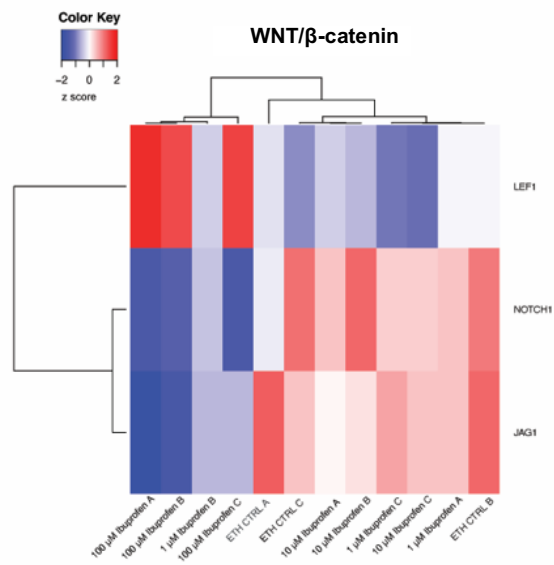
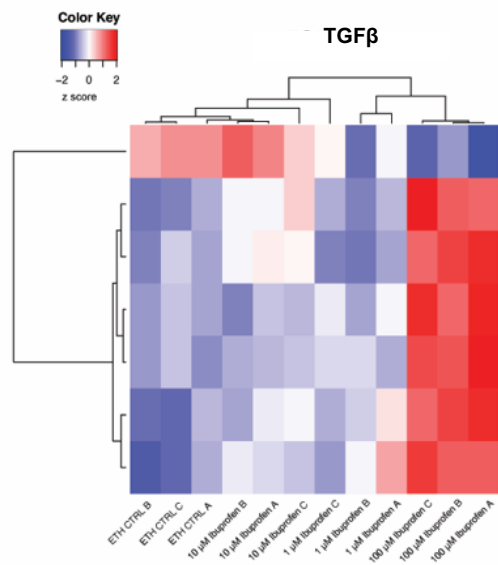
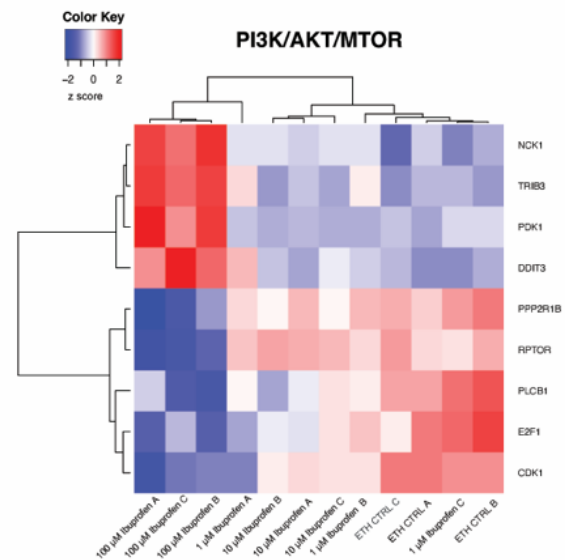
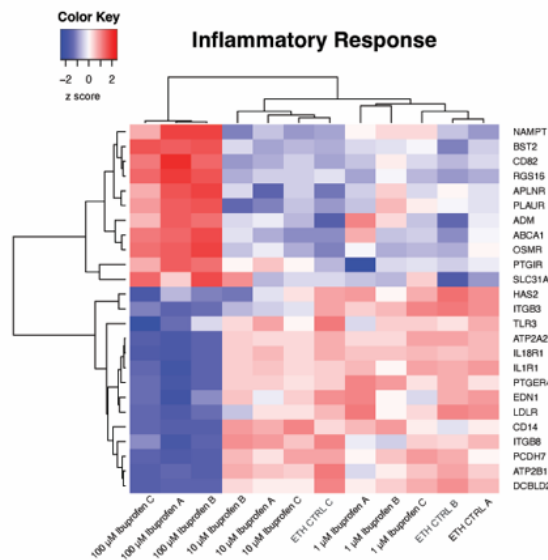
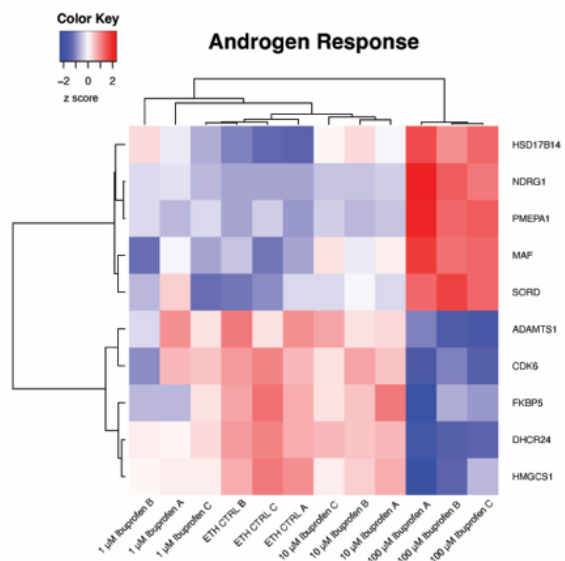


Figure 4.8. Heatmap of genes involved in cell junction regulation and inflammatory response gene sets from non-human primate primary Sertoli cells exposed to ibuprofen in vitro. Heatmap of genes significantly enriched in the Hallmark data gene sets: androgen response gene set (M5908), inflammatory response gene set (M5932), PI3K/AKT/mTOR signaling gene set (M5923), TGF- β signaling (M5896), and WNT/ β -catenin signaling gene set (M5895) using the gene set enrichment analysis of the non-human primate primary Sertoli cells after exposure to 1 μ M, 10 μ M, and 100 μ M ibuprofen compared to the 0.1% ethanol vehicle control. Each heatmap represents normalized gene expression by limma, normalized by each row.

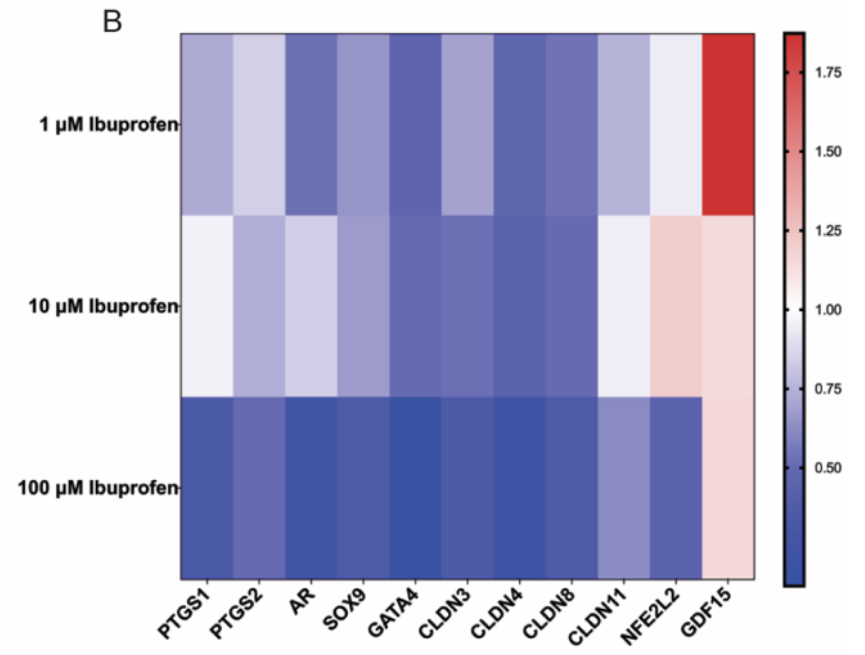
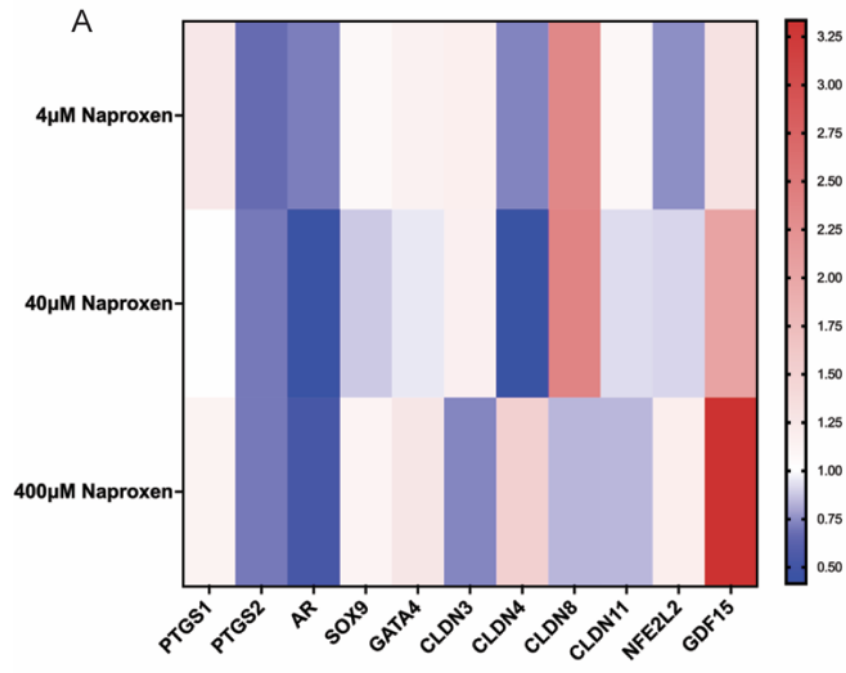


Figure 4.9. Validation of RNA-seq data by RT-qPCR. The results of RT-qPCR validation of genes involved in cyclooxygenase pathway (*PTGS1* and *PTGS2*), Sertoli cell function (Androgen Receptor: *AR*, *SOX9*, and *GATA4*), tight junctions (*CLDN 3,4,8*, and *11*), and inflammation response (*NFE2L2* and *GDF15*) from non-human primate primary Sertoli cells exposed to 4 μ M, 40 μ M, and 400 μ M naproxen compared to water vehicle control or to (A) 1 μ M, 10 μ M, and 100 μ M ibuprofen compared to the 0.1% ethanol vehicle control (B) compared to the normalized RNA-seq results table in Table 4.3.

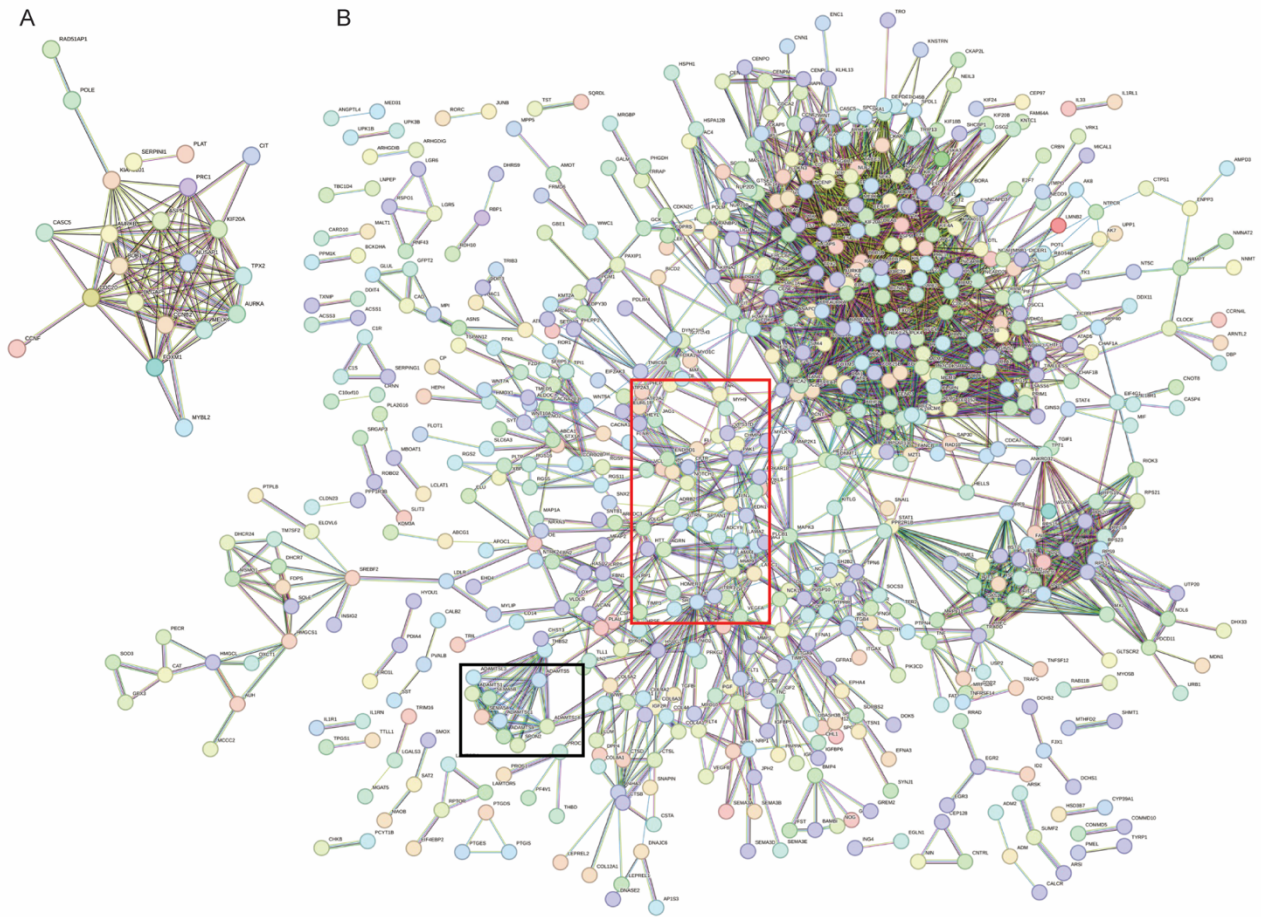


Figure 4.10. Predicted network interactions between proteins from non-human primate primary Sertoli cells exposed to naproxen and ibuprofen *in vitro*. (A)

STRING interaction among genes that were significantly upregulated or downregulated by 400 μ M naproxen with a fold change of 1.5. *Cit* (down regulated by naproxen) was identified as a central node in the protein interaction network and is a key regulator of adheren junction integrity. (B) STRING interaction among genes that were significantly upregulated or downregulated by 100 μ M ibuprofen with a fold change of 1.5. *ADAMTS5* (up regulated by ibuprofen) was identified as a central node in the protein interaction network (black box) and is a key regulator of adheren junction integrity. *AR* and *VCL* (down regulated by ibuprofen) were also identified as central nodes in the protein interaction network (red box) which assist in maintaining the integrity of the Blood-testis barrier. Genes that did not have any identified interactions were excluded from both graphs. The colors of the edges represent the following: light blue = known interactions from curated databases, purple = known interactions that were experimentally determined, green = predicted interactions from gene neighborhood, red = predicted interaction from gene fusions, blue = predicted interactions from gene co-occurrence, black = co-expression, and light purple = protein homology.

Table 4.1. Ibuprofen-induced non-human primate primary Sertoli cell gene enrichment using the Human phenotype ontology database. Genes that were enriched in the diseases associated with male factor infertility are listed below. Diseases with a $p_{adj} < 0.05$ were considered significant.

PHENOTYPE	1 μ M IBUPROFEN		10 μ M IBUPROFEN		100 μ M IBUPROFEN	
	$-\log_{10}(p_{adj})$	p_{adj}	$-\log_{10}(p_{adj})$	p_{adj}	$-\log_{10}(p_{adj})$	p_{adj}
CRYPTORCHIDISM (HP:0000028)	0.81882167	0.15176734	3.07967191	0.00083239	7.04626554	8.9895E-08
FUNCTIONAL ABNORMALITY OF MALE INTERNAL GENITALIA (HP:0000025)	1.02202654	0.09505467	2.9856728	0.00103354	3.26691469	0.00054086
APLASIA/HYPOPLASIA OF THE TESTES (HP:0010468)	0.9586435	0.10999084	2.98893714	0.0010258	3.23545956	0.00058149
INFERTILITY (HP:0000789)	0.27396643	0.53214939	3.02518252	0.00094366	2.49427552	0.00320424

Table 4.2. Naproxen-induced non-human primate primary Sertoli cell gene enrichment using the Human phenotype ontology database. Genes that were enriched in the diseases associated with male factor infertility are shown below. Diseases with a p-adjusted value (padj) < 0.05 were considered significant.

PHENOTYPE	4 μ M NAPROXEN		40 μ M NAPROXEN		400 μ M NAPROXEN	
	$-\log_{10}(\text{padj})$	padj	$-\log_{10}(\text{padj})$	padj	$-\log_{10}(\text{padj})$	padj
CRYPTORCHIDISM (HP:0000028)	1.094096107	0.08052002	1.088326763	0.08159682	0.897977507	0.12648019
FUNCTIONAL ABNORMALITY OF MALE INTERNAL GENITALIA (HP:0000025)	1.094096107	0.08052002	2.43011E-14	1	0.06833128	0.85441472
APLASIA/HYPOPLASIA OF THE TESTES (HP:0010468)	0.936758696	0.11567548	0.069880979	0.85137133	0.067201533	0.85664023
INFERTILITY (HP:0000789)	0.54346994	0.28610804	2.43011E-14	1	0.01161058	0.97361985

Table 4.3. Normalized RNA-seq results of genes from non-human primate primary Sertoli cells involved in the cyclooxygenase pathway (*PTGS1*, *PTGS2*, *PTGIS*, *PTGES*, *PTGIR*, *PTGER4*, *PTGDR*, *PTGER3*, *PTGER2*, *PTGDS*, *PTGES3*, *PTGR3*, *PTGR2*, and *PTGR1*), Sertoli cell function (*AR*, *SOX9*, and *GATA4*), tight junctions (*CLDN 3,4,8*, and *11*), and inflammation response (*NFE2L2* and *GDF15*), representing the log fold change and p-adjusted value (padj). Genes with a log fold change of 0.578 in either direction and a padj of < 0.01 were considered significant.

Gene	4 μ M Naproxen		40 μ M Naproxen		400 μ M Naproxen		1 μ M Ibuprofen		10 μ M Ibuprofen		100 μ M Ibuprofen	
	log fold change	padj	log fold change	padj	log fold change	padj	log fold change	padj	log fold change	padj	log fold change	padj
<i>PTGS1</i>	0.00686827	0.96118754	0.10387656	0.10624092	0.02232088	0.791978157	0.20942905	0.0110638	0.20942905	0.0110638	N/A	N/A
<i>PTGS2</i>	N/A	N/A	N/A	N/A	N/A	N/A	N/A	N/A	N/A	N/A	N/A	N/A
<i>AR</i>	-0.0424629	0.88683878	0.11262036	0.56360368	-0.0594209	0.756639324	0.00561496	0.98836418	0.00561496	0.98836418	-0.752292	8.02866E-05
<i>SOX9</i>	-0.0244845	0.85666987	0.11473923	0.12389484	0.35157269	1.35539E-06	-0.0360719	0.7992917	-0.0360719	0.62145481	N/A	N/A
<i>GATA4</i>	0.1550508	0.49215769	-0.1223206	0.6216548	0.09675929	0.611536288	-0.0249278	0.95794342	-0.0249278	0.89409869	N/A	N/A
<i>CLDN3</i>	N/A	N/A	N/A	N/A	N/A	N/A	N/A	N/A	N/A	N/A	N/A	N/A
<i>CLDN4</i>	-0.2939956	0.66425085	-0.1901474	0.8052816	-0.0302686	0.959163484	-0.3774419	0.58746627	-0.3774419	0.58746627	N/A	N/A
<i>CLDN8</i>	N/A	N/A	N/A	N/A	N/A	N/A	N/A	N/A	N/A	N/A	N/A	N/A

<i>CLDNI</i> 1	- 0.121 9729	0.1 337 863	0.0722 636	0.45 2150 12	- 0.0 620 437	0.4 257 621 21	0.28 3282 52	0.0 118 903 6	0.2 832 825 2	0.0 118 903 6	N/A	N/A
<i>NFE2L</i> 2	0.029 7658 9	0.7 223 149 7	0.0947 5895	0.08 1853 98	0.2 173 686 2	0.0 001 751 27	- 0.00 1344 8	0.9 947 125 6	- 0.0 013 448	0.9 947 125 6	N/A	N/A
<i>GDF15</i>	0.012 4635 6	0.9 734 364 3	0.0565 1566	0.85 7637 97	0.4 565 374	3.2 914 6E- 05	0.68 4190 13	0.0 071 905 6	0.3 894 564 8	0.0 078 767	0.86 0707 25	2.70 328E -06
<i>PTGIS</i>	0.010 6774 7	0.9 475 008 3	0.0843 7523	0.34 6038 24	- 0.1 238 714	0.0 918 115 3	- 0.05 3972 7	0.7 427 798 7	0.1 478 211 6	0.2 393 226 4	0.87 8400 78	3.24 E-08
<i>PTGES</i>	- 1.041 1309	0.1 424 565 7	- 0.7655 242	0.26 7277 27	- 0.0 853 335	0.1 110 047 1	- 0.00 9592 3	0.9 962 869 2	- 0.4 619 515	0.7 098 233 7	4.46 7140 89	0.00 1183 4
<i>PTGIR</i>	- 0.720 7861	0.4 612 559 9	- 0.5178 053	0.63 6969 38	0.1 741 369 4	0.8 230 986 7	- 0.76 6730 7	0.5 772 012 9	0.7 570 573 3	0.1 880 908 2	2.01 6224 65	0.00 0178 46
<i>PTGER</i> 4	- 0.011 4592	0.9 615 841	0.0819 0041	0.57 3725 39	0.2 344 425 4	0.0 181 716 5	0.10 1062 09	0.6 076 993 2	- 0.0 417 007	0.8 353 769 3	- 0.77 0314 1	1.12 E-05
<i>PTGD</i> R	0.340 6994 1	0.0 863 759	0.4275 9408	0.01 9442 08	0.2 906 346 7	0.1 036 018 9	0.17 9051 87	0.6 047 724	- 0.1 919 824	0.4 615 044 4	- 0.29 4219 9	0.24 1383 23
<i>PTGER</i> 3	- 0.584 204	0.3 634 963 4	- 0.3658 107	0.57 3725 39	- 0.3 784 567	0.4 171 272 5	- 0.64 2047 8	0.4 106 618 6	0.5 332 879 7	0.3 838 329	- 0.53 3588 4	0.28 0981 98
<i>PTGER</i> 2	- 0.036 5307	0.9 443 262 1	- 0.0723 01	0.85 3357 73	- 0.4 206 364	0.0 952 314 8	0.27 4639 42	0.2 669 549 9	0.2 791 926 6	0.2 099 026 4	- 0.00 0627	0.99 7330 71

<i>PTGDS</i>	- 0.147 0615	0.0 303 473 9	- 0.0289 506	0.81 4278 53	0.0 638 113 9	0.7 399 290 6	0.00 4937 71	0.0 049 377 1	0.2 164 858 4	0.0 427 110 3	1.03 5332 85	6.36 E-09
<i>PTGES</i> 3	- 0.048 8967	0.4 312 197	- 0.0298 049	0.72 2404 68	- 0.0 853 335	0.1 110 047 1	- 0.02 5612 7	0.8 512 861 6	- 0.4 619 515	0.7 098 233 7	- 0.07 7991 9	0.18 8058 28
<i>PTGR3</i>	- 0.083 7938	0.6 639 776 3	- 0.1131 158	0.47 8836 86	- 0.0 599 316	0.6 652 661 1	0.03 7216 01	0.8 807 978	0.0 391 248 4	0.8 653 066 7	0.03 0322 17	0.83 0417 7
<i>PTGR2</i>	0.003 8277 6	0.9 916 502 4	- 0.0960 505	0.44 0346 53	- 0.1 528 066	0.0 754 550 5	- 0.00 6896 5	0.9 753 730 7	- 0.0 347 467	0.8 418 765 2	- 0.34 9273	0.00 1136 24
<i>PTGR1</i>	- 0.025 1545	0.9 317 527 2	- 0.1720 802	0.30 3887 72	- 0.0 462 922	0.7 982 601 2	0.07 7354 41	0.7 112 457 4	0.0 796 443 1	0.6 776 082 8	0.17 3359 12	0.17 2570 24

Abbreviation: *PTGS1*, Prostaglandin-Endoperoxide Synthase 1; *PTGS2*, Prostaglandin-

Endoperoxide Synthase 2; *PTGIS*, Prostaglandin I2 Synthase; *PTGES*, Prostaglandin E

Synthase; *PTGIR*, Prostaglandin I2 Receptor; *PTGER4*, Prostaglandin E Receptor 4;

PTGDR, Prostaglandin D2 Receptor; *PTGER3*, Prostaglandin E Receptor 3; *PTGER2*,

Prostaglandin E Receptor 2; *PTGDS*, Prostaglandin D2 Synthase; *PTGES3*, Prostaglandin

E Synthase 3; *PTGR3*, Prostaglandin Reductase 3; *PTGR2*, Prostaglandin Reductase 2;

PTGR1, Prostaglandin Reductase 1; *AR*, Androgen Receptor; *SOX9*, SRY-Box

Transcription Factor 9; *GATA4*, GATA Binding Protein 4; *CLDN3*, Claudin 3; *CLDN4*,

Claudin 4; *CLDN8*, Claudin 8; *CLDN11*, Claudin 11; *NFE2L2*, NFE2 Like BZIP

Transcription Factor 2; *GDF15*, Growth Differentiation Factor 15; padj, adjusted p-value;
N/A, not applicable.

4.3 RESULTS: HUMAN TESTICULAR TISSUE EXPRESSES NSAID-INHIBITING ENZYMES IN VIVO

Ibuprofen and naproxen reduce pain and inflammation by inhibiting cyclooxygenase-1 (COX-1) and -2 (COX-2) enzymes that produce various prostaglandins, such as *PGE2* and *PGD2* [275-277]. Since several groups reported the importance of prostaglandins in male reproductive function (reviewed in [278]), we explored prostaglandin and COX expression in our *in vitro* NHP primary Sertoli cell model and in human testicular biopsies. Data from our mRNA-sequencing experiment revealed that NHP primary Sertoli cells exposed to 100 μ M ibuprofen differentially express prostaglandin synthases, *PTGES*, and *PTGIS*, and their receptors (e.g., EP4, which binds PGE and IP2, which binds PGI) [210, 279-281] (Table 4.3). The constitutive isoform COX-1, the prostaglandin synthases, and receptors *PTGDR* (which binds PTGDS), *PTGER2-4* (which binds *PTGES*), *PTGIR* (which binds *PTGIS*), and *PTGRI-3* (prostaglandin reductase 1-3) mRNA were also detected in the NSAID- exposed Sertoli samples, but not the inducible COX-2 isoenzyme (Table 4.3). Claudins 3 and 11, which aid in determining the permeability of the BTB [282], were not detected in the NSAID-exposed Sertoli cells (Table 4.3), indicating that NSAID-induced alterations in the BTB function could partially be driven by the absence of claudin expression. Interestingly, *PTGSI*, *SOX9*, *GATA4*, *CLDN4*, *CLDN11*, and *NFE2L2* were not expressed in the 100 μ M ibuprofen exposed Sertoli cells (Table 4.3), suggesting a dose-dependent effect on Sertoli cell and BTB function and inflammatory response. We also revealed the expression of COX-1 within the seminiferous tubules by immunofluorescence in the adult human testes without morphological abnormalities (Figure 4.11). Further, the *in*

vivo human Sertoli cells positively express COX-1 (Figure 4.11). Similar to other studies, we report that COX-2 is expressed in testicular biopsies of men diagnosed with inflammation and impaired fertility (Figure 4.12; B-C) [283] as well as in testicular cancer (Figure 4.13) [284], suggesting that diseased-states within the testis are capable of producing prostaglandins. Interestingly, the Sertoli cells in the male patient with Obstructive azoospermia with full spermatogenesis were positively identified to express COX-2 (Figure 4.12; A). While COX-1 and COX-2 expression were diffusely expressed throughout the seminiferous tubules, each enzyme did colocalize with *SOX9* in the Sertoli cells, revealing that COX/ prostaglandin pathway may locally modulate testicular activity through the BTB and regulate spermatogenesis (Table 4.5; [278]). Further, our results suggest the wide distribution of prostaglandin receptors and synthesizing enzymes in the testis may have key roles in male fertility [278].

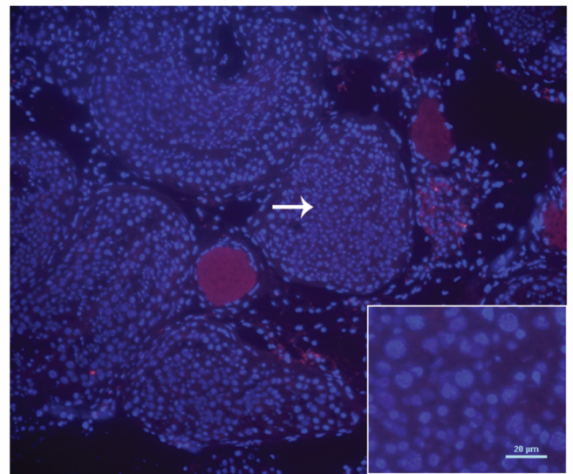
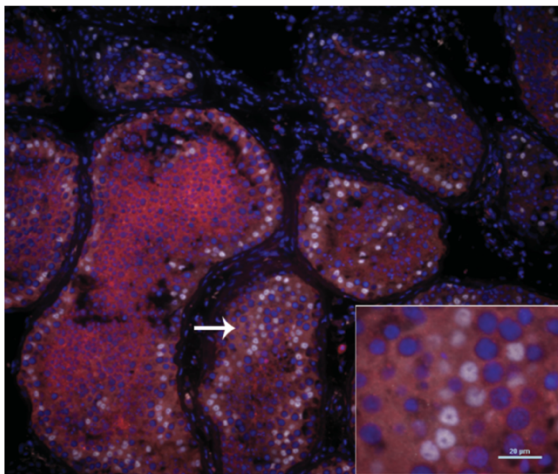
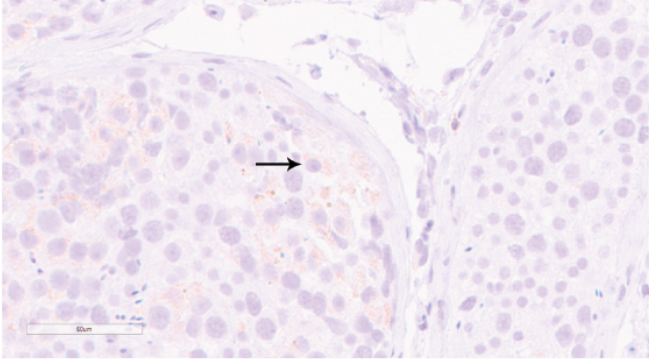
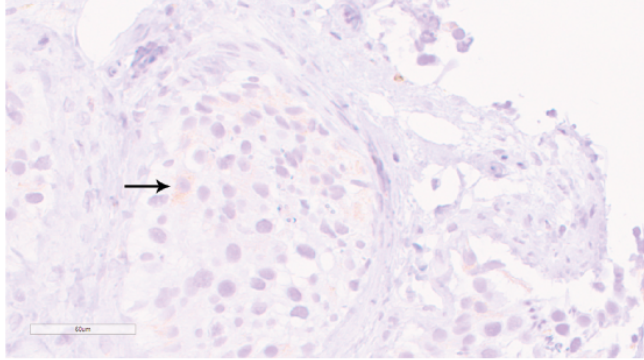


Figure 4.11. Sertoli cells in human testicular tissue express NSAID inhibiting enzyme, COX-1. (Left) Representative immunofluorescent images of COX-1 (red), *SOX9* (white), and DAPI (blue) in testicular tissue of a patient with Obstructive azoospermia with full spermatogenesis. Insert- Detail of COX-1 and *SOX9* colocalization immunofluorescence. Scale Bar 20 μm . **(Right)** Representative immunofluorescent secondary only images of rbIgG (red), gIgG (white), and DAPI (blue). Insert- Detail of rbIgG (red), gIgG (white), and DAPI (blue). Scale Bar 20 μm .

A



B



C

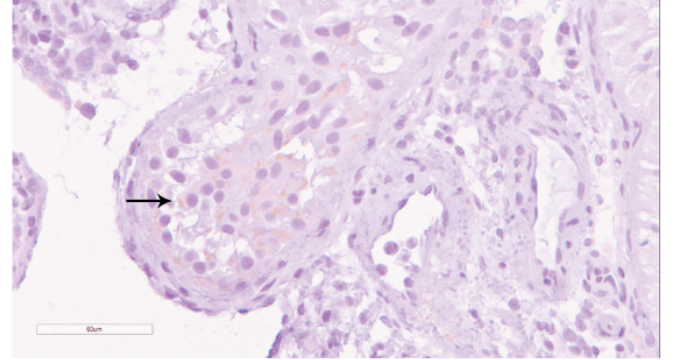


Figure 4.12. Sertoli cells in human testicular tissue express NSAID inhibiting enzyme, COX-2. (A-C) Representative Hematoxylin and immunohistochemistry images of COX-2 in human testicular biopsies from a male patient with Obstructive Azoospermia that had normal testicular morphology ($n = 1$; **A**), representative images of COX-2 staining from male patients diagnosed with non-obstructive azoospermia that did not have inflammation ($n = 4$; **B**), and representative COX-2 images from male patients diagnosed with non-obstructive azoospermia and testicular inflammation ($n = 8$; **C**). The arrows point to Sertoli cells positively expressing COX-2. Scale Bar 60 μm .

**Germ cell neoplasia
in situ (GCNIS)**

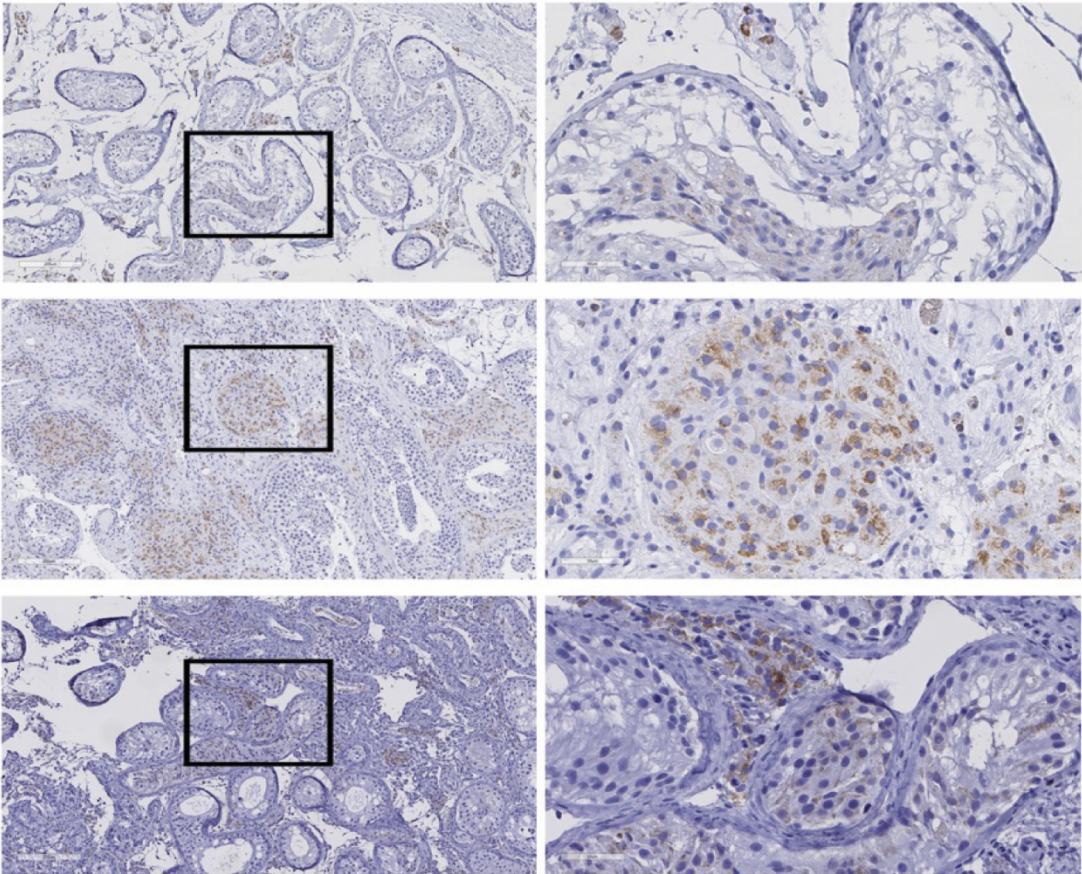


Figure 4.13. Human testicular tissue express NSAID inhibiting enzyme, COX-2.
Representative Hematoxylin and immunohistochemistry of COX-2 staining in human testicular biopsies from male patients ($n = 3$) diagnosed with Germ cell neoplasia *in situ* (GCNIS). Scale Bar 50 μm .

Table 4.4: Clinical patient data. Seventeen male patients consulted an andrologist for male infertility at the Clinic of Urology at the University of Zagreb School of Medicine, University Centre Zagreb, and were subjected to an open biopsy of the testis. Based on their clinical presentation and histology analysis, patients were classified as obstructive azoospermia with a diagnosis of full spermatogenesis or various degrees of testicular parenchyma damage.

	Number of Patients	Average Age of Patients	Diagnosis	Hormone Levels	Cryptorchidism	Varicocele
Obstructive Azoospermia	1	34	Full Spermatogenesis	FSH, LH, Testosterone are normal	No	No
Non-Inflammatory	4	39.5	Hypospermatogenesis	FSH, LH, Testosterone are normal	No	No
			Maturation Arrest	FSH, LH are normal, Testosterone is low	No	No
			SCOS	FSH (High), LH (High), Testosterone is normal	No	No
			Mixed Atrophy	FSH (High), LH, Testosterone are normal	No	No
Testicular Inflammation	8	39	Tubular fibrosis, SCOS	FSH (High), LH (High), Testosterone is normal	No	No
			Tubular fibrosis, SCOS, Mixed atrophy	FSH (High), LH (High), Testosterone is low	Yes	No

			Maturation arrest, mixed atrophy	FSH (High), LH, Testosterone are normal	No	No
			Maturation arrest, mixed atrophy	FSH (High), LH (High), Testosterone is normal	Yes	No
			Mixed atrophy	FSH (High), LH, Testosterone are normal	No	No
			Maturation arrest, mixed atrophy	FSH (High), LH, Testosterone are normal	No	No
			Maturation arrest, mixed atrophy	FSH (High), LH, Testosterone are normal	No	Yes
			Mixed atrophy	FSH (High), LH, Testosterone are normal	Yes	No
GCNIS	3	39.33	Mixed atrophy, GCNIS	FSH is normal, LH, Testosterone are unknown	No	No
			Mixed atrophy, tubular fibrosis, GCNIS	FSH (High), LH (High), Testosterone is normal	Yes	No
			GCNIS bilateral, Mixed atrophy	FSH, LH are normal, Testosterone is low	No	No

Abbreviations: FSH, follicle stimulating hormone; LH, luteinizing hormone; SCOS, Sertoli-cell only syndrome; GCNIS, germ cell neoplasia *in situ*.

4.4 DISCUSSION

Described as one of the most complex cells in the human body, Sertoli cells create a unique environment to support the development of male germ cells and are the main component of the BTB [285]. The BTB is constituted by different types of cellular junctions, such as tight junctions, gap junctions, desmosomes, and basal ectoplasmic specializations (including adherens junctions), in which these junctions co-exist [126] to form a physical barrier to separate the events of spermatogenesis and allow the development of the germ cells to take place in an immune-privileged state [112, 123, 144]. Because of the unique co-existing junctions that contribute to the barrier and adhesion function of the BTB, changes in gene expression could alter how these proteins interact to maintain barrier homeostasis. Considering the widespread and increasing use of the OTC analgesics naproxen and ibuprofen to relieve pain, fever, and inflammation, the goal of this study was to determine whether exposing NHP primary Sertoli cells to plasma serum levels of naproxen and ibuprofen altered the integrity of Sertoli cell tight junctions and in turn, compromises the function of the BTB.

This comprehensive study examined the effects of two common NSAIDs, ibuprofen and naproxen, on NHP primary Sertoli cell function. Because the testicular concentrations of NSAIDs are unknown in adult men, we used pharmacokinetic data to estimate human exposure and select the concentrations of ibuprofen and naproxen, equivalent to the plasma concentrations during standard analgesic usage [95, 238]. Using NHP adult primary Sertoli cells, we found that naproxen and ibuprofen may compromise male fertility by perturbing the integrity of the Sertoli cell junctions through modification of junctional protein expression and that this mechanism may be similar in humans.

We report here that ibuprofen and naproxen altered the permeability of the barrier formed by the NHP primary Sertoli cells. Both NSAIDs broadly increased the TER reflecting a change in the integrity of the Sertoli cell tight junctions. In our *in vitro* model, the higher the TER caused by each NSAID, the stronger the tight junctions should be between the Sertoli cells without causing any cytotoxic effects. For example, a decrease in TER would signify a decrease in barrier integrity, which could facilitate the movement of toxicants into the seminiferous epithelium causing further damage to germ cell production [286]; however, a tightening of the barrier could delay the entry of the spermatogonial stem cells into the lumen during differentiation or the dissociation of spermatids from the Sertoli cells into the lumen. In contrast to TER, neither NSAID altered the paracellular flux of small molecular weight fluorescent tracers. This implies that the tight junctions are dynamic in nature by adjusting their barrier function permeability in response to changes in the environment or physiological needs [287, 288]. Since the selectivity for different size molecules was unchanged, a mechanism within the Sertoli cells that allows the selective paracellular flux of different-sized molecules in the presence of strengthened tight junctions must have been altered.

Next, we demonstrated that the concentrations of naproxen and ibuprofen play a critical role in altering gene expression in the NHP primary Sertoli cells. Our data shows that the highest concentrations of naproxen and ibuprofen induce the most significant changes in gene expression compared to the lower doses tested (naproxen 4 μ M and 40 μ M; ibuprofen 1 μ M and 10 μ M), which show similar gene expression profiles to the control samples. In this study, we also observed slight alterations in gene expression of tight junction proteins *JAM3*, *OCN*, *MARVELD1*, and *MARVELD2* upon NSAID

exposure; specifically, 100 μ M ibuprofen resulted in a lack of *CLDN4* and *CLDN11* mRNA expression. Interestingly, collagen IV and laminin, major components of the seminiferous tubule basement membrane and can directly regulate tight junction dynamics in the testis, were also altered upon NSAID exposure. Furthermore, we observed alterations in cell-cell actin-based adhesion junctions which provide mechanical support between Sertoli cells (basal ectoplasmic specialization) and between Sertoli and germ cells (apical ectoplasmic specialization), playing a crucial role in the maintenance of the BTB, germ cell differentiation, morphogenesis, and translocation of germ cells from the basal to adluminal compartments of the seminiferous epithelium [289]. Since compromised BTB function is associated with impaired spermatogenesis [290], it is crucial to continue investigating the effects of NSAIDs on BTB function as NSAID usage in men continues to increase worldwide. Overall, at the BTB, naproxen and ibuprofen displayed broad cell junction-altering properties involving signaling pathways associated with tight, gap, and adheren junctions [271]. This specific but complex relationship between dose and effect may explain the broad alterations in cell junctions and signaling pathways involved in the BTB function.

Our study demonstrates that NHP primary Sertoli cells are susceptible to mild analgesics. However, the complex interactions between different cell junctions in the testis and the overall integrity of the BTB under NSAID therapy remain unclear. The results from our study are consistent with those suggesting ibuprofen directly impairs Sertoli cell function by inhibiting anti-Müllerian hormone (AMH) and decreasing the inhibin B/FSH ratio [95]. Additionally, testosterone has been shown to induce COX-2 expression in adult hamster Sertoli cells [281]; therefore, the COX/ prostaglandin system

may modulate Sertoli cell activity and, indirectly alter spermmaturation [278]. It is possible that the endocrine-disrupting nature of ibuprofen may also play an important role in the alteration of gene expression in our study. Although we could not simulate a longer dosing regimen that many reproductive-aged men and elite athletes experience, we could directly assess the impacts on adult Sertoli cells without germ cell contamination and other somatic cells (Figure 4.14). Additionally, by exposing the Sertoli cells to NSAIDs prior to plating on the Transwells, we aimed to model the *in vivo* effects of long-term NSAID usage which is predicted to act through the same mechanism on the BTB and cell junction formation, compared to other barriers in the human body. Thus, our comprehensive approach provides a foundation for future *in vivo* studies to determine the overall effect on sperm production and fertility in men that chronically use naproxen and ibuprofen.

Together, the results from our study add to the growing body of evidence that NSAID usage may be a contributing factor to the decline in male fertility (reviewed in [239]). However, since the BTB has an important role in immune regulation, perturbations of this delicate function could lead to inflammation and, ultimately, infertility [291]. In such cases, there is a shift in the location of macrophages and mast cells from the interstitial space to the seminiferous tubule compartment in the testes of men with infertility [292, 293]. Since COX-2 has been reported to be expressed in mast cells and macrophages of male patients with various infertility diagnoses [294-296], NSAIDs have a potential therapeutic role in treating sub-fertility and male factor infertility disorders and should be investigated further.

As naproxen and ibuprofen usage is increasing around the globe and throughout the U.S., understanding the long-term consequences is of the utmost importance for reproductive-aged men and may also shed light on the potential male fertility impacts of other commonly used OTC medications. In conclusion, we hope the increasing amount of scientific evidence regarding the effects on male reproductive hormones, the BTB, and sperm output following NSAID usage will encourage medical professionals to address OTC medication usage in evaluating male infertility and family planning.

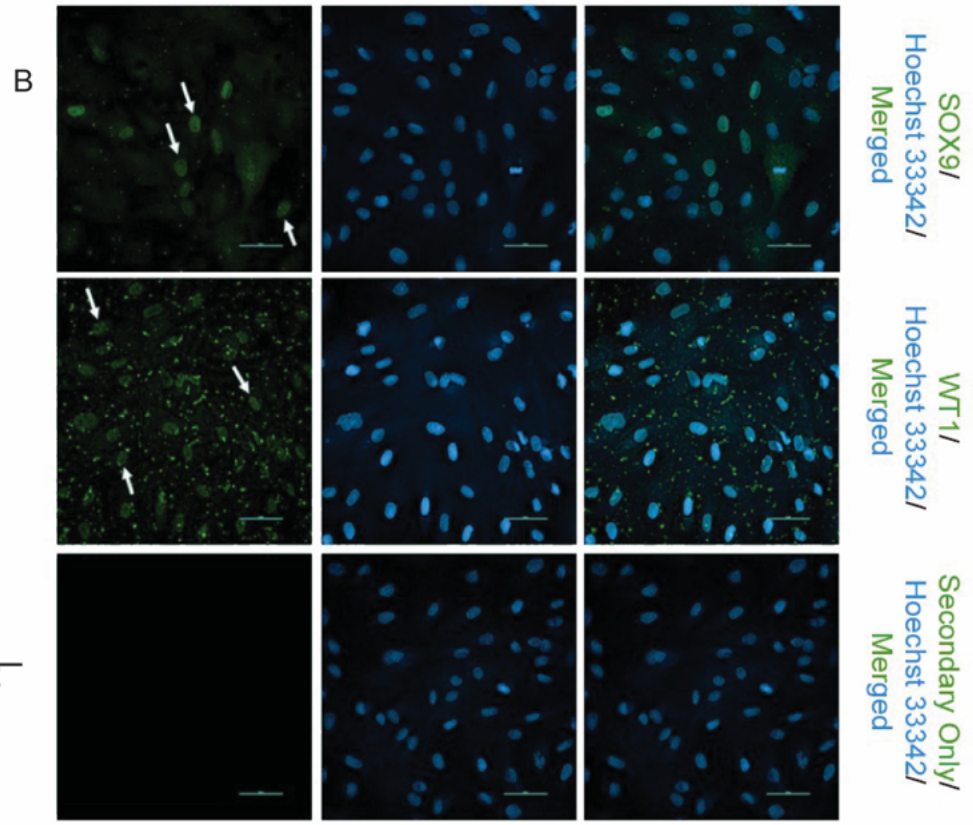
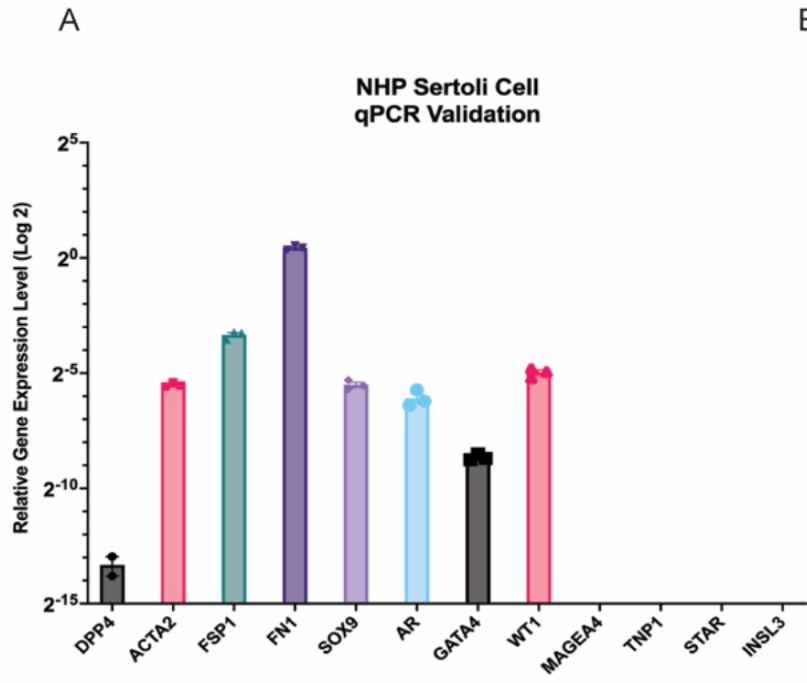


Figure 4.14. Non-human primate primary Sertoli cells validated in vitro using qPCR and fluorescence microscopy. NHP primary Sertoli cells validated in vitro using qPCR and fluorescence microscopy. **(A)** Graphical representation of individual relative gene expression levels in the NHP primary Sertoli cells: Fibroblast markers (*DPP4*, *FSP1*, and *FNI*), Sertoli cell markers (Androgen Receptor: *AR*, *SOX9*, *WT1*, and *GATA4*), Myoid markers (*ACTA2*), spermatogenic markers (*MAGEA4* and *TNPI*), and Leydig cell markers (*STAR* and *INSL3*). Each bar represents the mean \pm SEM. **(B)** Immunofluorescent staining reveals expression of characteristic Sertoli cell markers revealing expected nuclear staining for *SOX9* (green, Top Row), *WT1* (green, Middle Row), and Hoechst 33342 (Blue) dye. White arrows pointing to positively stained cells. The secondary only control (Bottom row) is negative for green fluorescence. Scale Bar: 50 μ m.

4.5 MATERIALS AND METHODS

Primary Non-human primate Sertoli cell isolation & validation

Isolation: The Sertoli cells were isolated from adult rhesus macaque testicular tissue as previously described [297]. Briefly, the Sertoli cells were isolated using a Percoll (Cytiva) gradient and purified by visual analysis and differential plating [297]. For this study, the cells routinely contained greater than 90-95% primary Sertoli cells.

Validation: The non-human primate (NHP) Sertoli cell cultures were validated by real-time quantitative polymerase chain reaction (RT-qPCR) and immunocytochemistry (ICC), as further described below. Briefly, the Sertoli cells were validated by various NHP Sertoli cell markers (*SOX9*, *AR*, *WT1*, and *GATA4*), Fibroblast markers (*DPP4* and *FSP1*), Peritubular cell marker (*FNI*), Myoid marker (*ACTA2*), spermatogenic markers (*MAGEA4* and *TNPI*), and Leydig cell markers (*STAR* and *INSL3*) (Integrated DNA Technologies, Table 6.7) by RT-qPCR. Additionally, these cells were validated by immunocytochemistry analysis for *SOX9* and *WT1* (EMD Millipore, Abcam, Invitrogen, Table 6.8), further described below.

Cell culture & NSAID treatment

Cell Culture: The NHP primary Sertoli cells were cultured and maintained in DMEM 1X (Gibco), supplemented with 10% Fetal Bovine Serum (Corning), 5% Penicillin-Streptomycin (Gibco), and 5% MEM Non-Essential Amino Acids Solution (Gibco) in a 5% CO₂ and 95% humidified air incubator at 35°C. Media was exchanged every 48 hours and passaged at 80- 90% confluency.

NSAID Treatment: The cells were treated with naproxen (MilliporeSigma) or ibuprofen (MilliporeSigma) at concentrations reflecting plasma levels in healthy adult

men ranging from 10^{-4} to 10^{-5} M [95, 238]. Confluent cultures were treated with naproxen at concentrations of 4 μ M, 40 μ M, or 400 μ M [238] or ibuprofen at concentrations of 1 μ M, 10 μ M, or 100 μ M [95]. The cells were maintained in 10% FBS DMEM media with naproxen dissolved in water and ibuprofen dissolved in 0.1% ethanol or water- or ethanol-only vehicle controls, with media changes occurring daily. A minimal volume of ethanol was used, which is unlikely to cause cell death and have negligible effects.

The primary NHP Sertoli cells were treated for three days in NSAID-containing media before the cell viability and apoptosis, and mitochondrial membrane potential assays due to reaching 95% confluency at three days of treatment. For the transepithelial electrical resistance (TER), barrier permeability assays, RT-qPCR gene expression studies, and RNA-seq analysis, confluent Sertoli cells were treated with either naproxen, ibuprofen, or vehicle control for 24 hours and were then trypsinized and seeded in 12 mm Transwells (Costar, Corning® Life Sciences) coated with Matrigel (Corning® Life Sciences) at 1×10^6 cells/ cm^2 per well, for continued growth in NSAID- containing media for an additional three days to develop tight junctions, simulate the BTB, and a longer dosing regimen, as described below.

Cell viability and apoptosis

By utilizing the Muse® Annexin V and Dead Cell Assay Kit (Luminex), cell viability was assessed by measuring the percentage of apoptotic cells in the cultures by staining unfixed cells with Annexin V and 7-AAD as per manufacturer's instructions in preparation for flow cytometry. Each sample was analyzed on the Muse® benchtop flow cytometer (MilliporeSigma) and analyzed at 1,000 events for three replications ($n = 3$) per analgesic concentration and water- or ethanol-only control.

Mitochondrial membrane potential

The mitochondrial membrane potential was assessed using the Muse[®] MitoPotential Kit (Luminex) to stain unfixed cells with the supplied dye and 7-AAD per the manufacturer's instructions to prepare the samples for flow cytometry. Each sample was analyzed on the Muse[®] benchtop flow cytometer (MilliporeSigma) and analyzed at 1,000 events for three replications ($n = 3$) per analgesic concentration and water- or ethanol-only control.

Transepithelial electrical resistance (TER) measurement

The functionality of the BTB was assessed by performing transepithelial electrical resistance (TER) and barrier permeability assays. Confluent cultures were treated with naproxen or ibuprofen for 24 hours and then trypsinized and seeded at 1×10^6 cells/ cm² in the apical (upper) chamber of the 12mm diameter Transwell (Costar) coated with Matrigel[®] (Corning[®]), as described above. The next day (Day 0), the TER of the cells in NSAID-containing media was measured using an Epithelial Voltohmmeter (EVOM, World Precision Instruments, Inc.) in ohms (Ω) x cm², as previously described [253, 298]. After the measurement, the cells were treated with ibuprofen, naproxen, or vehicle control, and 10 μ M testosterone (Sigma). The TER measurements were recorded, and media changes occurred for three consecutive days.

Paracellular flux (permeability) assay

After the TER was measured on the third day, the NSAID-treated NHP primary Sertoli cells were equilibrated with Ringer's solution for 15 minutes at 35°C, and then the apical chamber was replaced with Ringers and 50 μ g/mL Texas Red-labeled dextran (10 kDa; ThermoFisher) and 2 μ g/mL calcein (0.63 kDa; ThermoFisher) as described [166].

Over the course of two hours, 100 μ L of media was collected from the basal side of the chamber every 30 minutes and used for measuring the intensity of fluorescence at wavelengths Ex485/Em525 nanometers for calcein and Ex585/Em625 nanometers for dextran using a SpectraMax iD5 microplate reader (Molecular Devices). The amount of flux was determined by a standard curve and was graphed as the amount of calcein or dextran appearing in the lower chamber of the Transwell plotted versus time. The rate of diffusion of calcein and dextran was calculated using the slope of the flux curve as previously described [166, 299, 300].

RNA extraction and quantification

RNA was extracted following the manufacturer's instructions from the naproxen-, ibuprofen-, ethanol-only-, or water-only- treated NHP Sertoli cells using the RNeasy Plus Mini Kit (Qiagen) after the TER was measured on the third day to yield four biological replicates ($n = 4$). Using the NanoDrop[®] 2000c spectrophotometer (Thermo Scientific), RNA integrity was measured, and only 260/280 ratios >2.0 were accepted for further processing. The samples were stored at -80°C until Real-time quantitative polymerase chain reaction analysis and mRNA sequencing.

Real-time quantitative polymerase chain reaction (RT-qPCR) analysis

Each RNA sample (500ng) was reversed transcribed to cDNA for RT-qPCR using the iScript[™] cDNA Synthesis Kit (Bio-Rad) as per manufacturer's instructions.

Quantitative PCR was performed with 500 μ g cDNA and the iQ[™] SYBR Green Supermix (Bio-Rad) as per manufacturer's instructions using the CFX Connect Real-Time PCR Detection System (Bio-Rad). The amplification parameters were as follows: the initial denaturation of 3 min at 95°C , 40 cycles of 15-second denaturation at 95°C ,

and 1 minute at 57 °C for annealing and extension. After the final PCR cycle, a melt curve analysis was performed at the following parameters: 5 seconds per step, 65 °C to 95 °C at 0.5 °C increments.

All PCR primers (Integrated DNA Technologies, Table 6.7) were designed and validated for specificity and amplification efficiency to human genes *PTGS1*, *DPP4*, *FSP1*, *FNI*, and NHP genes *PTGS2*, *AR*, *SOX9*, *GATA4*, *CLDN3*, *CLDN4*, *CLDN8*, *CLDN11*, *NFE2L2*, *ACTA2*, *STAR*, *INSL3*, *WT1*, *MAGEA4*, *TNPI*, and *GDF15*. *GAPDH* was used as an internal control for normalization. For each experiment, there were 3 replicates for each gene, and 4 plates were run per vehicle control, and analgesic concentration representing 4 separate and distinct biological replicates ($n = 12$) except for the validation experiments where 3 replicates ($n = 3$) were run for genes *DPP4*, *ACTA2*, *FSP1*, *FNI*, *STAR*, *INSL3*, *WT1*, *MAGEA4*, and *TNPI*.

Immunocytochemistry (ICC)

NHP primary Sertoli cells cultured in the conditions described above were fixed in 4% paraformaldehyde (Electron Microscopy Solutions) for 15 minutes, then blocked with buffer containing 1X Phosphate-buffered Saline solution (PBS, Gibco), 0.1% Triton X (Sigma), and 5% normal goat serum (MP Biomedicals) or normal donkey serum (Jackson ImmunoResearch Laboratories) overnight at 4°C as described [62]. Primary antibodies, *SOX9* and *WT1* (Table 6.8) incubation was performed overnight at 4°C in blocking buffer followed by three washes in 1X PBS with 0.1% Triton X for 10 minutes each at room temperature on an LSE Orbital Shaker (Corning®). Secondary antibody incubation (1:1000, Alexa Fluor™ Invitrogen, Table 6.8) in blocking buffer occurred for 45 minutes at room temperature on Orbital Shaker or overnight at 4°C. Following the

three washes as described above, the samples were co-stained with Hoechst 33342 (1:1000, Invitrogen). All ICC samples were captured using a Nikon DS-Qi2 camera on a Nikon Eclipse Ti microscope. Images were processed using the NIS-Elements AR software (version 5.21.03 64-bit), with 3D deconvolution using the Richardson-Lucy deconvolution technique [301, 302], followed by the creation of an extended depth of focus (EDF) document.

Human testis samples preparation and histological processing

Participants: Sixteen patients with azoospermia or severe oligozoospermia were referred to an andrologist for male infertility at the Clinic of Urology at the University of Zagreb School of Medicine and were included in this study. Each patient was subjected to an open biopsy of the testis [303, 304], as detailed below.

Testicular biopsy: The testicular biopsies were performed under spinal anesthesia, and when possible, a bilateral biopsy was performed. After visualization of the testis and epididymis, a small surgical incision about 8-10 mm in length in the tunica albuginea of the testis was made, as described [305]. The testicular tissue was dissected using surgical micro-scissors and five testicular samples were collected from different parts of the testis to be used for histological analysis, potential sperm extraction, and research purposes. Histological analysis identified one patient ($n = 1$; age 34 years) with fully preserved spermatogenesis according to the Johnson's score [306]. This patient was diagnosed with obstructive azoospermia based on their clinical presentation and histological analysis. The remaining patients ($n = 12$) were diagnosed with various degrees of damage to the testicular parenchyma including: hypospermatogenesis, maturation arrest at either the spermatocyte or spermatid stages, Sertoli cell only syndrome, tubular fibrosis, and a

combination of the previous testicular disorders known as mixed atrophy [306, 307]. These patients were diagnosed with non-obstructive azoospermia. The average age of this group of patients was 39 years old, with an age range of 33-47 years. Three patients ($n = 3$) were diagnosed with germ cell neoplasia *in situ* (GCNIS), a noninvasive precursor to testicular germ cell tumors [308]. The average age of these patients was 39 years old, with an age range of 34-45 years.

Tissue processing: Briefly, testicular tissue was fixed in 10% neutral buffered formalin for 24 hours and rinsed in water overnight. The tissue samples were then dehydrated in a series of increasing ethanol solutions. Following two xylene immersions for clearing, four paraffin immersions were performed. The infiltrated tissue was removed from the cassette, and oriented within a metal mold. Then, the mold was filled with molten paraffin and transferred to the cold plate to set.

Immunohistochemistry (IHC) detection of Cyclooxygenase and Sertoli cell markers

Before proceeding with IHC, paraffin sections of 5 μM -fixed testicular biopsies were deparaffinized and rehydrated in a graded ethanol series. Following high-temperature TRIS buffer antigen retrieval, tissue sections were blocked for 60 minutes at room temperature and then stained with primary antibody COX-1 and SOX9 (Invitrogen, Millipore/FisherSci, R&D Systems, Table 6.8) in blocking buffer for 90 minutes at room temperature or overnight at 4°C. Primary antibodies were detected with secondary antibodies (1:200, Table 6.8) in blocking buffer for 45 minutes at room temperature. Sections were mounted with VectaShield mounting media containing DAPI (Vector Laboratories). All IHC samples were captured using a Nikon DS-Fi2 camera on a Nikon

Eclipse 90i microscope. Images were processed using the NIS-Elements AR software (version 4.06).

Following high-temperature Citrate buffer antigen retrieval, tissue sections were exposed to 3% hydrogen peroxide for 5 minutes. Samples were then blocked in Universal Blocking Reagent (BioGenex) for 5 minutes at room temperature. The samples were incubated for 60 minutes with an Anti-COX2 antibody (BD Transduction Laboratories™) in Renaissance Background Reducing Diluent (Biocare). Biotinylated horse anti-mouse secondary antibody (Vector Laboratories) was incubated on the tissue sections for 10 minutes at room temperature. The samples were labeled with 4plus Streptavidin HRP (Biocare Medical), and then submerged in Betazoid DAB Solution (Biocare Medical) for 12 minutes. The samples were then counterstained with hematoxylin, followed by a bluing reagent stain (Fisher Healthcare™) in preparation for imaging. Except for the antigen retrieval and counterstain steps, all other steps of the COX-2 staining were carried out on the intelliPATH™ (Biocare Medical).

mRNA sequencing, quantification of gene expression level, and differential gene expression analysis

Non-human primate primary Sertoli cell culture, naproxen and ibuprofen exposure, and RNA extraction were carried out as previously described to yield three biological replicates ($n = 3$). Following extraction, the RNA samples were sent to Azenta Life Sciences (Azenta US, Inc.) for mRNA-sequencing analyses. Similar mRNA-sequencing analyses using Azenta's service are shown here [309-311].

Library Preparation and Illumina Sequencing: Azenta Life Sciences checks RNA quantity and quality in two ways: Qubit™ 2.0 Fluorometer (Invitrogen) and Agilent

TapeStation (Agilent Technologies). All mRNA samples sent to Azenta for sequencing passed their quality control. The workstation is described as follows: The RNA sequencing libraries were prepared by using the NEBNext Ultra RNA Library Prep Kit for Illumina (NEB) following the manufacturer's instructions. Briefly, the mRNAs were enriched using Oligo(T) beads and then fragmented for 15 minutes at 94° C. Then, the first and second strand cDNA was subsequently synthesized. The cDNA fragments were end-repaired, and the 3' ends of the DNA fragments were adenylated. The cDNA fragments were ligated to universal adapters, followed by index addition. The library was then generated by PCR amplification with limited cycles. The sequencing library was validated on the Agilent TapeStation (Agilent Technologies) and quantified using the Qubit™ 2.0 Fluorometer (Invitrogen) and quantitative PCR (KAPA Biosystems). The libraries were clustered and sequenced on an Illumina HiSeq instrument with paired-end 150bp (PE150) sequencing. The initial data analysis, including the quality control, adapter sequence trimming, and alignment to the reference genome as described below, was performed at Azenta. From the Illumina instrument, the raw data files were transformed into raw sequenced reads by the Control base calling software. The raw sequence data were converted into FASTQ files and demultiplexed using Illumina's bcl2fastq (v. 2.17) software. Poor-quality adaptors and nucleotides were filtered out to leave clean reads using the Trimmomatic (v.0.36) [312] software. The clean paired-end reads were aligned to the reference genome (*Macaca mulatta*, build Mmul_10, downloaded from the ENSEMBL genome website browser) using the STAR aligner (v.2.5.2b) to generate BAM files.

Quantification of gene expression level and differential expression analysis: The unique gene hit counts were calculated by using featureCounts from the Subread package (v.1.5.2). Transcripts Per Kilobase Million (TPM) was used to estimate the gene expression levels and then used for the downstream differential expression analysis. On the Galaxy server (usegalaxy.org), differential expression analysis for each group of samples (three distinct biological replicates) exposed to naproxen or ibuprofen comparing to the control samples, water and 0.1% ethanol, respectively, were performed using the limma-voom (Galaxy version 3.50.1+galaxy0) method [313, 314]. Genes were considered to have very low expression if they were below a minimum of 0.5 count-per-million (CPM) and were then filtered out if they did not meet this minimum CPM in at least two samples [315-317]. The resulting p-values were adjusted using the Benjamini-Hochberg method to control for the false discovery rate. The trimmed mean of M-values (TMM) from the edgeR package (version 3.36.0) was used as the normalization method in this study. Genes were considered differentially expressed with an adjusted p-value < 0.01 and 1.5-fold change in either direction. The differential expression analysis data and the normalized read counts were used to generate graphs on the Galaxy server using the Volcano Plot (Galaxy version 0.0.5) and heatmap2 (Galaxy version 3.1.1+galaxy1) packages.

Gene set enrichment analysis: The Ensemble of Gene Set Enrichment Analysis (EGSEA; version 1.26.0) package was used to explore the biological signaling pathways and human phenotype ontology in the naproxen-treated samples compared to the water vehicle control and the ibuprofen-treated samples compared to the 0.1% ethanol vehicle control. The rhesus macaque gene symbols produced from limma-voom were matched to

the *Homo sapiens* hg19 reference genome, downloaded from the Ensembl genome website browser for enrichment analysis. The Molecular Signatures Database [318] (MSigDB; version 2022.1) and Human Phenotype Ontology [319] (HPO; version 2022.1) collections were used to explore the Hallmark gene sets and the phenotypic abnormalities in the human diseases collection. The terms from the Hallmark gene sets associated with Sertoli cells and human phenotypes associated with male factor infertility were used to further assess gene function, which were obtained from the NCBI Gene database (<https://www.ncbi.nlm.nih.gov/gene>), and biological relevance [271]. Enrichment results were considered significant if the adjusted p-value (FDR) was < 0.05 . The Gene Set Enrichment Analysis was performed in RStudio (version 2022.12.00) running on R Package (version R-4.2.2). Graphs of the Hallmark gene sets were generated using heatmap2 on the Galaxy server. Protein-protein interactions were visualized with STRING [320].

Statistical analysis

GraphPad Prism software (version 9) was used to analyze the cell viability, mitochondrial membrane potential, TER, paracellular flux, and RT-qPCR data. Significant differences in samples in comparison to the water-only control for naproxen and the ethanol-only control for ibuprofen were determined by the following methods: the cell viability and mitochondrial membrane potential were determined by two-tailed, unpaired *t*-test, where * is $p < 0.05$, ** is $p < 0.01$, and *** is $p < 0.001$. Significant differences for the TER and paracellular flux assays were determined by a two-way analysis of variance (ANOVA) with Dunnett's correction for multiple comparisons, where * is $p < 0.05$, ** is $p < 0.01$, and *** is $p < 0.001$. The results from the RT-qPCR

experiments were calculated by the $\Delta\Delta\text{CT}$ method as normalized fold differences in each target gene except for the NHP Sertoli cell validation experiments, where the relative fold change was calculated by the ΔCT method.

Study approval

Each patient provided their written and informed consent for the surgical procedure, histological analysis of the testicular biopsy, and the research studies. Approval was granted by the Ethics Committee of the School of Medicine at the University of Zagreb (380-59-10106-20-111/171).

4.6 AUTHOR CONTRIBUTIONS

Conceptualization: K.M.S.C., R.C.E, and C.A.E.; Methodology: K.M.S.C., R.C.E., K.F.E., I.K.C., A.P., N.Y., A.C.Z., C.C., C.S., G.S., K.O., D.J., M.K., and C.A.E., Investigation: K.M.S.C., R.C.E., I.K.C., K.F.E., E.W., J.S.M., and K.T.; Analysis: K.M.S.C., K.F.E., and I.K.C.; Writing: K.M.S.C. and C.A.E., Funding Acquisition: C.A.E., Resources: K.F.E., M.K., A.P., D.J., N.Y., K.O., and C.A.E., Supervision: C.A.E.

4.7 COMPETING INTERESTS

The authors declare no competing interests.

4.8 ACKNOWLEDGMENTS

The authors would like to thank Dr. Raymond Swetenburg, Aruna Bio Inc, for his expertise in using the SpectraMax iD5 for the Paracellular Flux (Permeability) assay, Drs. Megan Beaudry and Guanhui Bao (Azenta Life Sciences) for their mRNA sequencing expertise, and Dr. Anthony Chan (Center for Scientific Review, National Institutes of Health) for collecting the non-human primate testicular tissue while as a faculty member at the Yerkes National Primate Center. This work was supported by the National

Institutes of Health (NIH) grant's K22ES025418 and R01OD028223-01 to C.A.E for funding this work.

CHAPTER 5

TESTIBOW: A GENETIC MULTICOLOR PLATFORM FOR LABELING AND ANALYSING IN VITRO HUMAN SPERMATOGENIC CELL POPULATIONS

5.1 INTRODUCTION

5.1.1 Introduction to fluorescent reporters

As one of humans' most powerful sensory systems, vision allows us to see and understand complex information portrayed in a visual display [321]. Visualization tools are particularly useful for studying dynamic biological processes [321], such as spermatogenesis. In the testis, large colonies of differentiating daughter cells from one mature spermatogonium are connected by cytoplasmic bridges until the end of the differentiation, when the sperm are released into the lumen [322]. Similarly, in the *in vitro* human spermatogenesis model, the cells proliferate and differentiate into advanced spermatid-like cells. Analyzing the structure of the testis and seminiferous tubules and the differentiating *in vitro* cell colonies is spatiotemporally challenging without a powerful approach to identify all the different cell types throughout their development visually. Using unique color combinations, individual cells can be tagged for identification, and their behavior can be tracked [321].

In 1962, green fluorescent protein (GFP) was isolated from jellyfish (*Aequorea victoria*) [323]. Since then, other commonly used fluorescent proteins have also been derived from jellyfish, including yellow fluorescent protein (YFP), blue fluorescent protein (BFP), and cyan fluorescent protein (CFP) (reviewed in [324]). Additional

fluorescent proteins were derived from coral (*Discosoma* sp) such as dsRed, dTomato, mOrange, and mCherry [325], and the Bubble-tip anemone (*Entacmaea quadricolor*) such as mKate2 [326]. The development of fluorescent proteins with different excitation and emission spectra has allowed new applications to emerge, combining visual observations to identify specific cell populations with genetic analysis to quantify gene expression in those target populations [321]. Since fluorescent proteins can be used as a minimally invasive and precise tool, they have revolutionized the scientific field of cell or process labeling with contrasting colors [327].

In the mid-2000s, Livet and colleagues [328] developed Brainbow, a powerful technology that genetically labels every cell in a mouse brain with different fluorescent reporters. Using three or four fluorescent proteins, such as red fluorescent protein (RFP), CFP, GFP, and YFP, unique color profiles can be generated to distinguish and identify different mouse neuronal cell types easily. Since Brainbow's development, other fluorescent reporter systems have been used in various disciplines like neurobiology, stem cell biology, and organogenesis for assessing cell interactions, protein function and location, the effects of drugs on cell populations, and lineage tracing (reviewed in [329-332]) by fluorescent microscopy. Advancements in cell labeling techniques have allowed scientists to ask various questions regarding the function of individual cells within a given population and the ability to follow cells spatiotemporally in a variety of model systems such as mice, zebrafish, and *Drosophila* [321]. This advancement has led to our current work of developing Testibow, a fluorescent reporter platform coupled with our *in vitro* human spermatogenesis model. This model will label spermatogenic cells

throughout their development in order to identify potential male contraceptives and characterize potential male reproductive toxicants.

5.1.2 Current status on the development of a male contraceptive

Each year, unintended pregnancies represent nearly half of all pregnancies in the United States (U.S.), and nearly half are unwanted [333, 334]. Unfortunately, these unintended pregnancies account for a majority of abortions each year [335]. To put that into perspective, there are roughly six million pregnancies each year in the U.S. This means that three million of these pregnancies are unintended, of which the three million unintended pregnancies account for the vast majority of abortions annually [335]. Furthermore, unintended pregnancies pose extensive social (e.g., lower psychosocial well-being), health (e.g., increased maternal disability, lower psychological well-being, and poor child health), and economic risks (e.g., lack of health insurance and lower socioeconomic status) world-wide (reviewed in [336-342]). In the U.S. alone, unintended pregnancies cost the nation more than fifteen billion dollars annually [343]. Luckily, the rate of unintended pregnancies has dropped by roughly 10% during the last five years, mainly because women are using longer-acting methods of contraception. This suggests that (1) there is still a gap in contraceptive options and family planning services for couples, and (2) preventing unintended pregnancies is primarily the woman's responsibility [344, 345].

One of the earliest references to birth control dates back to the book of Genesis, in which men practiced coitus interruptus, also known as the “withdrawal” method. In 1827, scientists discovered the ovum, which became one of the first steps in understanding human reproduction. Before, it was only known that semen must enter the female body

for fertilization to occur. Shortly after that, in 1839, Charles Goodyear invented vulcanized rubber and began manufacturing rubber condoms, but in 1920, most condoms started to be made out of latex and, as a latex allergy alternative, polyurethane [335]. Four years later, scientists discovered that conception occurs when the sperm enters the egg. By the 1870s, various birth control devices could be purchased in the U.S., such as condoms, diaphragms, and douching syringes from catalogs, pharmacies, and stores. But between 1873-1974, several states created anti-birth control laws that prohibited the sale or advertisement of contraceptive devices. In some states, such as Massachusetts, it was a felony to sell, prescribe, or even give out information about birth control. In other states, like Connecticut, it was a crime for couples to use contraception. By 1960, a modern contraceptive method for women was developed, known as “the pill.” By 1990, “the pill” was considered safe and effective by the Food and Drug Administration (FDA), healthcare providers, and the general public, and now, most couples are choosing to use this to method to assist in their family planning needs (reviewed in [346]). Today, women have many contraceptive options, including patches, intrauterine devices, implants, and injections. Family planning is recognized as one of the top ten greatest public health achievements during the 20th century [347]. Access to family planning and contraceptive services has provided health (e.g., smaller family size, more time between the birth of children, a decrease in infant, child, and maternal deaths, and the use of barrier contraceptives to prevent pregnancies and the transmission of sexually transmitted diseases), and social benefits (e.g., increased opportunities for preconceptional counseling) [347].

Worldwide and in the U.S., millions of women use some form of hormonal contraception. While generally considered safe and effective at preventing unintended pregnancies, some women experience adverse side effects that lead to either voluntary cessation or medically required termination due to health conditions such as uterine bleeding, amenorrhea, or deep vein thrombosis [348]. In these cases, women are left with few reliable contraceptive options to assist in their family planning needs. As of 2014, it is estimated that 225 million women in developing countries need of contraception [349].

In contrast, men have had the same three options for over 100 years- condoms, withdrawal, and vasectomies [333]. Though it has been suggested that men are not involved in family planning, current male contraceptives account for 30% of all contraceptive use, with 6% of couples relying on vasectomies and 20% depending on condom use, both of which have significant drawbacks [350]. In the U.S., condoms have a failure rate of 15-20%, the withdrawal method fails slightly more at 20% of the time, and vasectomies have a failure rate of about 1% but are a permanent and nonreversible method [335, 351, 352]. Due to their limitations, these three methods may not be suitable for all men. Yet, international surveys have revealed men's desire to take on a larger role in family planning, including using reversible contraceptives [335, 351, 353].

Additionally, 13.5 million men living in the U.S. are believed to use a new contraceptive if one were available [351, 353, 354]. Furthermore, most contraceptive surveys report women would trust their partner to use a new contraceptive [351, 353] if one would become available; therefore, allowing both men and women to contribute to their family planning process in whatever way they deem appropriate. However,

developing new forms of male contraceptives has been challenging since men produce sperm throughout their entire adult life.

There are three approaches to developing a male contraceptive [335]. The first approach is to target the sperm in the ejaculate and inhibit the sperm's motility, function, or binding to the ovum. However, this is difficult to get medicine into the small volume of the ejaculate and to have it still work in the female reproductive tract. The second approach is to interfere with sperm production. Since men make about 1,000 sperm per heartbeat, current studies are looking to achieve severe oligozoospermia, or a sperm concentration of 1 million/mL [355], similar to a female contraceptive failure rate of 1% [356]. While the complete absence of sperm in the ejaculate, known as azoospermia, would make fertilization of an egg impossible and would ensure the efficacy of a contraceptive, achieving and maintaining this level has not been completed to date [335]. The third approach is preventing the sperm from reaching the egg through physical barriers, such as condoms and vasectomies. Thus, a male contraceptive that blocks spermatogenesis without causing damaging the spermatogonial stem cell population or causing reproductive health problems is ideal.

Scientists have been working to develop both hormonal and nonhormonal approaches. Several hormonal contraceptives have had an overall success rate greater than 90% but were abandoned in clinical trials due to unwanted side effects in men [357-361]. However, the most advanced male contraceptive is a progestin gel with testosterone called Nestorone[®] (Nes). This transdermal gel is an easy-reversible contraceptive that suppresses sperm production while maintaining normal levels of testosterone with minimal side effects [362] and is currently in Phase II clinical trials. Additional hormonal

contraceptives, Dimethandrolone and 11 β -Methyl Nortestosterone Dodecylcarbonate were in clinical trials, but the latest updates were posted in 2019 [363]. As an alternative to a vasectomy, an injectable polymer of styrene and maleic anhydride called RISUG[®] (Reversible Inhibition of Sperm Under Guidance) is currently in Phase III clinical trials in India, but experiments have slowed due to an insufficient number of participants [364]. Developing a male contraceptive has been slow and challenging, mainly due to the lack of an effective screening method.

Rodent models have primarily been used to assess potential male contraceptives. While animal models allowed some extrapolation to humans and provided valuable information, as Chapter 1 of this dissertation mentions, these models are kinetically and biologically distinct from humans [47, 365, 366]. In the context of male contraceptive development, rodent models tend to utilize genetically identical strains that do not accurately represent the genetic diversity within the human population. This may not identify potentially effective male contraceptives across multiple genetic backgrounds. Likewise, they can respond differently to certain chemicals than humans [59, 365], and thus potential contraceptives could be effective in rodents but not humans. While non-human primate models share similar biological reproductive mechanisms to humans [47], these experiments are often expensive. Therefore, we sought to develop a uniquely high-content/ high-throughput fluorescent reporter system that would allow rapid, unbiased, and efficient screening of potential male contraceptives. By examining potential male contraceptives for their reversibility and potential off-target alterations, we can address the current roadblocks plaguing the development of an effective male contraceptive.

5.2 STUDY INNOVATION

The current failures in developing a male contraceptive originate from the lack of a robust, rapid, and unbiased human spermatogenesis platform. We previously demonstrated that a human *in vitro* spermatogenesis model mimics several major stages of human spermatogenesis, including the production of spermatogonial stem cell-like cells, primary and secondary spermatocyte like-cells, and spermatid like-cells [62]. This model has been used to assess the reproductive toxicity of several environmental chemicals [12, 59, 64, 65] and pharmaceuticals (unpublished) on spermatogenesis using several genetically distinct human pluripotent stem cell lines. Thus, we sought to develop a novel fluorescent reporter system coupled with our *in vitro* human spermatogenesis model to provide the ideal platform for identifying potential contraceptives and to address the safety and efficacy challenges associated with male contraceptive development.

5.3 RESULTS: TESTIBOW 1.0: A FLUORESCENT REPORTER SYSTEM COUPLED WITH OUR IN VITRO MODEL OF HUMAN SPERMATOGENESIS

The overall goal of our project was to generate an *in vitro* fluorescent reporter system to enable high throughput and high content screening of potential male contraceptives in an unbiased way. To accomplish our goals, we developed a fluorescent reporter system, Testibow 1.0, coupled with our *in vitro* human spermatogenesis model. This system used stage-specific spermatogenic related genes to drive fluorescent expression throughout the spermatogenic differentiation process. For example, a *ZBTB16/ PLZF*, a zinc-finger transcription factor expressed in spermatogonial stem cells and progenitor spermatogonia [367-369], gene promoter would drive CFP expression. Then, as the cells continue to differentiate into primary spermatocyte-like cells, these

cells will express *PIWIL2/HILI*, a pre-meiotic spermatocyte marker, gene promoter driving GFP expression. Next, the cells in the secondary spermatocyte stage would express *PIWILI/ HIWI*, an essential protein involved in the spermatogenic progression from spermatogonial stem cells to round spermatids [370] gene promoter driving mCherry expression. Lastly, the spermatid-like cells would express the *PRMI/ Protamine 1*, a protein in which the sperm chromatin undergoes a transition where the histones are replaced by protamines by transition proteins [371] gene promoter driving tdTomato expression (Figure 5.1). Therefore, in order to identify potential male contraceptives with our model, we would want the compound to either block spermatogonia differentiation (as represented by only CFP+ cells and negative for GFP, mCherry, and tdTomato) or blocks meiotic entry (as represented by only CFP+ cells or CFP+ and GFP+ and negative for mCherry and tdTomato). If a compound would cause the death of our CFP+ spermatogonium, this compound would be eliminated because maintaining the viability of the spermatogonium is essential to not only allow the patients to produce offspring following cessation of the contraceptive, but it could have disastrous consequences such as causing sterility. Additionally, any compound that does not suppress tdTomato expression would be eliminated for further contraceptive consideration due to the potential fertilization capabilities of the remaining sperm.

In order to develop our platform, we purchased our lentiviral fluorescent promoter constructs from GeneCopoeia™, Inc., a biotechnology company located in Maryland. Compared to nonviral methods, viral transductions are usually more efficient [372]. Although adenoviruses have been used to accommodate different research purposes, we chose to use a lentiviral vector due to their higher stable transducing efficiency in human

embryonic stem cells [373], and that the transgenes would be permanently integrated into the host genome, so that the gene expression is stable and inheritable [374]. Therefore, Dr. Easley and our collaborator, Dr. Anthony Chan, generated high titer lentivirus for each construct. Before the transduction, we established the Puromycin Kill Curve to determine the minimal concentration to kill the non-transduced human embryonic stem cells (ESCs) over four days. During the first three years of my doctoral program, I optimized a protocol to produce genetically modified and stable human ESC cell lines. Briefly, this transduction protocol begins by seeding the human ESCs sparsely and in small aggregates on Matrigel[®] coated dishes. The following day, the cells were treated with polybrene, a polymer that enhances the efficiency of lentiviral infection in mammalian cells [375] during a one-hour spinoculation. Afterward, the cells were incubated with both polybrene and lentivirus for eight hours at 37° C, after which the cells receive fresh media. To develop Testibow 1.0, we completed three individual lentiviral transductions with the three viral transgenes. Three days following the lentiviral transductions, the cells were treated with puromycin in basal media to select colonies that express the plasmids. Following the puromycin selection, the cell colonies were manually propagated for cell line expansion and polymerase chain reaction (PCR)-based validation experiments. Once the cell lines were validated, they were differentiated in our *in vitro* spermatogenesis model to determine if the fluorescent reporter system was functioning properly.

Based on the preliminary results from the PCR analyses, we successfully generated three individual cell lines that express each fluorescent reporter (Figure 5.2 A-C). Although the bands in Lane 2 of A and B are faint, possibly due to a low transduction

efficiency and number of cells carrying the transgene, we decided to differentiate these cell lines anyways to determine whether the fluorescent reporter would function as we expected. With success, each of the three fluorescent reporters function as expected (Figure 5.2 D-F).

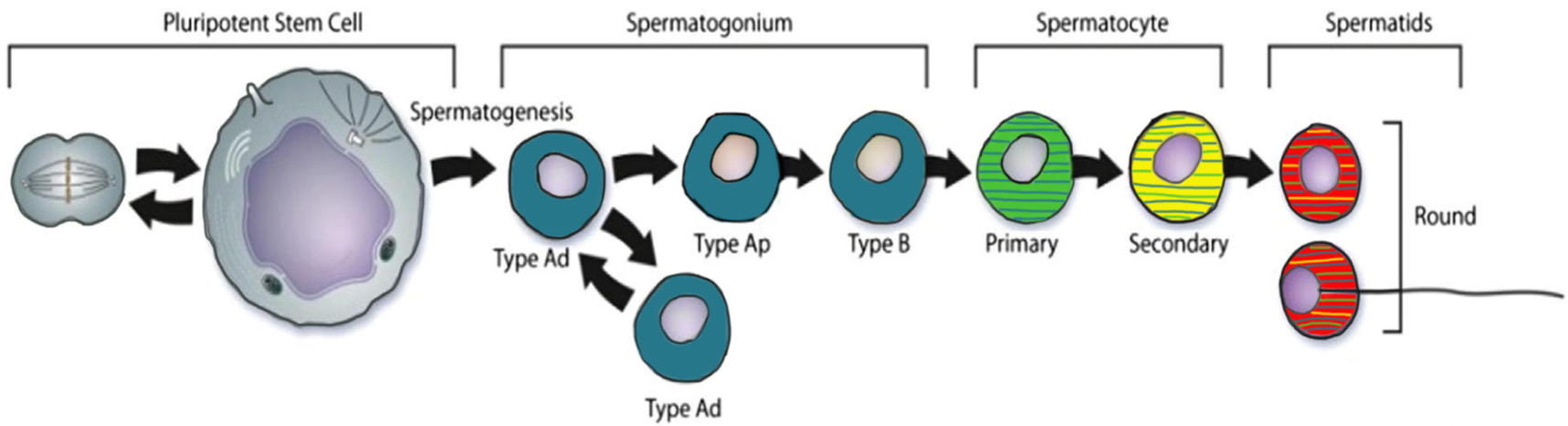


Figure 5.1. Diagram of the fluorescent reporter system, Testibow 1.0. A diagram of the fluorescent reporter system, Testibow 1.0, coupled with our established *in vitro* human spermatogenesis model. This schematic represents the various stages where we expect to observe each fluorescent reporter. The ideal male contraceptive would block spermatogonia differentiation (as represented by only CFP+ spermatogonia) or blocks meiotic entry (as represented by CFP+ spermatogonia or CFP+ spermatogonia and GFP+ primary spermatocytes) in our *in vitro* cultures.

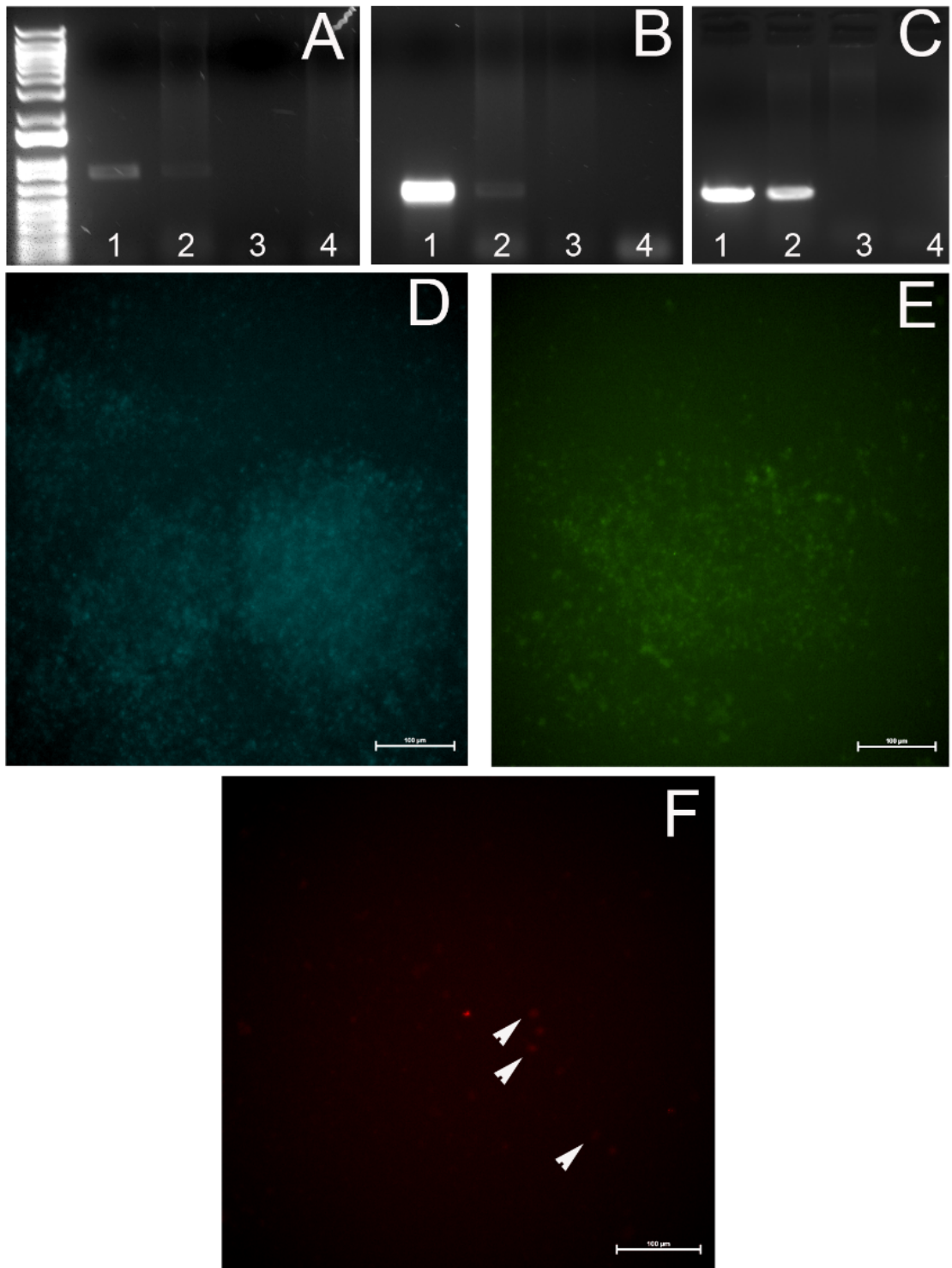


Figure 5.2. Characterization of human male ESCs transduced with the spermatogenic fluorescent reporters. (A-C) PCR validation of clonal human embryonic stem cells transduced with the spermatogenic promoters driving fluorescent protein expression. (A) *ZBTB16*-CFP (B) *PIWIL2*-GFP and (C) *PRMI*-tdTomato. The lanes for the PRC reactions are labeled as follows: Lane 1: Positive control/ Vector, 2: DNA from 1 clonal transduced cell line, 3: DNA from non-transduced human embryonic stem cells, 4: No template negative control. (D-F) Live cell fluorescent images showing functionality of the fluorescent reporter system coupled with our *in vitro* human spermatogenesis model. (D) CFP fluorescent protein expression in the differentiating human embryonic stem cell colonies signifying *ZBTB16* expression, representing the spermatogonium. (E) GFP fluorescent protein expression in the differentiating human embryonic stem cell colonies signifying *PIWIL2* expression, representing the primary spermatocytes. (F) tdTomato expression in certain cells signifying *PRMI* expression, representing the spermatids (arrows highlighting some examples). Scale Bars: 100 μ M.

5.3 RESULTS: TESTIBOW 2.0: A POLYCISTRONIC FLUORESCENT REPORTER SYSTEM COUPLED WITH OUR IN VITRO MODEL OF HUMAN SPERMATOGENESIS

To overcome the challenge of generating a stable human ESC line that expressed all three of our fluorescent reporters simultaneously, we designed and purchased a polycistronic version with each of the fluorescent reporters on one lentiviral vector from VectorBuilder Inc. to be integrated into our *in vitro* fluorescent reporter system (Figure 5.3). VectorBuilder synthesized the lentiviral vector and prepared the high-titer lentivirus for us. Known as Testibow 2.0, our polycistronic fluorescent reporter system used stage-specific spermatogenic related genes to drive fluorescent expression throughout the spermatogenic differentiation process. For example, *ZBTB16*/ PLZF promoter drove mOrange2 expression marking our spermatogonia/ spermatogonial stem cell-like cells. Then, as the cells continued to differentiate into primary spermatocyte-like cells, these cells expressed the *PIWIL2*/ HILI promoter driving GFP expression. Lastly, the spermatid-like cells expressed the *PRMI*/ Protamine 1 promoter driving mKate2 expression (Figure 5.4). In order to identify potential male contraceptives with this model, we would want the compound to either block spermatogonia differentiation (as represented by only mOrange2⁺ cells and negative for GFP and mKate2) or blocks meiotic entry (as represented by only mOrange2⁺ cells or mOrange2⁺ and GFP⁺ and negative for mKate2). Again, any compound that would cause death in the mOrange2⁺ spermatogonium would be eliminated because any impact on spermatogonia viability could have disastrous consequences in humans (e.g., sterility). Additionally, compounds

that do not suppress mKate2 expression would be eliminated for further consideration due to the potential fertilization capability of the remaining spermatids.

Prior to transduction, we re-established the Puromycin Kill Curve to determine the minimal concentration to kill the non-transduced human ESCs over the course of four days. Then, by utilizing our optimized lentiviral transduction, puromycin selection, and clonal line expansion protocols from Testibow 1.0 and the new puromycin kill curve, we successfully established a stable clonal hESC line that expressed our polycistronic fluorescent reporter. After establishing a stable, clonal Testibow 2.0 cell line, we performed PCR-based validation to confirm that the fluorescent reporters were stably integrated into the genome (Figure 5.5). Once the cell lines were validated, they were differentiated in our *in vitro* spermatogenesis model to determine if the fluorescent reporter system was functioning properly. Unfortunately, we could not observe robust fluorescence during the differentiation (Figure 5.6). The level of intensity of our fluorescence was too weak for our model to function as a high content approach.

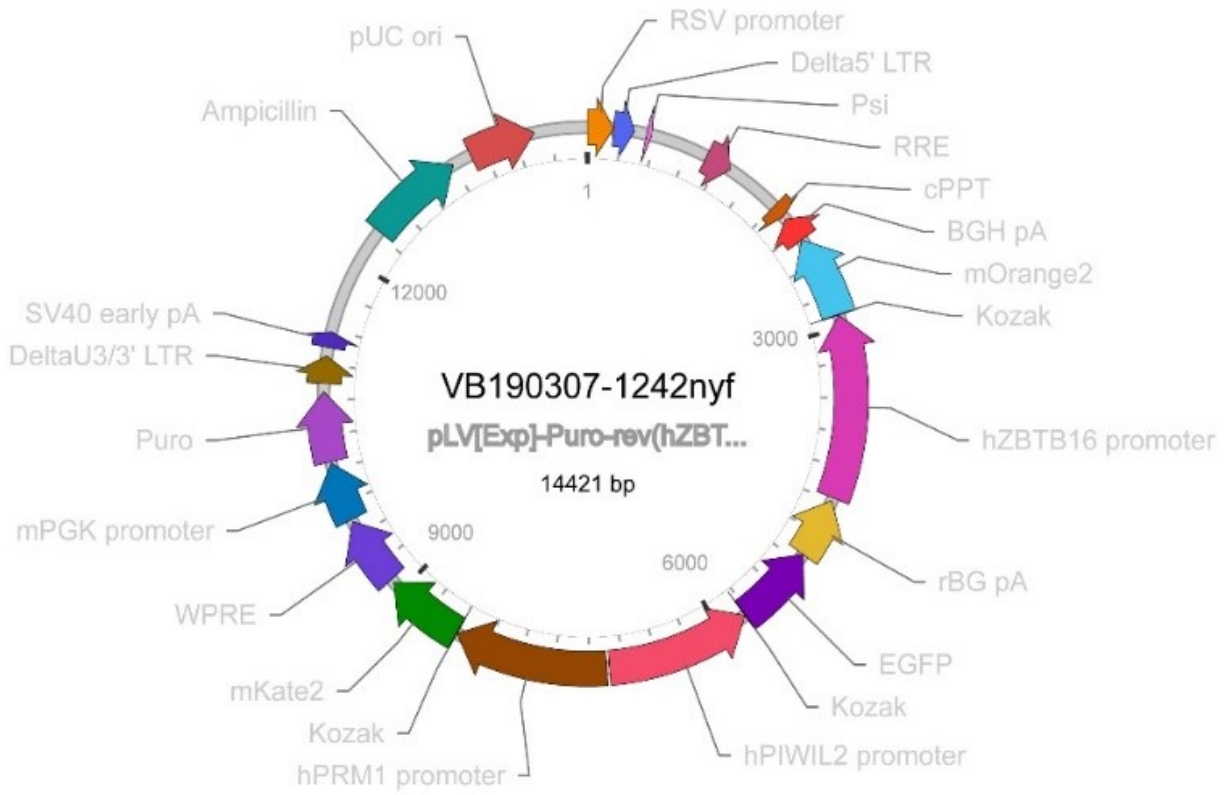


Figure 5.3. A polycistronic vector for the in vitro fluorescent reporter system.

Graphical illustration of the polycistronic fluorescent reporter that we designed and purchased from VectorBuilder, Inc. *ZBTB16*/PLZF promoter driving mOrange2 expression (marking spermatogonia/ spermatogonial stem cells), *PIWIL2*/HILI promoter driving GFP expression (marking primary spermatocytes), and *PRM1*/ Protamine 1 promoter driving mKate2 expression (marking spermatids). This construct contains a puromycin cassette for selecting lentiviral transduced cell lines.

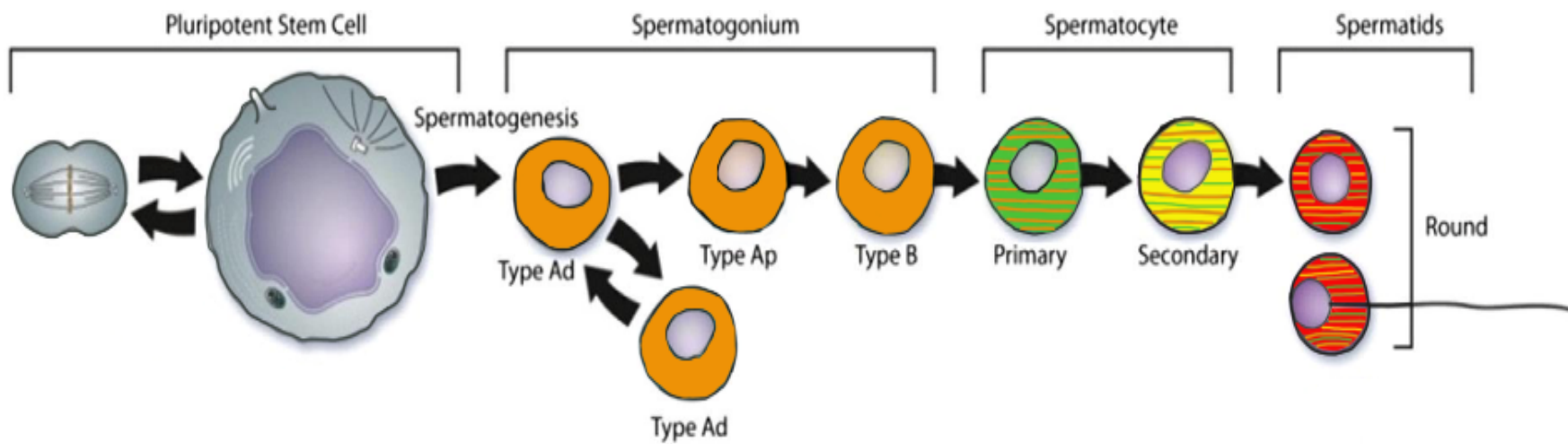


Figure 5.4. Diagram of the polycistronic fluorescent reporter system, Testibow 2.0.

The fluorescent reporter system integrated into our established *in vitro* spermatogenesis model represents the various stages where we expect to observe each fluorescent reporter. The ideal male contraceptive would block spermatogonia differentiation (as represented by only mOrange2⁺ spermatogonia) or blocks meiotic entry (as represented by mOrange2⁺ spermatogonia or mOrange2⁺ spermatogonia and GFP⁺ primary spermatocytes) in our cultures.

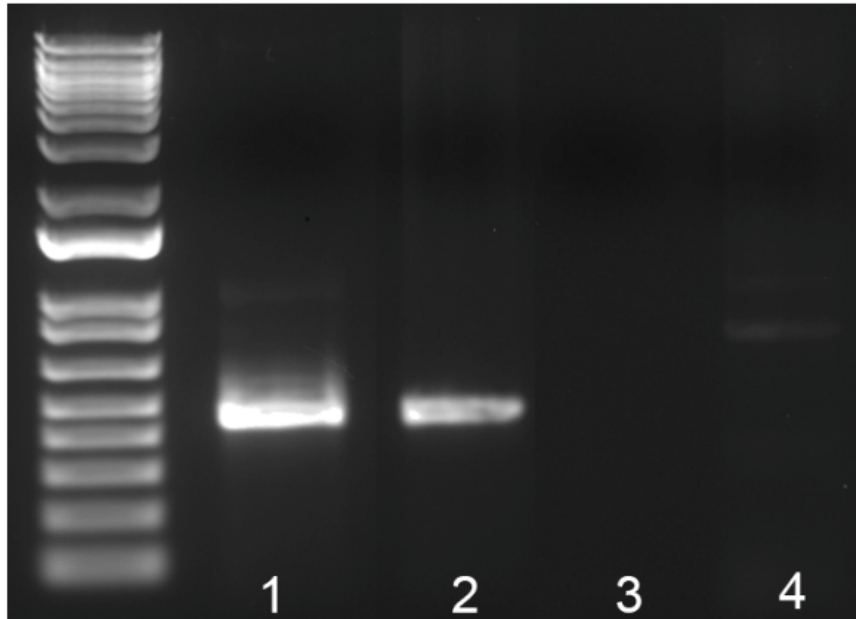
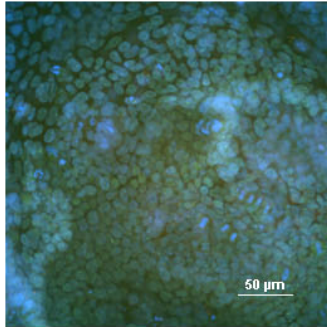


Figure 5.5. PCR Validation of the human male ESCs transduced with Testibow 2.0.

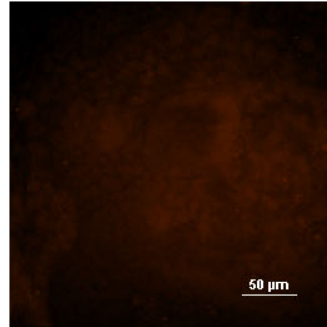
PCR validation of clonal human embryonic stem cells transduced with the Testibow 2.0 Polycistronic Fluorescent Reporter. The lanes for the PCR reaction are labeled as such:
Lane 1: Positive control/ Vector, 2: DNA from 1 clonal transduced line, 3: No template negative control, 4: DNA from non-transduced human embryonic stem cells.

Day 10

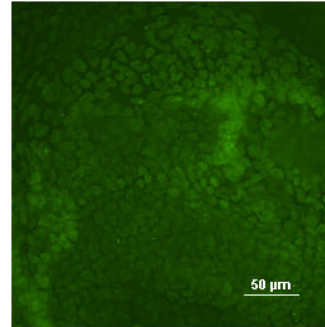
Merged



Testibow 2.0
ZBTB16-
mOrange2



ZBTB16



Hoechst
33342

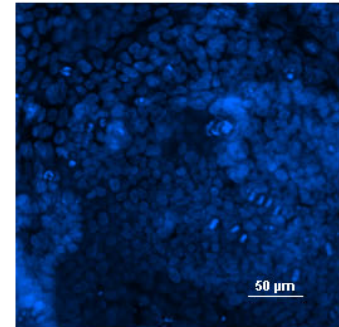


Figure 5.6. Functionality of Testibow 2.0. Co-immunostaining of fixed spermatogenic differentiations showing functionality of the fluorescent reporter system, Testibow 2.0, coupled with our *in vitro* human spermatogenesis model. mOrange2 fluorescent protein expression in the differentiating human embryonic stem cell colonies signifying *ZBTB16* expression, representing the spermatogonium (orange). Endogenous *ZBTB16* immunostaining in the differentiating human embryonic stem colonies also representing the spermatogonium (green). The cells were co-stained with Hoechst 33342 (blue). Scale Bars: 50 μ M.

5.4 OUTCOMES AND CHALLENGES ASSOCIATED WITH TESTIBOW 1.0 AND TESTIBOW 2.0

5.4.1 Proof of concept: Testibow 1.0

Here we showed that we could develop a fluorescent reporter system for our *in vitro* spermatogenesis model that labels spermatogenic cells throughout their development. Based on our preliminary results, we have generated stable cell lines that individually express each fluorescent reporter (Figure 5.2 A-C). Further, we confirmed each fluorescent reporter construct functions properly and fluoresces when the human ESCs were differentiated in our *in vitro* human spermatogenesis model (Figure 5.2 D-F). Overall, Testibow 1.0 served as proof that we can successfully generate a fluorescent reporter platform that can be coupled to our *in vitro* human spermatogenesis model, which could potentially serve as a high content and high throughput platform for screening potential male contraceptives. However, before we can use this model to screen compounds rapidly and unbiasedly, there are a few challenges that we need to overcome.

After optimizing the lentiviral transduction protocol, we decided to omit the *PIWILI*/HIWI mCherry construct since there was (1) spectral overlap with tdTomato that we could not resolve with our microscope setup, (2) both the secondary spermatocyte-like cells and spermatid-like cells are haploid cells and a marker for both would be redundant, and (3) the spermatid-like cells are more prevalent in our *in vitro* spermatogenic cultures than the secondary spermatocyte-like cells. We determined that for screening potential male contraceptives that do not impact the viability of the spermatogonial stem cells but blocks meiosis, having a spermatogonium, a primary spermatocyte, and a spermatid fluorescent reporter in our system would be sufficient for

our model to screen potential male contraceptives rapidly and unbiasedly. Furthermore, we were unable to transduce multiple lentiviral vectors into one cell line at one time. This was due to (1) the high requirement of lentivirus needed for a proper multiplicity of infection (MOI) to observe fluorescence in the differentiating human ESCs and (2) the amount of lentivirus needed to obtain a proper MOI for three different vectors causes cell death (viral overload). To overcome the challenge of generating a stable human ESC line that expressed all three fluorescent reporters simultaneously, we designed and purchased a polycistronic version of our fluorescent reporter system with each fluorescent reporter on one lentiviral construct through VectorBuilder Inc.

5.4.2 *Testibow 2.0: a polycistronic fluorescent reporter system*

With the new polycistronic version of our fluorescent reporter system, we successfully generated several stable cell lines that, when differentiated in our *in vitro* human spermatogenesis model, function as a fluorescent reporter system (Figures 5.5 and 5.6). However, we have been unsuccessful in observing robust fluorescence in the differentiating human ESCs (Figure 5.6). We believe this was due to the lentivirus being subjected to inactivation by the human ESCs. However, while lentiviruses have a transduction efficiency of up to 70% in human ESCs [376] viral vectors used as gene delivery vehicles may be subjected to silencing in the host cells [377]. This inactivation can occur immediately following the transduction and integration of the transgene into the host genome [377], during propagation [378], or differentiation [379]. This inactivation ultimately led to significantly lower lentiviral transgene expression in the human ESCs differentiated *in vitro*. To address this, we conducted various experiments utilizing different time points of our lentiviral transductions and spermatogenic

differentiation, resulting in the same faint fluorescence observed (not shown). As an alternative approach, we are currently utilizing CRISPR (Clustered, Regularly Interspaced Short Palindromic Repeats)/Cas9-mediated genome editing technology to fluorescently tag the endogenous genes of interest to generate our fluorescent reporter system.

5.5 CURRENTLY IN PRODUCTION: TESTIBOW 3.0

5.5.1 Introduction to genome editing technology mediated fluorescent tagging of endogenous proteins

In the 2000s, advancements in genome editing technologies (e.g., zinc-finger nucleases and transcription activator-like effector nucleases) have enabled site-specific genetic mutations in various cell types (reviewed in [380]) with high efficiency [381, 382]. Perhaps one of the most well-known modern genome editing technologies is the RNA-guided CRISPR/Cas9 nuclease system [383]. This editing system uses a guide RNA (gRNA) to target a protospacer-adjacent motif (PAM) and a Cas9 endonuclease to generate a double-stranded DNA break at the target genomic locus [384]. Genetic deletions or insertions can be generated by DNA damage repair mechanisms which can be used to achieve a desired editing outcome [383]. For example, the non-homologous DNA end joining repair mechanism can generate a genetic knockout. In contrast, when a DNA repair template is introduced, the homology directed repair mechanism can replace regions of the genome at the Cas9-induced DNA break [384]. Thus, the CRISPR/Cas9 mediated homology directed repair mechanism can be used to fluorescently tag endogenous proteins, such as BFP attached to *MAGEA4*, (a spermatogonia-related gene) in human cells. By adding the fluorescent tags to the endogenous spermatogenic-related

genes, we can circumnavigate the challenges associated with Testibow 1.0 and 2.0 to generate our *in vitro* fluorescent reporter system.

5.5.2 Testibow 3.0 idea

To overcome the challenges in Testibow 1.0 of generating a stable human ESC line that expressed all three of our fluorescent reporters simultaneously and inactivation of the lentiviral vector in Testibow 2.0, we designed and purchased a tri-reporter cell line in human BJ fibroblasts (ATCC; CRL-2522) from ThermoFisher Scientific. Following the generation of stable BJ cell lines with our tri-fluorescent reporters, these cells will then be reprogrammed into induced pluripotent stem cells and differentiated in our *in vitro* human spermatogenesis model to observe fluorescence. Known as Testibow 3.0, our *in vitro* fluorescent reporter system will use fluorescent tagging to stage-specific endogenous spermatogenic proteins to generate fluorescence in real-time. For example, the *MAGEA4* endogenous protein is fused with the BFP fluorescent protein representing our spermatogonia/ spermatogonial stem cell-like cells. Then, as the cells continue to differentiate into primary spermatocytes, these cells would express the endogenous *PIWIL2* protein fused with the YFP fluorescent protein. Lastly, the spermatid-like cells would express the endogenous *PRMI* protein fused with the mKate2 fluorescent protein (Figure 5.7). Therefore, in order to identify potential male contraceptives with this model, we would want the compound to either block spermatogonia differentiation (as represented by only BFP+ cells and negative for YFP and mKate2) or blocks meiotic entry (as represented by only BFP+ cells or BFP+ and YFP+ and negative for mKate2 cells). Thus, any compound that causes death in the BFP+ spermatogonium would be eliminated because any impact on spermatogonia viability could have disastrous

consequences in humans (e.g., sterility). Additionally, compounds that do not suppress mKate2 expression would also be eliminated for further consideration due to the potential fertilization capabilities of the remaining sperm.

5.5.3 Project milestones to date

To date (March 7, 2023), Life Technologies Corporation, operating as the Life Sciences Solutions Group of ThermoFisher Scientific, has worked diligently over the last several years to synthesize our tri-reporter cell line in the BJ fibroblast cells. Briefly, our colleagues at ThermoFisher have been successful in designing and synthesizing donor DNA, guide RNAs (gRNAs) or TALEN mRNA to target the *MAGEA4*, *PIWIL2*, and *PRMI* loci in the BJ cells, antibiotic kill curve validations, and stable pool generation of *MAGEA4*/BFP + *PIWIL2*/YFP. Currently, our colleagues are generating a stable cell pool with *PRMI*/mKate2 into the fully selected *MAGEA4*/BFP + *PIWIL2*/YFP cell pool. The protocols and milestones to generate the BJ fibroblast line with the fluorescent reporters integrated at the genes of interest are summarized below.

To perform the triple gene knock-in in the BJ cells, we chose to use the CRISPR/Cas9 system for the genome editing. We decided to change the spermatogonia marker to the *MAGEA4* gene for one of the CRISPR/Cas9-mediated gene knock-ins because it is a specific male germ cell marker [385]. Our colleagues at ThermoFisher successfully designed and synthesized donor DNA for our three knock-ins. The *MAGEA4* donor DNA was designed and prepared using the TrueTag™ Donor DNA Kit (ThermoFisher) and the TrueTag™ BFP-pPuro DNA template. This donor DNA will then be co-transfected with Cas9 and gRNA to promote the knock-in of the BFP+ pPuro at the c-terminus of *MAGEA4*. The *PRMI*/mKate2 and *PIWIL2*/YFP plasmids were

successfully generated using GeneArt[®] (ThermoFisher) and then will be paired with the CRISPRs or TALENS to facilitate gene knock-in (Figure 5.8). Next, our colleagues designed and synthesized three CRISPR gRNAs or TALEN mRNAs targeting our specific endogenous genes. CRISPR gRNA was designed to target the human *MAGEA4*, *PIWIL2*, and *PRMI* genes. If there were no suitable CRISPR cut sites within ten base pairs of the target site, TALEN mRNA was designed instead. The gRNAs were designed using the GeneArt[®] Precision gRNA Synthesis Kit (ThermoFisher) and then purified using the MEGAclean[™] Transcription Clean-Up Kit (ThermoFisher) to the *MAGEA4* and *PIWIL2* gene regions of interest to promote c-terminus knock-in (Table 5.1). TALEN mRNAs were designed and synthesized to target the *PRMI* gene region of interest to promote c-terminus knock-in (Table 5.2). In order to select the BJ cells with successful knock-ins at our three genes of interest, our colleagues determined the sensitivity of the BJ cells to three antibiotics, Blasticidin (Bsd), Puromycin (pPuro), and Hygromycin (pHyg). These results indicated that BJ cells were effectively killed with 3.13 µg/mL Blasticidin, 0.75 µg/mL Puromycin, and 0.2 mg/mL Hygromycin (Figure 5.9), and that these concentrations should be used for down-stream selection and analysis. Then, our colleagues performed CRISPR/Cas9-mediated *MAGEA4*/BFP knock-in. The BJ cells were transfected with the Cas9 + *MAGEA4* gRNA and donor DNA to promote the knock-in of BFP-pPuro at the c-terminus of *MAGEA4*. Briefly, the Cas9 protein (ThermoFisher), CRISPR gRNA, and C-*MAGE4*-BFP-pPuro donor were added to the transfection system buffer for the CRISPR transfections. After a short incubation period, the cells were added to the mixture, followed by electroporation. Following the transfection, the cells were allowed to expand and were then selected using puromycin.

These surviving cells were harvested and used for PCR confirmation and sequencing analysis. This milestones' result confirmed the insertion of the cassette at the correct location (Figure 5.10). Additionally, the BJ C-*MAGEA4*-BFP-pPuro stable pool cells were transfected with Cas9 + *PIWIL2* gRNA and donor DNA to promote knock-in of YFP-pBsd at the C-terminus of *PIWIL2* following the same protocol to generate the BJ C-*MAGEA4*-BFP-pPuro + C-*PIWIL2*-YFP-pBsd stable cell pool. These results indicated that the C-*PIWIL2*-YFP-pBsd cassette was successfully integrated at the correct location (Figure 5.11). Currently, our colleagues are working to initiate a stable cell pool with the *PRM1*-mKate2-pHyg cassette into the fully selected C-*MAGEA4*-BFP-pPuro + C-*PIWIL2*-YFP-pBsd pool.

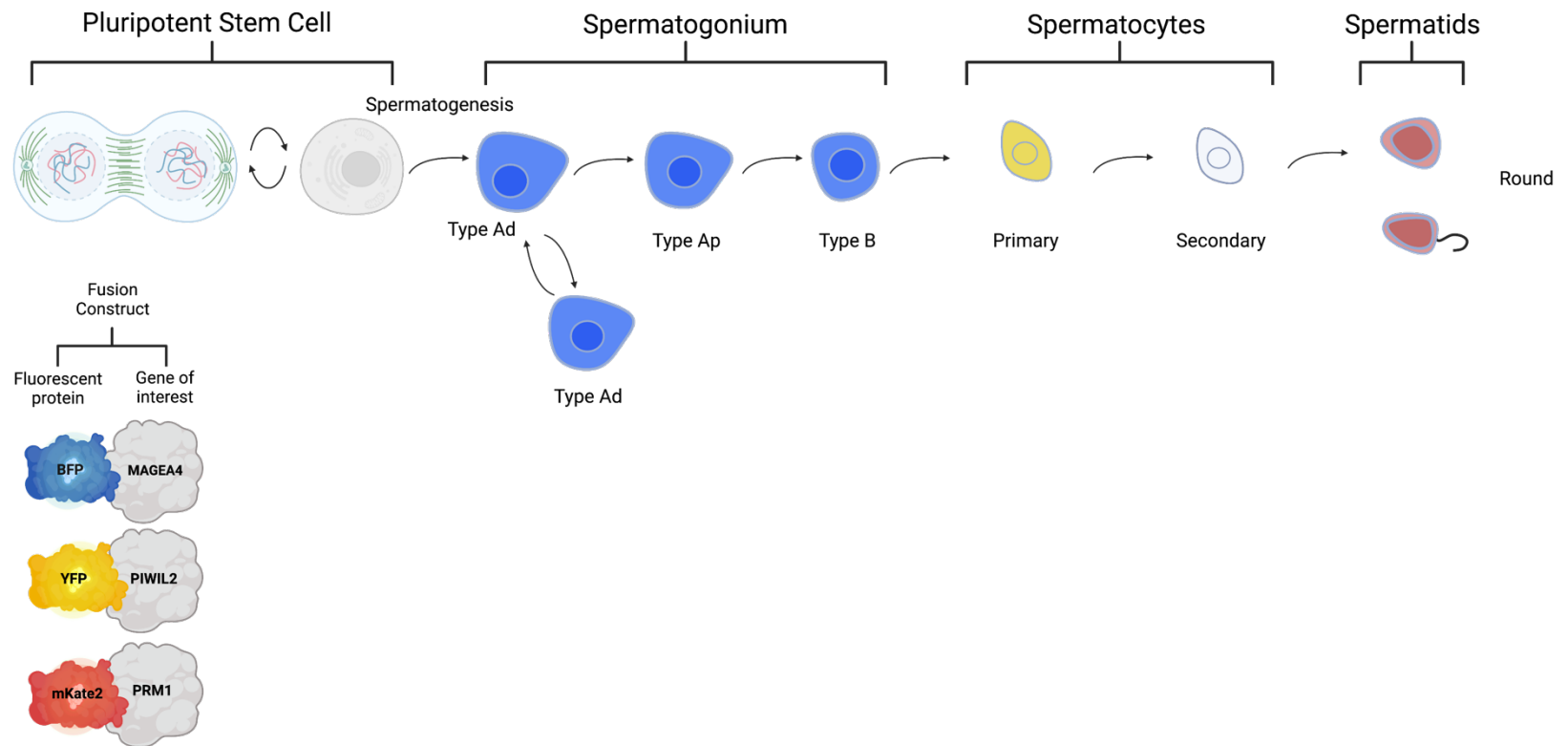


Figure 5.7. Diagram of the fluorescent reporter system, Testibow 3.0. The fluorescent reporter system integrated into our established *in vitro* human spermatogenesis model representing the various stages where we expect to observe each fluorescent reporter. The ideal male contraceptive would block spermatogonia differentiation as represented by only BFP+ spermatogonia or blocks meiotic entry as represented by BFP+ spermatogonia or BFP+ spermatogonia and YFP+ primary spermatocytes in our cultures.

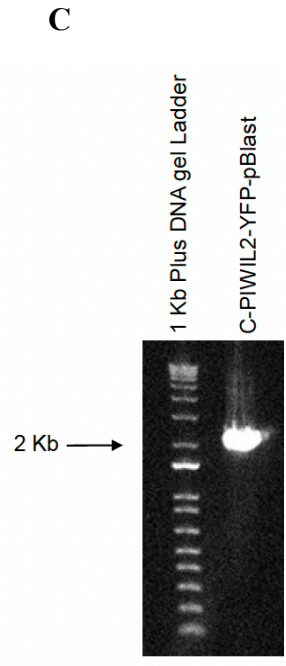
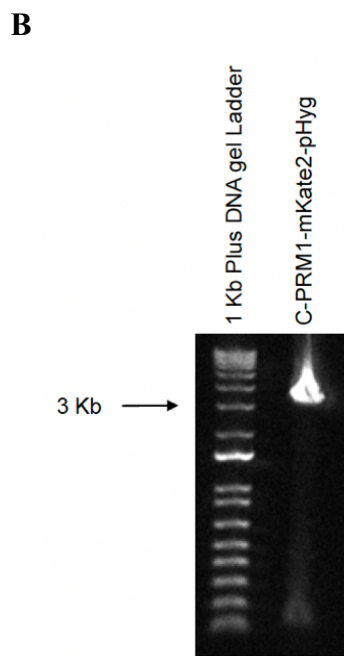
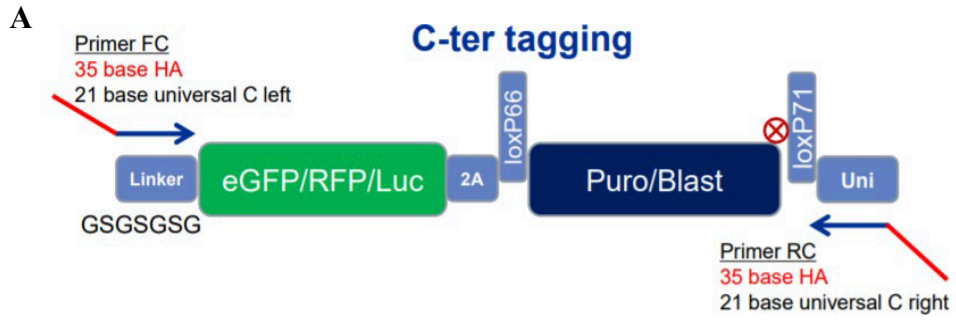


Figure 5.8. Donor DNA synthesis. (A) Schematic representation of the TrueTag™ BFP-pPuro cassette. The Primer FC and Primer RC indicate the *MAGEA4* TrueTag Forward primer and Reverse primers, respectively. (B) The *C-PRMI*-mKate2-pHyg donor fragment was amplified and loaded onto a 1% agarose gel and run alongside a 1 Kb Plus DNA gel ladder. The expected fragment size was 3,071 Kb. (C) The *C-PIWIL2*-YFP-pBlast (Bsd) donor fragment was amplified and loaded onto a 1% agarose gel and run alongside a 1 Kb Plus DNA gel ladder. The expected fragment size was 2,072 Kb.

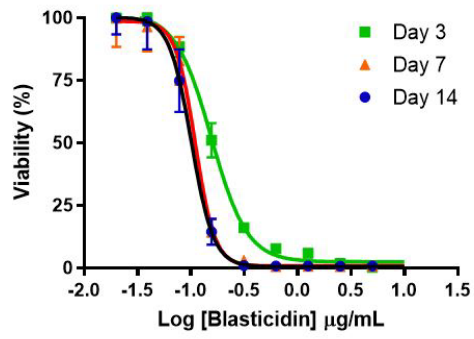
Table 5.1. CRISPR gRNA sequences. gRNA was designed to target *MAGEA4* and *PIWIL2* gene regions of interest to promote C-terminus knock-in.

CRISPR Name	Sequence (5' to 3')
MAGEA4	GCTTTGTTAGAGGAGGAAGA
PIWIL2	CTTCCTGTGACTGCACAGCT

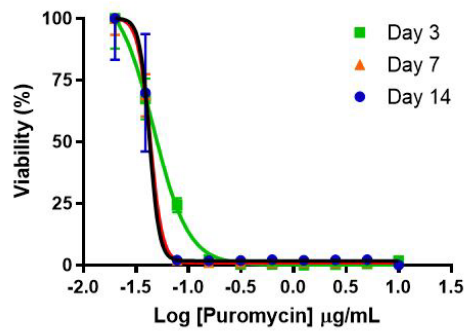
Table 5.2. TALEN mRNA. TALEN mRNA was designed to target *PRM1* gene region of interest to promote C-terminus knock-in.

TALEN	Left Sequence (5' to 3')	Right Sequence (5' to 3')
PRM1 TAL 1	GGTACAGACCGCGATGTA	GGTGGATGTGCTATTTTG
PRM1 TAL 2	GTACAGACCGCGATGTAG	TGGTGGATGTGCTATTTT
PRM1 TAL 3	CAGGTACAGACCGCGATG	TGGATGTGCTATTTTGTG

A



B



C

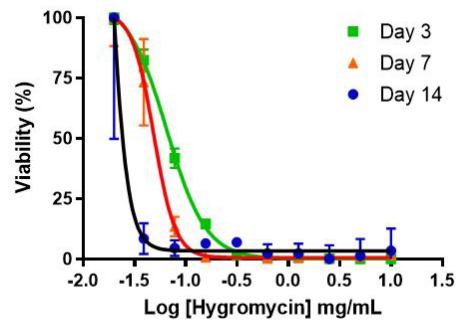
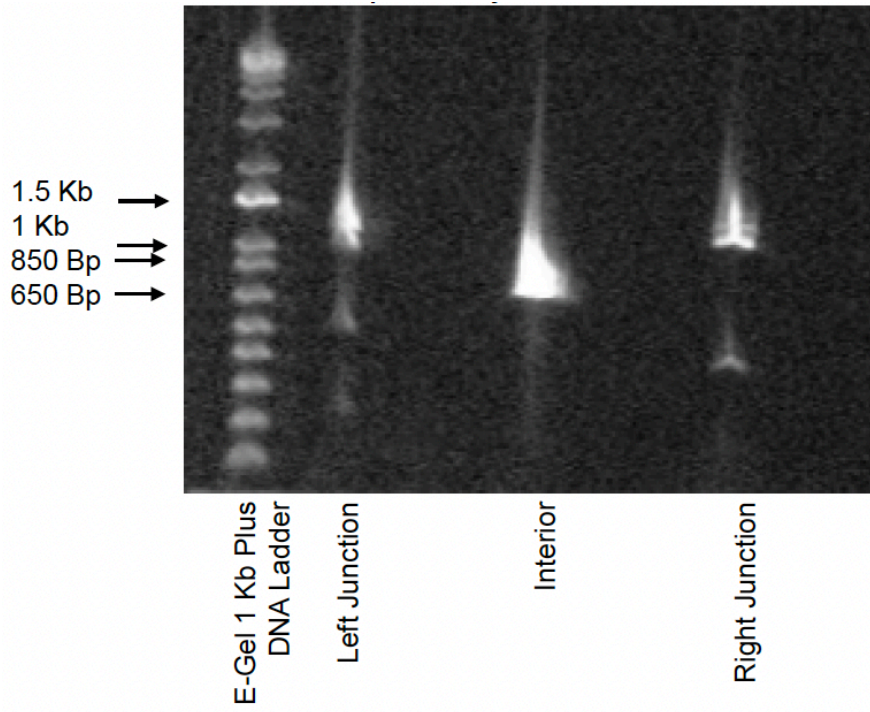


Figure 5.9. Antibiotic kill curve of BJ cells. Cell viability data was generated after 3, 7, and 14 days of cell exposure to antibiotics. Cells were treated with a titration of Blastidicin, Puromycin, or Hygromycin, and the resulting kill curve was plotted in the graph. **(A)** The data indicated that the BJ cells were effectively killed with 3.13 $\mu\text{g}/\text{mL}$ Blastidicin. **(B)** The data indicated that BJ cells were effectively killed with 0.75 $\mu\text{g}/\text{mL}$ Puromycin. **(C)** The data indicated that BJ cells were effectively killed with 0.2 mg/mL Hygromycin.

A



B

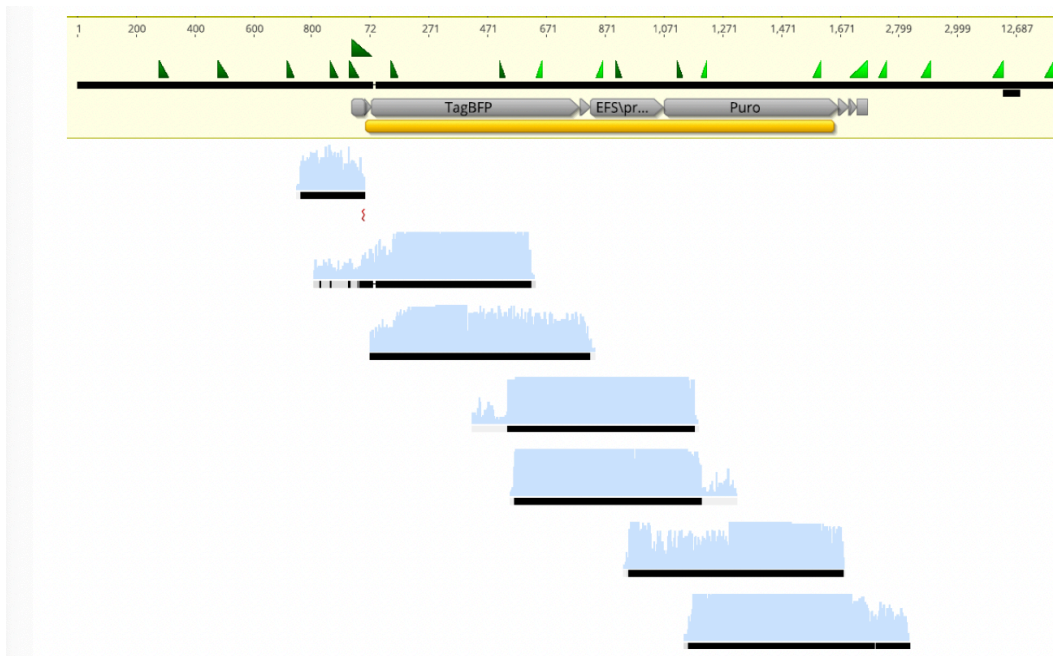
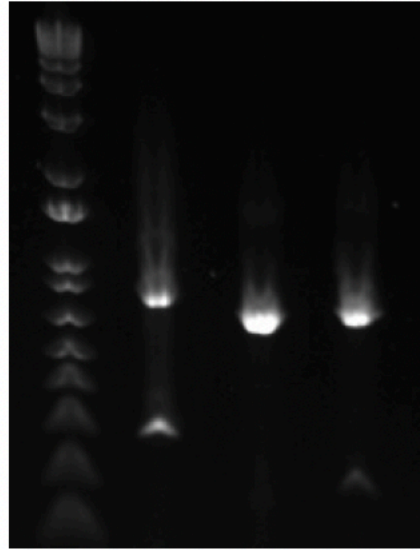


Figure 5.10. Stable pool generation. The BJ C-*MAGEA4*-BFP-pPuro cells were harvested and used for PCR amplification. **(A)** Primers were designed to flank the left and right junctions of the cassette and the interior region. The expected amplicon sizes were: Left: 1,135 bp, Right: 1,072 bp, and Interior: 707 bp. **(B)** The PCR products generated were Sanger sequenced and an alignment was generated against the reference (shown in the yellow box).

A

1.5 Kb →
1 Kb →
850 Bp →
650 Bp →



E-Gel 1 Kb Plus DNA
Ladder

Left Junction

Interior

Right Junction

B

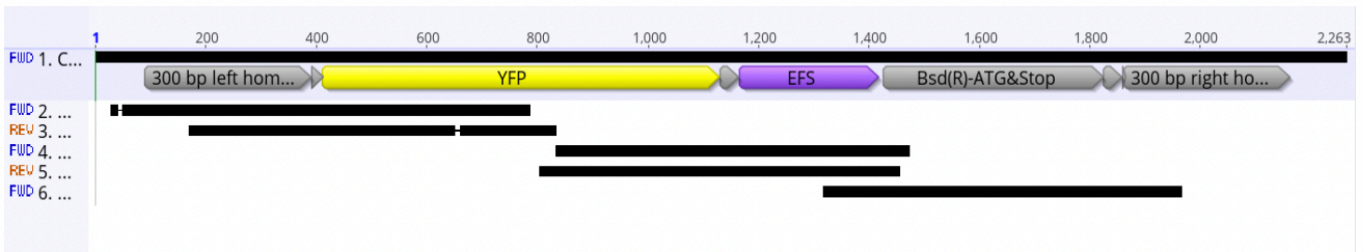


Figure 5.11. Stable pool generation. (A) The BJ *C-MAGEA4*-BFP-pPuro + *C-PIWIL2*-YFP-pBSD cells were harvested and used for PCR amplification. Primers were designed to flank the left and right junctions of the *C-PIWIL2*-YFP-pBsd cassette and the interior region. The expected amplicon sizes were: Left: 973 bp, Right: 1,100 bp, and Interior: 711 bp. (B) The PCR products generated from the BJ *C-MAGEA4*-BFP-pPuro + *C-PIWIL2*-YFP-pBSD cells were Sanger sequenced and an alignment was generated against the reference genome (shown in the black box).

5.6 SUMMARY AND FUTURE DIRECTIONS

As our colleagues have demonstrated, CRISPR/Cas9-mediated gene knock-in is a powerful technique for precise gene modification [386]. Additionally, they have generated a stable BJ cell pool containing two of the three cassettes. While this process has taken more than a few years with several challenges along the way, we are one step closer to generating our *in vitro* fluorescent reporter system to screen potential male contraceptives and addressing the current challenges plaguing contraceptive development. Our unconventional and novel approach will provide an ideal platform to identify effective, safe, and reversible male contraceptives.

Moreover, we will have the unique opportunity to utilize this powerful model to examine the impacts of environmental toxicants and pharmaceuticals, such as NSAIDs, on human spermatogenesis. This new system provides an ideal platform to evaluate the effects of environmental exposures and pharmaceutical usage on several windows of susceptibility where toxicants could affect the establishment, proliferation, survival, and differentiation of male germ cells. If any of these windows of susceptibility are altered, the risk of infertility increases. Testibow 3.0 has the potential to be an ideal platform to evaluate the effects of NSAIDs and other medications on four windows of susceptibility, including stem cell differentiation into spermatogonial stem cells/ differentiating spermatogonia, primary spermatocyte formation, the meiotic progression of primary spermatocytes to secondary spermatocytes, and spermatid maturation. With this model, we can identify a more targeted mechanistic approach for how each medication (streamlining the drug development process), or how environmental toxicants may disrupt sperm development based on the observation of each fluorescent reporter. These

compounds could then be evaluated for their potential deleterious effects and determine whether these effects are reversible. This approach will also prepare us for future studies to determine possible alterations in the sperm epigenome that could pose severe risks to future offspring.

Additionally, we could combine this model with three-dimensional culture systems to develop a more *in vivo*-like platform that allows complete spermatogenesis. This system would allow us to screen compounds for somatic-germ cell interactions and evaluate whether these compounds affect somatic cell viability, which could potentially cause sterility in men. In conclusion, our Testibow platform has the potential to be a valuable research tool, and I am looking forward to seeing the exciting and beautiful Testibow studies in the future.

5.7 MATERIALS AND METHODS

Generation of high titer lentivirus for Testibow 1.0

Working with our collaborator, Dr. Anthony Chan, we generated high titer lentivirus for each construct by transfecting 293Ta, a lentiviral packaging cell line (GeneCopoeia), with each of the plasmid constructs using the FuGene[®] 6 Transfection Reagent (Promega) as per manufacturer's instructions. Then, the lentivirus was obtained using the Lenti-Pac Lentiviral Packaging Kit (GeneCopoeia) as per manufacturer's instructions.

Puromycin Kill Curve Assessment for Testibow 1.0 and 2.0

The National Institutes of Health (NIH)-approved WA01 (H1, WiCell) male, human embryonic stem cell lines (hESCs) were seeded at a high density and at small to medium colony sizes into a twelve well Matrigel[®] (Corning[®])-coated dish. To provide a

control sample, the plate included two wells containing cells, but with an equal amount of medium without puromycin (ThermoFisher) as the others wells on the plate. A day after seeding, the cells were incubated with 0.2 µg/mL to 20 µg/mL puromycin. For the next three days, the cells received either fresh medium (mTeSR1™; STEMCELL Technologies) or medium + puromycin. At the end of the antibiotic selection, we determined that 0.4 µg/mL puromycin was the minimal concentration needed to kill the non-transduced human ESCs over the course of four days.

Testibow 1.0 and 2.0 Lentiviral Transduction

With guidance from Drs. Anthony Chan and Charles Easley, and utilizing a resource provided by Dr. Rick Cohen (<https://www.sigmaaldrich.com/US/en/technical-documents/protocol/genomics/advanced-gene-editing/protocol-for-transduction>), I developed an optimized human ESC lentiviral transduction protocol, since there is not a standardized method for human ESC lentiviral transductions. Using the WA01 human ESCs, these cells were passaged using Dispase (STEMCELL Technologies) and seeded densely and in small aggregates on Matrigel®- coated dishes the day before the transduction. The next day, the cells were treated with 6 µg/mL Polybrene Transfection Reagent during an hour-long “spinoculation” a process that consists of spinning the plated cells at 800 x G at room temperature for one hour. The cells were then incubated with 2 µL of the PLZF/CFP construct, HILI/GFP construct, or the PRM1/tdTomato construct in Polybrene for eight hours at 37° C. Following two washes with DMEM/F12 (Gibco), the cells received fresh mTeSR1™ medium for three days, prior to undergoing puromycin selection.

Puromycin Selection of Testibow 1.0

Four days following the lentiviral transduction, the cells were treated with 0.4 µg/mL puromycin in mTeSR1™. During the next three consecutive days, the cells were treated with puromycin to kill off any non-transduced cells.

Testibow 1.0 and Testibow 2.0 Clonal cell line expansion

The individual colonies that survived puromycin treatment, were manually broken into two clumps, where one clump was placed into one well of a 96 well dish. After five days of growth, one well selected at random was utilized for PCR-based validation of Testibow 1.0 and Testibow 2.0 into the genome. The other well was carried forward for expansion.

DNA extraction and quantification of Testibow 1.0 and Testibow 2.0

DNA was extracted following the manufacturer's instructions from the Testibow 1.0 PLZF/CFP, HILI/GFP, *PRMI*/ tdTomato and Testibow 2.0 transduced WA01 hESCs using the DNeasy Blood & Tissue Kit (Qiagen). Using the Qubit™ 3.0 Fluorometer (Invitrogen), DNA integrity was measured, and only 260/280 ratios ~1.8 were accepted for further processing. The samples were stored at -20°C until polymerase chain reaction analysis and gel electrophoresis.

Polymerase Chain Reaction (PCR) of Testibow 1.0 and Testibow 2.0

Polymerase chain reaction (PCR) was performed with 500 ng - 1 µg extracted DNA, viral vector DNA (0.1 ng/µL) to be used as a positive control, primers, and PCR Master Mix (ThermoFisher; total PCR reaction 50 µL) as per manufacturer's instructions using the T100 Thermal Cycler (Bio-Rad). The amplification parameters were as follows: the initial cycle of 5 min at 95° C, followed by 35 cycles each of 10 seconds at 95° C, 45

seconds at the designated annealing temperature (PLZF/ CFP- 60° C; PIWIL2/ GFP and PRM1/ tdTomato – 58° C), and 10 minutes at 72° C; an extension period of 10 minutes at 72° C completed the cycling sequence.

All PCR primers (Integrated DNA Technologies, Table 7.1) were designed and validated for specificity and amplification efficiency for *PRM1*/tdTomato (459 base pairs), *PIWIL2*/GFP (480 base pairs), and PLZF/CFP (810 base pairs) by Dr. Chan and colleagues.

Agarose gel electrophoresis of Testibow 1.0 and Testibow 2.0

The PCR products were separated by electrophoresis on 1.2% agarose gel in 1X Tris-acetate, EDTA (TAE; ThermoFisher) buffer. The gels were stained with ethidium bromide (Bio-Rad) and then ran for 35 minutes at 100 volts. The gels were photographed under UV light using the ChemiDoc Imaging System (Bio-Rad). A 1 Kb Plus DNA Ladder (ThermoFisher) was used as a molecular weight marker.

Cell culture of clonal Testibow 1.0 and Testibow 2.0 cell lines

The colonies determined to have successful integration of the lentiviral vector were maintained and expanded in mTeSR1™ media on Matrigel® (Corning® Life Sciences) as previously described [12, 62, 64, 65]. Briefly, the cells were cultured in 10 cm dishes and refed with mTeSR1™ (STEMCELL Technologies) daily for five to seven days. The human ESCs were passaged using Dispase in DMEM/F12 (STEM CELL) when the cell density reached approximately 80% confluency and plated onto Matrigel® coated plates [12, 62, 64, 65].

Spermatogenic differentiation of Testibow 1.0 and Testibow 2.0 human ESCs

Direct differentiation into spermatogenic lineages was performed as previously described [12, 59, 62, 64, 65]. Briefly, the differentiating cells were maintained in mouse spermatogonial stem cell (SSC) medium containing the following: MEMalpha + L-glutamine (ThermoFisher), 0.2% Bovine Serum Albumin (MilliporeSigma), 0.2 mg/mL ascorbic acid (MilliporeSigma), 0.2% Chemically Defined Lipid Mixture (MilliporeSigma), 5 µg/mL insulin (MilliporeSigma), 10 µg/mL (MilliporeSigma), 50 µM β-mercaptoethanol (MilliporeSigma), 30 nM sodium selenite (MilliporeSigma), 10 mM HEPES (Gibco), 0.5x Penicillin/Streptomycin (Gibco), 20 ng/mL glial-derived neurotrophic factor (GDNF, Peprotech), and 1 ng/mL human basic fibroblast growth factor (hbFGF, Peprotech) for 10 days. The SSC media was gassed with a blood gas mixture consisting of 5% carbon dioxide, 5% oxygen, and balanced with 90% nitrogen for 30 seconds, and inverted several times to mix following initial media preparation. After changing to the SSC medium, media changes occurred every other day for ten days.

In vitro live cell imaging analysis of Testibow 1.0

Differentiated WA01 spermatogenic cells transduced with the Testibow 1.0 construct were cultured in the conditions described above, and then live cell images were captured. During the imaging acquisition, the exposure time and light intensity were limited to reduce photobleaching [387]. Additionally, since we do not have a stage-top incubator or a way to control the temperature or CO₂ levels, we limited the amount of time to complete the imaging acquisition [387]. All live cell images were captured using a Nikon DS-Qi2 camera on a Nikon Eclipse Ti microscope. Images were processed using the NIS-Elements AR software with 3D deconvolution using the Richardson-Lucy

deconvolution technique [301, 302], followed by the creation of an extended depth of focus (EDF) document.

Puromycin selection of Testibow 2.0 non-transduced hESCs

Three days following the lentiviral transduction, the cells were treated with 0.4 µg/mL puromycin in mTeSR for two consecutive days to kill off any non-transduced cells. After the two days of treatment, the cells were then cultured in a maintenance dose of 0.2 µg/mL puromycin and allowed to grow for three more days.

Immunocytochemistry (ICC) analysis of Testibow 2.0

Differentiated WA01 spermatogenic cells transduced with the Testibow 2.0 construct cultured in the conditions described above were fixed in 4% paraformaldehyde (Electron Microscopy Solutions) for 15 minutes, then blocked with buffer containing 1X Phosphate-buffered Saline solution (PBS, Gibco), 0.1% Triton X (Sigma), and 5% normal goat serum (MP Biomedicals) overnight at 4°C as described [62]. Primary PLZF antibody (Table 7.2) incubation was performed overnight at 4°C in blocking buffer followed by three washes in 1X PBS with 0.1% Triton X for 10 minutes each at room temperature on an LSE Orbital Shaker (Corning). Secondary antibody incubation (1:1000, Alexa Fluor™ Invitrogen, Table 7.2) in blocking buffer occurred for 45 minutes overnight at 4°C. Following the three washes as described above, the samples were co-stained with Hoechst 33342 (1:1000, Invitrogen). All ICC samples were captured using a Nikon DS-Qi2 camera on a Nikon Eclipse Ti microscope. Images were processed using the NIS-Elements AR software (version 5.21.03 64-bit), with 3D deconvolution using the Richardson-Lucy deconvolution technique [301, 302], followed by the creation of an extended depth of focus (EDF) document.

Design and synthesis of donor DNA

Donor DNA was designed and synthesized to edit the *MAGEA4*-BFP-pPuro knock-in by developing chimeric oligos to amplify the BFP-pPuro cassette via the TrueTag™ manual. Then, the donor DNA was prepared using the chimeric oligos, the TrueTag™ Donor DNA Kit (ThermoFisher), and the TrueTag™ BFP-pPuro DNA template. The donor DNA gene sequences for *C-PRMI*-mKate2-Hyg and *C-PIWIL2*-YFP-pBlast were synthesized using GeneArt® via manufacturers protocols. The synthesized constructs were subcloned into a pMK-RQ (KanR, AmpR, respectively) vector backbone, and then transformed into *E. coli*. The cells were then harvested from the culture, and the plasmid DNA was purified using the PureLink® HiPure Plasmid Filter Maxiprep Kit (Invitrogen). The plasmids were then used to generate dsDNA, purified using the PureLink® PCR Purification Kit (ThermoFisher), and then quantified using a NanoDrop™ Spectrophotometer. The dsDNA donors will then be paired with the CRISPRs or TALENs to facilitate gene knock-in.

Design and synthesis of gRNA or TALEN mRNA

CRISPR gRNAs were designed to target the human *MAGEA4* and *PIWIL2* genes. The gRNAs were designed using the GeneArt™ Preision gRNA Synthesis Kit (ThermoFisher), and based on these designs, the DNA oligos were synthesized. PCR based reaction of the DNA oligos generated DNA templates that were then used with the GeneArt™ Preision gRNA Synthesis Kit to synthesize the gRNAs. The gRNAs were then purified using the MEGAclean™ Transcription Clean-Up Kit (ThermoFisher).

TALEN DNA templates were designed and synthesized corresponding to the *PRMI* gene. A linear TALEN DNA template was used to synthesize capped messenger

RNA using the mMESSAGE mMACHINE™ T7 Kit (ThermoFisher), and then the TALEN mRNA was purified using the MEGAclean™ Transcription Clean-Up Kit.

Blasticidin, Puromycin, and Hygromycin antibiotic kill curve assessment for BJ cells

The BJ fibroblast cells were seeded into 96 well plates at a cell density of 2.5×10^3 cells/well. Blasticidin or Puromycin was added to the plate at 0.1, 0.2, 0.4, 0.75, 1.5, 3.13, 6.25, 12.5, 25, or 50 $\mu\text{g}/\text{mL}$. Hygromycin was added to the plate at 0.025, 0.05, 0.1, 0.2, 0.4, 0.75, 1.25, 2.5, 5, or 10 mg/mL . These plates were assayed for cell survival at post-antibiotic addition days 3, 7, 14 using the PrestoBlue® cell viability reagent (ThermoFisher). Briefly, after the addition of PrestoBlue®, the cells were incubated at 37°C for three hours and then read on a fluorescence plate reader with an excitation wavelength of 560 nm and an emission wavelength of 600 nm.

Stable pool generation of C-MAGEA4-BFP-pPuro BJ cells

One million BJ cells were pelleted, washed with dPBS (ThermoFisher), and resuspended in Neon “R” buffer (ThermoFisher) to prepare a total of 2.0×10^5 cells per 10 μL reaction. For the CRISPR transfections, 0.5 μg TrueCut™ Cas9 v2 Protein (ThermoFisher), 200 ng CRISPR gRNA, and 200 ng C-MAGEA4-BFP-pPuro donor DNA per 10 μL reaction were added to the Neon “R” buffer and then incubated for five minutes at room temperature. The cells were then added to the mixture, and five rounds of electroporation using the Neon® Transfection System (ThermoFisher) were performed. Afterwards, the cells were transferred to a tissue culture plate, allowed to expand, and then selected for 72 hours using 0.75 μg Puromycin. Following a recovery period, the cells were harvested and prepared for PCR and sequencing.

Stable pool generation of C-MAGEA4-BFP-pPuro + C-PIWIL2-YFP-pBsd BJ cells

Two million BJ C-MAGEA4-BFP-pPuro cells were pelleted, washed with dPBS (ThermoFisher), and resuspended in Neon “R” buffer (ThermoFisher) to prepare a total of 2.0×10^5 cells per 10 μ L reaction. For the CRISPR transfections, 0.5 μ g TrueCut™ Cas9 v2 Protein (ThermoFisher), 200 ng CRISPR gRNA, and 500 ng C-PIWIL2-YFP-pBlast donor DNA per 10 μ L reaction were added to the Neon “R” buffer and then incubated for five minutes at room temperature. The cells were then added to the mixture, and ten rounds of electroporation using the Neon® Transfection System (ThermoFisher) were performed. Afterwards, the cells were transferred to a tissue culture flask, allowed to expand, and then selected for 72 hours using 3.13 μ g Blasticidin. Following a recovery period, the cells were harvested and prepared for PCR and sequencing.

CHAPTER 6

CONCLUDING REMARKS

Over-the-counter (OTC) pain relievers, such as non-steroidal anti-inflammatory drugs (NSAIDs), greatly benefit many people. These drugs typically relieve common aches, pains, and fevers. Taking the recommended doses of ibuprofen and naproxen, two common NSAIDs, are safe ways to relieve the aches and pains from exercising too hard. However, if one finds themselves going to the medicine cabinet for relief often, they could do more harm than good, particularly to their reproductive tract. This is especially important if couples are trying to conceive.

Worldwide, reproductive-aged men are using more OTC NSAIDs to treat their minor aches and pains than ever before. Yet, the effects of many medications, like NSAIDs, on the male reproductive system are not well established, mainly due to older literature, flaws in study design, and conflicting results. In combination with limited demographic information about the use of medications, there is a great need to improve our knowledge about how drugs affect fertility, and *in vitro*-based human model systems so these studies can be conducted efficiently and unbiasedly. From fast relief to future consequences, this dissertation described the impact of ibuprofen and naproxen on male reproductive health, particularly on spermatogenesis and the somatic niche. Using two powerful *in vitro* models, we first determined the spermatotoxic effects of naproxen and ibuprofen on human stem cells differentiated *in vitro*. In Chapter 3, we showed that human *in vitro* spermatogenic cells might be more susceptible to naproxen-induced

toxicity than to ibuprofen by directly altering mitochondrial membrane potential and affecting germ cell viability. Still, the overall effects appear to be minimal. Second, Chapter 4 revealed that short-term naproxen and ibuprofen increased the transepithelial electrical resistance, reflecting a strengthening of the Sertoli cell junctions. Through mRNA-sequencing analysis, serum levels of ibuprofen and naproxen altered gene expression in the non-human primate primary Sertoli cells. Gene set enrichment analysis was performed for the differentially expressed genes, which showed the broad effects of ibuprofen compared to naproxen. Ibuprofen appeared to alter genes involved in proper Blood-testis barrier function, cell junction regulation, and inflammatory response. Further, unlike naproxen, the differentially expressed genes altered upon ibuprofen exposure were significantly enriched in diseases associated with male factor infertility. Together, these results highlight the potential connection between NSAID therapy and male factor infertility.

This information is beneficial for other researchers by providing new avenues of research to determine mechanisms of action and potentially develop new strategies to decrease the reproductive toxicity of ibuprofen and naproxen. By developing our new *in vitro* fluorescent reporter system (Chapter 5), we can start to address the current limitations of drug testing and further our understanding of how Food and Drug Administration (FDA) approved medications can generate adverse effects on male fertility.

As we have seen throughout this dissertation, commonly used medications can be a contributing factor to the dramatic decline in sperm counts across the world. Due to the popularity of NSAIDs and acetaminophen among reproductive-aged men, all classes of

NSAIDs should undergo reproductive toxicity screening, especially since we and others have reported some reproductive toxicity. Further, as we continue to advance our knowledge about the role played by cyclooxygenase (COX) and prostaglandins in the male reproductive tract, new therapeutical approaches, such as repurposing NSAIDs, could be developed for treating idiopathic male infertility [203] and should be further investigated. Overall, additional work is needed at both the benchtop and during clinical trials to fill the gaps in our current knowledge.

So, what can we do? There are steps that we can take both as individuals and as a society to stay healthy and protect male reproduction. As individuals, we need to be aware of our dosage of NSAIDs, and if we find our pain is becoming chronic or our fever returns, we need to contact our physicians. As a society, the first thing we need to do is learn more about how common medications impact male fertility and to share our findings with people in- and outside the scientific community. It is my hope that future robust, well-designed studies will examine the male reproductive effects of other commonly used NSAIDs to help reproductive and infertility specialists counsel their patients on their medication usage. Second, through collaborative care with scientists, reproductive specialists, nurses, physicians, and pharmacists, we need to educate patients about the risks and doses needed to relieve pain and inflammation but not compromise fertility [388]. Together, we can better understand the connection between our environment and reproductive health.

REFERENCES

1. Swan, S.H. and S. Colino, *Count Down: How Our Modern World Is Threatening Sperm Counts, Altering Male and Female Reproductive Development, and Imperiling the Future of the Human Race*. 2021: Scribner.
2. Bak, C.W., et al., *Hormonal imbalances and psychological scars left behind in infertile men*. *J Androl*, 2012. **33**(2): p. 181-9.
3. Slade, P., et al., *The relationship between perceived stigma, disclosure patterns, support and distress in new attendees at an infertility clinic*. *Hum Reprod*, 2007. **22**(8): p. 2309-17.
4. Abbey, A., F.M. Andrews, and L.J. Halrnan, *GENDER'S ROLE IN RESPONSES TO INFERTILITY*. *Psychology of Women Quarterly*, 1991. **15**(2): p. 295-316.
5. Berg, B.J. and J.F. Wilson, *Psychological functioning across stages of treatment for infertility*. *Journal of Behavioral Medicine*, 1991. **14**(1): p. 11-26.
6. Wu, A.K., et al., *Time costs of fertility care: the hidden hardship of building a family*. *Fertil Steril*, 2013. **99**(7): p. 2025-30.
7. Downey, J., et al., *Mood disorders, psychiatric symptoms, and distress in women presenting for infertility evaluation*. *Fertil Steril*, 1989. **52**(3): p. 425-32.
8. Whiteford, L.M. and L. Gonzalez, *Stigma: the hidden burden of infertility*. *Soc Sci Med*, 1995. **40**(1): p. 27-36.
9. Carlsen, E., et al., *Evidence for decreasing quality of semen during past 50 years*. *Bmj*, 1992. **305**(6854): p. 609-13.

10. Levine, H., et al., *Temporal trends in sperm count: a systematic review and meta-regression analysis*. Hum Reprod Update, 2017. **23**(6): p. 646-659.
11. Levine, H., et al., *Temporal trends in sperm count: a systematic review and meta-regression analysis of samples collected globally in the 20th and 21st centuries*. Human Reproduction Update, 2022.
12. Steves, A.N., et al., *Ubiquitous Flame-Retardant Toxicants Impair Spermatogenesis in a Human Stem Cell Model*. iScience, 2018. **3**: p. 161-176.
13. Ma, Y., et al., *Effects of environmental contaminants on fertility and reproductive health*. Journal of Environmental Sciences, 2019. **77**: p. 210-217.
14. Bahadur, G., *Fertility issues for cancer patients*. Molecular and Cellular Endocrinology, 2000. **169**(1): p. 117-122.
15. Sharma, R., et al., *Lifestyle factors and reproductive health: taking control of your fertility*. Reprod Biol Endocrinol, 2013. **11**: p. 66.
16. Symosko, K.M., G. Schatten, and C.A. Easley, *Gamete Production from Stem Cells*, in *Female and Male Fertility Preservation*, M. Grynberg and P. Patrizio, Editors. 2022, Springer International Publishing: Cham. p. 395-407.
17. Drobnis, E. and A.K. Nangia, *Impacts of Medications on Male Fertility*. 1 ed. Advances in Experimental Medicine and Biology. 2017: Springer International Publishing. 325.
18. Bray, I., D. Gunnell, and G. Davey Smith, *Advanced paternal age: How old is too old?* Journal of Epidemiology and Community Health, 2006. **60**(10): p. 851-853.

19. Martinez, G., K. Daniels, and A. Chandra, *Fertility of men and women aged 15-44 years in the United States: National Survey of Family Growth, 2006-2010*. Natl Health Stat Report, 2012(51): p. 1-28.
20. Sartorius, G.A. and E. Nieschlag, *Paternal age and reproduction*. Hum Reprod Update, 2010. **16**(1): p. 65-79.
21. Zweifel, J.E., *Last chance or too late? Counseling prospective older parents*, in *Fertility counseling: Clinical guide and case studies*. 2015, Cambridge University Press: New York, NY, US. p. 150-165.
22. Eisenberg, M.L., et al., *Relationship between semen production and medical comorbidity*. Fertility and sterility, 2015. **103**(1): p. 66-71.
23. Eisenberg, M.L., et al., *Increased risk of incident chronic medical conditions in infertile men: analysis of United States claims data*. Fertility and sterility, 2016. **105**(3): p. 629-636.
24. Groos, S., W. Krause, and U.O. Mueller, *Men with subnormal sperm counts live shorter lives*. Social Biology, 2006. **53**(1-2): p. 46-60.
25. Jensen, T.K., et al., *Good Semen Quality and Life Expectancy: A Cohort Study of 43,277 Men*. American Journal of Epidemiology, 2009. **170**(5): p. 559-565.
26. Omu, A.E., *Sperm Parameters: Paradigmatic Index of Good Health and Longevity*. Medical Principles and Practice, 2013. **22(suppl 1)**(Suppl. 1): p. 30-42.
27. Salonia, A., et al., *Are Infertile Men Less Healthy than Fertile Men? Results of a Prospective Case-Control Survey*. European Urology, 2009. **56**(6): p. 1025-1032.

28. Tarín, J.J., et al., *Infertility etiologies are genetically and clinically linked with other diseases in single meta-diseases*. *Reproductive Biology and Endocrinology*, 2015. **13**(1): p. 31.
29. Samplaski, M.K. and A.K. Nangia, *Adverse effects of common medications on male fertility*. *Nat Rev Urol*, 2015. **12**(7): p. 401-13.
30. Pompe, S.V., et al., *Drug use among men with unfulfilled wish to father children: a retrospective analysis and discussion of specific drug classes*. *Pharmacoepidemiology and Drug Safety*, 2016. **25**(6): p. 668-677.
31. Hayashi, T., A. Miyata, and T. Yamada, *The impact of commonly prescribed drugs on male fertility*. *Hum Fertil (Camb)*, 2008. **11**(3): p. 191-6.
32. Administration, U.S.F.a.D., *Testicular toxicity: evaluation during drug development guidance for industry*. 2015.
33. Research, C.f.D.E.a., *Reproductive and Developmental Toxicities — Integrating Study Results to Assess concerns*, F.a.D. Administration, Editor. 2011.
34. Ding, J., et al., *FDA-approved medications that impair human spermatogenesis*. *Oncotarget*, 2017. **8**(6): p. 10714-10725.
35. Champion, S., et al., *Male reprotoxicity and endocrine disruption*. *Experientia supplementum* (2012), 2012. **101**: p. 315-360.
36. Skakkebaek, N.E., E. Rajpert-De Meyts, and K.M. Main, *Testicular dysgenesis syndrome: an increasingly common developmental disorder with environmental aspects*. *Hum Reprod*, 2001. **16**(5): p. 972-8.
37. Hughes, I.A., *Minireview: sex differentiation*. *Endocrinology*, 2001. **142**(8): p. 3281-3287.

38. Pinsky, L., R.P. Erickson, and R.N. Schimke, *Genetic disorders of human sexual development*. 1999: Oxford Monographs on Medical G.
39. Wu, H., et al., *Environmental Susceptibility of the Sperm Epigenome During Windows of Male Germ Cell Development*. *Current Environmental Health Reports*, 2015. **2**(4): p. 356-366.
40. Xiao, S., Symosko, K., Easley IV, C., *Reproductive and Developmental Toxicity: Toxic Effects on the Female and Male Reproductive Tracts and Offspring*, in *Principles of Toxicology*, S.M. Roberts, James, R.C., Williams, P.L., Editor. 2022, John Wiley & Sons, Inc: USA. p. 283-306.
41. Singh, S., et al., *Spermatogonial stem cells, infertility and testicular cancer*. *Journal of cellular and molecular medicine*, 2010. **15**: p. 468-83.
42. Chauvigné, F., et al., *Time- and dose-related effects of di-(2-ethylhexyl) phthalate and its main metabolites on the function of the rat fetal testis in vitro*. *Environ Health Perspect*, 2009. **117**(4): p. 515-21.
43. Hallmark, N., et al., *Effects of monobutyl and di(n-butyl) phthalate in vitro on steroidogenesis and Leydig cell aggregation in fetal testis explants from the rat: comparison with effects in vivo in the fetal rat and neonatal marmoset and in vitro in the human*. *Environmental health perspectives*, 2007. **115**(3): p. 390-396.
44. Li, H. and K.H. Kim, *Effects of mono-(2-ethylhexyl) phthalate on fetal and neonatal rat testis organ cultures*. *Biol Reprod*, 2003. **69**(6): p. 1964-72.
45. Stroheker, T., et al., *Effect of in utero exposure to di-(2-ethylhexyl)phthalate: distribution in the rat fetus and testosterone production by rat fetal testis in culture*. *Food Chem Toxicol*, 2006. **44**(12): p. 2064-9.

46. Bryda, E.C., *The Mighty Mouse: the impact of rodents on advances in biomedical research*. *Mo Med*, 2013. **110**(3): p. 207-11.
47. Fayomi, A.P. and K.E. Orwig, *Spermatogonial stem cells and spermatogenesis in mice, monkeys and men*. *Stem Cell Research*, 2018. **29**: p. 207-214.
48. Ehmcke, J. and S. Schlatt, *A revised model for spermatogonial expansion in man: lessons from non-human primates*. *Reproduction*, 2006. **132**(5): p. 673-680.
49. Brinster, R.L., *Germline stem cell transplantation and transgenesis*. *Science*, 2002. **296**(5576): p. 2174-2176.
50. Brinster, R.L., *Male germline stem cells: from mice to men*. *Science*, 2007. **316**(5823): p. 404-5.
51. Amann, R.P., *The cycle of the seminiferous epithelium in humans: a need to revisit?* *J Androl*, 2008. **29**(5): p. 469-87.
52. Clermont, Y. and M. Trott, *Duration of the cycle of the seminiferous epithelium in the mouse and hamster determined by means of 3H-thymidine and radioautography*. *Fertil Steril*, 1969. **20**(5): p. 805-17.
53. Heller, C.H. and Y. Clermont, *KINETICS OF THE GERMINAL EPITHELIUM IN MAN*. *Recent Prog Horm Res*, 1964. **20**: p. 545-75.
54. Oakberg, E.F., *Duration of spermatogenesis in the mouse and timing of stages of the cycle of the seminiferous epithelium*. *Am J Anat*, 1956. **99**(3): p. 507-16.
55. Li, L., et al., *Exposure to diethylhexyl phthalate (DEHP) results in a heritable modification of imprint genes DNA methylation in mouse oocytes*. *Mol Biol Rep*, 2014. **41**(3): p. 1227-35.

56. Greeson, K.W., et al., *Inheritance of paternal lifestyles and exposures through sperm DNA methylation*. Nature Reviews Urology, 2023.
57. *Administrator Wheeler Signs Memo to Reduce Animal Testing, Awards \$4.25 Million to Advance Research on Alternative Methods to Animal Testing*. 2019, United States Environmental Protection Agency.
58. Hubrecht, R.C. and E. Carter, *The 3Rs and Humane Experimental Technique: Implementing Change*. Animals (Basel), 2019. **9**(10).
59. Easley, C.A.t., et al., *Assessing reproductive toxicity of two environmental toxicants with a novel in vitro human spermatogenic model*. Stem Cell Res, 2015. **14**(3): p. 347-55.
60. *Stem Cell Catalog Search*. 2018 [cited 2023 March 1]; Available from: <https://www.wicell.org/home/stem-cells/catalog-of-stem-cell-lines/advanced-search.cmsx>.
61. Thomson, J.A., et al., *Embryonic stem cell lines derived from human blastocysts*. Science, 1998. **282**(5391): p. 1145-7.
62. Easley, C.A.t., et al., *Direct differentiation of human pluripotent stem cells into haploid spermatogenic cells*. Cell Rep, 2012. **2**(3): p. 440-6.
63. Khampang S, C.I., Punyawai K, Gill B, Langmo JN, Nath S, Greeson KW, Symosko KM, Fowler KL, Tian S, Statz JP, Steves AN, Parnpai R, White MA, Hennebold JD, Orwig KE, Simerly CR, Schatten G, Easley CA 4th, *Blastocyst Development after Fertilization with In vitro Spermatids Derived from Non-Human Primate Embryonic Stem Cells*. F S Sci, 2021. **2**(4): p. 365-375.

64. Steves, A.N., et al., *Per- and polyfluoroalkyl substances impact human spermatogenesis in a stem-cell-derived model*. *Systems biology in reproductive medicine*, 2018. **64**(4): p. 225-239.
65. Greeson, K.W., et al., *Detrimental effects of flame retardant, PBB153, exposure on sperm and future generations*. *Scientific Reports*, 2020. **10**(1): p. 8567.
66. Schrott, R., et al., *Cannabis alters DNA methylation at maternally imprinted and autism candidate genes in spermatogenic cells*. *Systems Biology in Reproductive Medicine*, 2022. **68**(5-6): p. 357-369.
67. Sakib, S., et al., *Testicular organoids to study cell-cell interactions in the mammalian testis*. *Andrology*, 2020. **8**(4): p. 835-841.
68. Krotz, S.P., et al., *In vitro maturation of oocytes via the pre-fabricated self-assembled artificial human ovary*. *Journal of assisted reproduction and genetics*, 2010. **27**(12): p. 743-750.
69. Laronda, M.M., et al., *Initiation of puberty in mice following decellularized ovary transplant*. *Biomaterials*, 2015. **50**: p. 20-29.
70. Xiao, S., et al., *A microfluidic culture model of the human reproductive tract and 28-day menstrual cycle*. *Nature communications*, 2017. **8**: p. 14584-14584.
71. Kristensen, D.M., et al., *Intrauterine exposure to mild analgesics is a risk factor for development of male reproductive disorders in human and rat*. *Human Reproduction*, 2010. **26**(1): p. 235-244.
72. Boisen, K., et al., *Difference in prevalence of congenital cryptorchidism in infants between two Nordic countries*. *The Lancet*, 2004. **363**(9417): p. 1264-1269.

73. Serrano, T., et al., *International geographic correlation study of the prevalence of disorders of male reproductive health*. Human reproduction, 2013. **28**(7): p. 1974-1986.
74. Berkowitz, G.S. and R.H. Lapinski, *Risk factors for cryptorchidism: a nested case-control study*. Paediatric and perinatal epidemiology, 1996. **10**(1): p. 39-51.
75. Jensen, M.S., et al., *Maternal Use of Acetaminophen, Ibuprofen, and Acetylsalicylic Acid During Pregnancy and Risk of Cryptorchidism*. Epidemiology, 2010. **21**(6): p. 779-785.
76. Correy, J., et al., *Use of prescription drugs in the first trimester and congenital malformations*. Australian and New Zealand journal of obstetrics and gynaecology, 1991. **31**(4): p. 340-344.
77. Lind, J.N., et al., *Maternal medication and herbal use and risk for hypospadias: data from the National Birth Defects Prevention Study, 1997–2007*. Pharmacoepidemiology and drug safety, 2013. **22**(7): p. 783-793.
78. Han, S., et al., *Endocrine disruption and consequences of chronic exposure to ibuprofen in Japanese medaka (*Oryzias latipes*) and freshwater cladocerans *Daphnia magna* and *Moina macrocopa**. Aquatic toxicology, 2010. **98**(3): p. 256-264.
79. Al-Rifai, J.H., C.L. Gabelish, and A.I. Schäfer, *Occurrence of pharmaceutically active and non-steroidal estrogenic compounds in three different wastewater recycling schemes in Australia*. Chemosphere, 2007. **69**(5): p. 803-815.

80. Ji, K., et al., *Effects of non-steroidal anti-inflammatory drugs on hormones and genes of the hypothalamic-pituitary-gonad axis, and reproduction of zebrafish*. *Journal of Hazardous Materials*, 2013. **254-255**: p. 242-251.
81. Yano, C.L. and H. Dolder, *Rat testicular structure and ultrastructure after paracetamol treatment*. *Contraception*, 2002. **66(6)**: p. 463-467.
82. Didolkar, A.K., et al., *Effects of Aspirin on Blood Plasma Levels of Testosterone, LH and FSH in Maturing Male Rats*. *International Journal of Andrology*, 1980. **3(1-6)**: p. 312-318.
83. Biswas, N., S. Sanyal, and P. Patra, *Antispermatogenic effect of aspirin and its prevention by prostaglandin E2*. *Andrologia*, 1978. **10(2)**: p. 137-141.
84. Scott, J.E. and T.V. Persaud, *A quantitative study of the effects of acetylsalicylic acid on spermatogenesis and organs of the rat*. *Int J Fertil*, 1978. **23(4)**: p. 282-7.
85. Kristensen, D.M., et al., *Intrauterine exposure to mild analgesics is a risk factor for development of male reproductive disorders in human and rat*. *Hum Reprod*, 2011. **26(1)**: p. 235-44.
86. Gupta, C. and A.S. Goldman, *The arachidonic acid cascade is involved in the masculinizing action of testosterone on embryonic external genitalia in mice*. *Proc Natl Acad Sci U S A*, 1986. **83(12)**: p. 4346-9.
87. Gupta, R.A., et al., *Prostacyclin-mediated activation of peroxisome proliferator-activated receptor δ in colorectal cancer*. *Proceedings of the National Academy of Sciences*, 2000. **97(24)**: p. 13275-13280.
88. Stutz, G., et al., *Functional activity of mouse sperm was not affected by low doses of aspirin-like drugs*. *Arch Androl*, 2000. **44(2)**: p. 117-28.

89. Uzun, B., et al., *Evaluation of the reproductive toxicity of naproxen sodium and meloxicam in male rats*. Human & Experimental Toxicology, 2015. **34**(4): p. 415-429.
90. Smarr, M.M., et al., *Urinary paracetamol and time-to-pregnancy*. Human Reproduction, 2016. **31**(9): p. 2119-2127.
91. Smarr, M.M., et al., *Male urinary paracetamol and semen quality*. Andrology, 2017. **5**(6): p. 1082-1088.
92. Topozada, M., et al., *Effect of prostaglandin E2 or prostaglandin synthesis inhibitors on human gonadotrophins and prolactin*. Eicosanoids, 1992. **5**(1): p. 23-7.
93. Knuth, U.A., et al., *Indomethacin and oxaprozin lower seminal prostaglandin levels but do not influence sperm motion characteristics and serum hormones of young healthy men in a placebo-controlled double-blind trial*. J Androl, 1989. **10**(2): p. 108-19.
94. Wei, N. and J.C. Hood, *Naproxen and ejaculatory dysfunction*. Ann Intern Med, 1980. **93**(6): p. 933.
95. Kristensen, D.M., et al., *Ibuprofen alters human testicular physiology to produce a state of compensated hypogonadism*. Proceedings of the National Academy of Sciences, 2018. **115**(4): p. E715-E724.
96. Tajar, A., et al., *Characteristics of secondary, primary, and compensated hypogonadism in aging men: evidence from the European Male Ageing Study*. J Clin Endocrinol Metab, 2010. **95**(4): p. 1810-8.

97. Jonas, K.C., et al., *Mouse models of altered gonadotrophin action: insight into male reproductive disorders*. *Reproduction*, 2014. **148**(4): p. R63-R70.
98. Banihani, S.A., *Effect of ibuprofen on semen quality*. *Andrologia*, 2019. **51**(4): p. e13228.
99. Roodbari, F., N. Abedi, and A.R. Talebi, *Early and late effects of Ibuprofen on mouse sperm parameters, chromatin condensation, and DNA integrity in mice*. *Iran J Reprod Med*, 2015. **13**(11): p. 703-10.
100. Bouffard, G., *Injection des couleurs de benzidine aux animaux normaux*. *Ann Inst Pasteur*, 1906. **20**: p. 539-546.
101. Goldmann, E.E., *Die äussere und innere Sekretion des gesunden und kranken Organismus im Lichte der 'vitalen Färbung*. *Beitr Klin Chir*, 1909. **64**: p. 192-265.
102. Ribbert, H., *Die Ausscheidung intravenos injizierten gelosten Karmins in den Geweben*. *Z allg Physiol*, 1904. **4**: p. 201-214.
103. Kormano, M., *Dye permeability and alkaline phosphatase activity of testicular capillaries in the postnatal rat*. *Histochemie*, 1967. **9**(4): p. 327-338.
104. Kormano, M., *Distribution of injected L-3, 4-dihydroxyphenylalanine (L-dopa) in the adult rat testis and epididymis*. *Acta physiologica Scandinavica*, 1967. **71**(1): p. 125-126.
105. Nordin, B., *Handbook of Physiology Section 7: Endocrinology*. *British Medical Journal*, 1976. **2**(6038): p. 761.
106. Setchell, B.P., *Blood-testis barrier, junctional and transport proteins and spermatogenesis*. *Adv Exp Med Biol*, 2008. **636**: p. 212-33.

107. Dym, M. and J.C. Cavicchia, *Further observations on the blood-testis barrier in monkeys*. *Biology of Reproduction*, 1977. **17**(3): p. 390-403.
108. Dym, M. and D.W. Fawcett, *The blood-testis barrier in the rat and the physiological compartmentation of the seminiferous epithelium*. *Biology of reproduction*, 1970. **3**(3): p. 308-326.
109. Fawcett, D., *Electron microscopic observations on the structural components of the bloodtestis barrier*. *J Reprod Fertil*, 1970. **10**: p. 105-122.
110. Russell, L.D. and R. Peterson, *Sertoli cell junctions: morphological and functional correlates*. *International review of cytology*, 1985. **94**: p. 177-211.
111. Gerber, J., J. Heinrich, and R. Brehm, *Blood-testis barrier and Sertoli cell function: lessons from SCCx43KO mice*. *Reproduction*, 2016. **151**(2): p. R15-27.
112. Cheng, C.Y. and D.D. Mruk, *The Blood-Testis Barrier and Its Implications for Male Contraception*. *Pharmacological Reviews*, 2012. **64**(1): p. 16-64.
113. Fijak, M., S. Bhushan, and A. Meinhardt, *Immunoprivileged sites: the testis*. *Methods Mol Biol*, 2011. **677**: p. 459-70.
114. Meinhardt, A. and M.P. Hedger, *Immunological, paracrine and endocrine aspects of testicular immune privilege*. *Molecular and cellular endocrinology*, 2011. **335**(1): p. 60-68.
115. Francavilla, F., et al., *Naturally-occurring antisperm antibodies in men: interference with fertility and clinical implications. An update*. *Frontiers in Bioscience-Landmark*, 2007. **12**(8): p. 2890-2911.
116. Dufour, J.M., et al., *Transgenic Sertoli cells as a vehicle for gene therapy*. *Cell transplantation*, 2004. **13**(1): p. 1-6.

117. Fallarino, F., et al., *Therapy of experimental type 1 diabetes by isolated Sertoli cell xenografts alone*. Journal of Experimental Medicine, 2009. **206**(11): p. 2511-2526.
118. Mital, P., G. Kaur, and J.M. Dufour, *Immunoprotective sertoli cells: making allogeneic and xenogeneic transplantation feasible*. Reproduction, 2010. **139**(3): p. 495.
119. Selawry, H.P. and D. Cameron, *Sertoli cell-enriched fractions in successful islet cell transplantation*. Cell transplantation, 1993. **2**(2): p. 123-129.
120. Shamekh, R., et al., *Sertoli cells induce systemic donor-specific tolerance in xenogenic transplantation model*. Cell transplantation, 2006. **15**(1): p. 45-53.
121. Yin, Z., et al., *Cotransplantation with xenogenetic neonatal porcine sertoli cells significantly prolongs islet allograft survival in nonimmunosuppressive rats*. Transplantation, 2009. **88**(3): p. 339-345.
122. Samy, E.T., et al., *Sertoli cell prostaglandin D2 synthetase is a multifunctional molecule: its expression and regulation*. Endocrinology, 2000. **141**(2): p. 710-721.
123. Mruk, D.D. and C.Y. Cheng, *Sertoli-Sertoli and Sertoli-Germ Cell Interactions and Their Significance in Germ Cell Movement in the Seminiferous Epithelium during Spermatogenesis*. Endocrine Reviews, 2004. **25**(5): p. 747-806.
124. Cheng, C.Y. and D.D. Mruk, *An intracellular trafficking pathway in the seminiferous epithelium regulating spermatogenesis: a biochemical and molecular perspective*. Critical reviews in biochemistry and molecular biology, 2009. **44**(5): p. 245-263.

125. Vogl, A., et al., *Molecular mechanisms in spermatogenesis*. Springer, 2008.
126. Cheng, C.Y. and D.D. Mruk, *A local autocrine axis in the testes that regulates spermatogenesis*. *Nat Rev Endocrinol*, 2010. **6**(7): p. 380-95.
127. Mruk, D.D. and C.Y. Cheng, *The Mammalian Blood-Testis Barrier: Its Biology and Regulation*. *Endocrine Reviews*, 2015. **36**(5): p. 564-591.
128. Vogl, A.W., K.S. Vaid, and J.A. Guttman, *The Sertoli cell cytoskeleton*. *Molecular mechanisms in spermatogenesis*, 2008: p. 186-211.
129. Cheng, C.Y. and F. Sun, *Molecular mechanisms in spermatogenesis*. Vol. 636. 2008: Springer.
130. Bass-Zubek, A.E., et al., *Plakophilins: multifunctional scaffolds for adhesion and signaling*. *Current opinion in cell biology*, 2009. **21**(5): p. 708-716.
131. Getsios, S., A.C. Huen, and K.J. Green, *Working out the strength and flexibility of desmosomes*. *Nature reviews Molecular cell biology*, 2004. **5**(4): p. 271-281.
132. Green, K.J., et al., *Intercellular junction assembly, dynamics, and homeostasis*. *Cold Spring Harbor perspectives in biology*, 2010. **2**(2): p. a000125.
133. Green, K.J. and C.L. Simpson, *Desmosomes: new perspectives on a classic*. *Journal of Investigative Dermatology*, 2007. **127**(11): p. 2499-2515.
134. Lie, P.P., C.Y. Cheng, and D.D. Mruk, *The biology of the desmosome-like junction: a versatile anchoring junction and signal transducer in the seminiferous epithelium*. *International review of cell and molecular biology*, 2011. **286**: p. 223-269.
135. Mruk, D.D. and C.Y. Cheng, *Desmosomes in the testis: moving into an uncharted territory*. *Spermatogenesis*, 2011. **1**(1): p. 47-51.

136. Thomason, H.A., et al., *Desmosomes: adhesive strength and signalling in health and disease*. Biochemical Journal, 2010. **429**(3): p. 419-433.
137. Pointis, G., et al., *Physiological and physiopathological aspects of connexins and communicating gap junctions in spermatogenesis*. Philosophical Transactions of the Royal Society B: Biological Sciences, 2010. **365**(1546): p. 1607-1620.
138. Cheng, C.Y., et al., *Regulation of blood-testis barrier dynamics by desmosome, gap junction, hemidesmosome and polarity proteins: An unexpected turn of events*. Spermatogenesis, 2011. **1**(2): p. 105-115.
139. Franca, L., et al., *Biology and regulation of blood-tissue barriers*. 2011.
140. Mital, P., B.T. Hinton, and J.M. Dufour, *The blood-testis and blood-epididymis barriers are more than just their tight junctions*. Biology of reproduction, 2011. **84**(5): p. 851-858.
141. De Kretser, D. and J. Kerr, *The physiology of reproduction*. The cytology of the testis, 1994. **2**: p. 1177-290.
142. Kerr, J., et al., *Knobil and Neill's Physiology of Reproduction*. 2006.
143. Russell, L., *Movement of spermatocytes from the basal to the adluminal compartment of the rat testis*. American Journal of Anatomy, 1977. **148**(3): p. 313-328.
144. Cheng, C.Y. and D.D. Mruk, *Cell junction dynamics in the testis: Sertoli-germ cell interactions and male contraceptive development*. Physiol Rev, 2002. **82**(4): p. 825-74.

145. Biotechnologies, i. *Human Sertoli Cells (HSerC)*. [cited 2023 March 6]; Available from: <https://www.ixcellsbiotech.com/human-primary-cells/human-sertoli-cells-hserc>.
146. Biotechnologies, i. *About Us*. [cited 2023 March 6]; Available from: <https://www.ixcellsbiotech.com/about-us-2/about>.
147. Biotechnologies, i. *Human Primary Cells*. [cited 2023 March 6]; Available from: https://www.ixcellsbiotech.com/product/human-primary-cells?sort_options=a.ordering-ASC&start=0.
148. Kaur, G. and J.M. Dufour, *Cell lines*. Spermatogenesis, 2012. **2**(1): p. 1-5.
149. Byers, S.W., et al., *Growth and characterization of polarized monolayers of epididymal epithelial cells and Sertoli cells in dual environment culture chambers*. J Androl, 1986. **7**(1): p. 59-68.
150. Janecki, A. and A. Steinberger, *Polarized Sertoli cell functions in a new two-compartment culture system*. J Androl, 1986. **7**(1): p. 69-71.
151. Russell, L.D. and M.D. Griswold, *The sertoli cell*. 1993: Cache River Press.
152. Siu, M.K., et al., *Sertoli-germ cell anchoring junction dynamics in the testis are regulated by an interplay of lipid and protein kinases*. Journal of Biological Chemistry, 2005. **280**(26): p. 25029-25047.
153. Li, M.W., et al., *Connexin 43 and plakophilin-2 as a protein complex that regulates blood–testis barrier dynamics*. Proceedings of the National Academy of Sciences, 2009. **106**(25): p. 10213-10218.
154. Lie, P.P., C.Y. Cheng, and D.D. Mruk, *Crosstalk between desmoglein-2/desmocollin-2/Src kinase and coxsackie and adenovirus receptor/ZO-1 protein*

- complexes, regulates blood-testis barrier dynamics. The international journal of biochemistry & cell biology, 2010. 42(6): p. 975-986.*
155. Chung, N.P. and C.Y. Cheng, *Is cadmium chloride-induced inter-Sertoli tight junction permeability barrier disruption a suitable in vitro model to study the events of junction disassembly during spermatogenesis in the rat testis?* Endocrinology, 2001. **142(5)**: p. 1878-1888.
156. Janecki, A., A. Jakubowiak, and A. Steinberger, *Effect of cadmium chloride on transepithelial electrical resistance of Sertoli cell monolayers in two-compartment cultures—a new model for toxicological investigations of the “blood-testis” barrier in vitro.* Toxicology and applied pharmacology, 1992. **112(1)**: p. 51-57.
157. OKANLAWON, A. and M. DYM, *Effect of chloroquine on the formation of tight junctions in cultured immature rat Sertoli cells.* Journal of andrology, 1996. **17(3)**: p. 249-255.
158. Siu, E.R., et al., *Cadmium-induced testicular injury.* Toxicology and applied pharmacology, 2009. **238(3)**: p. 240-249.
159. Koval, M., *Drug Delivery Across Physiological Barriers.* 2016.
160. Eaton, D.C., et al., *The contribution of epithelial sodium channels to alveolar function in health and disease.* Annual review of physiology, 2009. **71**: p. 403-423.
161. Venkatasubramanian, J., M. Ao, and M.C. Rao, *Ion transport in the small intestine.* Current opinion in gastroenterology, 2010. **26(2)**: p. 123-128.

162. Salama, N.N., N.D. Eddington, and A. Fasano, *Tight junction modulation and its relationship to drug delivery*. *Advanced Drug Delivery Reviews*, 2006. **58**(1): p. 15-28.
163. Grima, J., et al., *Testin Secreted by Sertoli Cells Is Associated with the Cell Surface, and Its Expression Correlates with the Disruption of Sertoli-Germ Cell Junctions but Not the Inter-Sertoli Tight Junction**. *Journal of Biological Chemistry*, 1998. **273**(33): p. 21040-21053.
164. Mruk, D.D. and C.Y. Cheng, *An in vitro system to study Sertoli cell blood-testis barrier dynamics*. *Methods Mol Biol*, 2011. **763**: p. 237-52.
165. Elbrecht, D.H., C.J. Long, and J.J. Hickman, *Transepithelial/endothelial Electrical Resistance (TEER) theory and applications for microfluidic body-on-a-chip devices*. *Journal of Rare Diseases Research & Treatment*, 2016. **1**(3).
166. Stewart, T., et al., *Calibrated flux measurements reveal a nanostructure-stimulated transcytotic pathway*. *Experimental Cell Research*, 2017. **355**(2): p. 153-161.
167. Gao, Y., D.D. Mruk, and C.Y. Cheng, *Sertoli cells are the target of environmental toxicants in the testis - a mechanistic and therapeutic insight*. *Expert Opin Ther Targets*, 2015. **19**(8): p. 1073-90.
168. Li, M.W., et al., *Disruption of the blood-testis barrier integrity by bisphenol A in vitro: is this a suitable model for studying blood-testis barrier dynamics?* *The international journal of biochemistry & cell biology*, 2009. **41**(11): p. 2302-2314.

169. Wong, C.-h., et al., *Blood-testis barrier dynamics are regulated by α 2-macroglobulin via the c-Jun N-terminal protein kinase pathway*. *Endocrinology*, 2005. **146**(4): p. 1893-1908.
170. Wan, H.T., et al., *Perfluorooctanesulfonate (PFOS) perturbs male rat Sertoli cell blood-testis barrier function by affecting F-actin organization via p-FAK-Tyr(407): an in vitro study*. *Endocrinology*, 2014. **155**(1): p. 249-62.
171. Qiu, L., et al., *Sertoli cell is a potential target for perfluorooctane sulfonate-induced reproductive dysfunction in male mice*. *toxicological sciences*, 2013. **135**(1): p. 229-240.
172. Su, L., et al., *A peptide derived from laminin- γ 3 reversibly impairs spermatogenesis in rats*. *Nature Communications*, 2012. **3**(1): p. 1185.
173. Lui, W.Y., et al., *TGF-beta3 regulates the blood-testis barrier dynamics via the p38 mitogen activated protein (MAP) kinase pathway: an in vivo study*. *Endocrinology*, 2003. **144**(4): p. 1139-42.
174. Wong, C.H., et al., *Regulation of blood-testis barrier dynamics: an in vivo study*. *J Cell Sci*, 2004. **117**(Pt 5): p. 783-98.
175. Reis, M.M., et al., *Sertoli cell as a model in male reproductive toxicology: Advantages and disadvantages*. *Journal of Applied Toxicology*, 2015. **35**(8): p. 870-883.
176. Boivin, J., et al., *International estimates of infertility prevalence and treatment-seeking: potential need and demand for infertility medical care*. *Hum Reprod*, 2007. **22**(6): p. 1506-12.

177. Rutstein, S.O. and I.H. Shah, *Infecundity, infertility, and childlessness in developing countries*, in *Infecundity, infertility, and childlessness in developing countries*. 2004. p. 56-56.
178. Kumar, N. and A.K. Singh, *Trends of male factor infertility, an important cause of infertility: A review of literature*. Journal of human reproductive sciences, 2015. **8**(4): p. 191-196.
179. Gassei, K. and K.E. Orwig, *Experimental methods to preserve male fertility and treat male factor infertility*. Fertility and sterility, 2016. **105**(2): p. 256-266.
180. Louis, J.F., et al., *The prevalence of couple infertility in the United States from a male perspective: evidence from a nationally representative sample*. Andrology, 2013. **1**(5): p. 741-748.
181. Chandra, A., C.E. Copen, and E.H. Stephen, *Infertility and impaired fecundity in the United States, 1982-2010: data from the National Survey of Family Growth*. Natl Health Stat Report, 2013(67): p. 1-18, 1 p following 19.
182. Kristensen, D.M., et al., *Analgesic use - prevalence, biomonitoring and endocrine and reproductive effects*. Nat Rev Endocrinol, 2016. **12**(7): p. 381-93.
183. Hudec, R., L. Božeková, and J. Tisoňová, *Consumption of three most widely used analgesics in six European countries*. Journal of Clinical Pharmacy and Therapeutics, 2012. **37**(1): p. 78-80.
184. Laine, L., *Approaches to nonsteroidal anti-inflammatory drug use in the high-risk patient*. Gastroenterology, 2001. **120**(3): p. 594-606.
185. Singh, G., *Gastrointestinal complications of prescription and over-the-counter nonsteroidal anti-inflammatory drugs: a view from the ARAMIS database*.

- Arthritis, Rheumatism, and Aging Medical Information System*. Am J Ther, 2000. 7(2): p. 115-21.
186. Kaufman, D.W., et al., *Recent patterns of medication use in the ambulatory adult population of the United States: the Slone survey*. JAMA, 2002. 287(3): p. 337-44.
187. Zhou, Y., D.M. Boudreau, and A.N. Freedman, *Trends in the use of aspirin and nonsteroidal anti-inflammatory drugs in the general U.S. population*. Pharmacoepidemiology and Drug Safety, 2014. 23(1): p. 43-50.
188. *Non-steroidal Anti-inflammatory Drugs Market Size, Share & Trends Analysis Report By Disease Indication (Arthritis, Migraine, Ophthalmic Diseases), By Route Of Administration, By Distribution Channel, By Region, And Segment Forecasts, 2022 - 2030*. Grand View Research, Inc. p. 150.
189. Thomson, W.M., et al., *Changes in medication use from age 26 to 32 in a representative birth cohort*. Intern Med J, 2007. 37(8): p. 543-9.
190. Stache, S., et al., *Nonprescription pain medication use in collegiate athletes: a comparison of samples*. Phys Sportsmed, 2014. 42(2): p. 19-26.
191. Rossignol, M., et al., *The CADEUS study: burden of nonsteroidal anti-inflammatory drug (NSAID) utilization for musculoskeletal disorders in blue collar workers*. Br J Clin Pharmacol, 2009. 67(1): p. 118-24.
192. Brune, K. and B. Hinz, *The discovery and development of antiinflammatory drugs*. Arthritis Rheum, 2004. 50(8): p. 2391-9.
193. Jones, R., *Nonsteroidal anti-inflammatory drug prescribing: past, present, and future*. Am J Med, 2001. 110(1a): p. 4s-7s.

194. Vane, J.R. and R.M. Botting, *Mechanism of action of nonsteroidal anti-inflammatory drugs*. Am J Med, 1998. **104**(3a): p. 2S-8S; discussion 21S-22S.
195. Smith, W.L., D.L. DeWitt, and R.M. Garavito, *Cyclooxygenases: structural, cellular, and molecular biology*. Annu Rev Biochem, 2000. **69**: p. 145-82.
196. Urade, Y., K. Watanabe, and O. Hayaishi, *Prostaglandin D, E, and F synthases*. Journal of Lipid Mediators and Cell Signalling, 1995. **12**(2): p. 257-273.
197. Watanabe, K., *Prostaglandin F synthase*. Prostaglandins Other Lipid Mediat, 2002. **68-69**: p. 401-7.
198. Moncada, S. and J.R. Vane, *Pharmacology and endogenous roles of prostaglandin endoperoxides, thromboxane A₂, and prostacyclin*. Pharmacological Reviews, 1978. **30**(3): p. 293-331.
199. Ferreira, S., *Prostaglandins and signs and symptoms of inflammation*. Prostaglandin synthetase inhibitors., 1974: p. 175-198.
200. Moncada, S. and J.R. Vane, *Mode of action of aspirin-like drugs*. Adv Intern Med, 1979. **24**: p. 1-22.
201. Vane, J.R., *Inhibition of prostaglandin synthesis as a mechanism of action for aspirin-like drugs*. Nature new biology, 1971. **231**: p. 232-235.
202. Vane, J.R., *The fight against rheumatism: from willow bark to COX-1 sparing drugs*. J Physiol Pharmacol, 2000. **51**(4 Pt 1): p. 573-86.
203. Frungieri, M., et al., *Sources and functions of prostaglandins in the testis: evidence for their relevance in male (in)fertility*. 2007.

204. Katori, M. and M. Majima, *Cyclooxygenase-2: its rich diversity of roles and possible application of its selective inhibitors*. *Inflammation Research*, 2000. **49**(8): p. 367-392.
205. Simmons, D.L., R.M. Botting, and T. Hla, *Cyclooxygenase isozymes: the biology of prostaglandin synthesis and inhibition*. *Pharmacol Rev*, 2004. **56**(3): p. 387-437.
206. Barkay, J., et al., *The prostaglandin inhibitor effect of antiinflammatory drugs in the therapy of male infertility*. *Fertil Steril*, 1984. **42**(3): p. 406-11.
207. Schaefer, M., et al., *A new prostaglandin E receptor mediates calcium influx and acrosome reaction in human spermatozoa*. *Proceedings of the National Academy of Sciences*, 1998. **95**(6): p. 3008-3013.
208. Cenedella, R.J., *Prostaglandins and male reproductive physiology*. *Adv Sex Horm Res*, 1975. **1**: p. 325-58.
209. Frungieri, M.B., *Cyclooxygenase 2 (COX2) and Prostaglandins: Emerging Roles in the Testis*. *Biology of Reproduction*, 2008. **78**(Suppl_1): p. 159-159.
210. Winnall, W.R., et al., *Constitutive Expression of Prostaglandin-Endoperoxide Synthase 2 by Somatic and Spermatogenic Cells Is Responsible for Prostaglandin E2 Production in the Adult Rat Testis1*. *Biology of Reproduction*, 2007. **76**(5): p. 759-768.
211. Conaghan, P.G., *A turbulent decade for NSAIDs: update on current concepts of classification, epidemiology, comparative efficacy, and toxicity*. *Rheumatol Int*, 2012. **32**(6): p. 1491-502.

212. Davies, N.M. and K.E. Anderson, *Clinical Pharmacokinetics of Naproxen*. *Clinical Pharmacokinetics*, 1997. **32**(4): p. 268-293.
213. *Naproxen vs ibuprofen: What's the difference?* 2022 March 21, 2022 [cited 2023 February 16, 2022]; Available from: <https://www.drugs.com/medical-answers/naproxen-ibuprofen-difference-3117722/>.
214. Davies, N.M. and K.E. Anderson, *Clinical pharmacokinetics of naproxen*. *Clin Pharmacokinet*, 1997. **32**(4): p. 268-93.
215. Day, R.O., G.G. Graham, and K.M. Williams, *Pharmacokinetics of non-steroidal anti-inflammatory drugs*. *Baillieres Clin Rheumatol*, 1988. **2**(2): p. 363-93.
216. Rainsford, K., *Ibuprofen: pharmacology, efficacy and safety*. *Inflammopharmacology*, 2009. **17**: p. 275-342.
217. Moore, N., C. Pollack, and P. Butkerait, *Adverse drug reactions and drug-drug interactions with over-the-counter NSAIDs*. *Ther Clin Risk Manag*, 2015. **11**: p. 1061-75.
218. Ternes, T.A., *Occurrence of drugs in German sewage treatment plants and rivers* *Dedicated to Professor Dr. Klaus Haberer on the occasion of his 70th birthday. I*. *Water Research*, 1998. **32**(11): p. 3245-3260.
219. Mompelat, S., B. Le Bot, and O. Thomas, *Occurrence and fate of pharmaceutical products and by-products, from resource to drinking water*. *Environment International*, 2009. **35**(5): p. 803-814.
220. Christensen, F., *Pharmaceuticals in the environment—a human risk?* *Regulatory toxicology and pharmacology*, 1998. **28**(3): p. 212-221.

221. Žur, J., et al., *Organic micropollutants paracetamol and ibuprofen—toxicity, biodegradation, and genetic background of their utilization by bacteria*. Environmental Science and Pollution Research, 2018. **25**: p. 21498-21524.
222. Bloom, M.S., et al., *Associations between urinary phthalate concentrations and semen quality parameters in a general population*. Human Reproduction, 2015. **30**(11): p. 2645-2657.
223. Revonta, M., et al., *Health and life style among infertile men and women*. Sex Reprod Healthc, 2010. **1**(3): p. 91-8.
224. Young, H.A., et al., *Environmental exposure to pyrethroids and sperm sex chromosome disomy: a cross-sectional study*. Environ Health, 2013. **12**: p. 111.
225. Bereiter-Hahn, J. and M. Vöth, *Dynamics of mitochondria in living cells: shape changes, dislocations, fusion, and fission of mitochondria*. Microscopy research and technique, 1994. **27**(3): p. 198-219.
226. Dykens, J.A., R.E. Davis, and W.H. Moos, *Introduction to mitochondrial function and genomics*. Drug development research, 1999. **46**(1): p. 2-13.
227. Lemasters, J.J., et al., *Role of mitochondrial inner membrane permeabilization in necrotic cell death, apoptosis, and autophagy*. Antioxidants and Redox Signaling, 2002. **4**(5): p. 769-781.
228. McBride, H.M., M. Neuspiel, and S. Wasiak, *Mitochondria: more than just a powerhouse*. Current biology, 2006. **16**(14): p. R551-R560.
229. Mitchell, P., *Coupling of phosphorylation to electron and hydrogen transfer by a chemi-osmotic type of mechanism*. Nature, 1961. **191**: p. 144-148.

230. Pacher, P. and G. Hajnóczky, *Propagation of the apoptotic signal by mitochondrial waves*. The EMBO journal, 2001. **20**(15): p. 4107-4121.
231. Krysko, D.V., et al., *Mitochondrial transmembrane potential changes support the concept of mitochondrial heterogeneity during apoptosis*. J Histochem Cytochem, 2001. **49**(10): p. 1277-84.
232. Nadanaciva, S. and Y. Will, *Investigating mitochondrial dysfunction to increase drug safety in the pharmaceutical industry*. Current drug targets, 2011. **12**(6): p. 774-782.
233. Attene-Ramos, M.S., et al., *Profiling of the Tox21 Chemical Collection for Mitochondrial Function to Identify Compounds that Acutely Decrease Mitochondrial Membrane Potential*. Environmental Health Perspectives, 2015. **123**(1): p. 49-56.
234. Moorthy, M., S. Fakurazi, and H. Ithnin, *Morphological alteration in mitochondria following diclofenac and ibuprofen administration*. Pak J Biol Sci, 2008. **11**(15): p. 1901-8.
235. Moreno-Sánchez, R., et al., *Inhibition and uncoupling of oxidative phosphorylation by nonsteroidal anti-inflammatory drugs: study in mitochondria, submitochondrial particles, cells, and whole heart*. Biochemical pharmacology, 1999. **57**(7): p. 743-752.
236. Upadhyay, A., et al., *Ibuprofen Induces Mitochondrial-Mediated Apoptosis Through Proteasomal Dysfunction*. Molecular Neurobiology, 2016. **53**(10): p. 6968-6981.

237. van Leeuwen, J.S., et al., *Differential involvement of mitochondrial dysfunction, cytochrome P450 activity, and active transport in the toxicity of structurally related NSAIDs*. *Toxicol In Vitro*, 2012. **26**(2): p. 197-205.
238. Ghosh, R., A. Alajbegovic, and A.V. Gomes, *NSAIDs and Cardiovascular Diseases: Role of Reactive Oxygen Species*. *Oxid Med Cell Longev*, 2015. **2015**: p. 536962.
239. Boizet-Bonhoure, B., et al., *Using Experimental Models to Decipher the Effects of Acetaminophen and NSAIDs on Reproductive Development and Health*. *Front Toxicol*, 2022. **4**: p. 835360.
240. Aly, H.A., *Aroclor 1254 induced oxidative stress and mitochondria mediated apoptosis in adult rat sperm in vitro*. *Environmental Toxicology and Pharmacology*, 2013. **36**(2): p. 274-283.
241. Ingram, M.J., et al., *A potential anti-implantation and spermicidal strategy: putative derivatives of nonoxynol-9 and anti-inflammatory agents and their spermicidal activity*. *Eur J Contracept Reprod Health Care*, 2006. **11**(4): p. 258-61.
242. Martini, A.C., et al., *Chronic administration of nonsteroidal-antiinflammatory drugs (NSAIDs): effects upon mouse reproductive functions*. *Rev Fac Cien Med Univ Nac Cordoba*, 2008. **65**(2): p. 41-51.
243. Johnson, D.G. and C.L. Walker, *Cyclins and cell cycle checkpoints*. *Annual review of pharmacology and toxicology*, 1999. **39**.

244. Shackelford, R.E., W.K. Kaufmann, and R.S. Paules, *Cell cycle control, checkpoint mechanisms, and genotoxic stress*. Environ Health Perspect, 1999. **107 Suppl 1**(Suppl 1): p. 5-24.
245. Leidgens, V., et al., *Ibuprofen and Diclofenac Restrict Migration and Proliferation of Human Glioma Cells by Distinct Molecular Mechanisms*. PLOS ONE, 2015. **10**(10): p. e0140613.
246. Varvel, N.H., et al., *NSAIDs prevent, but do not reverse, neuronal cell cycle reentry in a mouse model of Alzheimer disease*. The Journal of Clinical Investigation, 2009. **119**(12): p. 3692-3702.
247. Aydin, S., M.E. Aydin, and A. Ulvi, *Monitoring the release of anti-inflammatory and analgesic pharmaceuticals in the receiving environment*. Environmental Science and Pollution Research, 2019. **26**: p. 36887-36902.
248. de Santiago-Martín, A., et al., *Pharmaceuticals and trace metals in the surface water used for crop irrigation: Risk to health or natural attenuation?* Science of The Total Environment, 2020. **705**: p. 135825.
249. Nantaba, F., et al., *Occurrence, distribution, and ecotoxicological risk assessment of selected pharmaceutical compounds in water from Lake Victoria, Uganda*. Chemosphere, 2020. **239**: p. 124642.
250. Palma, P., et al., *Pharmaceuticals in a Mediterranean Basin: The influence of temporal and hydrological patterns in environmental risk assessment*. Science of the Total Environment, 2020. **709**: p. 136205.
251. Rabiet, M., et al., *Consequences of treated water recycling as regards pharmaceuticals and drugs in surface and ground waters of a medium-sized*

- Mediterranean catchment*. Environmental science & technology, 2006. **40**(17): p. 5282-5288.
252. Wee, S.Y. and A.Z. Aris, *Endocrine disrupting compounds in drinking water supply system and human health risk implication*. Environment international, 2017. **106**: p. 207-233.
253. Wang, F., et al., *Heterogeneity of claudin expression by alveolar epithelial cells*. Am J Respir Cell Mol Biol, 2003. **29**(1): p. 62-70.
254. Albert, O., et al., *Paracetamol, aspirin and indomethacin display endocrine disrupting properties in the adult human testis in vitro*. Human Reproduction, 2013. **28**(7): p. 1890-1898.
255. Conte, D., et al., *Aspirin inhibits androgen response to chorionic gonadotropin in humans*. American Journal of Physiology-Endocrinology and Metabolism, 1999. **277**(6): p. E1032-E1037.
256. Kim, M.-S., et al., *Naproxen induces cell-cycle arrest and apoptosis in human urinary bladder cancer cell lines and chemically induced cancers by targeting PI3K*. Cancer Prevention Research, 2014. **7**(2): p. 236-245.
257. Chang, J.-K., et al., *Nonsteroidal Anti-Inflammatory Drug Effects on Osteoblastic Cell Cycle, Cytotoxicity, and Cell Death*. Connective Tissue Research, 2005. **46**(4-5): p. 200-210.
258. Kaufman, D.W., et al., *Exceeding the daily dosing limit of nonsteroidal anti-inflammatory drugs among ibuprofen users*. Pharmacoepidemiology and Drug Safety, 2018. **27**(3): p. 322-331.

259. Andersson, A.M., et al., *Impaired Leydig cell function in infertile men: a study of 357 idiopathic infertile men and 318 proven fertile controls*. J Clin Endocrinol Metab, 2004. **89**(7): p. 3161-7.
260. Hurtado-Gonzalez, P., et al., *Effects of Exposure to Acetaminophen and Ibuprofen on Fetal Germ Cell Development in Both Sexes in Rodent and Human Using Multiple Experimental Systems*. Environ Health Perspect, 2018. **126**(4): p. 047006.
261. Barbosa, M.G., et al., *Pre-pubertal exposure to ibuprofen impairs sperm parameters in male adult rats and compromises the next generation*. Journal of toxicology and environmental health. Part A, 2020: p. 1-14.
262. Qato, D.M., et al., *Use of prescription and over-the-counter medications and dietary supplements among older adults in the United States*. JAMA, 2008. **300**(24): p. 2867-2878.
263. Banihani, S.A., *Effect of aspirin on semen quality: A review*. Andrologia, 2020. **52**(1): p. e13487.
264. Banihani, S.A., *Effect of paracetamol on semen quality*. Andrologia, 2018. **50**(1).
265. Koval, M., *Claudin heterogeneity and control of lung tight junctions*. Annu Rev Physiol, 2013. **75**: p. 551-67.
266. Kissinger, C., M.K. Skinner, and M.D. Griswold, *Analysis of Sertoli cell-secreted proteins by two-dimensional gel electrophoresis*. Biol Reprod, 1982. **27**(1): p. 233-40.
267. Mather, J.P., et al., *The hormonal and cellular control of Sertoli cell secretion*. J Steroid Biochem, 1983. **19**(1a): p. 41-51.

268. Lichtenberger, L.M., et al., *Insight into NSAID-induced membrane alterations, pathogenesis and therapeutics: Characterization of interaction of NSAIDs with phosphatidylcholine*. *Biochimica et Biophysica Acta (BBA) - Molecular and Cell Biology of Lipids*, 2012. **1821**(7): p. 994-1002.
269. Siu, M.K., W.M. Lee, and C.Y. Cheng, *The interplay of collagen IV, tumor necrosis factor-alpha, gelatinase B (matrix metalloproteinase-9), and tissue inhibitor of metalloproteinases-1 in the basal lamina regulates Sertoli cell-tight junction dynamics in the rat testis*. *Endocrinology*, 2003. **144**(1): p. 371-87.
270. Tung, P.S. and I.B. Fritz, *Interactions of Sertoli cells with laminin are essential to maintain integrity of the cytoskeleton and barrier functions of cells in culture in the two-chambered assembly*. *J Cell Physiol*, 1993. **156**(1): p. 1-11.
271. Ni, F.-D., S.-L. Hao, and W.-X. Yang, *Multiple signaling pathways in Sertoli cells: recent findings in spermatogenesis*. *Cell Death & Disease*, 2019. **10**(8): p. 541.
272. Paul, C. and B. Robaire, *Impaired function of the blood-testis barrier during aging is preceded by a decline in cell adhesion proteins and GTPases*. *PLoS One*, 2013. **8**(12): p. e84354.
273. Kelwick, R., et al., *The ADAMTS (A Disintegrin and Metalloproteinase with Thrombospondin motifs) family*. *Genome Biol*, 2015. **16**(1): p. 113.
274. Mulholland, D.J., S. Dedhar, and A.W. Vogl, *Rat seminiferous epithelium contains a unique junction (Ectoplasmic specialization) with signaling properties both of cell/cell and cell/matrix junctions*. *Biol Reprod*, 2001. **64**(1): p. 396-407.

275. Cashman, J.N., *The mechanisms of action of NSAIDs in analgesia*. *Drugs*, 1996. **52 Suppl 5**: p. 13-23.
276. Cha, Y.I., L. Solnica-Krezel, and R.N. DuBois, *Fishing for prostanoids: deciphering the developmental functions of cyclooxygenase-derived prostaglandins*. *Dev Biol*, 2006. **289**(2): p. 263-72.
277. Korbecki, J., et al., *Cyclooxygenase pathways*. *Acta Biochim Pol*, 2014. **61**(4): p. 639-49.
278. Frungieri, M.B., et al., *Cyclooxygenase and prostaglandins in somatic cell populations of the testis*. 2015. **149**(4): p. R169.
279. Ishikawa, T. and P. Morris, *A multistep kinase-based Sertoli cell autocrine amplifying loop regulates prostaglandins, their receptors, and cytokines*. *Endocrinology*, 2006. **147**: p. 1706-1716.
280. Kristensen, D., et al., *Many putative endocrine disruptors inhibit prostaglandin synthesis*. *Environmental Health Perspectives*, 2011. **119**: p. 534-541.
281. Matzkin, M., et al., *Exploring the cyclooxygenase 2 (COX2)/15d- Δ 12,14PGJ2 system in hamster Sertoli cells: regulation by FSH/testosterone and relevance to glucose uptake*. *General and Comparative Endocrinology*, 2012. **179**: p. 254-264.
282. Günzel, D. and A.S.L. Yu, *Claudins and the Modulation of Tight Junction Permeability*. *Physiological Reviews*, 2013. **93**(2): p. 525-569.
283. Frungieri, M., et al., *Proliferative action of mast-cell tryptase is mediated by PAR2, COX2, prostaglandins, and PPAR γ : possible relevance to human fibrotic disorders*. *PNAS*, 2002. **99**: p. 15072-15077.

284. Hase, T., et al., *Cyclooxygenase-1 and -2 in human testicular tumours*. European Journal of Cancer, 2003. **39**: p. 2043-2049.
285. Meroni, S.B., et al., *Molecular Mechanisms and Signaling Pathways Involved in Sertoli Cell Proliferation*. Frontiers in Endocrinology, 2019. **10**.
286. Chai, A.C., et al., *Ibuprofen regulates the expression and function of membrane-associated serine proteases prostasin and matriptase*. BMC Cancer, 2015. **15**(1): p. 1025.
287. Steed, E., M.S. Balda, and K. Matter, *Dynamics and functions of tight junctions*. Trends Cell Biol, 2010. **20**(3): p. 142-9.
288. Tsukita, S., M. Furuse, and M. Itoh, *Multifunctional strands in tight junctions*. Nat Rev Mol Cell Biol, 2001. **2**(4): p. 285-93.
289. Ozaki-Kuroda, K., et al., *Nectin couples cell-cell adhesion and the actin scaffold at heterotypic testicular junctions*. Curr Biol, 2002. **12**(13): p. 1145-50.
290. Cavicchia, J.C., F.L. Sacerdote, and L. Ortiz, *The Human Blood-Testis Barrier in Impaired Spermatogenesis*. Ultrastructural Pathology, 1996. **20**(3): p. 211-218.
291. Pérez, C., et al., *Dual role of immune cells in the testis: protective or pathogenic for germ cells?* Spermatogenesis, 2013. **3**: p. e23870.
292. Frungieri, M., et al., *Number, distribution pattern, and identification of macrophages in the testes of infertile men*. Fertility and Sterility, 2002. **78**: p. 298-306.
293. Meineke, V., et al., *Human testicular mast cells contain tryptase: increased mast cell number and altered distribution in the testes of infertile men*. Fertility and Sterility, 2000. **74**: p. 239-244.

294. Matzkin, M.E., et al., *Cyclooxygenase-2 in testes of infertile men: evidence for the induction of prostaglandin synthesis by interleukin-1 β* . *Fertil Steril*, 2010. **94**(5): p. 1933-6.
295. Welter, H., F. Kohn, and A. Mayerhofer, *Mast cells in human testicular biopsies from patients with mixed atrophy: increased numbers, heterogeneity, and expression of cyclooxygenase 2 and prostaglandin D2 synthase*. *Fertility and Sterility*, 2011. **96**: p. 309-313.
296. Rossi, S.P., et al., *Melatonin in testes of infertile men: evidence for anti-proliferative and anti-oxidant effects on local macrophage and mast cell populations*. *Andrology*, 2014. **2**(3): p. 436-49.
297. Gaur, M., et al., *Isolation of human testicular cells and co-culture with embryonic stem cells*. *Reproduction*, 2018. **155**(2): p. 153-166.
298. Ward, C., et al., *NF- κ B inhibitors impair lung epithelial tight junctions in the absence of inflammation*. *Tissue Barriers*, 2015. **3**(1-2): p. e982424.
299. Walsh, L., et al., *Nanotopography facilitates in vivo transdermal delivery of high molecular weight therapeutics through an integrin-dependent mechanism*. *Nano Lett*, 2015. **15**(4): p. 2434-41.
300. Kam, K.R., et al., *Nanostructure-mediated transport of biologics across epithelial tissue: enhancing permeability via nanotopography*. *Nano Lett*, 2013. **13**(1): p. 164-71.
301. Lucy, L.B., *An iterative technique for the rectification of observed distributions*. *The astronomical journal*, 1974. **79**: p. 745.

302. Richardson, W.H., *Bayesian-based iterative method of image restoration*. JoSA, 1972. **62**(1): p. 55-59.
303. Holstein, A., et al., *Morphology of normal and malignant germ cells*. International journal of andrology, 1987. **10**(1): p. 1-18.
304. Schulze, W., et al., *Processing of Testicular Biopsies—Fixed in Stieve's Solution—for Visualization of Substance P-and Methionine-Enkephalin-Like Immunoreactivity in Leydig Cells*. Andrologia, 1987. **19**(4): p. 419-422.
305. Goluža, T., et al., *Macrophages and Leydig cells in testicular biopsies of azoospermic men*. Biomed Res Int, 2014. **2014**: p. 828697.
306. Jezek, D., U. Knuth, and W. Schulze, *Successful testicular sperm extraction (TESE) in spite of high serum follicle stimulating hormone and azoospermia: correlation between testicular morphology, TESE results, semen analysis and serum hormone values in 103 infertile men*. Human reproduction (Oxford, England), 1998. **13**(5): p. 1230-1234.
307. Sigg, C. and C. Hedinger, *Quantitative and ultrastructural study of germinal epithelium in testicular biopsies with "mixed atrophy"*. Andrologia, 1981. **13**(5): p. 412-24.
308. Fink, C., et al., *On the origin of germ cell neoplasia in situ: Dedifferentiation of human adult Sertoli cells in cross talk with seminoma cells in vitro*. Neoplasia, 2021. **23**(7): p. 731-742.
309. Cheung, S., et al., *Genetic and epigenetic profiling of the infertile male*. PLOS ONE, 2019. **14**(3): p. e0214275.

310. Wu, Z.-J., et al., *CRISPR/Cas9-mediated ASXL1 mutations in U937 cells disrupt myeloid differentiation*. *Int J Oncol*, 2018. **52**(4): p. 1209-1223.
311. Taghbalout, A., et al., *Enhanced CRISPR-based DNA demethylation by Casilio-ME-mediated RNA-guided coupling of methylcytosine oxidation and DNA repair pathways*. *Nature Communications*, 2019. **10**(1): p. 4296.
312. Bolger, A.M., M. Lohse, and B. Usadel, *Trimmomatic: a flexible trimmer for Illumina sequence data*. *Bioinformatics*, 2014. **30**(15): p. 2114-2120.
313. Ritchie, M.E., et al., *limma powers differential expression analyses for RNA-sequencing and microarray studies*. *Nucleic Acids Research*, 2015. **43**(7): p. e47-e47.
314. Robinson, M.D., D.J. McCarthy, and G.K. Smyth, *edgeR: a Bioconductor package for differential expression analysis of digital gene expression data*. *Bioinformatics*, 2010. **26**(1): p. 139-40.
315. Law, C.W., et al., *voom: precision weights unlock linear model analysis tools for RNA-seq read counts*. *Genome Biology*, 2014. **15**(2): p. R29.
316. Phipson, B., et al., *ROBUST HYPERPARAMETER ESTIMATION PROTECTS AGAINST HYPERVARIABLE GENES AND IMPROVES POWER TO DETECT DIFFERENTIAL EXPRESSION*. *Ann Appl Stat*, 2016. **10**(2): p. 946-963.
317. Smyth, G.K., Ritchie, M., Thorne, N., Wettenhall, J., Shi, W., Hu, Yifang. *limma: Linear Models for Microarray and RNA-seq Data User's Guide*. 2022; Available from:
<http://bioconductor.org/packages/release/bioc/vignettes/limma/inst/doc/usersguide.pdf>.

318. Liberzon, A., et al., *The Molecular Signatures Database (MSigDB) hallmark gene set collection*. Cell Syst, 2015. **1**(6): p. 417-425.
319. Köhler, S., et al., *The Human Phenotype Ontology in 2021*. Nucleic Acids Research, 2020. **49**(D1): p. D1207-D1217.
320. Szklarczyk, D., et al., *STRING v10: protein-protein interaction networks, integrated over the tree of life*. Nucleic Acids Res, 2015. **43**(Database issue): p. D447-52.
321. Weissman, T.A. and Y.A. Pan, *Brainbow: new resources and emerging biological applications for multicolor genetic labeling and analysis*. Genetics, 2015. **199**(2): p. 293-306.
322. Alberts, B., Johnson, A., Lewis, J., Raff, M., Roberts, K., Walter, P., *Sperm*, in *Molecular Biology of the Cell*. 2002, Garland Science: New York.
323. Shimomura, O., F.H. Johnson, and Y. Saiga, *Extraction, purification and properties of aequorin, a bioluminescent protein from the luminous hydromedusan, Aequorea*. Journal of cellular and comparative physiology, 1962. **59**(3): p. 223-239.
324. Tsien, R.Y., *The green fluorescent protein*. Annual review of biochemistry, 1998. **67**(1): p. 509-544.
325. Shaner, N.C., et al., *Improved monomeric red, orange and yellow fluorescent proteins derived from Discosoma sp. red fluorescent protein*. Nature biotechnology, 2004. **22**(12): p. 1567-1572.
326. Merzlyak, E.M., et al., *Bright monomeric red fluorescent protein with an extended fluorescence lifetime*. Nature methods, 2007. **4**(7): p. 555-557.

327. Cai, D., et al., *Improved tools for the Brainbow toolbox*. Nature Methods, 2013. **10**(6): p. 540-547.
328. Livet, J., et al., *Transgenic strategies for combinatorial expression of fluorescent proteins in the nervous system*. Nature, 2007. **450**(7166): p. 56-62.
329. Day, R.N. and M.W. Davidson, *The fluorescent protein palette: tools for cellular imaging*. Chemical Society Reviews, 2009. **38**(10): p. 2887-2921.
330. Giepmans, B.N., et al., *The fluorescent toolbox for assessing protein location and function*. science, 2006. **312**(5771): p. 217-224.
331. Rodriguez, E.A., et al., *The growing and glowing toolbox of fluorescent and photoactive proteins*. Trends in biochemical sciences, 2017. **42**(2): p. 111-129.
332. Shaner, N.C., P.A. Steinbach, and R.Y. Tsien, *A guide to choosing fluorescent proteins*. Nature methods, 2005. **2**(12): p. 905-909.
333. Chao, J.H. and S.T. Page, *The current state of male hormonal contraception*. Pharmacology & Therapeutics, 2016. **163**: p. 109-117.
334. Finer, L.B. and M.R. Zolna, *Shifts in intended and unintended pregnancies in the United States, 2001-2008*. Am J Public Health, 2014. **104 Suppl 1**: p. S43-8.
335. Amory, J.K., *Male contraception*. Fertility and Sterility, 2016. **106**(6): p. 1303-1309.
336. Brown, S.S. and L. Eisenberg, *The best intentions: Unintended pregnancy and the well-being of children and families*. 1995.
337. Gipson, J.D., M.A. Koenig, and M.J. Hindin, *The effects of unintended pregnancy on infant, child, and parental health: a review of the literature*. Studies in family planning, 2008. **39**(1): p. 18-38.

338. Hardee, K., et al., *Unintended pregnancy and women's psychological well-being in Indonesia*. Journal of biosocial Science, 2004. **36**(5): p. 617-626.
339. Logan, C., et al., *The consequences of unintended childbearing*. Washington, DC: Child Trends and National Campaign to Prevent Teen Pregnancy, 2007. **28**: p. 142-151.
340. Marston, C. and J. Cleland, *Do unintended pregnancies carried to term lead to adverse outcomes for mother and child? An assessment in five developing countries*. Population studies, 2003. **57**(1): p. 77-93.
341. Tsui, A.O., R. McDonald-Mosley, and A.E. Burke, *Family planning and the burden of unintended pregnancies*. Epidemiologic reviews, 2010. **32**(1): p. 152-174.
342. Sedgh, G., S. Singh, and R. Hussain, *Intended and unintended pregnancies worldwide in 2012 and recent trends*. Studies in family planning, 2014. **45**(3): p. 301-314.
343. Sonfield, A. and K. Kost, *Public costs from unintended pregnancies and the role of public insurance programs in paying for pregnancy-related care. national and state estimates for 2010, 2015*: p. 2015.
344. *Unintended Pregnancy*. Reproductive Health 2019 [cited 2020 November 1]; Available from:
<https://www.cdc.gov/reproductivehealth/contraception/unintendedpregnancy/index.htm>

345. Balbach, M., et al., *On-demand male contraception via acute inhibition of soluble adenylyl cyclase*. Nature Communications, 2023. **14**(1): p. 637.
346. *A Timeline of Contraception*. The Pill Timeline 2020 [cited 2020 November 1]; Available from: <https://www.pbs.org/wgbh/americanexperience/features/pill-timeline/>.
347. *Ten great public health achievements--United States, 1900-1999*. MMWR Morb Mortal Wkly Rep, 1999. **48**(12): p. 241-3.
348. S., S., *Abnormal uterine bleeding associated with hormonal contraception*. *American family physician*. American Family Physician, 2002. **65**(10): p. 2073-2080.
349. Singh, S., Darroch, J.E., Ashford, L.S., *Adding It Up: The Costs and Benefits of Investing in Sexual and Reproductive Health 2014*, Guttmacher Institute.
350. Sundaram, A., et al., *Contraceptive Failure in the United States: Estimates from the 2006–2010 National Survey of Family Growth*. Perspectives on Sexual and Reproductive Health, 2017. **49**(1): p. 7-16.
351. Martin, C.W., et al., *Potential impact of hormonal male contraception: cross-cultural implications for development of novel preparations*. Hum Reprod, 2000. **15**(3): p. 637-45.
352. Fu, H., et al., *Contraceptive failure rates: new estimates from the 1995 National Survey of Family Growth*. Family planning perspectives, 1999: p. 56-63.
353. Glasier, A.F., et al., *Would women trust their partners to use a male pill?* Human Reproduction, 2000. **15**(3): p. 646-649.

354. Friedman, M., Nickels, L., Sokal, D., Hamlin, A., King, G., Levine, D., Vahdat, H., Shane, K., *Interest Among U.S. Men for New Male Contraceptive Options*. 2019, Male Contraceptive Initiative. p. 1-32.
355. Moreau, C., et al., *Contraceptive failure rates in France: results from a population-based survey*. Hum Reprod, 2007. **22**(9): p. 2422-7.
356. Roth, M.Y., S.T. Page, and W.J. Bremner, *Male hormonal contraception: looking back and moving forward*. Andrology, 2016. **4**(1): p. 4-12.
357. Behre, H.M., et al., *Efficacy and safety of an injectable combination hormonal contraceptive for men*. The Journal of Clinical Endocrinology & Metabolism, 2016. **101**(12): p. 4779-4788.
358. Griffin, P., et al., *Contraceptive efficacy of testosterone-induced azoospermia and oligozoospermia in normal men*. International Journal of Gynecology & Obstetrics, 1996. **55**(1): p. 83-83.
359. Gu, Y., et al., *Multicenter contraceptive efficacy trial of injectable testosterone undecanoate in Chinese men*. The Journal of Clinical Endocrinology & Metabolism, 2009. **94**(6): p. 1910-1915.
360. Gu, Y.-Q., et al., *A multicenter contraceptive efficacy study of injectable testosterone undecanoate in healthy Chinese men*. The Journal of Clinical Endocrinology & Metabolism, 2003. **88**(2): p. 562-568.
361. Turner, L., et al., *Contraceptive efficacy of a depot progestin and androgen combination in men*. The Journal of Clinical Endocrinology & Metabolism, 2003. **88**(10): p. 4659-4667.

362. Anawalt, B.D., et al., *Combined nesterone–testosterone gel suppresses serum gonadotropins to concentrations associated with effective hormonal contraception in men*. *Andrology*, 2019. **7**(6): p. 878-887.
363. Program, C.D. *CDP Research: Developing Hormonal Contraception Methods for Men*. 2022 February 16, 2022 [cited 2023 March 8]; Available from: https://www.nichd.nih.gov/about/org/dir/dph/officebranch/cdp/research/contraception_men.
364. Khilwani, B., et al., *RISUG(®) as a male contraceptive: journey from bench to bedside*. *Basic Clin Androl*, 2020. **30**: p. 2.
365. Ehmcke, J., J. Wistuba, and S. Schlatt, *Spermatogonial stem cells: questions, models and perspectives*. *Human Reproduction Update*, 2006. **12**(3): p. 275-282.
366. Schlatt, S., et al., *Germ cell transfer into rat, bovine, monkey and human testes*. *Hum Reprod*, 1999. **14**(1): p. 144-50.
367. Buaas, F.W., et al., *Plzf is required in adult male germ cells for stem cell self-renewal*. *Nature genetics*, 2004. **36**(6): p. 647-652.
368. Costoya, J.A., et al., *Essential role of Plzf in maintenance of spermatogonial stem cells*. *Nature Genetics*, 2004. **36**(6): p. 653-659.
369. Hobbs, R.M., et al., *Plzf regulates germline progenitor self-renewal by opposing mTORC1*. *Cell*, 2010. **142**(3): p. 468-479.
370. Deng, W. and H. Lin, *miwi, a Murine Homolog of piwi, Encodes a Cytoplasmic Protein Essential for Spermatogenesis*. 2002. **2**(6): p. 819-830.

371. Carrell, D.T., B.R. Emery, and S. Hammoud, *Altered protamine expression and diminished spermatogenesis: what is the link?* Hum Reprod Update, 2007. **13**(3): p. 313-27.
372. McMahon, J.M., et al., *Gene transfer into rat mesenchymal stem cells: a comparative study of viral and nonviral vectors.* Stem Cells Dev, 2006. **15**(1): p. 87-96.
373. Gropp, M., et al., *Stable genetic modification of human embryonic stem cells by lentiviral vectors.* Mol Ther, 2003. **7**(2): p. 281-7.
374. Cockrell, A.S. and T. Kafri, *HIV-1 vectors: fulfillment of expectations, further advancements, and still a way to go.* Curr HIV Res, 2003. **1**(4): p. 419-39.
375. Davis, H.E., J.R. Morgan, and M.L. Yarmush, *Polybrene increases retrovirus gene transfer efficiency by enhancing receptor-independent virus adsorption on target cell membranes.* Biophys Chem, 2002. **97**(2-3): p. 159-72.
376. Xiong, C., et al., *Genetic engineering of human embryonic stem cells with lentiviral vectors.* Stem Cells Dev, 2005. **14**(4): p. 367-77.
377. Xia, X., et al., *Transgenes delivered by lentiviral vector are suppressed in human embryonic stem cells in a promoter-dependent manner.* Stem cells and development, 2007. **16**(1): p. 167-176.
378. Cherry, S.R., et al., *Retroviral expression in embryonic stem cells and hematopoietic stem cells.* Mol Cell Biol, 2000. **20**(20): p. 7419-26.
379. Laker, C., et al., *Host cis-mediated extinction of a retrovirus permissive for expression in embryonal stem cells during differentiation.* J Virol, 1998. **72**(1): p. 339-48.

380. Gaj, T., C.A. Gersbach, and C.F. Barbas, *ZFN, TALEN, and CRISPR/Cas-based methods for genome engineering*. Trends in biotechnology, 2013. **31**(7): p. 397-405.
381. Cong, L., et al., *Multiplex genome engineering using CRISPR/Cas systems*. Science, 2013. **339**(6121): p. 819-823.
382. Mali, P., et al., *RNA-guided human genome engineering via Cas9*. Science, 2013. **339**(6121): p. 823-826.
383. Ran, F.A., et al., *Genome engineering using the CRISPR-Cas9 system*. Nature protocols, 2013. **8**(11): p. 2281-2308.
384. Sharma, A., et al., *CRISPR/Cas9-Mediated Fluorescent Tagging of Endogenous Proteins in Human Pluripotent Stem Cells*. Curr Protoc Hum Genet, 2018. **96**: p. 21.11.1-21.11.20.
385. Aubry, F., et al., *MAGE-A4, a germ cell specific marker, is expressed differentially in testicular tumors*. Cancer, 2001. **92**(11): p. 2778-2785.
386. Uemura, T., et al., *Fluorescent protein tagging of endogenous protein in brain neurons using CRISPR/Cas9-mediated knock-in and in utero electroporation techniques*. Scientific Reports, 2016. **6**(1): p. 35861.
387. Ettinger, A. and T. Wittmann, *Chapter 5 - Fluorescence live cell imaging*, in *Methods in Cell Biology*, J.C. Waters and T. Wittman, Editors. 2014, Academic Press. p. 77-94.
388. Ghichloo, I., Gerriets, V., *Nonsteroidal Anti-inflammatory Drugs (NSAIDs)*. StatPearls [Internet]. 2022, Treasure Island, Florida: StatPearls Publishing LLC.

APPENDIX A

TABLES ASSOCIATED WITH CHAPTER 4 ²

² Krista M. Symosko Crow, In Ki Cho, R. Clayton Edenfield, Kristen F. Easley, Ana Planinić, Nagham Younis, Elizabeth Waters, James S. McClellan, Amanda Colvin Zielen, Kylie Tager, Carlos Castro, Calvin Simerly, Gerald Schatten, Kyle Orwig, Davor Ježek, Michael Koval, Charles A. Easley IV. In preparation.

Table 6.1. 400 μ M naproxen significant differentially expressed genes. All genes up or downregulated by 400 μ M naproxen with a fold change ≥ 1.5 in either direction and an adjusted p-value of < 0.01 .

Gene Symbol	Rhesus Ensembl ID	Gene Name	logFC	p.value	adj.p.val
AKR1B10	ENSMMU G00000013 098	aldo-keto reductase family 1 member B10	0.72015443 5	3.68E-15	1.29E-11
ANLN	ENSMMU G00000021 186	anillin, actin binding protein	- 0.72636410 1	7.94E-06	0.00029807 9
ASB2	ENSMMU G00000012 400	ankyrin repeat and SOCS box containing 2	- 0.67289693 7	5.86E-05	0.00147964 9
ASGR1	ENSMMU G00000003 247	asialoglycop rotein receptor 1	1.13409711 2	0.00030038 5	0.00521300 1
ASPM	ENSMMU G00000000 245	assembly factor for spindle microtubule s	- 0.72901821 2	1.84E-07	1.59E-05
AURKA	ENSMMU G00000000 070	aurora kinase A	- 0.65002166 5	2.53E-06	0.00012053 9
AURKB	ENSMMU G00000002 997	aurora kinase B	- 1.00461405 8	1.01E-07	1.01E-05
BUB1	ENSMMU G00000017 653	BUB1 mitotic checkpoint serine/threo nine kinase	- 0.64002308 7	7.65E-09	1.20E-06
BUB1B	ENSMMU G00000016 686	BUB1 mitotic checkpoint serine/threo nine kinase B	- 0.68175946 6	5.26E-08	6.08E-06

CA9	ENSMMU G00000050 822	carbonic anhydrase 9	1.71057610 5	9.78E-05	0.00217171 6
CCL7	ENSMMU G00000009 782	C-C motif chemokine ligand 7	0.59747446 4	8.43E-06	0.00031217 1
CCNA2	ENSMMU G00000009 817	cyclin A2	-0.90300705	4.40E-13	5.20E-10
CCNB1	ENSMMU G00000018 142	cyclin B1	- 0.70064553 6	1.21E-11	7.04E-09
CCNB2	ENSMMU G00000029 628	cyclin B2	- 0.82193971 9	1.02E-07	1.01E-05
CCNF	ENSMMU G00000000 001	cyclin F	- 0.69721923 1	1.78E-08	2.41E-06
CDC20	ENSMMU G00000003 149	cell division cycle 20	-0.74279975	1.10E-10	4.06E-08
CDCA2	ENSMMU G00000010 582	cell division cycle associated 2	- 0.93597949 5	6.03E-08	6.76E-06
CDCA3	ENSMMU G00000005 191	cell division cycle associated 3	-0.71313103	0.00011111 9	0.00240157 5
CDCA8	ENSMMU G00000014 340	cell division cycle associated 8	-0.7476269	7.94E-08	8.30E-06
CDKN3	ENSMMU G00000012 323	cyclin dependent kinase inhibitor 3	- 0.96571108 5	7.46E-06	0.00028621 3

CEMIP	ENSMMU G00000002 038	cell migration inducing hyaluronida se 1	- 1.18585350 5	3.64E-07	2.70E-05
CENPA	ENSMMU G00000015 934	centromere protein A	-0.87789629	0.00022490 4	0.00410662 3
CENPE	ENSMMU G00000019 089	centromere protein E	-0.78960251	1.46E-09	3.27E-07
CENPL	ENSMMU G00000008 572	centromere protein L	-0.97715177	0.00044730 6	0.00692736
CENPU	ENSMMU G00000012 176	centromere protein U	- 0.74131654 4	2.56E-05	0.00076017 6
CENPW	ENSMMU G00000029 416	centromere protein W	- 0.63267501 9	5.58E-05	0.00142277
CEP55	ENSMMU G00000014 708	centrosomal protein 55	- 0.91821211 7	1.29E-06	7.54E-05
CFTR	ENSMMU G00000011 269	CF transmembr ane conductance regulator	0.58707639 2	0.00036015 1	0.00600466 5
CIT	ENSMMU G00000019 861	citron rho- interacting serine/threo nine kinase	- 0.71485826 2	5.00E-06	0.00020611 1
CKAP2	ENSMMU G00000018 720	cytoskeleton associated protein 2	- 0.58962487 6	3.34E-10	1.06E-07

CNN1	ENSMMU G00000001 473	calponin 1	1.10342246 4	0.00037541 6	0.00619281 5
CRLF1	ENSMMU G00000060 102	cytokine receptor like factor 1	0.78022497 7	1.75E-10	5.97E-08
CRTAC1	ENSMMU G00000018 154	cartilage acidic protein 1	- 1.18881611 1	0.00014725 7	0.00300193 8
DEPDC1	ENSMMU G00000017 766	DEP domain containing 1	- 0.83635183 2	2.76E-07	2.21E-05
DKK3	ENSMMU G00000022 862	dickkopf WNT signaling pathway inhibitor 3	- 0.84450392 5	5.65E-06	0.00022589 9
DLGAP5	ENSMMU G00000003 567	DLG associated protein 5	- 0.93664011 8	9.54E-11	3.61E-08
DUSP5	ENSMMU G00000057 793	dual specificity phosphatase 5	0.67338918	3.45E-12	2.42E-09
E2F8	ENSMMU G00000010 853	E2F transcription factor 8	- 0.86862697 1	1.10E-05	0.00038814 4
EGR2	ENSMMU G00000010 256	early growth response 2	0.69989446 9	3.62E-06	0.00016084

ERCC6L	ENSMMU G00000012 957	ERCC excision repair 6 like, spindle assembly checkpoint helicase	- 0.67063507 2	1.61E-05	0.00052411 6
ESPL1	ENSMMU G00000022 021	extra spindle pole bodies like 1, separase	- 0.73124121 6	1.18E-05	0.00040571 9
FAM89A	ENSMMU G00000008 191	family with sequence similarity 89 member A	0.58069166 1	2.76E-05	0.00081072 4
FCAMR	ENSMMU G00000011 221	Fc alpha and mu receptor	- 0.78898544 7	1.34E-08	1.94E-06
FOXC2	ENSMMU G00000019 498	forkhead box C2	0.84254980 4	5.32E-05	0.00137421 8
FOXM1	ENSMMU G00000019 385	forkhead box M1	- 0.62706489 3	2.61E-06	0.00012409 9
GPCPD1	ENSMMU G00000001 809	glycerophos phocholine phosphodies terase 1	1.18192570 6	4.57E-11	2.06E-08

GTSE1	ENSMMU G00000008 136	G2 and S- phase expressed 1	- 0.85857976 3	5.76E-06	0.00022940 8
HAS3	ENSMMU G00000010 922	hyaluronan synthase 3	-0.67693297	0.00017028 6	0.00336368 2
HASPIN	ENSMMU G00000056 072	histone H3 associated protein kinase	-0.62043479	6.43E-06	0.00025205 8
HBEGF	ENSMMU G00000060 742	heparin binding EGF like growth factor	0.60574663 5	0.00063898 8	0.00926399 6
HJURP	ENSMMU G00000021 221	Holliday junction recognition protein	- 0.95648584 9	7.18E-08	7.67E-06
HMMR	ENSMMU G00000019 553	hyaluronan mediated motility receptor	- 0.76450680 8	1.13E-06	6.72E-05
HMX1	ENSMMU G00000063 426	H6 family homeobox 1	0.67830258 5	0.00019420 2	0.00371228 2
HOMER1	ENSMMU G00000017 057	homer scaffold protein 1	0.64381573 4	1.12E-06	6.72E-05

IL11	ENSMMU G00000048 355	interleukin 11	0.64196973 2	1.14E-05	0.00039695 1
IQGAP3	ENSMMU G00000002 621	IQ motif containing GTPase activating protein 3	- 0.72898107 7	6.15E-08	6.79E-06
ITIH3	ENSMMU G00000014 522	inter-alpha- trypsin inhibitor heavy chain 3	- 0.59621348 3	0.00012544 4	0.00263789 7
KANK3	ENSMMU G00000016 699	KN motif and ankyrin repeat domains 3	0.82085765 3	1.80E-08	2.43E-06
KIF11	ENSMMU G00000023 266	kinesin family member 11	- 0.79904362 5	5.06E-11	2.21E-08
KIF14	ENSMMU G00000004 266	kinesin family member 14	- 0.84200865 3	1.59E-05	0.00052122
KIF15	ENSMMU G00000023 151	kinesin family member 15	- 0.69520819 9	6.57E-05	0.00161660 3
KIF18B	ENSMMU G00000013 113	kinesin family member 18B	- 0.91209824 5	2.08E-05	0.00063639 6
KIF20A	ENSMMU G00000001 511	kinesin family member 20A	- 0.71993634 1	2.66E-10	8.66E-08
KIF2C	ENSMMU G00000021 929	kinesin family member 2C	- 0.72313336 8	1.47E-09	3.27E-07

KIF4A	ENSMMU G00000013 940	kinesin family member 4A	-0.77051959	1.59E-07	1.43E-05
KIFC2	ENSMMU G00000002 661	kinesin family member C2	0.59505730 4	7.73E-06	0.00029267
KLHL4	ENSMMU G00000019 383	kelch like family member 4	0.75486422 8	0.00062140 5	0.00907485 1
KNL1	ENSMMU G00000048 910	kinetochore scaffold 1	- 0.58430712 5	4.57E-06	0.00019270 5
KNSTRN	ENSMMU G00000058 981	kinetochore localized astrin (SPAG5) binding protein	- 0.85578518 5	7.79E-07	4.91E-05
LAMA4	ENSMMU G00000013 782	laminin subunit alpha 4	- 0.70622302 2	2.62E-05	0.00077536 7
LENG8	ENSMMU G00000021 629	leukocyte receptor cluster member 8	0.62741001 7	6.14E-12	4.09E-09
LMNB1	ENSMMU G00000000 823	lamin B1	- 0.58993760 4	3.10E-09	5.79E-07
LRP3	ENSMMU G00000022 872	LDL receptor related protein 3	0.67532556 8	1.32E-06	7.60E-05
LST1	ENSMMU G00000008 853	leukocyte specific transcript 1	- 0.66846849 6	1.42E-11	7.96E-09

MDK	ENSMMU G00000038 138	midkine	1.91378786 4	9.37E-15	2.62E-11
MEDAG	ENSMMU G00000013 346	mesenteric estrogen dependent adiposis	1.20017963 8	0.00029273 2	0.00512464 2
MELK	ENSMMU G00000003 782	maternal embryonic leucine zipper kinase	- 0.65650431 3	8.90E-05	0.00203771 1
MISP3	ENSMMU G00000059 667	MISP family member 3	1.72851415 7	1.90E-06	9.70E-05
MKI67	ENSMMU G00000044 121	marker of proliferation Ki-67	- 0.73285408 3	1.17E-09	2.96E-07
MMP1	ENSMMU G00000002 037	matrix metallopepti dase 1	- 0.60737225 6	2.49E-06	0.00011954 1
MMP9	ENSMMU G00000016 549	matrix metallopepti dase 9	- 0.74707675 5	8.50E-07	5.27E-05
MTARC2	ENSMMU G00000057 631	mitochondri al amidoxime reducing component 2	0.78987032 7	0.00019440 6	0.00371228 2
MYBL2	ENSMMU G00000018 137	MYB proto- onco like 2	- 0.65425086 3	3.53E-07	2.66E-05
NCAPG	ENSMMU G00000018 070	non-SMC condensin I complex subunit G	- 0.76969903 5	4.40E-09	7.70E-07

NCAPG2	ENSMMU G00000013 719	non-SMC condensin II complex subunit G2	- 0.59292564 5	2.61E-09	5.14E-07
NDC80	ENSMMU G00000018 952	NDC80 kinetochore complex component	- 0.66728503 3	3.50E-06	0.00015662 1
NEIL3	ENSMMU G00000007 394	nei like DNA glycosylase 3	- 0.98222154 8	0.00023881 4	0.00431003 8
NEK2	ENSMMU G00000005 216	NIMA related kinase 2	- 0.74237832 7	8.08E-05	0.00189196 5
NEURL3	ENSMMU G00000000 006	neuralized E3 ubiquitin protein ligase 3	0.67904763 4	3.38E-05	0.00095814 4
NOTCH3	ENSMMU G00000013 637	notch receptor 3	0.62343490 8	1.81E-07	1.58E-05
NUF2	ENSMMU G00000001 152	NUF2 component of NDC80 kinetochore complex	- 0.85007015 1	5.40E-08	6.20E-06
NUSAP1	ENSMMU G00000012 681	nucleolar and spindle associated protein 1	- 0.72355017 9	2.20E-07	1.83E-05
ODC1	ENSMMU G00000020 441	ornithine decarboxyla se 1	0.86504155 7	1.72E-17	2.40E-13
PADI2	ENSMMU G00000001 616	peptidyl arginine deiminase 2	- 0.89433515 6	4.72E-13	5.20E-10

PALM3	ENSMMU G00000013 539	paralemmin 3	1.38327641 2	4.48E-05	0.00119502 4
PCLAF	ENSMMU G00000029 603	PCNA clamp associated factor	- 0.83322634 4	7.26E-07	4.65E-05
PCP2	ENSMMU G00000060 224	Purkinje cell protein 2	1.45185594 7	8.12E-05	0.00189424 5
PDGFB	ENSMMU G00000002 739	platelet derived growth factor subunit B	0.63597946	7.44E-08	7.90E-06
PIGR	ENSMMU G00000011 220	polymeric immunoglo bulin receptor	- 1.20009974 7	6.03E-09	1.03E-06
PIK3IP1	ENSMMU G00000019 661	phosphoinos itide-3- kinase interacting protein 1	- 0.70086835 9	4.23E-07	3.01E-05
PLAT	ENSMMU G00000014 432	plasminoge n activator, tissue type	- 0.58815091 8	1.27E-07	1.20E-05
PLK1	ENSMMU G00000017 306	polo like kinase 1	- 0.75603824 9	2.76E-11	1.29E-08
PLXDC1	ENSMMU G00000004 917	plexin domain containing 1	- 0.67586431 5	9.57E-05	0.00214155 7
POLE	ENSMMU G00000015 463	DNA polymerase epsilon, catalytic subunit	- 0.60099255 1	4.87E-07	3.36E-05
POLQ	ENSMMU G00000007 973	DNA polymerase theta	- 0.62701620 2	0.00026275 6	0.00467585 9

PPDPF	ENSMMU G00000048 418	pancreatic progenitor cell differentiation and proliferation factor	0.95048086	2.24E-12	1.85E-09
PPP1R3E	ENSMMU G00000014 745	protein phosphatase 1 regulatory subunit 3E	0.79192026 5	0.00064857 4	0.00938354 7
PRC1	ENSMMU G00000007 534	protein regulator of cytokinesis 1	- 0.62165947 4	2.59E-12	1.91E-09
PRR11	ENSMMU G00000003 390	proline rich 11	- 0.72289050 7	0.00025403 2	0.00457290 3
PRRT4	ENSMMU G00000037 473	proline rich transmembrane protein 4	- 0.66670137 9	0.00010439	0.00228435 1
PTCHD1	ENSMMU G00000001 088	patched domain containing 1	0.83553246 5	0.00034938 6	0.00589536 4
PTPRE	ENSMMU G00000005 383	protein tyrosine phosphatase receptor type E	0.63460947 4	6.72E-08	7.24E-06
PTTG1	ENSMMU G00000023 077	PTTG1 regulator of sister chromatid separation, securin	- 0.65759960 3	4.24E-09	7.52E-07
RACGAP1	ENSMMU G00000021 689	Rac GTPase activating protein 1	- 0.72002409 2	4.13E-06	0.00017671 4

RAD51AP1	ENSMMU G00000015 189	RAD51 associated protein 1	- 0.71587991 7	6.88E-06	0.00026682 9
RASA3	ENSMMU G00000007 434	RAS p21 protein activator 3	- 0.67603586 7	3.29E-06	0.00014844 9
RASD1	ENSMMU G00000006 493	ras related dexamethas one induced 1	0.90823791 6	2.56E-07	2.10E-05
RDM1	ENSMMU G00000006 847	RAD52 motif containing 1	- 0.86174337 9	0.00020825 3	0.00389918 2
RGS2	ENSMMU G00000049 590	regulator of G protein signaling 2	0.97897044 5	0.00037108 7	0.00614311 1
SERPINI1	ENSMMU G00000005 939	serpin family I member 1	- 0.62074767 2	8.77E-05	0.00201114 4
SGO2	ENSMMU G00000052 913	shugoshin 2	- 0.67865891 2	3.45E-05	0.00097104 2
SHCBP1	ENSMMU G00000012 376	SHC binding and spindle associated 1	- 0.72136286 3	5.11E-07	3.49E-05
SKA3	ENSMMU G00000016 560	spindle and kinetochore associated complex subunit 3	- 0.83664976 9	7.95E-05	0.0018714
SLC16A6	ENSMMU G00000011 094	solute carrier family 16 member 6	2.76028042 3	2.33E-06	0.00011346 1
SLC30A3	ENSMMU G00000010 272	solute carrier family 30 member 3	0.83980672 1	0.00034795 1	0.00587935 8
SLC6A1	ENSMMU G00000005 917	solute carrier	0.66646867	0.00025716 1	0.00461145 3

		family 6 member 1			
SLPI	ENSMMU G0000005091	secretory leukocyte peptidase inhibitor	-0.767235097	6.90E-07	4.48E-05
SMC2	ENSMMU G00000020463	structural maintenance of chromosomes 2	-0.608133792	1.97E-06	0.000100259
SPC25	ENSMMU G00000053972	SPC25 component of NDC80 kinetochore complex	-0.667478916	4.18E-07	2.99E-05
SPN	ENSMMU G00000016143	sialophorin	-0.731862274	4.42E-06	0.000187926
SRXN1	ENSMMU G00000047391	sulfiredoxin 1	0.740888304	2.44E-12	1.90E-09
STEAP4	ENSMMU G00000022697	STEAP4 metalloreductase	-0.914670373	1.30E-05	0.000445356
STIL	ENSMMU G00000020389	STIL centriolar assembly protein	-0.62335742	1.47E-05	0.000491462
THY1	ENSMMU G00000008923	Thy-1 cell surface antigen	-0.74862571	5.72E-05	0.001450822
TMEM158	ENSMMU G00000055346	transmembrane protein 158	0.800851148	0.000177139	0.003460013
TMOD1	ENSMMU G00000012278	tropomodulin 1	0.72598028	1.83E-06	9.48E-05

TOP2A	ENSMMU G00000008 941	DNA topoisomera se II alpha	- 0.74839069 8	3.20E-14	7.46E-11
TPX2	ENSMMU G00000000 966	TPX2 microtubule nucleation factor	- 0.77412208 1	6.82E-12	4.34E-09
UPK1B	ENSMMU G00000057 343	uroplakin 1B	- 0.62058949 1	2.18E-06	0.00010864 6
VIT	ENSMMU G00000001 278	vitrin	- 0.76182866 2	1.71E-08	2.38E-06
XPO1	ENSMMU G00000006 941	exportin 1	0.67308550 1	8.53E-16	3.98E-12
ZNF627	ENSMMU G00000001 715	zinc finger protein 627	0.61294848 9	3.93E-08	4.74E-06

Abbreviations: logFC, log fold change; adj. p. val, adjusted p- value.

Table 6.2. 40 μ M Naproxen Significant Differentially Expressed Genes. All genes up or downregulated by 40 μ M Naproxen with a fold change ≥ 1.5 in either direction and adjusted p-value of < 0.01 .

Gene Symbol	Rhesus Ensembl ID	Gene Name	logFC	p.value	adj.p.val
GCK	ENSMMUG0000002427	Glucokinase	-2.738421	9.49E-05	0.00729353
HMX1	ENSMMUG0000063426	H6 family homeobox 1	0.77236664	2.15E-05	0.00258349
IL21R	ENSMMUG0000008252	interleukin 21 receptor	-2.8662307	8.08E-05	0.00662655
PPP1R3E	ENSMMUG0000014745	protein phosphatase 1 regulatory subunit 3E	0.93431952	2.93E-05	0.00320907

Abbreviations: logFC, log fold change; adj. p. val, adjusted p-value.

Table 6.3. 4 μ M naproxen significant differentially expressed genes. All genes up or downregulated by 4 μ M Naproxen with a fold change ≥ 1.5 in either direction and an adjusted p-value of < 0.01 .

Gene Symbol	Rhesus Ensembl ID	Gene Name	logFC	p.value	adj.p.val
CENPW	ENSMMU G00000029 416	centromere protein W	-0.6065103	6.88E-05	0.00757501
CORO6	ENSMMU G00000014 411	coronin 6	0.86787806	1.74E-06	0.00055174
GABBR1	ENSMMU G00000021 483	gamma- aminobutyri c acid type B receptor subunit 1	0.68005349	4.05E-06	0.00099423
LENG8	ENSMMU G00000021 629	leukocyte receptor cluster member 8	0.59387675	2.10E-14	2.94E-10
MIR5047	ENSMMU G00000038 026	microRNA 5047	0.6735163	2.66E-06	0.00074382
RSRP1	ENSMMU G00000002 970	arginine and serine rich protein 1	0.59864494	6.04E-08	5.40E-05
SAC3D1	ENSMMU G00000031 168	SAC3 domain containing 1	-0.744768	1.86E-06	0.00057507

Abbreviations: logFC, log fold change; adj. p. val, adjusted p. value.

Table 6.4. 100 μ M ibuprofen significant differentially expressed genes. All genes up or downregulated by 100 μ M Ibuprofen with a fold change ≥ 1.5 in either direction and an adjusted p-value of < 0.01 .

Gene Symbol	Rhesus Ensembl ID	Gene Name	logFC	p.value	adj.p.val
A4GALT	ENSMMUG00000010194	alpha 1,4-galactosyltransferase	1.0769 4914	5.64E-05	0.0003 8056
AASDH	ENSMMUG00000016360	aminoadipate-semialdehyde dehydrogenase	0.6070 2307	0.0003 7836	0.0017 9797
ABCA1	ENSMMUG00000020608	ATP binding cassette subfamily A member 1	1.2203 2428	5.51E-05	0.0003 7348
ABCA12	ENSMMUG00000014813	ATP binding cassette subfamily A member 12	- 2.5445 283	0.0009 6942	0.0038 9343
ABCA4	ENSMMUG00000013858	ATP binding cassette subfamily A member 4	- 1.0737 573	0.0005 3586	0.0023 985
ABCC3	ENSMMUG00000003414	ATP binding cassette subfamily C member 3	1.0070 0778	0.0004 2081	0.0019 6203
ABCC9	ENSMMUG00000020806	ATP binding cassette subfamily C member 9	- 1.6153 938	8.14E-05	0.0005 1271
ABCG1	ENSMMUG00000018058	ATP binding cassette subfamily G member 1	2.7982 0584	2.25E-05	0.0001 7805
ABCG2	ENSMMUG00000008797	ATP binding cassette subfamily G member 2	- 1.2053 236	0.0022 7578	0.0079 1361
ABHD11	ENSMMUG00000014557	abhydrolase domain containing 11	0.6617 8854	1.37E-05	0.0001 1778
ABHD18	ENSMMUG00000020931	abhydrolase domain containing 18	1.1298 5752	2.72E-05	0.0002 0754
ABTB1	ENSMMUG00000000166	ankyrin repeat and BTB domain containing 1	0.9877 717	5.14E-07	8.65E-06
ACP7	ENSMMUG00000012787	acid phosphatase 7, tartrate resistant (putative)	1.8483 3749	0.0004 855	0.0022 0295
ACSM3	ENSMMUG00000016745	acyl-CoA synthetase medium chain family member 3	0.6123 4014	0.0004 132	0.0019 3501
ACSS1	ENSMMUG00000020597	acyl-CoA synthetase short chain family member 1	0.9647 383	7.96E-05	0.0005 0311

ACSS3	ENSMMUG0000013800	acyl-CoA synthetase short chain family member 3	2.45254706	5.89E-06	5.86E-05
ADAM12	ENSMMUG0000009661	ADAM metalloproteinase domain 12	-0.8175709	2.23E-09	1.50E-07
ADAM18	ENSMMUG0000022134	ADAM metalloproteinase domain 18	0.78268201	0.00033593	0.00162915
ADAM28	ENSMMUG0000005317	ADAM metalloproteinase domain 28	1.51692501	2.40E-07	4.85E-06
ADAMT S1	ENSMMUG0000013407	ADAM metalloproteinase with thrombospondin type 1 motif 1	-0.5934293	1.83E-07	3.91E-06
ADAMT S14	ENSMMUG0000012330	ADAM metalloproteinase with thrombospondin type 1 motif 14	-0.8490632	3.70E-08	1.09E-06
ADAMT S5	ENSMMUG0000013405	ADAM metalloproteinase with thrombospondin type 1 motif 5	1.11731202	9.87E-09	4.30E-07
ADAMT S9	ENSMMUG0000000265	ADAM metalloproteinase with thrombospondin type 1 motif 9	-1.1342989	8.77E-07	1.31E-05
ADAMT SL1	ENSMMUG00000044658	ADAMTS like 1	-0.8540081	0.00021636	0.00114764
ADAMT SL3	ENSMMUG0000013670	ADAMTS like 3	-0.7315658	5.05E-07	8.54E-06
ADAP1	ENSMMUG0000017064	ArfGAP with dual PH domains 1	0.61880792	0.00109166	0.00430181
ADCY9	ENSMMUG00000039943	adenylate cyclase 9	-1.1384514	0.00027763	0.00139479
ADD2	ENSMMUG0000010592	adducin 2	1.16979616	0.00251735	0.00861539
ADGRB1	ENSMMUG0000019877	adhesion G protein-coupled receptor B1	2.4275736	3.41E-05	0.00025059
ADGRF4	ENSMMUG0000017955	adhesion G protein-coupled receptor F4	0.65092019	0.00063077	0.00274969
ADGRG2	ENSMMUG0000020515	adhesion G protein-coupled receptor G2	0.70517413	0.00124862	0.00480165
ADGRG3	ENSMMUG0000015690	adhesion G protein-coupled receptor G3	1.44606428	2.70E-05	0.00020631
ADGRL4	ENSMMUG0000023345	adhesion G protein-coupled receptor L4	1.57059591	2.78E-05	0.00021168

ADIRF	ENSMMUG000 00030573	adipogenesis regulatory factor	1.1198 4292	1.28E- 06	1.74E- 05
ADM	ENSMMUG000 00016387	adrenomedullin	0.6728 4824	0.0016 7221	0.0060 9437
ADM2	ENSMMUG000 00062822	adrenomedullin 2	1.4348 4513	0.0022 6976	0.0078 9662
ADORA1	ENSMMUG000 00008714	adenosine A1 receptor	0.6027 1093	0.0016 4115	0.0060 0645
ADRB2	ENSMMUG000 00002214	adrenoceptor beta 2	- 1.8872 404	0.0003 599	0.0017 2562
AEBP1	ENSMMUG000 00002422	AE binding protein 1	2.6962 1219	8.34E- 07	1.26E- 05
AGBL4	ENSMMUG000 00008828	AGBL carboxypeptidase 4	2.5737 3728	1.01E- 05	9.07E- 05
AGPAT5	ENSMMUG000 00054376	1-acylglycerol-3- phosphate O- acyltransferase 5	0.7513 2428	6.68E- 08	1.72E- 06
AGRN	ENSMMUG000 00000838	agrin	- 0.6513 078	3.31E- 10	3.93E- 08
AHNAK2	ENSMMUG000 00064694	AHNAK nucleoprotein 2	- 0.7420 56	1.62E- 08	6.04E- 07
AIG1	ENSMMUG000 00006430	androgen induced 1	0.6008 8206	2.93E- 06	3.39E- 05
AK7	ENSMMUG000 00003397	adenylate kinase 7	- 0.9403 249	1.14E- 05	0.0001 0058
AK8	ENSMMUG000 00009916	adenylate kinase 8	1.1636 7423	0.0015 8248	0.0058 4726
AKR1E2	ENSMMUG000 00002473	aldo-keto reductase family 1 member E2	- 1.1216 58	0.0029 8003	0.0099 127
ALDOC	ENSMMUG000 00020322	aldolase, fructose- bisphosphate C	1.9417 5953	7.03E- 08	1.78E- 06
ALKAL1	ENSMMUG000 00042459	ALK and LTK ligand 1	- 1.4303 075	9.31E- 05	0.0005 7242
ALLC	ENSMMUG000 00004632	allantoicase	0.6703 0235	0.0015 1081	0.0056 2589
ALPK2	ENSMMUG000 00006635	alpha kinase 2	- 0.6183 278	2.70E- 05	0.0002 0631
AMN1	ENSMMUG000 00011180	antagonist of mitotic exit network 1 homolog	0.6319 0497	0.0001 4145	0.0008 128

AMOT	ENSMMUG000 00007688	angiomotin	- 0.6421 936	4.49E- 06	4.74E- 05
AMPD3	ENSMMUG000 00015785	adenosine monophosphate deaminase 3	- 0.6437 995	0.0002 3195	0.0012 0864
ANAPC1	ENSMMUG000 00012115	anaphase promoting complex subunit 1	- 0.6960 308	4.68E- 08	1.32E- 06
ANG	ENSMMUG000 00057652	angiogenin	0.7850 4182	1.62E- 05	0.0001 346
ANGPTL 4	ENSMMUG000 00000698	angiopoietin like 4	3.6088 0148	1.07E- 05	9.49E- 05
ANGPTL 7	ENSMMUG000 00006187	angiopoietin like 7	1.1056 2867	9.30E- 07	1.38E- 05
ANK3	ENSMMUG000 00003589	ankyrin 3	- 0.7758 155	3.24E- 09	1.96E- 07
ANKRD1 7	ENSMMUG000 00000790	ankyrin repeat domain 17	- 0.5868 047	1.83E- 08	6.60E- 07
ANKRD2 9	ENSMMUG000 00020328	ankyrin repeat domain 29	0.8250 9307	0.0001 2423	0.0007 2593
ANKRD3 7	ENSMMUG000 00062744	ankyrin repeat domain 37	2.6821 857	0.0001 3198	0.0007 6532
ANKRD5 2	ENSMMUG000 00008679	ankyrin repeat domain 52	- 0.8179 776	2.80E- 09	1.75E- 07
ANLN	ENSMMUG000 00021186	anillin, actin binding protein	- 1.2543 936	2.83E- 11	8.18E- 09
AP1S3	ENSMMUG000 00009710	adaptor related protein complex 1 subunit sigma 3	- 1.0809 392	0.0023 0258	0.0079 8279
APLNR	ENSMMUG000 00010627	apelin receptor	2.0453 1119	0.0007 8963	0.0032 9611
APOBEC 3G	ENSMMUG000 00039346	apolipoprotein B mRNA editing enzyme catalytic subunit 3G	1.4480 6112	7.42E- 11	1.41E- 08
APOBEC 3H	ENSMMUG000 00001016	apolipoprotein B mRNA editing enzyme catalytic subunit 3H	0.5958 5666	9.08E- 05	0.0005 6004
APOC1	ENSMMUG000 00028749	apolipoprotein C1	1.9948 3824	3.79E- 11	9.81E- 09
APOE	ENSMMUG000 00014305	apolipoprotein E	1.4939 1448	2.04E- 16	2.83E- 12

APOL2	ENSMMUG0000001537	apolipoprotein L2	0.66796651	0.00025828	0.00131231
APOL4	ENSMMUG00000020016	apolipoprotein L4	0.85157055	0.00019432	0.00105052
AR	ENSMMUG00000011437	androgen receptor	-0.752292	8.61E-06	8.03E-05
ARAP2	ENSMMUG00000006871	ArfGAP with RhoGAP domain, ankyrin repeat and PH domain 2	-0.7378142	0.00031148	0.00153104
ARF5	ENSMMUG00000046381	ADP ribosylation factor 5	0.59694871	9.89E-09	4.30E-07
ARHGAP11A	ENSMMUG00000012276	Rho GTPase activating protein 11A	-1.1897137	6.70E-11	1.41E-08
ARHGAP19	ENSMMUG00000047189	Rho GTPase activating protein 19	-0.62369	4.36E-05	0.00030919
ARHGAP22	ENSMMUG00000004063	Rho GTPase activating protein 22	0.78449974	0.00031623	0.00155218
ARHGAP26	ENSMMUG00000000419	Rho GTPase activating protein 26	-0.6319539	5.41E-06	5.48E-05
ARHGDI G	ENSMMUG00000000603	Rho GDP dissociation inhibitor gamma	1.06834046	0.00144135	0.00540498
ARHGEF10L	ENSMMUG00000010849	Rho guanine nucleotide exchange factor 10 like	1.23144886	2.33E-07	4.73E-06
ARHGEF16	ENSMMUG00000009354	Rho guanine nucleotide exchange factor 16	0.73164759	0.00107644	0.00425392
ARHGEF39	ENSMMUG00000016323	Rho guanine nucleotide exchange factor 39	-0.6004874	0.00086727	0.00355704
ARL4C	ENSMMUG00000011516	ADP ribosylation factor like GTPase 4C	0.93915228	3.27E-07	6.04E-06
ARMCX2	ENSMMUG00000015656	armadillo repeat containing X-linked 2	1.8601558	6.88E-05	0.00044588
ARMCX4	ENSMMUG00000045701	armadillo repeat containing X-linked 4	-0.8855765	0.00015291	0.0008664
ARMCX6	ENSMMUG00000032394	armadillo repeat containing X-linked 6	0.68771759	4.03E-05	0.00028881
ARNTL2	ENSMMUG00000023249	aryl hydrocarbon receptor nuclear translocator like 2	-0.8045707	4.31E-07	7.52E-06
ARPP21	ENSMMUG00000015959	cAMP regulated phosphoprotein 21	1.84709846	0.0001942	0.00105052

ARRDC3	ENSMMUG000 00003569	arrestin domain containing 3	1.4132 1139	5.55E- 11	1.24E- 08
ARSI	ENSMMUG000 00011565	arylsulfatase family member I	- 0.5854 43	2.64E- 06	3.12E- 05
ARSK	ENSMMUG000 00001209	arylsulfatase family member K	0.8174 2006	0.0010 5177	0.0041 7429
AS3MT	ENSMMUG000 00007662	arsenite methyltransferase	1.3701 9637	4.55E- 05	0.0003 2062
ASAP1	ENSMMUG000 00012145	ArfGAP with SH3 domain, ankyrin repeat and PH domain 1	- 0.6698 454	9.26E- 09	4.15E- 07
ASCL2	ENSMMUG000 00001322	achaete-scute family bHLH transcription factor 2	2.0699 0897	0.0003 6687	0.0017 5355
ASF1B	ENSMMUG000 00014135	anti-silencing function 1B histone chaperone	- 0.8680 185	3.12E- 08	9.73E- 07
ASGR1	ENSMMUG000 00003247	asialoglycoprotein receptor 1	4.2896 054	0.0001 8214	0.0010 0096
ASNS	ENSMMUG000 00019157	asparagine synthetase (glutamine-hydrolyzing)	0.8241 3963	5.47E- 06	5.53E- 05
ASPHD1	ENSMMUG000 00018992	aspartate beta- hydroxylase domain containing 1	- 0.8302 973	0.0004 6625	0.0021 3375
ASPM	ENSMMUG000 00000245	assembly factor for spindle microtubules	- 1.2743 483	1.34E- 10	2.06E- 08
ATAD2	ENSMMUG000 00020467	ATPase family AAA domain containing 2	- 0.8832 548	8.79E- 11	1.52E- 08
ATAD5	ENSMMUG000 00040177	ATPase family AAA domain containing 5	- 0.8238 12	8.35E- 06	7.86E- 05
ATF4	ENSMMUG000 00055780	activating transcription factor 4	0.5942 2257	2.07E- 09	1.41E- 07
ATP10A	ENSMMUG000 00054546	ATPase phospholipid transporting 10A (putative)	- 0.5802 142	0.0001 0382	0.0006 2752
ATP2A2	ENSMMUG000 00001739	ATPase sarcoplasmic/endoplasmic reticulum Ca ²⁺ transporting 2	- 0.7021 424	5.00E- 11	1.15E- 08
ATP2A3	ENSMMUG000 00008263	ATPase sarcoplasmic/endoplasmic	- 1.5474 536	2.63E- 12	2.02E- 09

		c reticulum Ca ²⁺ transporting 3			
ATP2B1	ENSMMUG000 00023378	ATPase plasma membrane Ca ²⁺ transporting 1	- 0.6666 309	1.48E- 09	1.11E- 07
ATP6V1 F	ENSMMUG000 00039360	ATPase H ⁺ transporting V1 subunit F	0.6201 6839	2.88E- 05	0.0002 1846
ATP8B1	ENSMMUG000 00019976	ATPase phospholipid transporting 8B1	- 0.5996 593	0.0003 0244	0.0014 9827
ATR	ENSMMUG000 00007927	ATR serine/threonine kinase	- 0.7887 546	5.51E- 08	1.48E- 06
AUH	ENSMMUG000 00015798	AU RNA binding methylglutaconyl-CoA hydratase	0.6432 4871	7.15E- 07	1.11E- 05
AURKA	ENSMMUG000 00000070	aurora kinase A	- 1.1635 223	4.90E- 10	4.99E- 08
AURKB	ENSMMUG000 00002997	aurora kinase B	- 0.7569 163	7.11E- 07	1.11E- 05
B3GNT5	ENSMMUG000 00031605	UDP-GlcNAc:betaGal beta-1,3-N- acetylglucosaminyltransf erase 5	- 0.6206 891	2.39E- 06	2.88E- 05
B9D2	ENSMMUG000 00064979	B9 domain containing 2	0.9490 6386	2.31E- 06	2.81E- 05
BAALC	ENSMMUG000 00019398	BAALC binder of MAP3K1 and KLF4	1.9235 3656	1.79E- 06	2.29E- 05
BAMBI	ENSMMUG000 00058108	BMP and activin membrane bound inhibitor	0.9809 7059	6.86E- 08	1.75E- 06
BATF3	ENSMMUG000 00015056	basic leucine zipper ATF-like transcription factor 3	1.8809 5693	0.0008 3288	0.0034 4552
BAX	ENSMMUG000 00003907	BCL2 associated X, apoptosis regulator	0.6599 9783	4.34E- 10	4.56E- 08
BBOF1	ENSMMUG000 00012683	basal body orientation factor 1	0.6772 4379	0.0002 044	0.0010 9383
BCKDH A	ENSMMUG000 00014346	branched chain keto acid dehydrogenase E1 subunit alpha	0.6668 1925	0.0001 0735	0.0006 4346
BCL7C	ENSMMUG000 00003225	BAF chromatin remodeling complex subunit BCL7C	0.6285 4869	0.0007 5753	0.0031 9189

BEST4	ENSMMUG0000050106	bestrophin 4	0.8817 794	0.0022 0653	0.0077 1339
BEX1	ENSMMUG0000002173	brain expressed X-linked 1	0.9654 2733	6.45E- 10	6.13E- 08
BEX4	ENSMMUG00000004150	brain expressed X-linked 4	2.4043 8844	0.0001 0634	0.0006 3863
BICD2	ENSMMUG00000001061	BICD cargo adaptor 2	- 0.7526 79	2.99E- 09	1.84E- 07
BMP4	ENSMMUG00000000429	bone morphotic protein 4	- 0.7691 273	5.03E- 05	0.0003 465
BNIP3	ENSMMUG00000022445	BCL2 interacting protein 3	1.5515 6433	0.0006 7727	0.0029 13
BNIP3L	ENSMMUG00000023646	BCL2 interacting protein 3 like	1.3463 6812	2.06E- 12	1.68E- 09
BORA	ENSMMUG00000000784	BORA aurora kinase A activator	- 0.7289 515	0.0001 7263	0.0009 5856
BRCA1	ENSMMUG00000001329	BRCA1 DNA repair associated	- 0.7617 842	1.87E- 09	1.32E- 07
BRCA2	ENSMMUG00000007197	BRCA2 DNA repair associated	- 1.2307 709	7.06E- 07	1.10E- 05
BRI3BP	ENSMMUG00000057428	BRI3 binding protein	- 1.1048 419	3.06E- 08	9.65E- 07
BRIP1	ENSMMUG00000009027	BRCA1 interacting helicase 1	- 1.2351 769	4.22E- 06	4.52E- 05
BST2	ENSMMUG00000005829	bone marrow stromal cell antigen 2	0.7941 2589	7.81E- 10	6.75E- 08
BTD	ENSMMUG00000020762	biotinidase	0.9193 615	1.71E- 05	0.0001 4097
BUB1	ENSMMUG00000017653	BUB1 mitotic checkpoint serine/threonine kinase	- 0.9452 47	2.16E- 10	2.88E- 08
BUB1B	ENSMMUG00000016686	BUB1 mitotic checkpoint serine/threonine kinase B	- 1.0040 105	2.21E- 10	2.89E- 08
C10H20o rf204	ENSMMUG00000055191	chromosome 10 C20orf204 homolog	1.5754 33	1.99E- 07	4.15E- 06
C18H18o rf54	ENSMMUG00000010914	chromosome 18 C18orf54 homolog	- 1.0152 302	0.0026 1146	0.0088 8267

C1GALT1C1L	ENSMMUG0000008076	C1GALT1 specific chaperone 1 like	0.62137939	0.00081429	0.0033787
C1H1orf112	ENSMMUG00000016582	chromosome 1 C1orf112 homolog	-0.7265521	0.00045273	0.0020801
C1H1orf198	ENSMMUG00000005886	chromosome 1 C1orf198 homolog	-0.5957957	2.25E-05	0.00017777
C1QL4	ENSMMUG00000007546	complement C1q like 4	1.82456043	0.00060943	0.00267216
C1QTNF9	ENSMMUG00000006945	C1q and TNF related 9	1.44999611	0.00078381	0.00327872
C1R	ENSMMUG00000006470	complement C1r	1.29327039	1.37E-11	5.45E-09
C1S	ENSMMUG00000012786	complement C1s	1.14826836	5.01E-14	9.61E-11
C6	ENSMMUG00000021034	complement C6	-1.0159943	2.93E-07	5.58E-06
C7H15orf62	ENSMMUG00000062039	chromosome 7 C15orf62 homolog	0.62436943	1.49E-07	3.28E-06
C8H8orf88	ENSMMUG00000049102	chromosome 8 C8orf88 homolog	0.57849949	0.00193905	0.00691429
C9H10orf90	ENSMMUG00000009663	chromosome 9 C10orf90 homolog	-2.7725311	0.00221546	0.00773486
CA12	ENSMMUG00000021338	carbonic anhydrase 12	1.97018421	6.77E-07	1.06E-05
CA2	ENSMMUG00000014891	carbonic anhydrase 2	-0.9474144	5.84E-08	1.54E-06
CA5B	ENSMMUG00000014052	carbonic anhydrase 5B	0.77609612	0.00112929	0.0044287
CABCOC01	ENSMMUG00000013152	ciliary associated calcium binding coiled-coil 1	1.6566442	0.00105276	0.00417581
CACNA1D	ENSMMUG00000019262	calcium voltage-gated channel subunit alpha1 D	-0.8097537	1.41E-05	0.00012084
CACNA2D1	ENSMMUG00000030244	calcium voltage-gated channel auxiliary subunit alpha2delta 1	-0.8714647	2.06E-10	2.77E-08
CAD	ENSMMUG00000010269	carbamoyl-phosphate synthetase 2, aspartate transcarbamylase, and dihydroorotase	-0.5784747	5.94E-09	3.02E-07

CALB2	ENSMMUG0000008403	calbindin 2	- 1.1702 476	4.08E- 06	4.40E- 05
CALCR	ENSMMUG0000014319	calcitonin receptor	- 0.9296 047	1.33E- 05	0.0001 1413
CAPN12	ENSMMUG0000006431	calpain 12	1.5434 2526	0.0026 9997	0.0091 2232
CARD10	ENSMMUG0000003007	caspase recruitment domain family member 10	- 0.6299 414	5.36E- 09	2.82E- 07
CASP4	ENSMMUG0000009850	caspase 4	0.7005 0481	2.45E- 07	4.90E- 06
CASS4	ENSMMUG0000000073	Cas scaffold protein family member 4	- 0.8432 21	0.0022 4138	0.0078 1554
CAT	ENSMMUG0000002429	catalase	0.6917 8575	3.60E- 08	1.07E- 06
CAVIN2	ENSMMUG0000011574	caveolae associated protein 2	- 0.8717 434	4.26E- 08	1.23E- 06
CBL	ENSMMUG0000004761	Cbl proto-onco	- 0.8334 61	4.66E- 07	8.02E- 06
CCDC13 4	ENSMMUG0000011531	coiled-coil domain containing 134	- 0.6515 119	0.0019 1949	0.0068 4981
CCDC15 9	ENSMMUG00000043134	coiled-coil domain containing 159	0.7684 0513	0.0006 72	0.0028 957
CCDC18	ENSMMUG0000016812	coiled-coil domain containing 18	- 0.9744 898	4.40E- 05	0.0003 118
CCDC30	ENSMMUG0000013128	coiled-coil domain containing 30	1.0478 6062	0.0001 128	0.0006 7094
CCDC77	ENSMMUG0000013892	coiled-coil domain containing 77	- 0.7191 79	3.78E- 05	0.0002 7344
CCDC80	ENSMMUG0000003061	coiled-coil domain containing 80	- 1.1237 873	2.08E- 05	0.0001 6651
CCDC88 A	ENSMMUG0000003003	coiled-coil domain containing 88A	- 0.6201 036	7.18E- 06	6.90E- 05
CCN4	ENSMMUG0000010199	cellular communication network factor 4	- 0.9986 606	3.55E- 07	6.42E- 06

CCNA2	ENSMMUG000 00009817	cyclin A2	- 0.9357 667	3.95E- 10	4.38E- 08
CCNB1	ENSMMUG000 00018142	cyclin B1	- 0.8476 408	9.17E- 11	1.54E- 08
CCNB2	ENSMMUG000 00029628	cyclin B2	- 0.9476 488	1.20E- 06	1.68E- 05
CCNDBP 1	ENSMMUG000 00022253	cyclin D1 binding protein 1	0.6106 7318	2.83E- 06	3.30E- 05
CCNE2	ENSMMUG000 00005358	cyclin E2	- 1.3484 713	1.30E- 07	2.91E- 06
CCNF	ENSMMUG000 00000001	cyclin F	- 1.2746 146	3.01E- 11	8.53E- 09
CCNJL	ENSMMUG000 00023073	cyclin J like	- 0.8200 005	0.0006 6755	0.0028 8011
CCNQ	ENSMMUG000 00011480	cyclin Q	0.6764 1177	9.85E- 06	8.94E- 05
CCNYL1	ENSMMUG000 00020211	cyclin Y like 1	- 0.6630 759	1.16E- 06	1.63E- 05
CD14	ENSMMUG000 00010007	CD14 molecule	- 0.7524 734	9.48E- 06	8.66E- 05
CD1D	ENSMMUG000 00020156	CD1d molecule	1.8551 3008	4.15E- 10	4.44E- 08
CD200	ENSMMUG000 00016076	CD200 molecule	0.6179 7811	0.0005 6073	0.0024 9372
CD82	ENSMMUG000 00019268	CD82 molecule	0.5799 1599	1.72E- 08	6.33E- 07
CDC20	ENSMMUG000 00003149	cell division cycle 20	- 1.0075 199	4.10E- 10	4.44E- 08
CDC25A	ENSMMUG000 00020954	cell division cycle 25A	- 1.0431 023	1.10E- 05	9.70E- 05
CDC25B	ENSMMUG000 00018922	cell division cycle 25B	- 0.7741 804	5.49E- 09	2.84E- 07
CDC25C	ENSMMUG000 00009025	cell division cycle 25C	- 0.7526 011	7.87E- 05	0.0004 9817

CDC45	ENSMMUG00000021904	cell division cycle 45	- 1.0202 139	1.22E- 07	2.78E- 06
CDC6	ENSMMUG00000004755	cell division cycle 6	- 1.0595 79	4.36E- 07	7.58E- 06
CDCA2	ENSMMUG00000010582	cell division cycle associated 2	- 1.2078 584	1.53E- 09	1.14E- 07
CDCA3	ENSMMUG00000005191	cell division cycle associated 3	- 0.8576 057	1.26E- 06	1.73E- 05
CDCA5	ENSMMUG00000018767	cell division cycle associated 5	- 0.9424 526	1.66E- 06	2.16E- 05
CDCA7	ENSMMUG00000014228	cell division cycle associated 7	- 0.6806 751	5.16E- 05	0.0003 5273
CDCA7L	ENSMMUG00000022766	cell division cycle associated 7 like	0.6993 3814	2.97E- 06	3.41E- 05
CDCA8	ENSMMUG00000014340	cell division cycle associated 8	- 1.0650 01	6.66E- 10	6.22E- 08
CDCP1	ENSMMUG00000005742	CUB domain containing protein 1	1.0827 0183	0.0009 4158	0.0038 0111
CDH13	ENSMMUG00000020114	cadherin 13	- 0.7686 451	3.49E- 08	1.05E- 06
CDH24	ENSMMUG00000006009	cadherin 24	- 0.6530 534	9.89E- 06	8.95E- 05
CDK1	ENSMMUG00000019876	cyclin dependent kinase 1	- 1.0928 48	3.33E- 10	3.93E- 08
CDK5RAP2	ENSMMUG00000023255	CDK5 regulatory subunit associated protein 2	- 0.5824 335	3.79E- 08	1.12E- 06
CDK6	ENSMMUG00000008698	cyclin dependent kinase 6	- 0.8962 206	2.67E- 08	8.78E- 07
CDKL5	ENSMMUG00000005063	cyclin dependent kinase like 5	- 0.7572 802	0.0001 1624	0.0006 8672
CDKN2C	ENSMMUG00000019057	cyclin dependent kinase inhibitor 2C	- 0.7578 595	5.76E- 07	9.44E- 06

CDKN3	ENSMMUG0000012323	cyclin dependent kinase inhibitor 3	- 0.6850 004	0.0003 5587	0.0017 1103
CDR2	ENSMMUG0000022035	cerebellar deration related protein 2	- 0.7059 922	1.04E- 06	1.52E- 05
CELF2	ENSMMUG0000037449	CUGBP Elav-like family member 2	- 0.6610 919	2.00E- 08	7.07E- 07
CEMIP	ENSMMUG0000002038	cell migration inducing hyaluronidase 1	- 2.3635 521	4.87E- 09	2.65E- 07
CENPA	ENSMMUG0000015934	centromere protein A	- 0.8020 346	0.0002 4633	0.0012 6974
CENPE	ENSMMUG0000019089	centromere protein E	- 1.0788 365	3.88E- 10	4.33E- 08
CENPF	ENSMMUG0000015634	centromere protein F	- 1.0405 164	2.52E- 09	1.62E- 07
CENPI	ENSMMUG0000007601	centromere protein I	- 1.3291 7	8.62E- 07	1.29E- 05
CENPJ	ENSMMUG0000014611	centromere protein J	- 1.0378 334	1.09E- 06	1.56E- 05
CENPL	ENSMMUG0000008572	centromere protein L	- 1.2962 697	1.04E- 05	9.29E- 05
CENPM	ENSMMUG0000003360	centromere protein M	- 0.7164 882	9.09E- 06	8.39E- 05
CENPO	ENSMMUG0000009599	centromere protein O	- 0.7416 093	0.0006 5772	0.0028 4658
CENPU	ENSMMUG0000012176	centromere protein U	- 1.2302 03	1.63E- 07	3.55E- 06
CEP128	ENSMMUG0000019710	centrosomal protein 128	- 1.2256 879	1.31E- 06	1.78E- 05
CEP152	ENSMMUG0000009829	centrosomal protein 152	- 0.9988 268	0.0001 2301	0.0007 2116

CEP55	ENSMMUG000 00014708	centrosomal protein 55	- 0.9279 53	9.23E- 08	2.20E- 06
CEP97	ENSMMUG000 00015062	centrosomal protein 97	- 0.6262 873	0.0002 2145	0.0011 6573
CERS1	ENSMMUG000 00059247	ceramide synthase 1	0.7564 2847	0.0005 1389	0.0023 0911
CFI	ENSMMUG000 00021226	complement factor I	0.7787 9305	0.0001 1866	0.0006 998
CFTR	ENSMMUG000 00011269	CF transmembrane conductance regulator	1.0230 422	0.0004 8002	0.0021 8449
CHAC1	ENSMMUG000 00014542	ChaC glutathione specific gamma- glutamylcyclotransferase 1	1.6489 032	1.87E- 10	2.62E- 08
CHAC2	ENSMMUG000 00010639	ChaC glutathione specific gamma- glutamylcyclotransferase 2	- 0.6597 239	0.0022 137	0.0077 3068
CHAF1A	ENSMMUG000 00016706	chromatin assembly factor 1 subunit A	- 0.7185 394	1.79E- 08	6.52E- 07
CHAF1B	ENSMMUG000 00007399	chromatin assembly factor 1 subunit B	- 0.6780 502	0.0001 0211	0.0006 1822
CHAMP1	ENSMMUG000 00023599	chromosome alignment maintaining phosphoprotein 1	- 0.5894 815	6.27E- 06	6.20E- 05
CHCHD6	ENSMMUG000 00016719	coiled-coil-helix-coiled- coil-helix domain containing 6	1.1743 2052	5.07E- 06	5.22E- 05
CHD7	ENSMMUG000 00011584	chromodomain helicase DNA binding protein 7	- 0.6491 161	8.61E- 07	1.29E- 05
CHEK1	ENSMMUG000 00010010	checkpoint kinase 1	- 0.9106 925	1.24E- 06	1.71E- 05
CHI3L1	ENSMMUG000 00008711	chitinase 3 like 1	0.9343 2569	0.0016 9079	0.0061 492
CHI3L2	ENSMMUG000 00002455	chitinase 3 like 2	1.7768 1512	1.90E- 05	0.0001 5417
CHKB	ENSMMUG000 00057498	choline kinase beta	0.7036 2356	2.02E- 06	2.53E- 05
CHL1	ENSMMUG000 00001349	cell adhesion molecule L1 like	1.4843 114	0.0015 9251	0.0058 7493

CHMP4C	ENSMMUG000 00002625	charged multivesicular body protein 4C	0.7336 9695	3.08E- 05	0.0002 3038
CHST3	ENSMMUG000 00052336	carbohydrate sulfotransferase 3	- 0.6872 798	2.18E- 06	2.69E- 05
CHST4	ENSMMUG000 00061967	carbohydrate sulfotransferase 4	- 0.9504 198	1.21E- 05	0.0001 056
CHTF18	ENSMMUG000 00000843	chromosome transmission fidelity factor 18	- 0.7971 727	1.56E- 06	2.04E- 05
CILP2	ENSMMUG000 00011352	cartilage intermediate layer protein 2	- 1.8614 366	3.57E- 05	0.0002 6106
CIT	ENSMMUG000 00019861	citron rho-interacting serine/threonine kinase	- 0.9387 396	7.64E- 08	1.88E- 06
CKAP2	ENSMMUG000 00018720	cytoskeleton associated protein 2	- 0.9293 189	1.77E- 11	6.31E- 09
CKAP2L	ENSMMUG000 00019773	cytoskeleton associated protein 2 like	- 1.1783 682	2.35E- 08	7.96E- 07
CKAP5	ENSMMUG000 00003631	cytoskeleton associated protein 5	- 0.6413 442	5.27E- 09	2.79E- 07
CKB	ENSMMUG000 00049145	creatine kinase B	- 1.3569 728	1.82E- 11	6.32E- 09
CLDN23	ENSMMUG000 00058938	claudin 23	1.1812 9999	0.0003 0928	0.0015 2237
CLEC12 B	ENSMMUG000 00002954	C-type lectin domain family 12 member B	- 1.2268 403	5.73E- 09	2.94E- 07
CLIP3	ENSMMUG000 00051879	CAP-Gly domain containing linker protein 3	0.8428 5545	1.47E- 05	0.0001 2422
CLOCK	ENSMMUG000 00001919	clock circadian regulator	- 0.6627 083	1.48E- 05	0.0001 2501
CLSPN	ENSMMUG000 00010961	claspin	- 1.4134 242	5.46E- 09	2.84E- 07
CLU	ENSMMUG000 00021516	clusterin	1.1248 0661	8.26E- 15	2.87E- 11

CLUH	ENSMMUG00000020527	clustered mitochondria homolog	- 0.6130 842	1.15E-08	4.73E-07
CMTM7	ENSMMUG00000009931	CKLF like MARVEL transmembrane domain containing 7	0.7341 4916	1.78E-09	1.26E-07
CNN1	ENSMMUG00000001473	calponin 1	- 1.1662 586	0.0001 8829	0.0010 2581
CNOT8	ENSMMUG00000008318	CCR4-NOT transcription complex subunit 8	0.6313 453	1.39E-08	5.42E-07
CNPY4	ENSMMUG00000013452	canopy FGF signaling regulator 4	0.6372 8273	4.74E-06	4.96E-05
CNTN3	ENSMMUG00000021241	contactin 3	- 1.0370 755	4.13E-05	0.0002 9497
CNTRL	ENSMMUG00000012668	centriolin	- 0.6379 227	0.0003 5715	0.0017 1599
COBLL1	ENSMMUG00000009400	cordon-bleu WH2 repeat protein like 1	- 0.6758 95	7.73E-08	1.90E-06
COL12A1	ENSMMUG00000019261	collagen type XII alpha 1 chain	- 1.5829 373	8.21E-15	2.87E-11
COL1A1	ENSMMUG00000001467	collagen type I alpha 1 chain	- 0.8785 639	2.13E-08	7.37E-07
COL4A1	ENSMMUG00000022280	collagen type IV alpha 1 chain	- 1.1406 938	1.12E-12	1.19E-09
COL4A2	ENSMMUG00000022282	collagen type IV alpha 2 chain	- 0.9584 269	3.89E-13	4.90E-10
COL4A4	ENSMMUG00000013233	collagen type IV alpha 4 chain	- 1.2401 731	0.0016 3663	0.0059 9791
COL5A2	ENSMMUG00000021290	collagen type V alpha 2 chain	- 0.5962 581	1.69E-08	6.29E-07
COL6A3	ENSMMUG00000014049	collagen type VI alpha 3 chain	2.0658 6132	4.59E-05	0.0003 2272
COL8A1	ENSMMUG00000002935	collagen type VIII alpha 1 chain	- 0.6129 607	7.11E-08	1.80E-06

COLEC1 2	ENSMMUG000 00004663	collectin subfamily member 12	- 0.8517 027	0.0001 6572	0.0009 2691
COMMD 10	ENSMMUG000 00008738	COMM domain containing 10	0.6216 4675	1.05E- 06	1.52E- 05
COMMD 5	ENSMMUG000 00011549	COMM domain containing 5	0.8640 1709	1.64E- 07	3.55E- 06
COMP	ENSMMUG000 00006511	cartilage oligomeric matrix protein	1.8343 7917	1.18E- 06	1.65E- 05
COPRS	ENSMMUG000 00057946	coordinator of PRMT5 and differentiation stimulator	0.6029 8943	9.51E- 07	1.40E- 05
COPZ2	ENSMMUG000 00021934	COPI coat complex subunit zeta 2	0.7079 8516	2.13E- 05	0.0001 6955
CORO2B	ENSMMUG000 00006356	coronin 2B	0.6979 6611	0.0006 1654	0.0026 9779
COX20	ENSMMUG000 00031175	cytochrome c oxidase assembly factor COX20	- 0.5978 461	1.36E- 06	1.83E- 05
CP	ENSMMUG000 00005529	ceruloplasmin	1.6607 9517	2.85E- 14	6.59E- 11
CPEB4	ENSMMUG000 00019926	cytoplasmic polyadenylation element binding protein 4	- 0.8051 969	7.61E- 09	3.60E- 07
CPZ	ENSMMUG000 00006237	carboxypeptidase Z	1.6409 8052	4.04E- 11	1.02E- 08
CRABP2	ENSMMUG000 00002295	cellular retinoic acid binding protein 2	1.8801 4261	5.34E- 08	1.46E- 06
CRACD	ENSMMUG000 00016358	capping protein inhibiting regulator of actin dynamics	1.1734 5933	6.54E- 06	6.41E- 05
CRBN	ENSMMUG000 00017986	cereblon	0.5919 4917	3.80E- 06	4.14E- 05
CREB3L 2	ENSMMUG000 00016833	cAMP responsive element binding protein 3 like 2	- 0.8658 146	1.67E- 11	6.09E- 09
CRIM1	ENSMMUG000 00048261	cysteine rich transmembrane BMP regulator 1	- 0.8310 097	7.41E- 09	3.53E- 07
CRLF1	ENSMMUG000 00060102	cytokine receptor like factor 1	1.0310 0846	1.46E- 09	1.11E- 07
CRNN	ENSMMUG000 00009040	cornulin	- 4.0274 178	7.70E- 05	0.0004 8953
CRTAC1	ENSMMUG000 00018154	cartilage acidic protein 1	1.2270 239	6.32E- 08	1.64E- 06

CRYGN	ENSMMUG000 00006249	crystallin gamma N	1.7109 2434	0.0010 2384	0.0040 8565
CRYL1	ENSMMUG000 00004560	crystallin lambda 1	0.6773 5875	0.0013 1428	0.0050 0012
CSPG4	ENSMMUG000 00016104	chondroitin sulfate proteoglycan 4	- 0.8715 145	1.76E- 06	2.27E- 05
CSRP2	ENSMMUG000 00018257	cysteine and glycine rich protein 2	0.6420 4723	0.0009 9889	0.0039 9641
CSTA	ENSMMUG000 00056258	cystatin A	1.3142 5278	7.44E- 05	0.0004 7619
CTHRC1	ENSMMUG000 00019402	collagen triple helix repeat containing 1	1.0296 2899	3.09E- 08	9.69E- 07
CTPS1	ENSMMUG000 00017101	CTP synthase 1	- 0.6492 579	1.11E- 08	4.61E- 07
CTSB	ENSMMUG000 00019212	cathepsin B	0.6605 0999	4.08E- 10	4.44E- 08
CTSD	ENSMMUG000 00003874	cathepsin D	0.7987 7054	3.05E- 05	0.0002 2825
CTSF	ENSMMUG000 00002496	cathepsin F	0.7069 7717	1.12E- 08	4.64E- 07
CTSL	ENSMMUG000 00017609	cathepsin L	0.7245 1456	7.01E- 10	6.38E- 08
CXCL16	ENSMMUG000 00004891	C-X-C motif chemokine ligand 16	- 0.6488 883	3.05E- 07	5.77E- 06
CYGB	ENSMMUG000 00056406	cytoglobin	1.4650 8955	0.0029 7814	0.0099 1117
CYP2A2 9	ENSMMUG000 00063763	cytochrome P450 family 2 subfamily A member 29	0.8414 5764	0.0017 0079	0.0061 807
CYP2S1	ENSMMUG000 00009608	cytochrome P450 family 2 subfamily S member 1	1.8003 1508	0.0005 8079	0.0025 6975
CYP39A 1	ENSMMUG000 00055199	cytochrome P450 family 39 subfamily A member 1	0.7254 6248	0.0014 3189	0.0053 8113
CYYR1	ENSMMUG000 00012107	cysteine and tyrosine rich 1	1.6868 2693	0.0017 5804	0.0063 5046
DALRD3	ENSMMUG000 00005652	DALR anticodon binding domain containing 3	0.6849 1531	8.99E- 06	8.33E- 05
DBF4B	ENSMMUG000 00005456	DBF4 zinc finger B	- 0.5947 314	0.0008 2323	0.0034 0868
DBP	ENSMMUG000 00022160	D-box binding PAR bZIP transcription factor	0.7953 3564	0.0001 6911	0.0009 4356

DCBLD2	ENSMMUG0000017438	discoidin, CUB and LCCL domain containing 2	- 0.7644 084	1.26E- 11	5.45E- 09
DCHS1	ENSMMUG00000007754	dachsous cadherin-related 1	1.7329 8938	0.0005 2246	0.0023 4303
DCHS2	ENSMMUG00000014024	dachsous cadherin-related 2	- 1.6928 424	7.91E- 11	1.46E- 08
DDAH1	ENSMMUG00000014573	dimethylarginine dimethylaminohydrolase 1	- 1.0761 325	3.32E- 09	1.98E- 07
DDIAS	ENSMMUG00000007841	DNA damage induced apoptosis suppressor	- 1.2815 548	2.29E- 06	2.80E- 05
DDIT3	ENSMMUG00000011286	DNA damage inducible transcript 3	0.5931 4594	0.0002 0208	0.0010 8353
DDIT4	ENSMMUG00000055226	DNA damage inducible transcript 4	1.2063 4129	5.48E- 07	9.09E- 06
DDIT4L	ENSMMUG00000056608	DNA damage inducible transcript 4 like	0.8265 6597	0.0011 139	0.0043 7579
DDX11	ENSMMUG00000022864	DEAD/H-box helicase 11	- 0.5996 559	0.0015 6648	0.0057 9536
DENND2 C	ENSMMUG00000014497	DENN domain containing 2C	- 0.8168 7	0.0014 1675	0.0053 3289
DENND3	ENSMMUG00000013578	DENN domain containing 3	0.8012 2926	0.0002 4104	0.0012 4617
DEPDC1	ENSMMUG00000017766	DEP domain containing 1	- 1.1957 202	1.01E- 09	8.47E- 08
DEPDC1 B	ENSMMUG00000018379	DEP domain containing 1B	- 0.6394 066	0.0001 4376	0.0008 2262
DEPP1	ENSMMUG00000055586	DEPP1 autophagy regulator	1.7956 1465	2.56E- 05	0.0001 974
DHCR24	ENSMMUG00000021577	24-dehydrocholesterol reductase	- 1.6967 601	3.61E- 12	2.50E- 09
DHCR7	ENSMMUG00000011976	7-dehydrocholesterol reductase	- 1.2493 032	1.41E- 09	1.10E- 07
DHDH	ENSMMUG00000003905	dihydrodiol dehydrogenase	0.6814 9427	0.0013 0463	0.0049 7021
DHRS2	ENSMMUG00000021849	dehydrogenase/reductase 2	0.8395 0027	0.0001 1113	0.0006 6242

DHRS7	ENSMMUG000 00002540	dehydrogenase/reductase 7	0.6792 2599	9.81E- 07	1.44E- 05
DHX33	ENSMMUG000 00006594	DEAH-box helicase 33	- 0.5991 795	0.0004 2666	0.0019 8662
DHX35	ENSMMUG000 00003385	DEAH-box helicase 35	- 0.7486 214	2.38E- 07	4.83E- 06
DIAPH3	ENSMMUG000 00013780	diaphanous related formin 3	- 0.9705 019	2.87E- 10	3.46E- 08
DICER1	ENSMMUG000 00023305	dicer 1, ribonuclease III	- 0.8800 637	1.82E- 08	6.59E- 07
DIRAS2	ENSMMUG000 00007223	DIRAS family GTPase 2	- 0.6924 1	0.0005 0595	0.0022 8156
DIRAS3	ENSMMUG000 00013333	DIRAS family GTPase 3	- 0.6543 69	2.21E- 05	0.0001 754
DLG4	ENSMMUG000 00010536	discs large MAGUK scaffold protein 4	0.6571 1336	2.98E- 07	5.67E- 06
DLGAP5	ENSMMUG000 00003567	DLG associated protein 5	- 0.9684 965	1.23E- 09	9.95E- 08
DNAJC6	ENSMMUG000 00017259	DnaJ heat shock protein family (Hsp40) member C6	- 0.8430 018	3.09E- 08	9.69E- 07
DNAL4	ENSMMUG000 00004868	dynein axonemal light chain 4	0.6708 2938	5.51E- 05	0.0003 7348
DNASE1 L1	ENSMMUG000 00050873	deoxyribonuclease 1 like 1	- 0.6082 134	3.15E- 05	0.0002 3468
DNASE2	ENSMMUG000 00028866	deoxyribonuclease 2, lysosomal	0.6970 1461	1.99E- 08	7.06E- 07
DNMT1	ENSMMUG000 00014604	DNA methyltransferase 1	- 0.7927 626	2.68E- 10	3.29E- 08
DNPEP	ENSMMUG000 00017929	aspartyl aminopeptidase	0.6001 1746	7.90E- 08	1.93E- 06
DNTTIP1	ENSMMUG000 00021022	deoxynucleotidyltransfer ase terminal interacting protein 1	0.8686 1318	6.22E- 08	1.61E- 06
DOK5	ENSMMUG000 00007090	docking protein 5	1.1818 843	8.58E- 05	0.0005 3489

DPP4	ENSMMUG000 00008387	dipeptidyl peptidase 4	- 1.0112 8	6.83E- 05	0.0004 441
DPY30	ENSMMUG000 00014481	dpy-30 histone methyltransferase complex regulatory subunit	0.6243 23	3.57E- 07	6.42E- 06
DSCC1	ENSMMUG000 00002788	DNA replication and sister chromatid cohesion 1	- 0.9038 938	8.85E- 05	0.0005 4876
DTL	ENSMMUG000 00010176	denticleless E3 ubiquitin	- 1.2140 676	1.05E- 07	2.44E- 06
DTWD1	ENSMMUG000 00013496	DTW domain containing 1	0.6427 7665	1.83E- 07	3.91E- 06
DTX2	ENSMMUG000 00017570	deltex E3 ubiquitin ligase 2	1.0623 3609	1.91E- 08	6.83E- 07
DUSP10	ENSMMUG000 00004379	dual specificity phosphatase 10	0.8154 8818	8.00E- 08	1.95E- 06
DUSP16	ENSMMUG000 00018580	dual specificity phosphatase 16	- 0.6949 698	2.41E- 07	4.85E- 06
DUSP23	ENSMMUG000 00018444	dual specificity phosphatase 23	0.6419 0502	0.0004 2716	0.0019 8684
DUSP4	ENSMMUG000 00049727	dual specificity phosphatase 4	0.6648 6027	4.87E- 05	0.0003 3716
DYNC1H 1	ENSMMUG000 00005780	dynein cytoplasmic 1 heavy chain 1	- 0.6570 165	0.0007 8744	0.0032 8895
DYRK3	ENSMMUG000 00023566	dual specificity tyrosine phosphorylation regulated kinase 3	- 0.5827 625	8.17E- 06	7.72E- 05
E2F1	ENSMMUG000 00023550	E2F transcription factor 1	- 1.0270 138	0.0004 2037	0.0019 6064
E2F2	ENSMMUG000 00011832	E2F transcription factor 2	- 1.0024 381	0.0001 7252	0.0009 5837
E2F3	ENSMMUG000 00017649	E2F transcription factor 3	- 0.9732 722	0.0002 2796	0.0011 913
E2F7	ENSMMUG000 00022846	E2F transcription factor 7	- 0.6693 569	1.07E- 05	9.52E- 05

E2F8	ENSMMUG00000010853	E2F transcription factor 8	- 1.1587 537	6.53E-07	1.03E-05
EBF1	ENSMMUG00000021696	EBF transcription factor 1	- 1.2489 496	0.00070224	0.00299533
EBF3	ENSMMUG00000011447	EBF transcription factor 3	- 1.2509 902	2.16E-05	0.00017159
ECT2	ENSMMUG00000017014	epithelial cell transforming 2	- 0.9871 824	1.28E-11	5.45E-09
EDN1	ENSMMUG00000051532	endothelin 1	- 1.1565 317	9.21E-06	8.46E-05
EEPD1	ENSMMUG00000010702	endonuclease/exonuclease/phosphatase family domain containing 1	0.84045291	0.00129962	0.00495385
EFHD1	ENSMMUG00000050546	EF-hand domain family member D1	- 0.7936 509	0.00044684	0.00205919
EFNA1	ENSMMUG00000005350	ephrin A1	1.49469217	1.56E-07	3.42E-06
EFNA3	ENSMMUG00000023350	ephrin A3	1.17767414	1.06E-05	9.44E-05
EGLN1	ENSMMUG00000053396	egl-9 family hypoxia inducible factor 1	0.66903131	3.07E-06	3.52E-05
EGR2	ENSMMUG00000010256	early growth response 2	0.93853436	0.00046927	0.00214544
EGR3	ENSMMUG00000058396	early growth response 3	0.8455578	0.00234026	0.00809265
EHD4	ENSMMUG00000003846	EH domain containing 4	- 0.6693 519	1.89E-09	1.32E-07
EID2B	ENSMMUG00000053767	EP300 interacting inhibitor of differentiation 2B	0.75713483	4.90E-05	0.00033849
EIF2AK3	ENSMMUG00000009254	eukaryotic translation initiation factor 2 alpha kinase 3	- 0.7028 134	5.65E-07	9.30E-06
EIF4EBP2	ENSMMUG00000055936	eukaryotic translation initiation factor 4E binding protein 2	- 0.5862 278	3.30E-07	6.06E-06
EIF4G1	ENSMMUG00000010934	eukaryotic translation initiation factor 4 gamma 1	- 0.6037 662	1.43E-10	2.15E-08

ELFN2	ENSMMUG00000052785	extracellular leucine rich repeat and fibronectin type III domain containing 2	- 0.5937 252	0.0007 9218	0.0033 0375
ELMO3	ENSMMUG00000020259	engulfment and cell motility 3	0.7379 2571	8.88E- 05	0.0005 5006
ELOVL2	ENSMMUG00000013908	ELOVL fatty acid elongase 2	- 0.7924 664	2.47E- 07	4.92E- 06
ELOVL6	ENSMMUG00000050694	ELOVL fatty acid elongase 6	- 1.3723 849	3.19E- 07	5.94E- 06
EMID1	ENSMMUG00000021372	EMI domain containing 1	0.8962 9376	2.11E- 07	4.36E- 06
ENC1	ENSMMUG00000019996	ectodermal-neural cortex 1	- 0.8504 217	1.55E- 09	1.14E- 07
ENDOD1	ENSMMUG00000047793	endonuclease domain containing 1	- 0.7177 997	5.45E- 08	1.47E- 06
ENO2	ENSMMUG00000009443	enolase 2	2.2121 8798	5.21E- 05	0.0003 5587
ENOSF1	ENSMMUG00000004051	enolase superfamily member 1	0.6950 4287	0.0003 3994	0.0016 4756
ENTPD7	ENSMMUG00000023761	ectonucleoside triphosphate diphosphohydrolase 7	- 0.6598 026	1.80E- 06	2.29E- 05
EPG5	ENSMMUG00000003562	ectopic P-granules 5 autophagy tethering factor	- 0.5808 985	2.71E- 05	0.0002 0677
EPHA4	ENSMMUG00000012364	EPH receptor A4	- 0.9044 721	3.04E- 05	0.0002 2782
EPOR	ENSMMUG00000038989	erythropoietin receptor	0.5893 3646	3.50E- 05	0.0002 5659
ERCC6L	ENSMMUG00000012957	ERCC excision repair 6 like, spindle assembly checkpoint helicase	- 1.5148 746	1.01E- 09	8.47E- 08
ERO1A	ENSMMUG00000029350	endoplasmic reticulum oxidoreductase 1 alpha	1.1504 4547	7.77E- 09	3.63E- 07
ERVME R34-1	ENSMMUG00000007951	endogenous retrovirus group MER34 member 1, envelope	- 0.5782 917	7.18E- 05	0.0004 627
ESCO2	ENSMMUG00000016018	establishment of sister chromatid cohesion N-acetyltransferase 2	- 1.3233 571	1.20E- 07	2.73E- 06

ESPL1	ENSMMUG000 00022021	extra spindle pole bodies like 1, separase	- 1.2042 412	1.05E- 08	4.43E- 07
EVA1A	ENSMMUG000 00048322	eva-1 homolog A, regulator of programmed cell death	0.6215 4606	3.56E- 06	3.93E- 05
EVA1B	ENSMMUG000 00057604	eva-1 homolog B	1.0072 1312	4.01E- 09	2.27E- 07
EXO1	ENSMMUG000 00008761	exonuclease 1	- 1.1432 587	8.09E- 10	6.93E- 08
EXOC8	ENSMMUG000 00005243	exocyst complex component 8	- 0.5922 794	0.0002 7303	0.0013 7696
EXOSC7	ENSMMUG000 00019130	exosome component 7	0.5897 5579	1.63E- 05	0.0001 3516
FAIM	ENSMMUG000 00008664	Fas apoptotic inhibitory molecule	0.6425 6168	7.54E- 05	0.0004 8108
FAM107 A	ENSMMUG000 00064614	family with sequence similarity 107 member A	- 1.6155 659	4.11E- 09	2.30E- 07
FAM107 B	ENSMMUG000 00017169	family with sequence similarity 107 member B	- 0.8303 194	1.31E- 11	5.45E- 09
FAM111 B	ENSMMUG000 00010273	FAM111 trypsin like peptidase B	- 1.2497 069	2.01E- 07	4.18E- 06
FAM120 C	ENSMMUG000 00008760	family with sequence similarity 120C	- 0.9264 482	2.37E- 05	0.0001 8577
FAM13C	ENSMMUG000 00003706	family with sequence similarity 13 member C	- 3.0833 908	0.0015 2541	0.0056 7415
FAM162 A	ENSMMUG000 00016377	family with sequence similarity 162 member A	0.9667 2695	4.34E- 08	1.24E- 06
FAM167 A	ENSMMUG000 00021191	family with sequence similarity 167 member A	- 1.3050 558	0.0011 5855	0.0045 1284
FAM189 A1	ENSMMUG000 00019340	family with sequence similarity 189 member A1	- 0.7781 158	0.0001 8435	0.0010 1033
FAM20C	ENSMMUG000 00052328	FAM20C golgi associated secretory pathway kinase	1.6967 2331	8.23E- 09	3.79E- 07

FAM241 A	ENSMMUG000 00050382	family with sequence similarity 241 member A	- 0.6642 48	0.0003 6282	0.0017 3723
FAM241 B	ENSMMUG000 00016240	family with sequence similarity 241 member B	0.6138 8483	0.0001 2341	0.0007 2231
FAM50B	ENSMMUG000 00039209	family with sequence similarity 50 member B	0.7060 7972	0.0008 6138	0.0035 3918
FAM53B	ENSMMUG000 00015216	family with sequence similarity 53 member B	- 0.7420 351	6.36E- 07	1.02E- 05
FAM81A	ENSMMUG000 00016390	family with sequence similarity 81 member A	- 1.3157 131	0.0015 1317	0.0056 3318
FAM89A	ENSMMUG000 00008191	family with sequence similarity 89 member A	0.6118 4099	9.53E- 05	0.0005 8327
FANCB	ENSMMUG000 00017839	FA complementation group B	- 2.2324 69	6.28E- 05	0.0004 1454
FANCD2	ENSMMUG000 00008966	FA complementation group D2	- 0.7264 179	3.02E- 07	5.72E- 06
FANCI	ENSMMUG000 00011155	FA complementation group I	- 0.6654 204	6.15E- 08	1.61E- 06
FARP1	ENSMMUG000 00009890	FERM, ARH/RhoGEF and pleckstrin domain protein 1	- 0.6786 806	1.36E- 09	1.08E- 07
FASN	ENSMMUG000 00012811	fatty acid synthase	- 0.6779 358	4.90E- 09	2.65E- 07
FAT1	ENSMMUG000 00018051	FAT atypical cadherin 1	- 0.9009 008	0.0003 273	0.0015 9355
FAU	ENSMMUG000 00018776	FAU ubiquitin like and ribosomal protein S30 fusion	0.6378 7109	2.47E- 09	1.60E- 07
FBLN2	ENSMMUG000 00017659	fibulin 2	0.9440 8055	0.0003 5159	0.0016 9452
FBN1	ENSMMUG000 00004239	fibrillin 1	- 0.5785 472	3.65E- 09	2.13E- 07
FBN2	ENSMMUG000 00010682	fibrillin 2	- 1.5782 219	2.07E- 13	3.20E- 10

FBXL7	ENSMMUG000 00013364	F-box and leucine rich repeat protein 7	- 0.9311 345	8.77E- 09	4.02E- 07
FBXO32	ENSMMUG000 00023778	F-box protein 32	1.4029 6634	2.50E- 13	3.47E- 10
FBXO44	ENSMMUG000 00032251	F-box protein 44	0.7182 2933	0.0001 9963	0.0010 716
FBXO5	ENSMMUG000 00019076	F-box protein 5	- 0.8121 625	2.83E- 07	5.45E- 06
FBXO6	ENSMMUG000 00023668	F-box protein 6	0.5964 834	0.0008 8872	0.0036 3427
FCRL6	ENSMMUG000 00011335	Fc receptor like 6	0.9747 8721	0.0024 1662	0.0083 158
FDPS	ENSMMUG000 00023144	farnesyl diphosphate synthase	- 0.5912 419	7.33E- 08	1.83E- 06
FGF12	ENSMMUG000 00000949	fibroblast growth factor 12	- 0.7437 754	1.26E- 07	2.85E- 06
FGF18	ENSMMUG000 00019401	fibroblast growth factor 18	- 0.7016 952	0.0012 3086	0.0047 4785
FGF7	ENSMMUG000 00009842	fibroblast growth factor 7	1.4362 3696	0.0001 825	0.0010 0248
FHIP1A	ENSMMUG000 00041800	FHF complex subunit HOOK interacting protein 1A	- 0.9473 044	0.0001 9542	0.0010 5514
FIBCD1	ENSMMUG000 00012713	fibrinogen C domain containing 1	1.6197 2621	0.0013 1951	0.0050 1726
FIBIN	ENSMMUG000 00013358	fin bud initiation factor homolog	1.3611 8694	0.0004 034	0.0018 968
FICD	ENSMMUG000 00017123	FIC domain protein adenylyltransferase	- 1.0118 303	5.77E- 07	9.44E- 06
FJX1	ENSMMUG000 00004331	four-jointed box kinase 1	- 0.6741 337	6.35E- 05	0.0004 1778
FKBP14	ENSMMUG000 00012528	FKBP prolyl isomerase 14	- 0.7269 612	6.41E- 07	1.02E- 05
FKBP5	ENSMMUG000 00011520	FKBP prolyl isomerase 5	- 0.5815 166	1.19E- 05	0.0001 0383

FLNA	ENSMMUG000 00013668	filamin A	- 0.5975 797	6.10E- 09	3.06E- 07
FLNB	ENSMMUG000 00000706	filamin B	- 0.8553 868	6.71E- 12	3.86E- 09
FLNC	ENSMMUG000 00006296	filamin C	- 0.6122 029	6.37E- 08	1.65E- 06
FLOT1	ENSMMUG000 00014071	flotillin 1	0.8873 8786	1.53E- 10	2.23E- 08
FLRT3	ENSMMUG000 00002916	fibronectin leucine rich transmembrane protein 3	- 0.6007 004	0.0002 0634	0.0011 0207
FLT1	ENSMMUG000 00021538	fms related receptor tyrosine kinase 1	- 1.0462 313	5.69E- 08	1.52E- 06
FLT4	ENSMMUG000 00018693	fms related receptor tyrosine kinase 4	2.4123 22	7.12E- 07	1.11E- 05
FMO5	ENSMMUG000 00000476	flavin containing dimethylaniline monooxygenase 5	2.2197 8985	0.0010 8425	0.0042 787
FNDC4	ENSMMUG000 00005101	fibronectin type III domain containing 4	0.7499 5915	0.0003 9914	0.0018 7995
FOXA1	ENSMMUG000 00056013	forkhead box A1	- 1.6037 582	0.0003 5365	0.0017 0209
FOXF2	ENSMMUG000 00004540	forkhead box F2	- 0.5923 048	0.0018 2447	0.0065 5627
FOXM1	ENSMMUG000 00019385	forkhead box M1	- 0.9661 436	2.44E- 09	1.59E- 07
FOXQ1	ENSMMUG000 00059043	forkhead box Q1	- 1.3360 183	9.54E- 05	0.0005 839
FRMD4A	ENSMMUG000 00017164	FERM domain containing 4A	- 1.1260 213	1.85E- 05	0.0001 5075
FRMD6	ENSMMUG000 00018274	FERM domain containing 6	- 0.5962 816	1.09E- 07	2.55E- 06
FRY	ENSMMUG000 00007192	FRY microtubule binding protein	- 0.7544 21	6.95E- 08	1.77E- 06

FSCN2	ENSMMUG000 00001583	fascin actin-bundling protein 2, retinal	- 0.8937 4	0.0003 8682	0.0018 2936
FST	ENSMMUG000 00004860	follistatin	- 0.6956 927	1.49E- 08	5.69E- 07
FUOM	ENSMMUG000 00006324	fucose mutarotase	0.9570 6287	2.24E- 08	7.64E- 07
FUT11	ENSMMUG000 00013695	fucosyltransferase 11	0.8794 9223	2.30E- 09	1.53E- 07
FUZ	ENSMMUG000 00011614	fuzzy planar cell polarity protein	0.8058 8126	0.0003 8064	0.0018 057
FZD4	ENSMMUG000 00004048	frizzled class receptor 4	- 0.5989 73	3.77E- 05	0.0002 7335
G0S2	ENSMMUG000 00045482	G0/G1 switch 2	0.9614 645	6.39E- 07	1.02E- 05
GADD45 B	ENSMMUG000 00003468	growth arrest and DNA damage inducible beta	1.1014 4045	3.66E- 09	2.13E- 07
GAL3ST 4	ENSMMUG000 00018404	galactose-3-O- sulfotransferase 4	1.7402 6713	0.0018 4463	0.0066 2221
GALM	ENSMMUG000 00008248	galactose mutarotase	1.0265 4469	0.0015 0193	0.0055 9732
GALNT1 7	ENSMMUG000 00022555	polypeptide N- acetylgalactosaminyltran sferase 17	- 1.1388 922	0.0021 9586	0.0076 8191
GALNT3	ENSMMUG000 00019177	polypeptide N- acetylgalactosaminyltran sferase 3	- 0.8147 734	1.60E- 10	2.32E- 08
GAPDH	ENSMMUG000 00018679	glyceraldehyde-3- phosphate dehydrogenase	0.6812 6344	2.18E- 07	4.48E- 06
GAS2L3	ENSMMUG000 00020360	growth arrest specific 2 like 3	- 1.1669 067	2.48E- 06	2.97E- 05
GAS7	ENSMMUG000 00018092	growth arrest specific 7	0.6418 1997	0.0001 3546	0.0007 8288
GASK1B	ENSMMUG000 00008547	golgi associated kinase 1B	1.0966 5265	0.0001 617	0.0009 0851
GBE1	ENSMMUG000 00015877	1,4-alpha-glucan branching enzyme 1	0.6280 6628	4.16E- 09	2.31E- 07
GBP7	ENSMMUG000 00000663	guanylate binding protein 7	1.3591 4662	0.0006 1229	0.0026 8257
GCK	ENSMMUG000 00002427	glucokinase	3.5263 354	1.74E- 06	2.25E- 05

GCNT2	ENSMMUG00000020132	glucosaminyl (N-acetyl) transferase 2	- 0.9497 029	5.02E- 07	8.50E- 06
GDF15	ENSMMUG00000050122	growth differentiation factor 15	0.8607 0725	1.18E- 07	2.70E- 06
GEN1	ENSMMUG00000012058	GEN1 Holliday junction 5' flap endonuclease	- 0.8863 906	4.31E- 06	4.60E- 05
GFOD1	ENSMMUG00000061899	glucose-fructose oxidoreductase domain containing 1	- 0.6236 104	8.60E- 05	0.0005 3611
GFPT2	ENSMMUG00000001731	glutamine-fructose-6-phosphate transaminase 2	1.4177 4688	0.0008 0927	0.0033 6391
GFRA1	ENSMMUG00000020080	GDNF family receptor alpha 1	- 1.1765 582	1.15E- 06	1.63E- 05
GHR	ENSMMUG00000001336	growth hormone receptor	- 0.5876 438	0.0012 3823	0.0047 683
GIN2	ENSMMUG00000020594	GIN2 complex subunit 2	- 0.7795 871	4.73E- 05	0.0003 3014
GIN3	ENSMMUG00000009109	GIN3 complex subunit 3	- 0.6085 572	0.0002 4861	0.0012 7625
GJA5	ENSMMUG00000001803	gap junction protein alpha 5	- 1.5362 129	5.64E- 06	5.68E- 05
GJB2	ENSMMUG00000010522	gap junction protein beta 2	0.7785 6187	0.0004 7523	0.0021 6838
GKAP1	ENSMMUG00000063374	G kinase anchoring protein 1	0.9866 1241	0.0003 2061	0.0015 6979
GLIPR2	ENSMMUG00000010213	GLI pathosis related 2	- 0.6263 257	2.85E- 07	5.49E- 06
GLUL	ENSMMUG00000022884	glutamate-ammonia ligase	1.3912 6235	5.87E- 07	9.56E- 06
GM2A	ENSMMUG00000022869	ganglioside GM2 activator	0.8670 6343	1.43E- 05	0.0001 2209
GNB4	ENSMMUG00000004083	G protein subunit beta 4	- 0.7658 252	3.38E- 08	1.03E- 06
GNB5	ENSMMUG00000017374	G protein subunit beta 5	1.2404 2543	5.17E- 06	5.30E- 05

GPANK1	ENSMMUG000 00005293	G-patch domain and ankyrin repeats 1	0.5965 8848	1.33E- 06	1.80E- 05
GPD2	ENSMMUG000 00004897	glycerol-3-phosphate dehydrogenase 2	- 0.6855 35	7.29E- 07	1.12E- 05
GPNMB	ENSMMUG000 00012648	glycoprotein nmb	0.6769 9151	2.07E- 08	7.21E- 07
GPR146	ENSMMUG000 00007208	G protein-coupled receptor 146	2.2045 8978	0.0001 8724	0.0010 2113
GPR63	ENSMMUG000 00055593	G protein-coupled receptor 63	- 0.6212 49	0.0004 0152	0.0018 8919
GPX3	ENSMMUG000 00042643	glutathione peroxidase 3	1.3175 0906	2.32E- 10	3.01E- 08
GRAMD 1B	ENSMMUG000 00015522	GRAM domain containing 1B	- 0.8655 525	1.52E- 05	0.0001 2843
GREM1	ENSMMUG000 00001810	gremlin 1, DAN family BMP antagonist	- 0.8724 809	3.52E- 09	2.07E- 07
GREM2	ENSMMUG000 00064824	gremlin 2, DAN family BMP antagonist	- 0.6709 123	6.47E- 05	0.0004 2355
GSTA3	ENSMMUG000 00017137	glutathione S-transferase alpha 3	- 1.1132 918	0.0014 2662	0.0053 6361
GTF3C1	ENSMMUG000 00008254	ral transcription factor IIIC subunit 1	- 0.6717 129	1.49E- 09	1.12E- 07
GTSE1	ENSMMUG000 00008136	G2 and S-phase expressed 1	- 1.1652 999	6.19E- 10	5.93E- 08
H2AX	ENSMMUG000 00044496	H2A.X variant histone	- 0.6573 563	5.21E- 08	1.44E- 06
HACD2	ENSMMUG000 00002232	3-hydroxyacyl-CoA dehydratase 2	- 0.7149 456	1.83E- 06	2.32E- 05
HACD4	ENSMMUG000 00019068	3-hydroxyacyl-CoA dehydratase 4	0.6336 9899	0.0005 9344	0.0026 1488
HAS2	ENSMMUG000 00045043	hyaluronan synthase 2	- 1.2653 683	0.0002 1481	0.0011 4075
HAS3	ENSMMUG000 00010922	hyaluronan synthase 3	- 0.7007 59	0.0022 2916	0.0077 7684

HASPIN	ENSMMUG00000056072	histone H3 associated protein kinase	- 1.0617 486	4.72E- 08	1.33E- 06
HBP1	ENSMMUG00000015409	HMG-box transcription factor 1	0.7331 3803	2.07E- 08	7.21E- 07
HCN4	ENSMMUG00000016564	hyperpolarization activated cyclic nucleotide gated potassium channel 4	- 1.5056 613	0.0023 4069	0.0080 9265
HDAC4	ENSMMUG00000006077	histone deacetylase 4	- 0.6908 683	7.11E- 06	6.85E- 05
HEATR5 A	ENSMMUG00000011779	HEAT repeat containing 5A	- 0.7303 738	1.58E- 08	5.93E- 07
HELLS	ENSMMUG00000017255	helicase, lymphoid specific	- 0.9241 284	1.04E- 08	4.43E- 07
HERC1	ENSMMUG00000012117	HECT and RLD domain containing E3 ubiquitin protein ligase family member 1	- 0.6812 594	8.92E- 05	0.0005 5182
HERC2	ENSMMUG00000004370	HECT and RLD domain containing E3 ubiquitin protein ligase 2	- 0.6518 788	9.24E- 06	8.47E- 05
HES1	ENSMMUG00000058672	hes family bHLH transcription factor 1	0.8385 3013	4.82E- 06	5.04E- 05
HEXD	ENSMMUG00000019221	hexosaminidase D	0.5947 2597	0.0002 0281	0.0010 8619
HEYL	ENSMMUG00000050019	hes related family bHLH transcription factor with YRPW motif like	- 1.5061 51	1.08E- 06	1.55E- 05
HIPK2	ENSMMUG00000002481	homeodomain interacting protein kinase 2	- 0.9084 65	9.04E- 08	2.17E- 06
HIVEP3	ENSMMUG00000016215	HIVEP zinc finger 3	- 0.7716 011	4.45E- 05	0.0003 1444
HJURP	ENSMMUG00000021221	Holliday junction recognition protein	- 1.1292 391	4.06E- 10	4.44E- 08
HLA- DMB	ENSMMUG00000022626	major histocompatibility complex, class II, DM beta	0.7180 391	4.24E- 06	4.54E- 05

HMCN1	ENSMMUG0000010474	hemicentin 1	- 0.6916 134	1.80E- 05	0.0001 4697
HMGCL	ENSMMUG0000019548	3-hydroxy-3-methylglutaryl-CoA lyase	0.6646 4441	5.77E- 06	5.78E- 05
HMGCS1	ENSMMUG0000001226	3-hydroxy-3-methylglutaryl-CoA synthase 1	- 0.7284 049	2.77E- 06	3.25E- 05
HMMR	ENSMMUG0000019553	hyaluronan mediated motility receptor	- 0.9075 055	1.43E- 08	5.54E- 07
HMOX1	ENSMMUG00000007221	heme oxygenase 1	1.0498 5043	0.0007 2175	0.0030 6441
HNRNPL L	ENSMMUG00000002338	heteroous nuclear ribonucleoprotein L like	0.8807 5931	0.0027 7877	0.0093 5768
HOMER1	ENSMMUG00000017057	homer scaffold protein 1	- 0.6256 51	0.0001 7102	0.0009 5347
HOXB2	ENSMMUG00000057001	homeobox B2	0.9817 2838	0.0005 0704	0.0022 8573
HOXB7	ENSMMUG00000055324	homeobox B7	0.9851 1302	1.73E- 05	0.0001 4215
HPS5	ENSMMUG00000017958	HPS5 biosis of lysosomal organelles complex 2 subunit 2	- 0.5986 851	1.56E- 06	2.05E- 05
HPSE	ENSMMUG00000013342	heparanase	- 0.8310 859	1.59E- 06	2.07E- 05
HSD11B 1L	ENSMMUG00000020705	hydroxysteroid 11-beta dehydrogenase 1 like	0.9976 3525	5.71E- 06	5.74E- 05
HSD17B 14	ENSMMUG00000028736	hydroxysteroid 17-beta dehydrogenase 14	0.6881 3037	5.21E- 08	1.44E- 06
HSD3B7	ENSMMUG00000037727	hydroxy-delta-5-steroid dehydrogenase, 3 beta- and steroid delta-isomerase 7	0.9483 5981	0.0004 766	0.0021 7178
HSPA12 B	ENSMMUG00000022077	heat shock protein family A (Hsp70) member 12B	0.9118 6377	0.0023 3123	0.0080 6799
HSPG2	ENSMMUG00000014828	heparan sulfate proteoglycan 2	- 0.9759 053	6.77E- 06	6.58E- 05
HSPH1	ENSMMUG00000013707	heat shock protein family H (Hsp10) member 1	- 0.7822 914	1.43E- 09	1.11E- 07

HTR2A	ENSMMUG000 00004210	5-hydroxytryptamine receptor 2A	- 0.9631 655	1.25E- 05	0.0001 0869
HTRA3	ENSMMUG000 00022672	HtrA serine peptidase 3	1.5422 0552	3.32E- 06	3.73E- 05
HTT	ENSMMUG000 00008392	huntingtin	- 0.6230 197	6.62E- 09	3.20E- 07
HYLS1	ENSMMUG000 00048333	HYLS1 centriolar and ciliosis associated	- 0.6958 258	0.0004 1748	0.0019 5111
HYOU1	ENSMMUG000 00030891	hypoxia up-regulated 1	- 0.8032 699	8.51E- 11	1.49E- 08
ICA1	ENSMMUG000 00005435	islet cell autoantigen 1	0.6794 8754	0.0007 7642	0.0032 5173
ICA1L	ENSMMUG000 00017364	islet cell autoantigen 1 like	- 0.9724 941	0.0006 586	0.0028 477
ID2	ENSMMUG000 00003237	inhibitor of DNA binding 2	0.7153 7076	5.06E- 09	2.71E- 07
IER5L	ENSMMUG000 00049227	immediate early response 5 like	0.6198 496	2.83E- 07	5.45E- 06
IFI27	ENSMMUG000 00023780	interferon alpha inducible protein 27	2.1844 1017	8.34E- 06	7.86E- 05
IFI27L2	ENSMMUG000 00056668	interferon alpha inducible protein 27 like 2	1.0387 6422	1.97E- 11	6.36E- 09
IFIT1	ENSMMUG000 00017533	interferon induced protein with tetratricopeptide repeats 1	1.3390 4407	3.80E- 05	0.0002 7485
IFIT3	ENSMMUG000 00005001	interferon induced protein with tetratricopeptide repeats 3	0.9908 6882	2.35E- 09	1.54E- 07
IFIT5	ENSMMUG000 00017534	interferon induced protein with tetratricopeptide repeats 5	1.2355 3711	1.91E- 05	0.0001 5448
IFITM2	ENSMMUG000 00013256	interferon induced transmembrane protein 2	1.1855 3223	2.46E- 11	7.43E- 09
IFNGR1	ENSMMUG000 00062426	interferon gamma receptor 1	0.6838 301	2.67E- 09	1.69E- 07
IGF2	ENSMMUG000 00047449	insulin like growth factor 2	3.0252 4825	1.01E- 05	9.08E- 05

IGF2R	ENSMMUG0000015658	insulin like growth factor 2 receptor	- 0.6027 381	1.30E-08	5.19E-07
IGFBP2	ENSMMUG0000054183	insulin like growth factor binding protein 2	1.0949 645	4.32E-10	4.56E-08
IGFBP5	ENSMMUG0000041480	insulin like growth factor binding protein 5	- 1.2718 972	2.31E-15	1.60E-11
IGFBP6	ENSMMUG0000051123	insulin like growth factor binding protein 6	1.6443 0693	6.74E-05	0.0004 3892
IGKC	ENSMMUG0000054391	immunoglobulin kappa constant	- 1.8329 395	0.0023 1882	0.0080 2903
IGSF9	ENSMMUG0000004706	immunoglobulin superfamily member 9	1.6374 8067	4.86E-07	8.28E-06
IKZF2	ENSMMUG0000000381	IKAROS family zinc finger 2	- 0.7285 379	5.73E-05	0.0003 8491
IL13RA1	ENSMMUG0000053844	interleukin 13 receptor subunit alpha 1	0.7972 5405	4.45E-11	1.06E-08
IL18R1	ENSMMUG0000009244	interleukin 18 receptor 1	- 0.6184 782	7.09E-10	6.38E-08
IL1R1	ENSMMUG0000020737	interleukin 1 receptor type 1	- 0.9118 784	1.12E-09	9.18E-08
IL1RL1	ENSMMUG0000009238	interleukin 1 receptor like 1	- 1.2404 612	1.20E-12	1.19E-09
IL24	ENSMMUG0000023572	interleukin 24	- 3.6948 763	0.0005 9416	0.0026 1723
IL33	ENSMMUG0000021344	interleukin 33	2.2145 5995	8.30E-08	2.01E-06
IL34	ENSMMUG0000020415	interleukin 34	0.9609 6672	1.32E-05	0.0001 1357
ILDR2	ENSMMUG0000023462	immunoglobulin like domain containing receptor 2	- 0.9634 177	0.0003 7101	0.0017 7093
INCENP	ENSMMUG0000004420	inner centromere protein	- 0.9436 789	2.70E-10	3.29E-08
ING4	ENSMMUG0000016985	inhibitor of growth family member 4	0.9916 6645	1.39E-09	1.09E-07
INHA	ENSMMUG0000007483	inhibin subunit alpha	0.8718 8297	1.13E-06	1.60E-05

INKA1	ENSMMUG00000020979	inka box actin regulator 1	1.31205729	5.93E-06	5.89E-05
INPP5D	ENSMMUG00000009772	inositol polyphosphate-5-phosphatase D	0.69813933	0.00179735	0.00647225
INSIG2	ENSMMUG00000006354	insulin induced 2	1.00423768	1.52E-05	0.00012843
INSL4	ENSMMUG00000058221	insulin like 4	-1.3019419	0.00015705	0.00088484
INSR	ENSMMUG00000028907	insulin receptor	-0.6257138	0.00021993	0.00116083
INSYN2A	ENSMMUG00000018550	inhibitory synaptic factor 2A	-1.4459151	8.91E-05	0.00055113
IPPK	ENSMMUG00000004642	inositol-pentakisphosphate 2-kinase	-0.6088984	0.00011454	0.00067836
IQGAP3	ENSMMUG00000002621	IQ motif containing GTPase activating protein 3	-1.0908365	9.19E-11	1.54E-08
IRF9	ENSMMUG00000040817	interferon regulatory factor 9	0.75354856	1.51E-08	5.71E-07
IRGQ	ENSMMUG00000004468	immunity related GTPase Q	-0.8909763	0.00110864	0.00435846
IRS2	ENSMMUG00000021790	insulin receptor substrate 2	0.70624107	8.11E-07	1.23E-05
ISG20	ENSMMUG00000007669	interferon stimulated exonuclease 20	1.16948572	0.00015387	0.00087082
ISLR2	ENSMMUG00000001835	immunoglobulin superfamily containing leucine rich repeat 2	2.93292983	2.92E-06	3.37E-05
ISOC2	ENSMMUG00000012704	isochorismatase domain containing 2	0.62478256	9.08E-06	8.39E-05
ITGA9	ENSMMUG00000021927	integrin subunit alpha 9	1.38171939	0.00129102	0.00493163
ITGAX	ENSMMUG00000014349	integrin subunit alpha X	0.93382451	7.72E-05	0.00049062
ITGB3	ENSMMUG00000003289	integrin subunit beta 3	-0.9101942	1.89E-11	6.36E-09
ITGB4	ENSMMUG00000021763	integrin subunit beta 4	1.08552463	9.20E-09	4.15E-07

ITGB8	ENSMMUG000 00006898	integrin subunit beta 8	- 0.9845 566	1.62E- 07	3.54E- 06
ITPR1	ENSMMUG000 00012574	inositol 1,4,5- trisphosphate receptor type 1	- 0.6997 089	1.20E- 07	2.73E- 06
ITSN1	ENSMMUG000 00007626	intersectin 1	- 0.6021 185	1.38E- 08	5.41E- 07
IYD	ENSMMUG000 00010802	iodotyrosine deiodinase	- 1.1041 726	0.0006 8892	0.0029 5028
JAG1	ENSMMUG000 00018116	jagged canonical Notch ligand 1	- 0.6321 609	2.42E- 06	2.91E- 05
JPH1	ENSMMUG000 00050527	junctionophilin 1	- 0.6584 8	5.67E- 05	0.0003 8206
JPH2	ENSMMUG000 00022865	junctionophilin 2	- 1.1790 804	8.37E- 07	1.26E- 05
JPH3	ENSMMUG000 00052495	junctionophilin 3	1.9992 0189	0.0015 717	0.0058 0897
JRK	ENSMMUG000 00022452	Jrk helix-turn-helix protein	- 0.7593 702	9.60E- 06	8.74E- 05
JUNB	ENSMMUG000 00005688	JunB proto-onco, AP-1 transcription factor subunit	0.8705 232	7.04E- 08	1.78E- 06
KALRN	ENSMMUG000 00003851	kalirin RhoGEF kinase	1.0264 3256	0.0004 5959	0.0021 0532
KANK1	ENSMMUG000 00019862	KN motif and ankyrin repeat domains 1	- 0.9907 098	0.0007 8627	0.0032 868
KANK3	ENSMMUG000 00016699	KN motif and ankyrin repeat domains 3	3.3562 1444	0.0002 789	0.0013 9916
KCNC4	ENSMMUG000 00004614	potassium voltage-gated channel subfamily C member 4	1.4763 1283	0.0014 3463	0.0053 856
KCNK2	ENSMMUG000 00016931	potassium two pore domain channel subfamily K member 2	- 0.8521 974	0.0003 5334	0.0017 0119
KCNN4	ENSMMUG000 00021267	potassium calcium- activated channel subfamily N member 4	0.6741 0367	0.0021 3872	0.0075 1044

KCNQ5	ENSMMUG000 00015320	potassium voltage-gated channel subfamily Q member 5	- 0.9694 695	5.49E- 05	0.0003 7236
KCTD15	ENSMMUG000 00011319	potassium channel tetramerization domain containing 15	1.2165 7001	7.95E- 06	7.54E- 05
KCTD16	ENSMMUG000 00029791	potassium channel tetramerization domain containing 16	0.6265 7001	8.10E- 06	7.65E- 05
KCTD9	ENSMMUG000 00010151	potassium channel tetramerization domain containing 9	- 0.6736 905	4.34E- 08	1.24E- 06
KDM3A	ENSMMUG000 00013124	lysine demethylase 3A	0.6407 5485	2.57E- 06	3.06E- 05
KHDRBS 3	ENSMMUG000 00022248	KH RNA binding domain containing, signal transduction associated 3	0.6635 3013	7.65E- 05	0.0004 8715
KIAA082 5	ENSMMUG000 00002508	KIAA0825	1.1627 8841	0.0020 3423	0.0072 0737
KIF11	ENSMMUG000 00023266	kinesin family member 11	- 1.0007 923	5.25E- 10	5.27E- 08
KIF14	ENSMMUG000 00004266	kinesin family member 14	- 0.9685 436	0.0002 2068	0.0011 6303
KIF15	ENSMMUG000 00023151	kinesin family member 15	- 0.8352 571	4.04E- 07	7.09E- 06
KIF18B	ENSMMUG000 00013113	kinesin family member 18B	- 1.3802 739	3.41E- 07	6.21E- 06
KIF1A	ENSMMUG000 00021802	kinesin family member 1A	1.9399 6118	0.0003 4091	0.0016 4994
KIF20A	ENSMMUG000 00001511	kinesin family member 20A	- 0.8428 151	3.31E- 07	6.07E- 06
KIF20B	ENSMMUG000 00013485	kinesin family member 20B	- 0.7369 111	1.28E- 08	5.17E- 07
KIF23	ENSMMUG000 00014887	kinesin family member 23	- 1.1216 804	9.41E- 11	1.55E- 08
KIF24	ENSMMUG000 00018726	kinesin family member 24	- 0.8238 405	0.0001 7721	0.0009 801

KIF2C	ENSMMUG000 00021929	kinesin family member 2C	- 1.0028 857	2.57E- 10	3.21E- 08
KIF4A	ENSMMUG000 00013940	kinesin family member 4A	- 1.1171 257	5.60E- 10	5.48E- 08
KIFC1	ENSMMUG000 00007477	kinesin family member C1	- 0.9440 2	4.16E- 10	4.44E- 08
KITLG	ENSMMUG000 00051340	KIT ligand	- 0.8605 527	0.0005 4111	0.0024 181
KLC4	ENSMMUG000 00011668	kinesin light chain 4	0.6130 0246	7.82E- 07	1.19E- 05
KLF10	ENSMMUG000 00018815	Kruppel like factor 10	0.8394 2176	6.41E- 09	3.15E- 07
KLF12	ENSMMUG000 00019097	Kruppel like factor 12	- 0.6946 559	6.35E- 05	0.0004 1778
KLF2	ENSMMUG000 00028855	Kruppel like factor 2	0.8748 3356	6.95E- 05	0.0004 4993
KLF4	ENSMMUG000 00006088	Kruppel like factor 4	2.1132 483	9.89E- 07	1.45E- 05
KLHDC1	ENSMMUG000 00003914	kelch domain containing 1	0.9832 9591	0.0028 6465	0.0095 9942
KLHDC9	ENSMMUG000 00002007	kelch domain containing 9	1.2550 4717	6.00E- 06	5.96E- 05
KLHL13	ENSMMUG000 00002293	kelch like family member 13	- 0.8456 274	0.0017 0214	0.0061 8235
KLHL15	ENSMMUG000 00037633	kelch like family member 15	- 0.6841 492	0.0001 4682	0.0008 3704
KLK8	ENSMMUG000 00015445	kallikrein related peptidase 8	- 1.5929 014	9.77E- 05	0.0005 954
KMT2A	ENSMMUG000 00005482	lysine methyltransferase 2A	- 0.5832 502	5.67E- 06	5.70E- 05
KMT2D	ENSMMUG000 00015718	lysine methyltransferase 2D	- 0.7281 766	0.0029 691	0.0098 8821
KNL1	ENSMMUG000 00048910	kinetochore scaffold 1	- 0.9372 926	3.24E- 08	1.00E- 06

KNSTRN	ENSMMUG00000058981	kinetochore localized astrin (SPAG5) binding protein	- 0.9222 275	2.06E-08	7.21E-07
KNTC1	ENSMMUG00000007556	kinetochore associated 1	- 0.9943 646	1.70E-08	6.30E-07
KPNA2	ENSMMUG00000016685	karyopherin subunit alpha 2	- 0.8643 212	1.94E-10	2.69E-08
KRBA1	ENSMMUG00000017159	KRAB-A domain containing 1	0.6512 867	0.0028 6431	0.0095 9942
L2HGDH	ENSMMUG00000007468	L-2-hydroxyglutarate dehydrogenase	- 0.6899 123	0.0004 8941	0.0022 1639
LAMA2	ENSMMUG00000022136	laminin subunit alpha 2	- 1.1459 732	0.0001 0447	0.0006 306
LAMA3	ENSMMUG00000004321	laminin subunit alpha 3	- 0.9708 126	1.13E-07	2.62E-06
LAMA4	ENSMMUG00000013782	laminin subunit alpha 4	- 0.9537 121	1.82E-08	6.59E-07
LAMC1	ENSMMUG00000015084	laminin subunit gamma 1	- 0.7500 486	3.33E-11	9.24E-09
LAMTOR4	ENSMMUG00000018401	late endosomal/lysosomal adaptor, MAPK and MTOR activator 4	0.7224 775	5.97E-09	3.02E-07
LAMTOR5	ENSMMUG00000049848	late endosomal/lysosomal adaptor, MAPK and MTOR activator 5	0.6668 5255	2.37E-07	4.81E-06
LAPTM5	ENSMMUG00000008744	lysosomal protein transmembrane 5	- 2.7172 451	0.0023 1322	0.0080 1366
LARP6	ENSMMUG00000004429	La ribonucleoprotein 6, translational regulator	0.6596 8651	1.10E-06	1.57E-05
LCLAT1	ENSMMUG00000059622	lysocardiolipin acyltransferase 1	- 0.9703 31	0.0001 2056	0.0007 0949
LCOR	ENSMMUG00000010427	ligand dependent nuclear receptor corepressor	- 0.7254 05	3.49E-06	3.87E-05

LDAF1	ENSMMUG000 00016758	lipid droplet assembly factor 1	0.6787 3349	1.61E- 05	0.0001 3404
LDLR	ENSMMUG000 00003611	low density lipoprotein receptor	- 0.8012 679	6.11E- 09	3.06E- 07
LEF1	ENSMMUG000 00023256	lymphoid enhancer binding factor 1	1.1624 1875	2.47E- 06	2.96E- 05
LGALS3	ENSMMUG000 00003565	galectin 3	1.0854 3413	8.37E- 11	1.49E- 08
LGR5	ENSMMUG000 00020942	leucine rich repeat containing G protein- coupled receptor 5	- 1.0955 761	1.69E- 05	0.0001 397
LIG1	ENSMMUG000 00014591	DNA ligase 1	- 0.5922 045	4.64E- 06	4.87E- 05
LIG4	ENSMMUG000 00008874	DNA ligase 4	- 0.5860 267	1.08E- 05	9.54E- 05
LMNB1	ENSMMUG000 00000823	lamin B1	- 0.9327 459	6.82E- 10	6.31E- 08
LMNB2	ENSMMUG000 00001192	lamin B2	- 0.7391 129	1.07E- 09	8.86E- 08
LMO1	ENSMMUG000 00015017	LIM domain only 1	1.3279 0891	1.43E- 05	0.0001 2196
LNPEP	ENSMMUG000 00018542	leucyl and cystinyl aminopeptidase	- 0.6540 951	4.97E- 06	5.15E- 05
LOX	ENSMMUG000 00056626	lysyl oxidase	2.2132 3413	3.37E- 06	3.77E- 05
LPP	ENSMMUG000 00016823	LIM domain containing preferred translocation partner in lipoma	- 0.7203 394	4.57E- 08	1.29E- 06
LRP1	ENSMMUG000 00021782	LDL receptor related protein 1	- 0.5948 662	3.32E- 06	3.73E- 05
LRP2BP	ENSMMUG000 00003519	LRP2 binding protein	1.6604 0808	0.0001 8081	0.0009 9526
LRP3	ENSMMUG000 00022872	LDL receptor related protein 3	2.0465 0865	1.74E- 08	6.39E- 07
LRP8	ENSMMUG000 00007612	LDL receptor related protein 8	- 1.0079 602	9.70E- 08	2.29E- 06
LRRC32	ENSMMUG000 00022403	leucine rich repeat containing 32	1.8751 0198	3.51E- 08	1.05E- 06

LRRC59	ENSMMUG000 00017234	leucine rich repeat containing 59	- 0.6692 885	1.32E- 10	2.06E- 08
LRRC61	ENSMMUG000 00005233	leucine rich repeat containing 61	2.0888 5028	0.0014 2024	0.0053 4458
LRRC75 B	ENSMMUG000 00010673	leucine rich repeat containing 75B	1.3435 1917	0.0030 0908	0.0099 7584
LRRN1	ENSMMUG000 00049373	leucine rich repeat neuronal 1	1.3570 4601	3.97E- 05	0.0002 8522
LRRN4	ENSMMUG000 00064554	leucine rich repeat neuronal 4	- 0.7604 333	2.03E- 10	2.76E- 08
LSP1	ENSMMUG000 00003335	lymphocyte specific protein 1	1.9870 1822	0.0007 001	0.0029 8896
LTBP1	ENSMMUG000 00021436	latent transforming growth factor beta binding protein 1	0.5821 6286	0.0002 1863	0.0011 5598
LTBP4	ENSMMUG000 00020798	latent transforming growth factor beta binding protein 4	0.6211 2777	9.44E- 05	0.0005 7937
LUM	ENSMMUG000 00016995	lumican	- 0.6759 652	5.48E- 06	5.54E- 05
LYPD6B	ENSMMUG000 00009475	LY6/PLAUR domain containing 6B	- 0.8118 861	0.0010 3446	0.0041 1708
LYSMD2	ENSMMUG000 00017437	LysM domain containing 2	- 0.8598 009	7.83E- 05	0.0004 9604
MAF	ENSMMUG000 00037756	MAF bZIP transcription factor	0.9463 6651	1.46E- 08	5.62E- 07
MAFF	ENSMMUG000 00045506	MAF bZIP transcription factor F	0.7367 4227	2.39E- 06	2.88E- 05
MALT1	ENSMMUG000 00014235	MALT1 paracaspase	- 0.6217 073	1.98E- 07	4.13E- 06
MAMDC 2	ENSMMUG000 00008343	MAM domain containing 2	- 0.6467 192	2.22E- 06	2.73E- 05
MAN2A1	ENSMMUG000 00003316	mannosidase alpha class 2A member 1	- 0.6695 804	5.33E- 09	2.81E- 07
MAOB	ENSMMUG000 00019492	monoamine oxidase B	2.9271 4363	1.03E- 05	9.21E- 05

MAP1A	ENSMMUG0000007255	microtubule associated protein 1A	- 0.6715 888	0.0013 5271	0.0051 2382
MAP2K1	ENSMMUG0000016840	mitogen-activated protein kinase kinase 1	0.6355 2175	1.26E- 06	1.73E- 05
MAP3K9	ENSMMUG0000005786	mitogen-activated protein kinase kinase kinase 9	- 1.1762 809	0.0002 0903	0.0011 1475
MAPK3	ENSMMUG0000017758	mitogen-activated protein kinase 3	0.5884 9919	1.18E- 06	1.65E- 05
MARCH F1	ENSMMUG0000041688	membrane associated ring-CH-type finger 1	- 1.4611 577	0.0020 7135	0.0073 1645
MARCH F11	ENSMMUG0000007069	membrane associated ring-CH-type finger 11	- 0.6985 922	0.0014 8383	0.0055 4027
MARCH F2	ENSMMUG0000043959	membrane associated ring-CH-type finger 2	0.7165 0596	2.38E- 08	8.05E- 07
MARCH F3	ENSMMUG0000021547	membrane associated ring-CH-type finger 3	0.7101 242	3.22E- 05	0.0002 3886
MARCK SL1	ENSMMUG0000009951	MARCKS like 1	0.6397 8206	2.81E- 08	9.16E- 07
MASTL	ENSMMUG0000016407	microtubule associated serine/threonine kinase like	- 0.7767 867	2.98E- 06	3.42E- 05
MATN2	ENSMMUG0000020072	matrilin 2	- 1.1371 529	0.0009 2018	0.0037 2666
MBOAT1	ENSMMUG0000017425	membrane bound O-acyltransferase domain containing 1	- 0.6842 698	1.75E- 08	6.40E- 07
MCCC2	ENSMMUG0000015175	methylcrotonyl-CoA carboxylase subunit 2	- 0.6313 019	5.57E- 05	0.0003 7665
MCM10	ENSMMUG0000005602	minichromosome maintenance 10 replication initiation factor	- 1.2857 312	1.61E- 08	6.02E- 07
MCM3	ENSMMUG0000021149	minichromosome maintenance complex component 3	- 0.9884 477	1.31E- 08	5.21E- 07
MCM4	ENSMMUG0000015360	minichromosome maintenance complex component 4	- 0.8122 128	9.38E- 09	4.17E- 07

MCM5	ENSMMUG00000021054	minichromosome maintenance complex component 5	- 0.9203 047	3.71E- 09	2.15E- 07
MCM6	ENSMMUG00000017486	minichromosome maintenance complex component 6	- 0.6950 311	1.31E- 07	2.92E- 06
MCM7	ENSMMUG00000013442	minichromosome maintenance complex component 7	- 0.6149 124	6.58E- 08	1.69E- 06
MDGA2	ENSMMUG00000015110	MAM domain containing glycosylphosphatidylinositol anchor 2	- 0.6868 901	0.0009 9104	0.0039 7253
MDK	ENSMMUG00000038138	midkine	1.5253 8858	4.95E- 09	2.67E- 07
MDN1	ENSMMUG00000003464	midasin AAA ATPase 1	- 0.6764 996	1.44E- 05	0.0001 2285
MED31	ENSMMUG00000058158	mediator complex subunit 31	0.6023 712	5.90E- 05	0.0003 9364
MEDAG	ENSMMUG00000013346	mesenteric estrogen dependent adiposis	2.5464 8122	6.31E- 06	6.23E- 05
MEIS3	ENSMMUG00000013009	Meis homeobox 3	0.9397 7406	1.25E- 06	1.73E- 05
MELK	ENSMMUG00000003782	maternal embryonic leucine zipper kinase	- 0.9770 344	1.39E- 06	1.86E- 05
Metazoa_SRP	ENSMMUG00000059393	Metazoan signal recognition particle RNA	1.1832 5487	1.02E- 07	2.37E- 06
Metazoa_SRP	ENSMMUG00000060067	Metazoan signal recognition particle RNA	1.1585 1927	1.02E- 11	4.71E- 09
MFAP2	ENSMMUG00000053451	microfibril associated protein 2	1.8819 2556	5.45E- 07	9.06E- 06
MFAP3L	ENSMMUG00000040113	microfibril associated protein 3 like	- 0.6123 506	0.0007 4319	0.0031 3911
MGAT5	ENSMMUG00000010563	alpha-1,6-mannosylglycoprotein 6-beta-N-acetylglucosaminyltransferase	- 0.7432 381	1.14E- 07	2.62E- 06
MGST3	ENSMMUG00000015948	microsomal glutathione S-transferase 3	0.5804 0075	3.16E- 07	5.91E- 06
MICAL1	ENSMMUG00000023221	microtubule associated monooxygenase, calponin and LIM domain containing 1	- 0.6415 721	4.95E- 05	0.0003 4153

MICAL2	ENSMMUG00000020953	microtubule associated monooxygenase, calponin and LIM domain containing 2	- 0.7741 989	7.21E-11	1.41E-08
MID1	ENSMMUG00000020179	midline 1	- 0.7417 1	8.85E-06	8.23E-05
MIF	ENSMMUG00000009106	solute carrier family 2 member 11	1.2164 0136	0.0002 1652	0.0011 4764
MKI67	ENSMMUG00000044121	marker of proliferation Ki-67	- 1.3349 79	2.87E-06	3.33E-05
MLPH	ENSMMUG00000012089	melanophilin	1.1564 5149	1.08E-06	1.55E-05
mml-mir-675	ENSMMUG00000032643	mml-mir-675	3.2260 3764	0.0009 0065	0.0036 7057
MMP1	ENSMMUG00000002037	matrix metalloproteinase 1	0.7711 1803	1.20E-06	1.67E-05
MMP28	ENSMMUG00000022229	matrix metalloproteinase 28	0.7001 7739	0.0004 7099	0.0021 5186
MMP9	ENSMMUG00000016549	matrix metalloproteinase 9	0.7848 8497	0.0006 6255	0.0028 6389
MMS22L	ENSMMUG00000040203	MMS22 like, DNA repair protein	- 0.7570 041	2.68E-05	0.0002 0536
MNS1	ENSMMUG00000019485	meiosis specific nuclear structural 1	- 1.0132 935	0.0002 03	0.0010 8678
MORN2	ENSMMUG00000021067	MORN repeat containing 2	0.7240 7796	0.0029 1747	0.0097 4669
MOSPD3	ENSMMUG00000002949	motile sperm domain containing 3	0.6302 6387	8.01E-07	1.22E-05
MPI	ENSMMUG00000005227	mannose phosphate isomerase	0.5969 534	1.53E-05	0.0001 287
MPND	ENSMMUG00000028926	MPN domain containing	0.5852 8081	0.0001 9071	0.0010 3456
MR1	ENSMMUG00000020023	major histocompatibility complex, class I-related	1.2241 9407	0.0017 0468	0.0061 8997
MRAP	ENSMMUG00000059677	melanocortin 2 receptor accessory protein	- 1.0934 19	0.0002 5953	0.0013 182
MRGBP	ENSMMUG00000046848	MRG domain binding protein	0.6029 6686	3.39E-06	3.79E-05
MROH2A	ENSMMUG00000021219	maestro heat like repeat family member 2A	- 1.1688 148	0.0022 9635	0.0079 7314

MRPL11	ENSMMUG000 00008876	mitochondrial ribosomal protein L11	0.6191 2153	3.36E- 08	1.03E- 06
MRPS26	ENSMMUG000 00063622	mitochondrial ribosomal protein S26	0.6789 0009	9.04E- 08	2.17E- 06
MSMO1	ENSMMUG000 00056040	methylsterol monooxygenase 1	- 0.7616 764	5.64E- 10	5.48E- 08
MSRB1	ENSMMUG000 00007936	methionine sulfoxide reductase B1	0.6059 9367	4.93E- 06	5.12E- 05
MSRB2	ENSMMUG000 00010388	methionine sulfoxide reductase B2	0.8123 6447	0.0029 3828	0.0098 0087
MT1X	ENSMMUG000 00056419	metallothionein 1X	0.9768 6534	1.46E- 06	1.94E- 05
MTHFD2	ENSMMUG000 00009739	methylenetetrahydrofolat e dehydrogenase (NADP+ dependent) 2, methenyltetrahydrofolate cyclohydrolase	0.5929 6014	1.71E- 09	1.24E- 07
MX1	ENSMMUG000 00015329	MX dynamin like GTPase 1	1.4767 9185	4.64E- 07	8.01E- 06
MX2	ENSMMUG000 00044257	MX dynamin like GTPase 2	2.3998 3398	3.20E- 08	9.92E- 07
MXD3	ENSMMUG000 00009047	MAX dimerization protein 3	- 0.6904 018	0.0002 1868	0.0011 5598
MXI1	ENSMMUG000 00014350	MAX interactor 1, dimerization protein	1.1581 9857	7.67E- 10	6.69E- 08
MXRA8	ENSMMUG000 00003582	matrix remodeling associated 8	0.6734 7677	0.0017 6735	0.0063 7412
MYBL1	ENSMMUG000 00013974	MYB proto-onco like 1	- 0.8000 762	1.50E- 06	1.97E- 05
MYBL2	ENSMMUG000 00018137	MYB proto-onco like 2	- 0.8970 17	2.31E- 09	1.53E- 07
MYH9	ENSMMUG000 00006101	myosin heavy chain 9	- 0.6936 436	2.22E- 11	6.85E- 09
MYLIP	ENSMMUG000 00057657	myosin regulatory light chain interacting protein	0.7311 3416	4.68E- 07	8.03E- 06
MYLK	ENSMMUG000 00014818	myosin light chain kinase	- 0.6605 103	1.33E- 07	2.96E- 06
MYO10	ENSMMUG000 00012672	myosin X	- 0.7968 626	7.33E- 10	6.47E- 08

MYO1C	ENSMMUG000 00002371	myosin IC	- 0.6174 192	3.39E- 10	3.93E- 08
MYO5B	ENSMMUG000 00003041	myosin VB	- 0.7759 809	4.58E- 09	2.52E- 07
MYORG	ENSMMUG000 00039762	myosis regulating glycosidase (putative)	- 1.0448 371	1.60E- 07	3.51E- 06
MZT1	ENSMMUG000 00060508	mitotic spindle organizing protein 1	- 0.6487 661	2.87E- 06	3.33E- 05
N4BP2L1	ENSMMUG000 00007198	NEDD4 binding protein 2 like 1	2.3267 1359	1.21E- 07	2.74E- 06
NABP1	ENSMMUG000 00009460	nucleic acid binding protein 1	- 0.6279 472	0.0010 723	0.0042 424
NAMPT	ENSMMUG000 00003572	nicotinamide phosphoribosyltransferas e	0.6393 855	3.09E- 07	5.84E- 06
NARF	ENSMMUG000 00019224	nuclear prelamin A recognition factor	0.5793 2437	1.57E- 06	2.05E- 05
NAT14	ENSMMUG000 00052201	N-acetyltransferase 14 (putative)	0.6511 7732	6.28E- 07	1.01E- 05
NCAM2	ENSMMUG000 00004300	neural cell adhesion molecule 2	- 1.2688 222	0.0012 2738	0.0047 3572
NCAPD2	ENSMMUG000 00018677	non-SMC condensin I complex subunit D2	- 0.9029 63	4.51E- 11	1.06E- 08
NCAPD3	ENSMMUG000 00007102	non-SMC condensin II complex subunit D3	- 0.6266 742	3.89E- 06	4.23E- 05
NCAPG	ENSMMUG000 00018070	non-SMC condensin I complex subunit G	- 1.2120 258	2.18E- 08	7.49E- 07
NCAPG2	ENSMMUG000 00013719	non-SMC condensin II complex subunit G2	- 0.7625 834	7.09E- 10	6.38E- 08
NCAPH	ENSMMUG000 00023269	non-SMC condensin I complex subunit H	- 0.6865 612	1.08E- 06	1.55E- 05
NCF4	ENSMMUG000 00008160	neutrophil cytosolic factor 4	0.8416 9134	4.42E- 06	4.69E- 05
NCK1	ENSMMUG000 00055871	NCK adaptor protein 1	0.7377 1449	3.54E- 07	6.40E- 06

NCLN	ENSMMUG000 00017036	nicalin	- 0.5858 606	1.84E- 07	3.92E- 06
NDC80	ENSMMUG000 00018952	NDC80 kinetochore complex component	- 0.9324 953	5.96E- 09	3.02E- 07
NDRG1	ENSMMUG000 00010200	N-myc downstream regulated 1	1.8311 0992	0.0012 6596	0.0048 5355
NDUFB7	ENSMMUG000 00050251	NADH:ubiquinone oxidoreductase subunit B7	0.6346 6835	1.02E- 08	4.40E- 07
NEDD9	ENSMMUG000 00016135	neural cell expressed, developmentally down- regulated 9	0.6860 7992	1.15E- 07	2.63E- 06
NEIL2	ENSMMUG000 00019209	nei like DNA glycosylase 2	0.7233 3989	3.72E- 06	4.07E- 05
NEIL3	ENSMMUG000 00007394	nei like DNA glycosylase 3	- 1.1267 722	3.20E- 07	5.94E- 06
NEK2	ENSMMUG000 00005216	NIMA related kinase 2	- 0.7184 342	1.29E- 05	0.0001 1155
NENF	ENSMMUG000 00002142	neudesin neurotrophic factor	0.5784 6063	0.0012 5746	0.0048 3164
NETO2	ENSMMUG000 00028921	neuropilin and tolloid like 2	- 1.0944 916	2.84E- 08	9.19E- 07
NEURL1 B	ENSMMUG000 00008848	neuralized E3 ubiquitin protein ligase 1B	- 1.0704 296	0.0027 851	0.0093 6989
NEURL3	ENSMMUG000 00000006	neuralized E3 ubiquitin protein ligase 3	1.1089 6581	8.31E- 05	0.0005 2141
NEXN	ENSMMUG000 00010352	nexilin F-actin binding protein	- 0.5894 873	1.52E- 05	0.0001 2785
NFAT5	ENSMMUG000 00018255	nuclear factor of activated T cells 5	- 0.6700 352	1.23E- 05	0.0001 0735
NFIB	ENSMMUG000 00014697	nuclear factor I B	- 0.6408 943	4.05E- 06	4.38E- 05
NFIL3	ENSMMUG000 00023257	nuclear factor, interleukin 3 regulated	1.0363 1498	1.42E- 08	5.51E- 07
NID1	ENSMMUG000 00012716	nidogen 1	- 0.9975 406	6.52E- 09	3.18E- 07

NID2	ENSMMUG000 00018201	nidogen 2	- 1.0551 311	2.03E- 10	2.76E- 08
NIM1K	ENSMMUG000 00001224	NIM1 serine/threonine protein kinase	2.4436 5304	3.40E- 06	3.79E- 05
NIN	ENSMMUG000 00014658	ninein	- 0.7446 791	1.31E- 08	5.21E- 07
NKX1-2	ENSMMUG000 00054006	NK1 homeobox 2	- 1.3518 689	0.0007 5507	0.0031 8249
NMNAT 2	ENSMMUG000 00001481	nicotinamide nucleotide adenylyltransferase 2	- 0.7967 813	1.34E- 09	1.07E- 07
NNMT	ENSMMUG000 00007086	nicotinamide N- methyltransferase	1.6581 5243	0.0004 0623	0.0019 0944
NOCT	ENSMMUG000 00004983	nocturnin	- 0.7734 16	2.44E- 06	2.93E- 05
NOG	ENSMMUG000 00005798	noggin	1.2112 2984	1.08E- 05	9.55E- 05
NOL3	ENSMMUG000 00020268	nucleolar protein 3	0.8546 0054	0.0025 8584	0.0088 0848
NOL6	ENSMMUG000 00000389	nucleolar protein 6	- 0.6845 833	1.19E- 08	4.85E- 07
NOP53	ENSMMUG000 00013348	NOP53 ribosome biosis factor	0.7489 4886	7.17E- 11	1.41E- 08
NOTCH1	ENSMMUG000 00017022	notch receptor 1	- 0.6045 495	3.81E- 05	0.0002 7536
NOTCH3	ENSMMUG000 00013637	notch receptor 3	0.6469 9816	9.66E- 05	0.0005 9021
NPAS4	ENSMMUG000 00015982	neuronal PAS domain protein 4	- 2.7957 616	0.0015 0592	0.0056 092
NPC2	ENSMMUG000 00006563	NPC intracellular cholesterol transporter 2	0.6179 6587	3.85E- 10	4.33E- 08
NPHP1	ENSMMUG000 00022802	nephrocystin 1	0.6907 2038	0.0001 5954	0.0008 9813
NPNT	ENSMMUG000 00023428	nephronectin	- 0.8705 414	5.44E- 08	1.47E- 06
NPTX1	ENSMMUG000 00001286	neuronal pentraxin 1	- 0.9525 445	3.51E- 05	0.0002 5725

NR2C2A P	ENSMMUG000 00010723	nuclear receptor 2C2 associated protein	1.9384 0574	0.0012 6584	0.0048 5355
NR4A1	ENSMMUG000 00022922	nuclear receptor subfamily 4 group A member 1	1.1490 3566	6.31E- 06	6.23E- 05
NR4A3	ENSMMUG000 00011410	nuclear receptor subfamily 4 group A member 3	- 1.5751 364	9.89E- 08	2.33E- 06
NREP	ENSMMUG000 00002768	neuronal reration related protein	1.7855 8603	8.46E- 06	7.95E- 05
NRP1	ENSMMUG000 00017588	neuropilin 1	- 1.2841 211	5.19E- 06	5.31E- 05
NRP2	ENSMMUG000 00020052	neuropilin 2	- 1.2093 422	2.39E- 05	0.0001 8705
NRXN3	ENSMMUG000 00013842	neurexin 3	- 0.8927 274	0.0011 3184	0.0044 3423
NT5C	ENSMMUG000 00029832	5', 3'-nucleotidase, cytosolic	1.0622 4825	1.09E- 05	9.64E- 05
NTHL1	ENSMMUG000 00002807	nth like DNA glycosylase 1	0.7739 9438	4.08E- 05	0.0002 9195
NTPCR	ENSMMUG000 00063981	nucleoside- triphosphatase, cancer- related	0.7551 9969	7.58E- 08	1.88E- 06
NTRK2	ENSMMUG000 00023117	neurotrophic receptor tyrosine kinase 2	1.5340 7583	4.16E- 11	1.03E- 08
NUDT11	ENSMMUG000 00043712	nudix hydrolase 11	1.1022 2106	0.0010 4256	0.0041 4483
NUDT18	ENSMMUG000 00049401	nudix hydrolase 18	0.8378 3455	2.35E- 06	2.84E- 05
NUF2	ENSMMUG000 00001152	NUF2 component of NDC80 kinetochore complex	- 0.6361 412	1.75E- 06	2.26E- 05
NUP153	ENSMMUG000 00001993	nucleoporin 153	- 0.6112 028	1.90E- 08	6.82E- 07
NUP205	ENSMMUG000 00016384	nucleoporin 205	- 0.6807 558	7.04E- 07	1.10E- 05
NUP210	ENSMMUG000 00015979	nucleoporin 210	- 1.0135 34	3.50E- 07	6.35E- 06

NUSAP1	ENSMMUG000 00012681	nucleolar and spindle associated protein 1	- 1.0358 562	7.32E- 10	6.47E- 08
NXPH2	ENSMMUG000 00005176	neurexophilin 2	- 3.0701 084	0.0006 0455	0.0026 6128
OAS1	ENSMMUG000 00012782	2'-5'-oligoadenylate synthetase 1	2.0989 2448	0.0002 2192	0.0011 6759
OCIAD2	ENSMMUG000 00014869	OCIA domain containing 2	0.9829 9335	0.0001 2876	0.0007 4856
OGDH	ENSMMUG000 00002651	oxoglutarate dehydrogenase	- 0.6020 6	1.75E- 09	1.25E- 07
OGDHL	ENSMMUG000 00000275	oxoglutarate dehydrogenase L	- 0.6912 531	3.79E- 05	0.0002 7421
OPCML	ENSMMUG000 00047242	opioid binding protein/cell adhesion molecule like	- 0.7458 08	0.0001 3154	0.0007 6341
OPN3	ENSMMUG000 00005669	opsin 3	- 0.9930 643	5.16E- 05	0.0003 5288
ORC1	ENSMMUG000 00052294	origin recognition complex subunit 1	- 0.9719 252	3.50E- 05	0.0002 5624
OSMR	ENSMMUG000 00001609	oncostatin M receptor	0.6171 634	2.49E- 07	4.95E- 06
OTOGL	ENSMMUG000 00000121	otogelin like	- 1.6619 753	3.59E- 05	0.0002 6234
OTUD3	ENSMMUG000 00010764	OTU deubiquitinase 3	- 0.9525 817	6.39E- 05	0.0004 2012
OXCT1	ENSMMUG000 00011027	3-oxoacid CoA- transferase 1	- 0.6557 328	1.15E- 07	2.63E- 06
P2RY6	ENSMMUG000 00003138	pyrimidinergic receptor P2Y6	1.1490 8074	0.0003 4195	0.0016 5325
P3H2	ENSMMUG000 00000623	prolyl 3-hydroxylase 2	- 1.0803 65	1.63E- 11	6.09E- 09
P3H3	ENSMMUG000 00005189	prolyl 3-hydroxylase 3	3.8802 9982	0.0009 7439	0.0039 1083
P4HA3	ENSMMUG000 00017399	prolyl 4-hydroxylase subunit alpha 3	0.6295 6623	5.89E- 07	9.57E- 06

PABIR2	ENSMMUG000 00016948	PABIR family member 2	- 0.6659 75	1.06E- 05	9.42E- 05
PADI2	ENSMMUG000 00001616	peptidyl arginine deiminase 2	1.0398 9098	7.51E- 08	1.86E- 06
PAK1	ENSMMUG000 00001387	p21 (RAC1) activated kinase 1	0.8696 9293	0.0004 394	0.0020 3231
PALS1	ENSMMUG000 00021417	protein associated with LIN7 1, MAGUK p55 family member	- 0.7252 463	1.07E- 06	1.54E- 05
PAPPA	ENSMMUG000 00013099	pappalysin 1	- 1.1423 106	1.49E- 08	5.69E- 07
PARPBP	ENSMMUG000 00005506	PARP1 binding protein	- 1.0555 143	7.65E- 06	7.30E- 05
PASK	ENSMMUG000 00016207	PAS domain containing serine/threonine kinase	- 0.7396 784	1.79E- 06	2.29E- 05
PAXIP1	ENSMMUG000 00006331	PAX interacting protein 1	- 0.6718 356	0.0001 0634	0.0006 3863
PBK	ENSMMUG000 00016019	PDZ binding kinase	- 0.8292 393	2.22E- 07	4.54E- 06
PCDH20	ENSMMUG000 00053482	protocadherin 20	1.5846 5995	0.0001 988	0.0010 6843
PCDH7	ENSMMUG000 00011898	protocadherin 7	- 0.7875 494	1.52E- 08	5.76E- 07
PCLAF	ENSMMUG000 00029603	PCNA clamp associated factor	- 0.8938 409	2.80E- 07	5.42E- 06
PCMTD1	ENSMMUG000 00003347	protein-L-isoaspartate (D-aspartate) O- methyltransferase domain containing 1	0.7485 9988	1.40E- 08	5.45E- 07
PCNT	ENSMMUG000 00012914	pericentrin	- 0.6909 98	5.77E- 07	9.44E- 06
PCSK6	ENSMMUG000 00011829	proprotein convertase subtilisin/kexin type 6	2.8288 3683	0.0001 0409	0.0006 286
PCYT1B	ENSMMUG000 00012821	phosphate cytidyltransferase 1B, choline	1.1804 9418	0.0008 826	0.0036 135

PDCD11	ENSMMUG0000007058	programmed cell death 11	- 0.7083 918	4.22E-08	1.22E-06
PDE10A	ENSMMUG00000023614	phosphodiesterase 10A	- 0.7715 657	3.97E-05	0.00028522
PDE1C	ENSMMUG00000001625	phosphodiesterase 1C	- 1.4144 202	3.33E-08	1.02E-06
PDE7B	ENSMMUG00000003708	phosphodiesterase 7B	- 1.4293 798	7.95E-08	1.94E-06
PDIA4	ENSMMUG00000042048	protein disulfide isomerase family A member 4	- 0.7280 552	3.43E-11	9.33E-09
PDK1	ENSMMUG00000022553	pyruvate dehydrogenase kinase 1	1.1775 7387	3.36E-06	3.77E-05
PDLIM2	ENSMMUG00000018520	PDZ and LIM domain 2	0.6812 4173	3.97E-08	1.17E-06
PDLIM4	ENSMMUG00000009298	PDZ and LIM domain 4	0.6550 1941	2.14E-05	0.00017054
PDZD4	ENSMMUG00000003377	PDZ domain containing 4	1.0396 8168	0.0005505	0.0024553
PEAK1	ENSMMUG00000042378	pseudopodium enriched atypical kinase 1	- 1.1699 505	6.15E-09	3.06E-07
PECR	ENSMMUG00000017964	peroxisomal trans-2-enoyl-CoA reductase	0.9963 8944	1.52E-07	3.35E-06
PELI3	ENSMMUG00000003387	pellino E3 ubiquitin protein ligase family member 3	0.7616 1199	0.001467	0.00548778
PEPD	ENSMMUG00000006128	peptidase D	0.8074 291	3.48E-09	2.06E-07
PF4V1	ENSMMUG00000001295	platelet factor 4 variant 1	1.0998 7705	0.00067531	0.00290727
PFDN5	ENSMMUG00000022030	prefoldin subunit 5	1.0225 6972	4.34E-11	1.06E-08
PFKL	ENSMMUG00000004173	phosphofructokinase, liver type	0.7175 9275	2.47E-07	4.92E-06
PGF	ENSMMUG00000002909	placental growth factor	1.8081 187	0.00299854	0.00995042
PGGHG	ENSMMUG00000004625	protein-glucosylgalactosylhydroxylysine glucosidase	1.1602 0893	6.20E-08	1.61E-06
PGM1	ENSMMUG00000020049	phosphoglucomutase 1	0.7909 8951	2.19E-10	2.89E-08

PHF19	ENSMMUG000 00010623	PHD finger protein 19	- 0.6796 319	6.18E- 08	1.61E- 06
PHF7	ENSMMUG000 00016984	PHD finger protein 7	0.7515 5586	0.0003 4745	0.0016 7692
PHGDH	ENSMMUG000 00023089	phosphoglycerate dehydrogenase	3.5133 4353	0.0018 6084	0.0066 719
PHLPP1	ENSMMUG000 00005145	PH domain and leucine rich repeat protein phosphatase 1	- 0.6048 168	1.53E- 05	0.0001 2865
PHLPP2	ENSMMUG000 00012007	PH domain and leucine rich repeat protein phosphatase 2	- 0.7669 723	3.10E- 05	0.0002 3124
PHYHIP L	ENSMMUG000 00003705	phytanoyl-CoA 2- hydroxylase interacting protein like	- 1.2588 636	8.60E- 06	8.03E- 05
PIEZO1	ENSMMUG000 00007254	piezo type mechanosensitive ion channel component 1	- 0.6615 365	4.57E- 10	4.72E- 08
PIEZO2	ENSMMUG000 00057787	piezo type mechanosensitive ion channel component 2	- 0.8465 474	7.42E- 11	1.41E- 08
PIF1	ENSMMUG000 00006366	PIF1 5'-to-3' DNA helicase	- 1.2761 689	2.35E- 05	0.0001 8409
PIGR	ENSMMUG000 00011220	polymeric immunoglobulin receptor	- 1.1605 274	0.0002 2838	0.0011 9229
PIK3CD	ENSMMUG000 00006224	phosphatidylinositol-4,5- bisphosphate 3-kinase catalytic subunit delta	- 0.7840 564	1.70E- 10	2.41E- 08
PIK3IP1	ENSMMUG000 00019661	phosphoinositide-3- kinase interacting protein 1	0.8851 48	1.38E- 05	0.0001 1812
PIMREG	ENSMMUG000 00017760	PICALM interacting mitotic regulator	- 0.6022 151	0.0002 7607	0.0013 8796
PITRM1	ENSMMUG000 00004938	pitrilysin metallopeptidase 1	- 0.6562 367	2.87E- 07	5.51E- 06
PKMYT1	ENSMMUG000 00004214	protein kinase, membrane associated tyrosine/threonine 1	- 0.8255 102	2.55E- 07	5.03E- 06
PKN3	ENSMMUG000 00010143	protein kinase N3	- 0.6741 911	0.0028 6509	0.0095 9942

PLA2G3	ENSMMUG0000050471	phospholipase A2 group III	- 1.0928 62	9.88E- 09	4.30E- 07
PLAAT3	ENSMMUG0000005775	phospholipase A and acyltransferase 3	0.8641 6738	1.01E- 08	4.36E- 07
PLAU	ENSMMUG00000009906	plasminogen activator, urokinase	1.1830 7113	3.74E- 11	9.81E- 09
PLAUR	ENSMMUG00000004616	plasminogen activator, urokinase receptor	0.6114 5287	2.19E- 06	2.70E- 05
PLCB1	ENSMMUG00000004313	phospholipase C beta 1	- 0.7412 023	2.22E- 05	0.0001 7588
PLD5	ENSMMUG00000004265	phospholipase D family member 5	1.4400 5882	1.04E- 06	1.51E- 05
PLEC	ENSMMUG00000000388	plectin	- 0.7502 031	1.04E- 10	1.67E- 08
PLEK2	ENSMMUG00000021420	pleckstrin 2	0.7171 7273	0.0017 0203	0.0061 8235
PLEKHA7	ENSMMUG00000017628	pleckstrin homology domain containing A7	- 0.9089 566	0.0006 9123	0.0029 5763
PLEKHG3	ENSMMUG00000019170	pleckstrin homology and RhoGEF domain containing G3	- 0.6237 546	3.09E- 07	5.84E- 06
PLEKHG6	ENSMMUG00000000375	pleckstrin homology and RhoGEF domain containing G6	- 0.7561 017	0.0006 0673	0.0026 6751
PLEKHO1	ENSMMUG00000013681	pleckstrin homology domain containing O1	0.7311 6969	2.63E- 09	1.67E- 07
PLIN2	ENSMMUG00000013997	perilipin 2	2.1730 3697	9.62E- 05	0.0005 8784
PLK1	ENSMMUG00000017306	polo like kinase 1	- 0.9713 214	3.34E- 10	3.93E- 08
PLK4	ENSMMUG00000003320	polo like kinase 4	- 0.7177 417	4.94E- 06	5.12E- 05
PLOD2	ENSMMUG00000011577	procollagen-lysine,2-oxoglutarate 5-dioxygenase 2	0.7458 9169	0.0016 1742	0.0059 4467
PLSCR4	ENSMMUG00000007976	phospholipid scramblase 4	1.1880 746	9.22E- 06	8.46E- 05
PLTP	ENSMMUG00000009963	phospholipid transfer protein	0.9814 8943	1.34E- 11	5.45E- 09

PMEL	ENSMMUG000 00018816	premelanosome protein	0.8487 5389	1.77E- 06	2.27E- 05
PMEPA1	ENSMMUG000 00022589	prostate transmembrane protein, androgen induced 1	0.7171 064	8.65E- 09	3.97E- 07
PNMA8A	ENSMMUG000 00005827	PNMA family member 8A	1.0871 5131	1.68E- 06	2.17E- 05
PNOC	ENSMMUG000 00007479	prepronociceptin	3.1322 2226	2.67E- 06	3.15E- 05
POC1A	ENSMMUG000 00012485	POC1 centriolar protein A	- 0.7339 167	0.0001 8056	0.0009 9466
POLA1	ENSMMUG000 00018433	DNA polymerase alpha 1, catalytic subunit	- 0.6260 813	7.74E- 07	1.18E- 05
POLA2	ENSMMUG000 00022031	DNA polymerase alpha 2, accessory subunit	- 0.9406 181	2.27E- 08	7.70E- 07
POLE	ENSMMUG000 00015463	DNA polymerase epsilon, catalytic subunit	- 0.9727 325	1.53E- 09	1.14E- 07
POLE2	ENSMMUG000 00003913	DNA polymerase epsilon 2, accessory subunit	- 0.9462 712	9.89E- 05	0.0006 014
POLM	ENSMMUG000 00002421	DNA polymerase mu	1.0914 2878	1.51E- 05	0.0001 2743
POLN	ENSMMUG000 00001156	DNA polymerase nu	- 0.7901 971	5.14E- 06	5.27E- 05
POLQ	ENSMMUG000 00007973	DNA polymerase theta	- 1.1298 678	4.18E- 08	1.22E- 06
PON3	ENSMMUG000 00008013	paraoxonase 3	0.9343 4538	9.51E- 06	8.68E- 05
POSTN	ENSMMUG000 00012307	periostin	0.8832 1552	1.68E- 09	1.23E- 07
POT1	ENSMMUG000 00020587	protection of telomeres 1	0.5800 9026	2.17E- 06	2.69E- 05
PPA1	ENSMMUG000 00006397	inorganic pyrophosphatase 1	- 0.5988 742	4.27E- 08	1.23E- 06
PPIL3	ENSMMUG000 00006638	peptidylprolyl isomerase like 3	0.6312 9514	4.33E- 07	7.54E- 06
PPM1K	ENSMMUG000 00004561	protein phosphatase, Mg ²⁺ /Mn ²⁺ dependent 1K	- 0.9154 855	0.0002 6909	0.0013 6026

PPM1M	ENSMMUG0000008236	protein phosphatase, Mg ²⁺ /Mn ²⁺ dependent 1M	0.92847486	2.54E-06	3.03E-05
PPME1	ENSMMUG0000017398	protein phosphatase methylesterase 1	0.64615416	5.67E-08	1.51E-06
PPP1R1A	ENSMMUG0000000113	protein phosphatase 1 regulatory inhibitor subunit 1A	2.21708217	0.00029055	0.00144763
PPP1R35	ENSMMUG0000012728	protein phosphatase 1 regulatory subunit 35	0.64799668	0.00015376	0.00087054
PPP1R3B	ENSMMUG0000050623	protein phosphatase 1 regulatory subunit 3B	1.05191038	0.0016313	0.00598776
PPP1R3C	ENSMMUG0000000242	protein phosphatase 1 regulatory subunit 3C	2.04232653	0.00022283	0.0011699
PPP1R3G	ENSMMUG00000061878	protein phosphatase 1 regulatory subunit 3G	2.50006086	0.00137808	0.00521137
PPP2R1B	ENSMMUG0000014001	protein phosphatase 2 scaffold subunit Abeta	-0.6948897	1.95E-06	2.45E-05
PPP4R4	ENSMMUG0000021295	protein phosphatase 4 regulatory subunit 4	-0.5924517	5.05E-05	0.00034728
PRC1	ENSMMUG0000007534	protein regulator of cytokinesis 1	-0.8952958	4.86E-12	3.07E-09
PRDX4	ENSMMUG0000021366	peroxiredoxin 4	0.84118454	3.09E-09	1.89E-07
PRIM1	ENSMMUG0000004522	DNA primase subunit 1	-0.6474417	6.43E-05	0.00042177
PRKAR1B	ENSMMUG0000053014	protein kinase cAMP-dependent type I regulatory subunit beta	0.75396637	5.04E-05	0.00034708
PRKDC	ENSMMUG0000015347	protein kinase, DNA-activated, catalytic subunit	-0.7870932	6.61E-07	1.04E-05
PROC	ENSMMUG0000049035	protein C, inactivator of coagulation factors Va and VIIIa	3.43363779	2.10E-05	0.00016808
PROS1	ENSMMUG0000020334	protein S	1.1507985	1.63E-09	1.20E-07
PRR11	ENSMMUG0000003390	proline rich 11	-1.2613157	3.54E-07	6.40E-06

PRR14L	ENSMMUG000 00020746	proline rich 14 like	- 0.6610 447	4.67E- 05	0.0003 2741
PRRC2A	ENSMMUG000 00005297	proline rich coiled-coil 2A	- 0.6308 215	1.46E- 10	2.17E- 08
PRRC2C	ENSMMUG000 00013639	proline rich coiled-coil 2C	- 0.6972 359	1.64E- 07	3.56E- 06
PRRX2	ENSMMUG000 00050493	paired related homeobox 2	1.5686 5302	3.76E- 07	6.70E- 06
PRTFDC 1	ENSMMUG000 00018728	phosphoribosyl transferase domain containing 1	1.6614 9745	8.88E- 06	8.24E- 05
PRUNE2	ENSMMUG000 00001043	prune homolog 2 with BCH domain	- 1.0839 373	2.06E- 08	7.21E- 07
PRXL2A	ENSMMUG000 00021773	peroxiredoxin like 2A	1.0193 4843	3.33E- 09	1.98E- 07
PRXL2C	ENSMMUG000 00008295	peroxiredoxin like 2C	0.6000 373	3.70E- 06	4.06E- 05
PSD4	ENSMMUG000 00011572	pleckstrin and Sec7 domain containing 4	0.6821 7495	0.0005 6972	0.0025 2641
PTGDS	ENSMMUG000 00052688	prostaglandin D2 synthase	1.0353 3285	1.96E- 11	6.36E- 09
PTGER4	ENSMMUG000 00016167	prostaglandin E receptor 4	- 0.7703 141	7.21E- 07	1.12E- 05
PTGES	ENSMMUG000 00059501	prostaglandin E synthase	4.4671 4089	0.0002 2575	0.0011 834
PTGIR	ENSMMUG000 00017922	prostaglandin I2 receptor	2.0162 2465	2.26E- 05	0.0001 7846
PTGIS	ENSMMUG000 00021692	prostaglandin I2 synthase	0.8784 0078	2.62E- 10	3.24E- 08
PTPN4	ENSMMUG000 00005610	protein tyrosine phosphatase non- receptor type 4	- 0.6783 46	0.0003 8082	0.0018 0591
PTPN6	ENSMMUG000 00010203	protein tyrosine phosphatase non- receptor type 6	0.6163 2634	0.0009 6874	0.0038 9266
PTPRD	ENSMMUG000 00006952	protein tyrosine phosphatase receptor type D	- 0.7283 39	1.02E- 06	1.49E- 05
PTPRR	ENSMMUG000 00011075	protein tyrosine phosphatase receptor type R	1.0756 3502	4.29E- 08	1.23E- 06

PVALB	ENSMMUG000 00008778	parvalbumin	1.8683 8763	0.0002 2052	0.0011 6259
QPCT	ENSMMUG000 00016442	glutaminy-peptide cyclotransferase	0.6123 923	3.32E- 05	0.0002 4536
QSER1	ENSMMUG000 00001536	glutamine and serine rich 1	- 0.6189 921	8.00E- 09	3.71E- 07
RAB11B	ENSMMUG000 00010225	RAB11B, member RAS onco family	0.6276 3961	3.65E- 08	1.08E- 06
RAB2B	ENSMMUG000 00014992	RAB2B, member RAS onco family	1.1470 1478	3.12E- 08	9.73E- 07
RAB30	ENSMMUG000 00007842	RAB30, member RAS onco family	- 0.8102 265	0.0029 8547	0.0099 213
RAB36	ENSMMUG000 00015204	RAB36, member RAS onco family	- 1.7627 641	0.0016 7127	0.0060 9416
RAB3B	ENSMMUG000 00014035	RAB3B, member RAS onco family	- 0.6724 799	0.0026 4073	0.0089 6234
RACGAP 1	ENSMMUG000 00021689	Rac GTPase activating protein 1	- 0.9120 776	3.77E- 09	2.17E- 07
RAD18	ENSMMUG000 00020013	RAD18 E3 ubiquitin protein ligase	- 0.9553 663	2.64E- 05	0.0002 031
RAD51	ENSMMUG000 00004579	RAD51 recombinase	- 0.7998 173	4.84E- 05	0.0003 3553
RAD51A P1	ENSMMUG000 00015189	RAD51 associated protein 1	- 0.9848 92	5.33E- 07	8.89E- 06
RAD54B	ENSMMUG000 00005659	RAD54 homolog B	- 0.7931 952	0.0001 3598	0.0007 8559
RAD54L	ENSMMUG000 00011568	RAD54 like	- 0.9476 837	3.50E- 06	3.88E- 05
RALGDS	ENSMMUG000 00015274	ral guanine nucleotide dissociation stimulator	0.6571 0406	0.0001 1939	0.0007 0353
RANBP2	ENSMMUG000 00021019	RAN binding protein 2	- 0.6407 384	2.89E- 09	1.79E- 07
RAP1GA P2	ENSMMUG000 00022989	RAP1 GTPase activating protein 2	- 1.2393 944	0.0010 8761	0.0042 8831

RAPH1	ENSMMUG0000000314	Ras association (RalGDS/AF-6) and pleckstrin homology domains 1	- 0.6725 732	5.97E-08	1.57E-06
RARRES2	ENSMMUG00000005232	retinoic acid receptor responder 2	1.7458 1628	3.20E-07	5.94E-06
RASAL1	ENSMMUG00000021793	RAS protein activator like 1	0.6229 8857	2.22E-07	4.54E-06
RASD1	ENSMMUG00000006493	ras related dexamethasone induced 1	0.8398 8685	6.84E-05	0.0004 443
RASD2	ENSMMUG00000061659	RASD family member 2	1.1419 9956	0.0012 5892	0.0048 3589
RASSF10	ENSMMUG00000031015	Ras association domain family member 10	1.1857 7179	2.43E-08	8.18E-07
RASSF7	ENSMMUG00000054421	Ras association domain family member 7	1.3771 494	1.38E-09	1.09E-07
RBKS	ENSMMUG00000014458	ribokinase	0.6221 6551	0.0002 7861	0.0013 9821
RBP1	ENSMMUG00000000290	retinol binding protein 1	1.7534 9517	2.67E-06	3.15E-05
RBPM2	ENSMMUG00000013270	RNA binding protein, mRNA processing factor 2	- 0.8128 089	4.55E-05	0.0003 2062
RDH10	ENSMMUG00000005143	retinol dehydrogenase 10	- 0.6563 195	4.26E-05	0.0003 0297
RECQL4	ENSMMUG00000015588	RecQ like helicase 4	- 0.8218 845	7.11E-06	6.85E-05
REL	ENSMMUG00000010834	REL proto-onco, NF-kB subunit	- 0.8874 62	0.0005 5972	0.0024 9003
RFC3	ENSMMUG00000003371	replication factor C subunit 3	- 0.6763 642	3.01E-05	0.0002 2644
RFC4	ENSMMUG00000003704	replication factor C subunit 4	- 0.7203 581	4.18E-06	4.48E-05
RFC5	ENSMMUG00000010235	replication factor C subunit 5	- 0.6162 914	8.83E-06	8.21E-05
RGS11	ENSMMUG00000000602	regulator of G protein signaling 11	0.7768 6937	1.28E-05	0.0001 1098
RGS16	ENSMMUG00000055481	regulator of G protein signaling 16	1.2077 0619	9.15E-10	7.79E-08

RGS2	ENSMMUG00000049590	regulator of G protein signaling 2	1.62805712	2.34E-09	1.54E-07
RGS5	ENSMMUG00000005186	regulator of G protein signaling 5	0.66489287	1.03E-06	1.50E-05
RGS9	ENSMMUG00000014521	regulator of G protein signaling 9	0.85643975	0.00104405	0.00414719
RHPN2	ENSMMUG00000028798	rhophilin Rho GTPase binding protein 2	-0.7499093	2.46E-06	2.95E-05
RILP	ENSMMUG00000002377	Rab interacting lysosomal protein	1.12069566	5.87E-06	5.85E-05
RIOK3	ENSMMUG00000021478	RIO kinase 3	0.6769076	1.96E-07	4.12E-06
RMI1	ENSMMUG00000018875	RecQ mediated genome instability 1	-0.6564566	0.00061591	0.00269591
RNASE4	ENSMMUG00000005496	ribonuclease A family member 4	1.1217569	7.30E-11	1.41E-08
RNaseP_nuc	ENSMMUG00000036452	Nuclear RNase P	1.09985872	0.00254333	0.00868501
RNF128	ENSMMUG00000021412	ring finger protein 128	-0.6252297	9.04E-05	0.00055813
RNF144A	ENSMMUG00000045908	ring finger protein 144A	1.44540762	2.37E-10	3.04E-08
RNF145	ENSMMUG00000021699	ring finger protein 145	0.67826102	3.13E-09	1.90E-07
RNF183	ENSMMUG00000005848	ring finger protein 183	2.55650314	0.00025723	0.00130858
RNF212	ENSMMUG00000015507	ring finger protein 212	0.76187776	8.17E-05	0.00051449
RNF43	ENSMMUG00000007004	ring finger protein 43	-0.9756553	0.0014932	0.00556628
ROBO2	ENSMMUG00000012609	roundabout guidance receptor 2	-1.7719852	0.00068537	0.00293874
ROR1	ENSMMUG00000004668	receptor tyrosine kinase like orphan receptor 1	-0.9630443	0.00186903	0.00669645
RORC	ENSMMUG00000012138	RAR related orphan receptor C	1.39027219	1.11E-06	1.58E-05
RPA2	ENSMMUG00000018172	replication protein A2	-0.6645763	1.97E-07	4.12E-06

RPAIN	ENSMMUG000 00010468	RPA interacting protein	0.7699 2796	2.84E- 06	3.31E- 05
RPL18	ENSMMUG000 00022158	ribosomal protein L18	0.6920 3645	4.40E- 10	4.59E- 08
RPL35	ENSMMUG000 00005260	ribosomal protein L35	0.6937 4375	5.55E- 08	1.49E- 06
RPL5	ENSMMUG000 00005072	ribosomal protein L5	0.9194 2969	6.64E- 11	1.41E- 08
RPP40	ENSMMUG000 00004966	ribonuclease P/MRP subunit p40	- 0.6703 52	0.0013 9506	0.0052 6266
RPS14	ENSMMUG000 00002848	ribosomal protein S14	0.8780 9252	6.74E- 12	3.86E- 09
RPS15	ENSMMUG000 00061470	ribosomal protein S15	0.5988 1682	4.02E- 08	1.18E- 06
RPS18	ENSMMUG000 00003867	ribosomal protein S18	0.9392 978	1.34E- 12	1.24E- 09
RPS19	ENSMMUG000 00013429	ribosomal protein S19	0.7653 5808	2.61E- 11	7.69E- 09
RPS20	ENSMMUG000 00053276	ribosomal protein S20	0.6250 4272	2.54E- 09	1.63E- 07
RPS21	ENSMMUG000 00005006	ribosomal protein S21	0.7352 3052	6.56E- 06	6.42E- 05
RPS23	ENSMMUG000 00003578	ribosomal protein S23	0.5963 2928	1.85E- 08	6.63E- 07
RPS5	ENSMMUG000 00008729	ribosomal protein S5	0.6561 8865	7.32E- 10	6.47E- 08
RPS9	ENSMMUG000 00060498	ribosomal protein S9	0.6823 7266	3.40E- 10	3.93E- 08
RPTOR	ENSMMUG000 00006761	regulatory associated protein of MTOR complex 1	- 0.7187 5	6.02E- 09	3.04E- 07
RRAD	ENSMMUG000 00049583	RRAD, Ras related glycolysis inhibitor and calcium channel regulator	0.9040 6028	5.65E- 05	0.0003 8136
RRM1	ENSMMUG000 00003962	ribonucleotide reductase catalytic subunit M1	- 0.6667 661	5.58E- 10	5.48E- 08
RRM2	ENSMMUG000 00002057	ribonucleotide reductase regulatory subunit M2	- 0.9111 683	8.07E- 11	1.46E- 08
RSPH3	ENSMMUG000 00020011	radial spoke head 3	0.6663 5781	1.27E- 05	0.0001 1027
RSPO1	ENSMMUG000 00008420	R-spondin 1	1.6720 9466	0.0026 4647	0.0089 7098

RTL5	ENSMMUG000 00059483	retrotransposon Gag like 5	- 0.8056 111	4.98E- 08	1.39E- 06
RTN4RL 2	ENSMMUG000 00010982	reticulon 4 receptor like 2	2.9668 2527	0.0006 3736	0.0027 7142
S100A1	ENSMMUG000 00008145	S100 calcium binding protein A1	0.7601 824	1.71E- 09	1.24E- 07
SAMD12	ENSMMUG000 00004846	sterile alpha motif domain containing 12	- 0.6025 906	0.0025 7509	0.0087 7834
SAMD13	ENSMMUG000 00000402	sterile alpha motif domain containing 13	1.4139 1721	0.0012 934	0.0049 3693
SAMD14	ENSMMUG000 00014687	sterile alpha motif domain containing 14	1.4893 1842	4.41E- 06	4.69E- 05
SAMD4A	ENSMMUG000 00010315	sterile alpha motif domain containing 4A	- 0.6377 467	1.18E- 06	1.65E- 05
SAMD9	ENSMMUG000 00000170	sterile alpha motif domain containing 9	- 0.5811 335	0.0009 0077	0.0036 7057
SAMD9L	ENSMMUG000 00020803	sterile alpha motif domain containing 9 like	- 1.2355 273	2.75E- 05	0.0002 097
SAP130	ENSMMUG000 00021287	Sin3A associated protein 130	- 0.7018 614	6.18E- 05	0.0004 0916
SAP30	ENSMMUG000 00002401	Sin3A associated protein 30	0.9753 8969	1.57E- 05	0.0001 3158
SASS6	ENSMMUG000 00004240	SAS-6 centriolar assembly protein	- 1.0638 563	4.67E- 06	4.89E- 05
SAT2	ENSMMUG000 00013511	spermidine/spermine N1- acetyltransferase family member 2	0.5922 7544	3.56E- 07	6.42E- 06
SCAND1	ENSMMUG000 00009306	SCAN domain containing 1	0.6359 7029	7.50E- 08	1.86E- 06
SCARA3	ENSMMUG000 00021517	scavenger receptor class A member 3	0.8046 2404	2.83E- 08	9.19E- 07
SCARB2	ENSMMUG000 00020913	scavenger receptor class B member 2	0.7112 2597	3.67E- 10	4.17E- 08
SCML1	ENSMMUG000 00012899	Scm polycomb group protein like 1	- 0.9398 744	0.0001 9434	0.0010 5052
SEC14L2	ENSMMUG000 00013404	SEC14 like lipid binding 2	0.6532 725	1.76E- 07	3.77E- 06

SEL1L3	ENSMMUG000 00020349	SEL1L family member 3	- 0.6128 559	1.65E- 06	2.15E- 05
SELENO M	ENSMMUG000 00037662	selenoprotein M	0.5873 5766	1.28E- 08	5.16E- 07
SEMA3A	ENSMMUG000 00007555	semaphorin 3A	- 0.6558 35	8.53E- 05	0.0005 3245
SEMA3B	ENSMMUG000 00020117	semaphorin 3B	0.8070 8423	2.52E- 05	0.0001 9475
SEMA3D	ENSMMUG000 00021730	semaphorin 3D	- 0.9841 375	1.59E- 05	0.0001 3248
SEMA3E	ENSMMUG000 00001979	semaphorin 3E	- 0.7197 977	1.38E- 05	0.0001 1835
SEMA4B	ENSMMUG000 00023816	semaphorin 4B	0.8155 2508	4.90E- 08	1.37E- 06
SEMA5A	ENSMMUG000 00020160	semaphorin 5A	- 1.1957 657	4.69E- 09	2.57E- 07
SEMA5B	ENSMMUG000 00010034	semaphorin 5B	0.7121 0499	0.0006 7759	0.0029 1346
SERP2	ENSMMUG000 00044916	stress associated endoplasmic reticulum protein family member 2	1.0645 6826	0.0002 6067	0.0013 2348
SERPIN A1	ENSMMUG000 00020426	serpin family A member 1	4.0623 7655	0.0004 6985	0.0021 4736
SERPIN G1	ENSMMUG000 00012618	serpin family G member 1	2.0083 6539	2.76E- 07	5.38E- 06
SERTAD 1	ENSMMUG000 00016027	SERTA domain containing 1	0.5964 1782	8.48E- 07	1.28E- 05
SETD1B	ENSMMUG000 00012842	SET domain containing 1B, histone lysine methyltransferase	- 0.6403 208	1.71E- 07	3.68E- 06
SFMBT1	ENSMMUG000 00014527	Scm like with four mbt domains 1	- 0.6440 908	0.0002 9143	0.0014 5097
SFRP5	ENSMMUG000 00064002	secreted frizzled related protein 5	2.1862 8361	1.96E- 08	6.98E- 07
SFXN3	ENSMMUG000 00022620	sideroflexin 3	0.6120 6946	0.0007 1422	0.0030 3709
SGCE	ENSMMUG000 00016394	sarcoglycan epsilon	0.6834 5846	5.25E- 05	0.0003 5792

SGO1	ENSMMUG000 00020341	shugoshin 1	- 0.7481 497	0.0008 9016	0.0036 3647
SGO2	ENSMMUG000 00052913	shugoshin 2	- 1.2009 014	2.00E- 07	4.17E- 06
SH2B2	ENSMMUG000 00010329	SH2B adaptor protein 2	1.1144 7264	0.0016 3048	0.0059 8635
SH3GL3	ENSMMUG000 00013669	SH3 domain containing GRB2 like 3, endophilin A3	0.6094 456	0.0009 0592	0.0036 829
SHCBP1	ENSMMUG000 00012376	SHC binding and spindle associated 1	- 1.0550 065	6.12E- 09	3.06E- 07
SHF	ENSMMUG000 00008757	Src homology 2 domain containing F	1.2979 306	0.0001 6878	0.0009 4211
SHMT1	ENSMMUG000 00013535	serine hydroxymethyltransferas e 1	- 0.6837 359	0.0001 1543	0.0006 8276
SHROOM1	ENSMMUG000 00010312	shroom family member 1	0.8766 6543	0.0001 8873	0.0010 2668
SHROOM2	ENSMMUG000 00006193	shroom family member 2	- 0.6614 237	0.0003 5863	0.0017 2071
SHROOM3	ENSMMUG000 00020919	shroom family member 3	- 0.9559 593	7.84E- 10	6.75E- 08
SIAE	ENSMMUG000 00008476	sialic acid acetyltransferase	1.0669 565	9.47E- 05	0.0005 8127
SIPA1L2	ENSMMUG000 00012068	signal induced proliferation associated 1 like 2	- 0.6066 415	0.0029 138	0.0097 391
SIX1	ENSMMUG000 00058852	SIX homeobox 1	0.7773 3627	0.0003 9807	0.0018 7621
SKA1	ENSMMUG000 00000719	spindle and kinetochore associated complex subunit 1	- 0.8672 963	0.0003 0291	0.0014 9904
SKA3	ENSMMUG000 00016560	spindle and kinetochore associated complex subunit 3	- 1.0685 076	1.86E- 06	2.35E- 05
SLAMF7	ENSMMUG000 00017327	SLAM family member 7	- 1.3340 561	0.0019 1873	0.0068 4886
SLC12A2	ENSMMUG000 00011214	solute carrier family 12 member 2	- 0.6562 003	1.03E- 08	4.40E- 07

SLC16A1 1	ENSMMUG000 00021176	solute carrier family 16 member 11	1.6772 4457	0.0019 0084	0.0067 9025
SLC1A1	ENSMMUG000 00000135	solute carrier family 1 member 1	- 0.5781 935	1.23E- 08	5.02E- 07
SLC22A1 7	ENSMMUG000 00014748	solute carrier family 22 member 17	0.6697 8598	9.34E- 06	8.55E- 05
SLC24A3	ENSMMUG000 00002321	solute carrier family 24 member 3	- 1.4254 008	1.35E- 08	5.31E- 07
SLC25A2 2	ENSMMUG000 00007513	solute carrier family 25 member 22	- 0.6532 692	8.52E- 06	7.99E- 05
SLC25A3 0	ENSMMUG000 00037790	solute carrier family 25 member 30	- 0.8692 611	6.51E- 07	1.03E- 05
SLC26A1 1	ENSMMUG000 00002850	solute carrier family 26 member 11	0.7222 0853	1.88E- 05	0.0001 5285
SLC2A3	ENSMMUG000 00046124	solute carrier family 2 member 3	1.2165 6569	0.0013 4447	0.0051 0098
SLC2A5	ENSMMUG000 00016307	solute carrier family 2 member 5	1.9565 6074	8.60E- 06	8.03E- 05
SLC2A6	ENSMMUG000 00010981	solute carrier family 2 member 6	- 0.8795 442	0.0008 1755	0.0033 902
SLC30A2	ENSMMUG000 00012328	solute carrier family 30 member 2	- 1.6738 367	1.15E- 08	4.73E- 07
SLC31A2	ENSMMUG000 00000172	solute carrier family 31 member 2	0.6959 0714	0.0014 864	0.0055 4542
SLC35F1	ENSMMUG000 00022354	solute carrier family 35 member F1	0.8298 0078	0.0003 2368	0.0015 8091
SLC38A5	ENSMMUG000 00016975	solute carrier family 38 member 5	1.6973 9211	5.01E- 05	0.0003 454
SLC43A2	ENSMMUG000 00017561	solute carrier family 43 member 2	0.8052 59	3.61E- 08	1.07E- 06
SLC6A3	ENSMMUG000 00005198	solute carrier family 6 member 3	- 0.8724 513	1.54E- 05	0.0001 2908
SLC6A9	ENSMMUG000 00015158	solute carrier family 6 member 9	0.5910 76	2.28E- 06	2.79E- 05
SLC7A6	ENSMMUG000 00037975	solute carrier family 7 member 6	- 0.7843 484	4.12E- 07	7.21E- 06

SLC7A6 OS	ENSMMUG000 00061757	solute carrier family 7 member 6 opposite strand	0.7124 0391	3.01E- 05	0.0002 2644
SLC7A8	ENSMMUG000 00019653	solute carrier family 7 member 8	- 0.7946 592	0.0015 9833	0.0058 9169
SLC8A1	ENSMMUG000 00015508	solute carrier family 8 member A1	- 0.7184 656	9.64E- 07	1.42E- 05
SLF1	ENSMMUG000 00001392	SMC5-SMC6 complex localization factor 1	- 0.7539 428	0.0004 5838	0.0021 0174
SLIT3	ENSMMUG000 00017087	slit guidance ligand 3	- 0.8591 109	3.29E- 09	1.98E- 07
SLX4	ENSMMUG000 00007574	SLX4 structure-specific endonuclease subunit	- 0.9843 192	0.0001 527	0.0008 6593
SMC1A	ENSMMUG000 00009293	structural maintenance of chromosomes 1A	- 0.5864 465	1.19E- 08	4.85E- 07
SMC2	ENSMMUG000 00020463	structural maintenance of chromosomes 2	- 0.9103 558	6.07E- 10	5.84E- 08
SMDT1	ENSMMUG000 00013061	single-pass membrane protein with aspartate rich tail 1	0.7047 3263	6.62E- 09	3.20E- 07
SMO	ENSMMUG000 00012110	smoothed, frizzled class receptor	1.9509 0909	0.0001 9856	0.0010 6838
SMOX	ENSMMUG000 00020912	spermine oxidase	0.9494 207	8.45E- 06	7.94E- 05
SNAI1	ENSMMUG000 00063295	snail family transcriptional repressor 1	1.3263 8978	0.0003 5564	0.0017 1049
SNAP47	ENSMMUG000 00001869	synaptosome associated protein 47	0.6109 345	2.65E- 05	0.0002 0361
SNAPC1	ENSMMUG000 00017303	small nuclear RNA activating complex polypeptide 1	0.5791 8545	4.91E- 06	5.11E- 05
SNAPIN	ENSMMUG000 00053224	SNAP associated protein	0.6008 6608	2.64E- 07	5.17E- 06
SNED1	ENSMMUG000 00004968	sushi, nidogen and EGF like domains 1	0.7583 2714	0.0002 6747	0.0013 5308
SNORA7 0	ENSMMUG000 00024570	Small nucleolar RNA SNORA70	- 2.7688 161	0.0024 1955	0.0083 2174

SNORD5 2	ENSMMUG000 00024056	small nucleolar RNA, C/D box 52	- 2.2612 274	0.0024 3615	0.0083 726
SNTB1	ENSMMUG000 00002607	syntrophin beta 1	0.8488 0722	0.0025 2402	0.0086 3394
SNX21	ENSMMUG000 00023515	sorting nexin family member 21	0.6472 7954	2.84E- 05	0.0002 1616
SNX27	ENSMMUG000 00016920	sorting nexin 27	- 0.6523 595	0.0011 3672	0.0044 4906
SOCS3	ENSMMUG000 00058428	suppressor of cytokine signaling 3	1.6030 4214	1.31E- 07	2.92E- 06
SOD3	ENSMMUG000 00002612	superoxide dismutase 3	- 0.8827 464	0.0001 4155	0.0008 1299
SOGA1	ENSMMUG000 00005579	suppressor of glucose, autophagy associated 1	- 0.9429 753	8.15E- 08	1.98E- 06
SON	ENSMMUG000 00005511	SON DNA and RNA binding protein	- 0.6369 846	4.35E- 09	2.40E- 07
SORBS2	ENSMMUG000 00015733	sorbin and SH3 domain containing 2	- 0.7241 268	2.01E- 08	7.08E- 07
SORCS1	ENSMMUG000 00000433	sortilin related VPS10 domain containing receptor 1	1.1939 457	0.0028 4146	0.0095 3407
SORD	ENSMMUG000 00015971	sorbitol dehydrogenase	1.2247 0101	2.98E- 06	3.42E- 05
SOX13	ENSMMUG000 00008460	SRY-box transcription factor 13	- 0.6465 048	0.0001 4703	0.0008 3758
SPAG5	ENSMMUG000 00006018	sperm associated antigen 5	- 0.7819 775	2.26E- 09	1.51E- 07
SPC24	ENSMMUG000 00003612	SPC24 component of NDC80 kinetochore complex	- 0.7402 644	7.12E- 05	0.0004 597
SPC25	ENSMMUG000 00053972	SPC25 component of NDC80 kinetochore complex	- 0.8882 511	1.53E- 07	3.36E- 06
SPDL1	ENSMMUG000 00009365	spindle apparatus coiled- coil protein 1	- 0.5947 134	4.15E- 06	4.46E- 05

SPHKAP	ENSMMUG000 00013254	SPHK1 interactor, AKAP domain containing	1.1819 2471	0.0001 9409	0.0010 5052
SPINT1	ENSMMUG000 00063461	serine peptidase inhibitor, Kunitz type 1	0.7355 6481	2.57E- 08	8.56E- 07
SPNS2	ENSMMUG000 00022858	sphingolipid transporter 2	- 1.0389 183	2.11E- 05	0.0001 6854
SPOCK3	ENSMMUG000 00006851	SPARC (osteonectin), cwcv and kazal like domains proteoglycan 3	1.1296 3337	2.40E- 10	3.05E- 08
SPON2	ENSMMUG000 00020856	spondin 2	1.0070 4539	1.39E- 06	1.86E- 05
SPP1	ENSMMUG000 00008793	secreted phosphoprotein 1	0.7806 8346	1.74E- 06	2.25E- 05
SPRY1	ENSMMUG000 00001848	sprouty RTK signaling antagonist 1	0.9593 6319	3.86E- 07	6.84E- 06
SPTAN1	ENSMMUG000 00009327	spectrin alpha, non- erythrocytic 1	- 0.6284 087	3.44E- 08	1.04E- 06
SQLE	ENSMMUG000 00003535	squalene epoxidase	- 1.5157 122	1.38E- 10	2.10E- 08
SQOR	ENSMMUG000 00015749	sulfide quinone oxidoreductase	0.8872 3019	1.25E- 10	1.97E- 08
SREBF2	ENSMMUG000 00003357	sterol regulatory element binding transcription factor 2	- 0.5789 881	3.46E- 09	2.05E- 07
SRGAP3	ENSMMUG000 00020014	SLIT-ROBO Rho GTPase activating protein 3	- 0.8558 79	6.58E- 07	1.04E- 05
SRMS	ENSMMUG000 00050161	src-related kinase lacking C-terminal regulatory tyrosine and N-terminal myristylation sites	1.8302 0689	0.0028 963	0.0096 9463
SRPX	ENSMMUG000 00013135	sushi repeat containing protein X-linked	1.9202 4759	0.0017 6632	0.0063 7206
SSC5D	ENSMMUG000 00005014	scavenger receptor cysteine rich family member with 5 domains	0.8386 4416	0.0026 4953	0.0089 7694
SSH2	ENSMMUG000 00014413	slingshot protein phosphatase 2	- 0.7649 711	2.33E- 07	4.74E- 06
SST	ENSMMUG000 00000850	somatostatin	- 2.8536 987	4.27E- 08	1.23E- 06

ST6GAL NAC6	ENSMMUG000 00018686	ST6 N- acetylgalactosaminide alpha-2,6- sialyltransferase 6	0.7636 4377	1.24E- 08	5.02E- 07
ST8SIA1	ENSMMUG000 00003685	ST8 alpha-N-acetyl- neuraminide alpha-2,8- sialyltransferase 1	0.7107 8794	0.0023 2168	0.0080 3693
STARD8	ENSMMUG000 00015291	StAR related lipid transfer domain containing 8	- 1.0528 525	6.87E- 05	0.0004 4579
STAT1	ENSMMUG000 00005613	signal transducer and activator of transcription 1	- 1.0230 193	8.76E- 12	4.50E- 09
STAT4	ENSMMUG000 00005617	signal transducer and activator of transcription 4	- 1.3010 172	0.0008 6891	0.0035 6258
STC2	ENSMMUG000 00014782	stanniocalcin 2	2.9173 2207	0.0029 2007	0.0097 53
STIL	ENSMMUG000 00020389	STIL centriolar assembly protein	- 1.3008 727	9.05E- 09	4.10E- 07
STK16	ENSMMUG000 00019626	serine/threonine kinase 16	0.6200 4012	1.10E- 06	1.57E- 05
STX1A	ENSMMUG000 00014555	syntaxin 1A	0.7348 5441	1.38E- 06	1.85E- 05
STXBP5 L	ENSMMUG000 00011161	syntaxin binding protein 5L	- 1.0194 313	7.69E- 09	3.61E- 07
SUMF2	ENSMMUG000 00015275	sulfatase modifying factor 2	0.6465 8532	8.90E- 06	8.25E- 05
SVBP	ENSMMUG000 00059313	small vasohibin binding protein	1.0164 9055	7.65E- 08	1.88E- 06
SVIL	ENSMMUG000 00001374	supervillin	0.8100 981	6.87E- 07	1.07E- 05
SWT1	ENSMMUG000 00013882	SWT1 RNA endoribonuclease homolog	0.8289 4701	0.0002 7087	0.0013 6774
SYNDIG 1	ENSMMUG000 00015852	synapse differentiation inducing 1	2.9681 1396	2.67E- 06	3.15E- 05
SYNGR1	ENSMMUG000 00012101	synaptogyrin 1	1.4963 9376	0.0005 6364	0.0025 0265
SYNJ1	ENSMMUG000 00004624	synaptojanin 1	- 0.6082 05	8.73E- 05	0.0005 4268

SYT1	ENSMMUG000 00005530	synaptotagmin 1	- 0.8921 509	2.52E- 07	4.99E- 06
SYT10	ENSMMUG000 00010712	synaptotagmin 10	- 0.7643 842	7.49E- 07	1.15E- 05
TACC3	ENSMMUG000 00011191	transforming acidic coiled-coil containing protein 3	- 0.9985 47	7.38E- 11	1.41E- 08
TAGAP	ENSMMUG000 00011994	T cell activation RhoGTPase activating protein	- 1.2974 331	0.0006 6707	0.0028 7893
TAMALI N	ENSMMUG000 00006199	trafficking regulator and scaffold protein tamalin	2.3461 593	9.62E- 05	0.0005 881
TANC1	ENSMMUG000 00006180	tetratricopeptide repeat, ankyrin repeat and coiled-coil containing 1	- 0.6985 208	2.18E- 09	1.47E- 07
TASOR2	ENSMMUG000 00013180	transcription activation suppressor family member 2	- 0.6532 209	7.69E- 09	3.61E- 07
TBC1D4	ENSMMUG000 00021197	TBC1 domain family member 4	- 0.5840 322	0.0002 1988	0.0011 6083
TBCC	ENSMMUG000 00001305	tubulin folding cofactor C	0.6406 1719	2.37E- 06	2.86E- 05
TBL1Y	ENSMMUG000 00046495	transducin beta like 1 Y- linked	1.9922 3025	0.0006 1803	0.0027 0346
TCAF2C	ENSMMUG000 00013955	TRPM8 channel associated factor 2C	0.8000 6535	0.0013 453	0.0051 0132
TCEA2	ENSMMUG000 00018878	transcription elongation factor A2	1.1182 8652	1.36E- 08	5.34E- 07
TCEAL3	ENSMMUG000 00003501	transcription elongation factor A like 3	2.5941 9133	9.90E- 05	0.0006 0152
TCEAL8	ENSMMUG000 00052429	transcription elongation factor A like 8	0.8590 1004	2.19E- 08	7.53E- 07
TCF19	ENSMMUG000 00015682	transcription factor 19	- 0.9264 592	1.02E- 05	9.21E- 05
TCP11L1	ENSMMUG000 00002539	t-complex 11 like 1	- 0.7721 313	4.00E- 06	4.33E- 05
TCP11L2	ENSMMUG000 00003711	t-complex 11 like 2	0.5934 066	2.44E- 05	0.0001 8983
TDRD12	ENSMMUG000 00015608	tudor domain containing 12	0.7884 784	0.0029 9459	0.0099 397

TEAD2	ENSMMUG000 00014791	TEA domain transcription factor 2	0.5999 6112	4.31E- 06	4.60E- 05
TEDC2	ENSMMUG000 00000002	tubulin epsilon and delta complex 2	- 0.8194 497	0.0002 153	0.0011 4292
TENM3	ENSMMUG000 00007240	teneurin transmembrane protein 3	- 0.8732 941	2.06E- 08	7.21E- 07
TENM4	ENSMMUG000 00042218	teneurin transmembrane protein 4	- 0.6190 261	2.24E- 05	0.0001 7777
TFAP4	ENSMMUG000 00044729	transcription factor AP-4	0.7377 4667	4.03E- 05	0.0002 8886
TFPI2	ENSMMUG000 00020581	tissue factor pathway inhibitor 2	- 1.0297 172	9.18E- 06	8.44E- 05
TGFA	ENSMMUG000 00010591	transforming growth factor alpha	- 0.7279 361	0.0001 141	0.0006 7695
TGFBI	ENSMMUG000 00000332	transforming growth factor beta induced	1.6400 7192	0.0005 089	0.0022 9186
TGIF1	ENSMMUG000 00005086	TGFB induced factor homeobox 1	0.5853 8011	2.96E- 08	9.39E- 07
THAP11	ENSMMUG000 00013240	THAP domain containing 11	0.6499 0425	3.31E- 07	6.07E- 06
THBD	ENSMMUG000 00016814	thrombomodulin	1.3254 5941	0.0012 6066	0.0048 3991
THBS2	ENSMMUG000 00051514	thrombospondin 2	0.5816 9267	5.10E- 05	0.0003 4959
THOC6	ENSMMUG000 00007666	THO complex 6	1.1695 2361	9.89E- 08	2.33E- 06
THRA	ENSMMUG000 00002931	thyroid hormone receptor alpha	0.6714 8992	0.0001 2337	0.0007 2231
THYN1	ENSMMUG000 00007103	thymocyte nuclear protein 1	0.6004 3386	5.28E- 06	5.38E- 05
TIAM2	ENSMMUG000 00011169	TIAM Rac1 associated GEF 2	- 0.9838 523	8.84E- 05	0.0005 4837
TICRR	ENSMMUG000 00001254	TOPBP1 interacting checkpoint and replication regulator	- 1.0914 546	1.43E- 07	3.17E- 06
TIMELE SS	ENSMMUG000 00021878	timeless circadian regulator	- 0.6311 452	6.21E- 05	0.0004 1041

TIMM8B	ENSMMUG00000043558	translocase of inner mitochondrial membrane 8 homolog B	0.60513333	0.00018893	0.00102729
TIMP2	ENSMMUG00000005355	TIMP metalloproteinase inhibitor 2	0.62964721	3.45E-05	0.00025344
TIMP3	ENSMMUG00000062825	TIMP metalloproteinase inhibitor 3	0.99403247	6.25E-05	0.0004127
TK1	ENSMMUG00000021867	thymidine kinase 1	-0.8253707	1.06E-05	9.44E-05
TLL1	ENSMMUG00000015799	tolloid like 1	-0.8793944	3.20E-07	5.94E-06
TLN1	ENSMMUG00000031856	talin 1	-0.6035744	1.68E-10	2.40E-08
TLR3	ENSMMUG00000021762	toll like receptor 3	-0.8589515	0.00083382	0.00344841
TM7SF2	ENSMMUG00000018773	transmembrane 7 superfamily member 2	1.01115562	3.21E-06	3.64E-05
TMED5	ENSMMUG00000045421	transmembrane p24 trafficking protein 5	-0.5915431	1.15E-07	2.63E-06
TMEM107	ENSMMUG00000055944	transmembrane protein 107	0.66438177	4.95E-05	0.00034179
TMEM144	ENSMMUG00000004448	transmembrane protein 144	0.70028247	0.00111868	0.00439332
TMEM160	ENSMMUG00000057454	transmembrane protein 160	0.70630997	2.05E-05	0.00016458
TMEM171	ENSMMUG00000015433	transmembrane protein 171	-1.2530021	0.00155875	0.00577259
TMEM184A	ENSMMUG00000013080	transmembrane protein 184A	-0.6650189	0.00167215	0.00609437
TMEM229A	ENSMMUG00000049185	transmembrane protein 229A	-1.4689352	7.44E-08	1.85E-06
TMEM234	ENSMMUG00000008453	transmembrane protein 234	0.61703539	0.00024616	0.00126934
TMEM258	ENSMMUG00000006656	transmembrane protein 258	0.74793732	7.25E-08	1.82E-06
TMEM45A	ENSMMUG00000002861	transmembrane protein 45A	0.97230449	0.00044419	0.00205172

TMEM59	ENSMMUG000 00007183	transmembrane protein 59	0.6022 9159	6.60E- 10	6.22E- 08
TMEM86 A	ENSMMUG000 00041731	transmembrane protein 86A	0.9173 2889	7.30E- 05	0.0004 6832
TMEM9	ENSMMUG000 00013500	transmembrane protein 9	0.5837 9156	2.73E- 07	5.33E- 06
TMPO	ENSMMUG000 00023719	thymopoietin	- 0.6135 511	5.76E- 08	1.52E- 06
TMPRSS 9	ENSMMUG000 00001190	transmembrane serine protease 9	0.6242 9007	6.95E- 06	6.72E- 05
TNC	ENSMMUG000 00003356	tenascin C	- 1.7699 082	1.43E- 11	5.50E- 09
TNF	ENSMMUG000 00045654	tumor necrosis factor	- 1.4533 275	4.44E- 06	4.70E- 05
TNFRSF 11B	ENSMMUG000 00016485	TNF receptor superfamily member 11b	- 2.0561 914	4.01E- 12	2.65E- 09
TNFRSF 14	ENSMMUG000 00016329	TNF receptor superfamily member 14	1.1268 8841	0.0001 1158	0.0006 648
TNFRSF 6B	ENSMMUG000 00045470	TNF receptor superfamily member 6b	0.6034 6476	1.10E- 05	9.75E- 05
TNFSF12	ENSMMUG000 00006327	TNF superfamily member 12	0.9900 9156	8.43E- 06	7.93E- 05
TNIP3	ENSMMUG000 00004415	TNFAIP3 interacting protein 3	- 0.6141 069	0.0001 8013	0.0009 9345
TNNT1	ENSMMUG000 00006169	troponin T1, slow skeletal type	1.1392 7112	8.10E- 11	1.46E- 08
TNRC6B	ENSMMUG000 00021345	trinucleotide repeat containing adaptor 6B	- 0.5806 432	2.84E- 06	3.31E- 05
TOP2A	ENSMMUG000 00008941	DNA topoisomerase II alpha	- 1.1788 718	6.96E- 12	3.86E- 09
TOR1AIP 2	ENSMMUG000 00031279	torsin 1A interacting protein 2	- 0.5815 255	0.0001 5355	0.0008 697
TPGS1	ENSMMUG000 00008590	tubulin polyglutamylase complex subunit 1	0.6518 0397	3.65E- 06	4.01E- 05
TPI1	ENSMMUG000 00052852	triosephosphate isomerase 1	1.1312 4586	0.0006 3278	0.0027 5755

TPMT	ENSMMUG000 00016627	thiopurine S- methyltransferase	- 0.7256 139	5.14E- 05	0.0003 5161
TPST1	ENSMMUG000 00001744	tyrosylprotein sulfotransferase 1	0.6330 3092	4.60E- 05	0.0003 2305
TPT1	ENSMMUG000 00022979	tumor protein, translationally-controlled 1	0.7345 6983	9.62E- 12	4.71E- 09
TPX2	ENSMMUG000 00000966	TPX2 microtubule nucleation factor	- 0.9744 1	1.06E- 10	1.68E- 08
TRABD2 B	ENSMMUG000 00032139	TraB domain containing 2B	0.7174 4702	0.0019 6084	0.0069 7617
TRADD	ENSMMUG000 00060314	TNFRSF1A associated via death domain	0.8598 6568	3.34E- 08	1.03E- 06
TRAF1	ENSMMUG000 00041498	TNF receptor associated factor 1	- 0.6367 544	6.18E- 05	0.0004 0913
TRAF5	ENSMMUG000 00031427	TNF receptor associated factor 5	0.5916 3179	8.04E- 06	7.60E- 05
TRAM2	ENSMMUG000 00013718	translocation associated membrane protein 2	- 0.5943 605	4.60E- 10	4.72E- 08
TRAPPC 5	ENSMMUG000 00040778	trafficking protein particle complex subunit 5	0.8428 2266	6.58E- 09	3.20E- 07
TRIB3	ENSMMUG000 00012600	tribbles pseudokinase 3	1.0374 312	6.02E- 11	1.30E- 08
TRIL	ENSMMUG000 00020183	TLR4 interactor with leucine rich repeats	1.1082 9442	0.0003 4576	0.0016 6934
TRIM16	ENSMMUG000 00054196	tripartite motif containing 16	- 0.7925 448	5.24E- 07	8.81E- 06
TRIM67	ENSMMUG000 00017449	tripartite motif containing 67	- 0.6232 303	0.0012 9657	0.0049 4495
TRIP13	ENSMMUG000 00014740	thyroid hormone receptor interactor 13	- 0.6881 491	1.68E- 07	3.62E- 06
TRMT11 2	ENSMMUG000 00019647	tRNA methyltransferase activator subunit 11-2	0.6840 2343	8.36E- 08	2.02E- 06
TRO	ENSMMUG000 00008422	trophinin	1.5464 4861	1.23E- 06	1.70E- 05
TROAP	ENSMMUG000 00007544	trophinin associated protein	- 1.0762 971	1.18E- 05	0.0001 0375

TRPC3	ENSMMUG0000009820	transient receptor potential cation channel subfamily C member 3	- 1.2543 398	0.0005 5049	0.0024 553
TRPM6	ENSMMUG00000013102	transient receptor potential cation channel subfamily M member 6	1.0037 3806	0.0002 8687	0.0014 324
TRPV2	ENSMMUG00000015614	transient receptor potential cation channel subfamily V member 2	0.6778 1677	4.91E- 06	5.11E- 05
TRPV4	ENSMMUG00000003942	transient receptor potential cation channel subfamily V member 4	- 0.6481 155	0.0003 2486	0.0015 8465
TRRAP	ENSMMUG00000023318	transformation/transcription domain associated protein	- 0.6043 565	0.0004 7655	0.0021 7178
TRUB2	ENSMMUG00000014146	TruB pseudouridine synthase family member 2	0.6380 8155	5.24E- 06	5.35E- 05
TSC22D3	ENSMMUG00000057348	TSC22 domain family member 3	0.7287 2834	4.89E- 07	8.31E- 06
TSPAN1 2	ENSMMUG00000023310	tetraspanin 12	0.6456 5287	1.07E- 05	9.47E- 05
TSPAN1 3	ENSMMUG00000017049	tetraspanin 13	- 0.7491 747	0.0012 7731	0.0048 8759
TSPAN2	ENSMMUG00000017421	tetraspanin 2	1.2633 7988	8.01E- 06	7.59E- 05
TST	ENSMMUG00000012349	thiosulfate sulfurtransferase	1.0097 285	3.75E- 09	2.16E- 07
TTC30B	ENSMMUG00000043597	tetratricopeptide repeat domain 30B	0.7904 0975	0.0008 4275	0.0034 7395
TTC5	ENSMMUG00000016250	tetratricopeptide repeat domain 5	0.8271 2663	7.44E- 08	1.85E- 06
TTF2	ENSMMUG00000016905	transcription termination factor 2	- 0.9508 762	3.91E- 07	6.90E- 06
TTK	ENSMMUG00000020207	TTK protein kinase	- 0.8379 267	1.44E- 05	0.0001 2283
TTL1	ENSMMUG00000008728	TTL family tubulin polyglutamylase complex subunit L1	0.6256 3635	4.36E- 05	0.0003 0902
TTL7	ENSMMUG00000016591	tubulin tyrosine ligase like 7	- 0.8414 149	1.61E- 05	0.0001 3407

TXNIP	ENSMMUG000 00007338	thioredoxin interacting protein	1.1374 8712	0.0002 8613	0.0014 3001
TYRP1	ENSMMUG000 00062815	tyrosinase related protein 1	1.6819 1122	0.0007 0061	0.0029 9022
UAP1L1	ENSMMUG000 00047506	UDP-N- acetylglucosamine pyrophosphorylase 1 like 1	1.0867 1548	7.58E- 09	3.60E- 07
UBASH3 B	ENSMMUG000 00002919	ubiquitin associated and SH3 domain containing B	- 0.9616 368	1.97E- 09	1.36E- 07
UBE2T	ENSMMUG000 00013795	ubiquitin conjugating enzyme E2 T	- 0.9442 098	5.18E- 06	5.31E- 05
UBL5	ENSMMUG000 00007877	ubiquitin like 5	0.5847 7529	7.13E- 08	1.80E- 06
UBXN1	ENSMMUG000 00005761	UBX domain protein 1	0.6921 9348	5.65E- 10	5.48E- 08
UCP2	ENSMMUG000 00002605	uncoupling protein 2	- 1.4595 456	0.0011 4021	0.0044 5894
UGDH	ENSMMUG000 00001892	UDP-glucose 6- dehydrogenase	- 0.8132 361	7.13E- 07	1.11E- 05
UGGT1	ENSMMUG000 00023321	UDP-glucose glycoprotein glucosyltransferase 1	- 0.9168 409	7.14E- 08	1.80E- 06
UHRF1	ENSMMUG000 00012705	ubiquitin like with PHD and ring finger domains 1	- 0.9867 459	5.51E- 08	1.48E- 06
UNC119	ENSMMUG000 00012239	unc-119 lipid binding chaperone	1.0444 3268	9.68E- 11	1.58E- 08
UPK1B	ENSMMUG000 00057343	uroplakin 1B	- 1.2353 393	9.32E- 09	4.16E- 07
UPK3B	ENSMMUG000 00047349	uroplakin 3B	0.6797 8636	2.35E- 05	0.0001 8409
UPP1	ENSMMUG000 00007037	uridine phosphorylase 1	0.9656 71	2.69E- 06	3.17E- 05
URB1	ENSMMUG000 00010295	URB1 ribosome biosis homolog	- 0.7662 662	1.17E- 06	1.65E- 05
USP2	ENSMMUG000 00008921	ubiquitin specific peptidase 2	- 1.2976 498	1.60E- 05	0.0001 3371

UTP20	ENSMMUG0000012891	UTP20 small subunit processome component	- 0.7043 017	2.21E- 06	2.72E- 05
UTRN	ENSMMUG0000019438	utrophin	- 0.6871 953	2.32E- 06	2.81E- 05
VAMP5	ENSMMUG00000058122	vesicle associated membrane protein 5	0.5915 5762	0.0009 0236	0.0036 7379
VAT1L	ENSMMUG00000011797	vesicle amine transport 1 like	0.8907 6191	8.27E- 05	0.0005 1979
VCAM1	ENSMMUG00000022906	vascular cell adhesion molecule 1	- 1.0517 45	0.0001 6687	0.0009 3259
VCAN	ENSMMUG00000011513	versican	- 0.6729 524	1.65E- 05	0.0001 3661
VCL	ENSMMUG00000020823	vinculin	- 0.7076 045	6.95E- 11	1.41E- 08
VEGFA	ENSMMUG00000004577	vascular endothelial growth factor A	0.6366 1037	0.0025 0966	0.0085 912
VEGFB	ENSMMUG00000012944	vascular endothelial growth factor B	0.6753 4168	1.12E- 07	2.61E- 06
VGLL3	ENSMMUG00000000519	vestigial like family member 3	- 0.8059 048	0.0011 5062	0.0044 8863
VIT	ENSMMUG00000001278	vitrin	0.9902 8873	1.17E- 05	0.0001 0275
VLDLR	ENSMMUG00000015093	very low density lipoprotein receptor	1.3759 568	0.0007 4441	0.0031 4234
VMP1	ENSMMUG00000048926	vacuole membrane protein 1	0.6145 3239	1.46E- 09	1.11E- 07
VPS13D	ENSMMUG00000021449	vacuolar protein sorting 13 homolog D	- 0.6348 345	6.66E- 05	0.0004 3459
VPS37D	ENSMMUG00000001623	VPS37D subunit of ESCRT-I	2.8296 936	7.10E- 06	6.85E- 05
VRK1	ENSMMUG00000003443	VRK serine/threonine kinase 1	- 0.6787 377	9.51E- 07	1.40E- 05
VSIG1	ENSMMUG00000007189	V-set and immunoglobulin domain containing 1	0.8998 1224	0.0007 6322	0.0032 1002
VWA1	ENSMMUG00000053801	von Willebrand factor A domain containing 1	0.9176 1344	1.24E- 06	1.71E- 05

VWA5A	ENSMMUG00000020491	von Willebrand factor A domain containing 5A	2.26065821	1.47E-09	1.11E-07
VWF	ENSMMUG00000022893	von Willebrand factor	- 1.2536018	2.31E-06	2.81E-05
WDHD1	ENSMMUG00000000302	WD repeat and HMG-box DNA binding protein 1	- 0.8593649	4.12E-07	7.21E-06
WDR45	ENSMMUG00000010620	WD repeat domain 45	0.61464159	7.24E-07	1.12E-05
WDR54	ENSMMUG00000002719	WD repeat domain 54	0.88547799	4.90E-07	8.32E-06
WDR62	ENSMMUG00000019704	WD repeat domain 62	- 0.9343532	1.41E-06	1.88E-05
WDR76	ENSMMUG00000022774	WD repeat domain 76	- 0.6950323	1.22E-06	1.69E-05
WDR86	ENSMMUG00000006248	WD repeat domain 86	0.95351731	1.04E-05	9.33E-05
WFDC2	ENSMMUG00000002751	WAP four-disulfide core domain 2	1.32650691	1.74E-07	3.73E-06
WNT10A	ENSMMUG00000055913	Wnt family member 10A	- 0.8929861	5.56E-05	0.00037633
WNT5A	ENSMMUG00000061281	Wnt family member 5A	- 0.6636926	3.78E-07	6.72E-06
WNT7A	ENSMMUG00000018445	Wnt family member 7A	- 0.9702323	1.33E-09	1.07E-07
WWC1	ENSMMUG00000007457	WW and C2 domain containing 1	- 0.8326491	1.02E-11	4.71E-09
WWC3	ENSMMUG00000016290	WWC family member 3	- 0.6053087	1.62E-05	0.0001346
XKR9	ENSMMUG00000007429	XK related 9	- 1.4112307	0.00272888	0.00920307
XPO4	ENSMMUG00000013371	exportin 4	- 0.6110819	0.00011901	0.00070158
XRCC2	ENSMMUG00000002878	X-ray repair cross complementing 2	- 0.6793446	0.00161613	0.00594153

YOD1	ENSMMUG000 00022171	YOD1 deubiquitinase	- 1.0534 223	0.0017 6192	0.0063 6116
YPEL3	ENSMMUG000 00000980	yippee like 3	1.0184 8601	1.47E- 08	5.66E- 07
YPEL4	ENSMMUG000 00012620	yippee like 4	1.1676 6973	0.0003 5893	0.0017 2156
YPEL5	ENSMMUG000 00006615	yippee like 5	0.6073 6523	2.98E- 08	9.45E- 07
ZBED2	ENSMMUG000 00055898	zinc finger BED-type containing 2	- 2.8057 717	1.12E- 09	9.15E- 08
ZBTB22	ENSMMUG000 00003876	zinc finger and BTB domain containing 22	0.6573 2771	1.78E- 06	2.29E- 05
ZC2HC1 A	ENSMMUG000 00001653	zinc finger C2HC-type containing 1A	0.6418 7884	4.26E- 05	0.0003 0297
ZC3H12 C	ENSMMUG000 00048435	zinc finger CCCH-type containing 12C	- 0.5836 314	2.02E- 05	0.0001 6207
ZCCHC1 2	ENSMMUG000 00017574	zinc finger CCHC-type containing 12	1.0769 6151	0.0006 3902	0.0027 7691
ZCWPW 1	ENSMMUG000 00012720	zinc finger CW-type and PWWP domain containing 1	1.2955 9206	0.0003 8709	0.0018 3001
ZFAT	ENSMMUG000 00004918	zinc finger and AT-hook domain containing	0.9761 4739	3.18E- 07	5.93E- 06
ZFP30	ENSMMUG000 00053870	ZFP30 zinc finger protein	0.6139 4702	0.0002 5035	0.0012 8377
ZGRF1	ENSMMUG000 00023591	zinc finger GRF-type containing 1	- 1.4164 863	1.38E- 06	1.86E- 05
ZMAT5	ENSMMUG000 00064854	zinc finger matrin-type 5	0.6589 07	0.0003 3602	0.0016 2915
ZMYND 12	ENSMMUG000 00001034	zinc finger MYND-type containing 12	0.8006 842	0.0015 5606	0.0057 6652
ZNF154	ENSMMUG000 00047887	zinc finger protein 154	0.7811 7106	0.0004 8433	0.0021 9908
ZNF185	ENSMMUG000 00015264	zinc finger protein 185 with LIM domain	- 0.6681 481	2.65E- 08	8.74E- 07
ZNF286A	ENSMMUG000 00002354	zinc finger protein 286A	0.7358 4441	3.34E- 05	0.0002 4636
ZNF345	ENSMMUG000 00049498	zinc finger protein 345	0.6986 9904	0.0016 5464	0.0060 4808

ZNF367	ENSMMUG000 00060597	zinc finger protein 367	- 0.8803 461	0.0011 7596	0.0045 6447
ZNF395	ENSMMUG000 00060762	zinc finger protein 395	1.0435 8111	1.48E- 06	1.96E- 05
ZNF416	ENSMMUG000 00009290	zinc finger protein 416	0.5912 3002	0.0006 8767	0.0029 4584
ZNF423	ENSMMUG000 00021261	zinc finger protein 423	- 0.7765 402	0.0008 6545	0.0035 5167
ZNF428	ENSMMUG000 00053175	zinc finger protein 428	0.5908 4847	5.88E- 07	9.56E- 06
ZNF432	ENSMMUG000 00041450	zinc finger protein 432	1.1924 1377	0.0001 8636	0.0010 1773
ZNF469	ENSMMUG000 00046821	zinc finger protein 469	- 0.9500 571	6.95E- 10	6.38E- 08
ZNF521	ENSMMUG000 00008600	zinc finger protein 521	0.6975 446	0.0002 5077	0.0012 8543
ZNF536	ENSMMUG000 00063586	zinc finger protein 536	- 0.5943 365	0.0019 1872	0.0068 4886
ZNF581	ENSMMUG000 00004805	zinc finger protein 581	1.0702 1174	5.06E- 11	1.15E- 08
ZNF596	ENSMMUG000 00020598	zinc finger protein 596	0.7032 3516	0.0012 2501	0.0047 2792
ZNF606	ENSMMUG000 00020495	zinc finger protein 606	1.5261 7478	0.0003 2001	0.0015 6849
ZNF615	ENSMMUG000 00003712	zinc finger protein 615	0.7646 0469	0.0029 5962	0.0098 6136
ZNF667	ENSMMUG000 00003256	zinc finger protein 667	2.1562 1514	0.0004 6419	0.0021 2572
ZNF789	ENSMMUG000 00020139	zinc finger protein 789	- 0.7076 513	0.0002 6741	0.0013 5308
ZNF804A	ENSMMUG000 00012423	zinc finger protein 804A	- 0.7334 168	3.45E- 06	3.85E- 05
ZNF853	ENSMMUG000 00038892	zinc finger protein 853	0.7929 0846	0.0004 8455	0.0021 9935
ZP3	ENSMMUG000 00003637	zona pellucida glycoprotein 3	1.2969 422	0.0008 3652	0.0034 5545
ZSCAN1 6	ENSMMUG000 00003331	zinc finger and SCAN domain containing 16	0.7696 2601	0.0002 3578	0.0012 2354
ZSCAN1 8	ENSMMUG000 00020503	zinc finger and SCAN domain containing 18	1.7643 257	4.79E- 07	8.17E- 06

ZWINT	ENSMMUG000 00022376	ZW10 interacting kinetochore protein	- 0.7045 013	1.09E- 06	1.56E- 05
-------	------------------------	---	--------------------	--------------	--------------

Abbreviations: logFC, log fold change; adj. p. val, adjusted p- value.

Table 6.5. 10 μ M ibuprofen significant differentially expressed genes. All genes up or downregulated by 10 μ M Ibuprofen with a fold change ≥ 1.5 in either direction and an adjusted p-value of < 0.01 .

Gene Symbol	Rhesus Ensembl ID	Gene Name	logFC	p.value	adj.p.val
BCAT1	ENSMMUG0000001223	branched chain amino acid transaminase 1	-0.677977	0.000154	0.009406
CCNE2	ENSMMUG00000005358	cyclin E2	-0.697132	1.93E-05	0.002405
CENPU	ENSMMUG00000012176	centromere protein U	-0.666274	4.67E-06	0.001068
CLSPN	ENSMMUG00000010961	claspin	-0.649557	3.48E-07	0.000274
COL3A1	ENSMMUG00000021286	collagen type III alpha 1 chain	0.591462	7.23E-05	0.005537
CYP2S1	ENSMMUG00000009608	cytochrome P450 family 2 subfamily S member 1	0.588112	1.33E-06	0.000529
DTL	ENSMMUG00000010176	denticleless E3 ubiquitin	-0.588907	1.27E-05	0.001997
EGR2	ENSMMUG00000010256	early growth response 2	1.288492	7.49E-09	2.57E-05
EXO1	ENSMMUG00000008761	exonuclease 1	-0.636514	2.20E-07	0.000225
FOSB	ENSMMUG00000014430	FosB proto-oncogene, AP-1 transcription factor subunit	0.881203	9.25E-06	0.001786

HEYL	ENSMMUG 0000005001 9	hes related family bHLH transcription factor with YRPW motif	-0.685015	8.65E-05	0.006402
RAD51AP1	ENSMMUG 0000001518 9	RAD51 associated protein 1	-0.621265	3.28E-06	0.000833

Abbreviations: logFC, log fold change; adj. p. val, adjusted p- value.

Table 6.6. 1 μ M ibuprofen significant differentially expressed genes. All genes up or downregulated by 1 μ M Ibuprofen with a fold change ≥ 1.5 in either direction and an adjusted p-value of < 0.01 .

Gene Symbol	Rhesus Ensembl ID	Gene Name	logFC	p.value	adj.p.val
AHNAK	ENSMMU G00000022301	AHNAK nucleoprotein	-0.616307	4.71E-05	0.009541
CIITA	ENSMMU G00000007777	class II major histocompatibility complex transactivator	1.327601	1.46E-05	0.005134
DCHS2	ENSMMU G00000014024	dachshund cadherin-related 2	-0.652168	5.31E-07	0.00066
GPNMB	ENSMMU G00000012648	glycoprotein nmb	0.659145	5.83E-07	0.000665
HLA-DRA	ENSMMU G00000039082	major histocompatibility complex, class II, DR alpha	1.598196	3.40E-05	0.008308
HLA-DRB5	ENSMMU G00000029799	major histocompatibility complex, class II, DR beta 5	1.568884	5.44E-06	0.002566
HSPG2	ENSMMU G00000014828	heparan sulfate proteoglycan 2	-0.622591	7.57E-10	1.04E-05
NR4A3	ENSMMU G00000011410	nuclear receptor subfamily 4 group A member 3	0.583734	1.59E-05	0.005187

PIGR	ENSMMU G00000011 220	polymeric immunoglo bulin receptor	-0.660282	1.96E-05	0.005952
PTX3	ENSMMU G00000062 582	pentraxin 3	0.600426	5.06E-05	0.009757
SYNE2	ENSMMU G00000001 008	spectrin repeat containing nuclear envelope protein 2	-1.057441	2.51E-06	0.00172
TENM4	ENSMMU G00000042 218	teneurin transmembr ane protein 4	-0.662371	1.53E-07	0.000299

Abbreviations: logFC, log fold change; adj. p. val, adjusted p- value.

Table 6.7. Oligonucleotide primer sequences. Oligonucleotide primers used for PCR amplification of cDNAs isolated from vehicle control or NSAID treated NHP Sertoli cells.

Gene	Forward Primer Sequence (5' – 3')	Reverse Primer Sequence (5'-3')
<i>PTGS1</i>	AACCTTATCCCCAGTCCCCC	CAACTGCTTCTTCCCTTTGGT T
<i>PTGS2</i>	AGGCTTCCATTGACCAGAGC	GCAGACATTTCTTTTCTCCT GT
<i>AR</i>	GGATGGGGCTCATGGTGTTT	GCCCATCCACTGGAATAATGC
<i>SOX9</i>	GGGCAAGCTCTGGAGACTTCTG	GGGAGATGTGCGTCTGCTC
<i>GATA4</i>	CGGCACCCCAATCTCGTAG	GCGGGAGGCAGACAGC
<i>CLDN3</i>	CGAGTCGTACACCTTGCACT	GGCAGCAACATCATCACGTC
<i>CLDN4</i>	AAAGTGCCTTTGTTGGCCTG	CGAGTGTGAGCAGACCAGTT
<i>CLDN8</i>	GCACTCGTGCTCATTGTTGG	GATCTGGAGTAGACGCTCGG
<i>CLDN11</i>	CACCAATGACTGGGTGGTGA	CAGGACTGAGGCAGCAATCA
<i>NFE2L2</i>	AACTACTCCAGGTTGCCA	ATGTGGCCGGGAATATCAGG
<i>DPP4</i>	TGGTCTCCAAACGGCACTTT	TGCCCATGTCACATCACACA
<i>ACTA2</i>	AGCGTGGCTATTCCTTCGTT	TGAAGGATGGCTGGAACAGG
<i>FSP1</i>	CAGAACTAAAGGAGCTGCTGA CC	CTTGGAAGTCCACCTCGTTGT C
<i>FN1</i>	CCCATCAGCAGGAACACCTT	GTGGGAGCATCCAGTTTGGT
<i>STAR</i>	GAGACCCAGCAGGACAATGG	ATTAGGGTTCCACTCCCCCA
<i>INSL3</i>	GATATGCCTGATAAGTTGGTCG G	ATGTCGTCTCTCCAGCCACT
<i>WT1</i>	TGAGACCAGTGAGAAACGCC	ATGAGTCCTGGTGTGGGTCT
<i>MAGEA 4</i>	GAGGCAAGGTTTTCAGGGGA	GCAGCCTCCTTCTCCTCAGT
<i>TNPI</i>	TGACAGCACAATAGAGCCCC	GGCTGGTCGACATGGTAAGT
<i>GAPDH</i>	ACAACCTTGGTATCGTGGAAGG	GCCATCACGCCACAGTTTC

Table 6.8. Antibodies used for immunocytochemistry and immunohistochemistry.

Antibodies used for immunocytochemistry and immunohistochemistry.

Antibody	Company	Catalog Number
Recombinant Anti-COX-1/ COX1(Rabbit)	Abcam	ab109025
PTGS2	Abcam	ab23672
Anti-SOX9 (Rabbit)	EMD Millipore	AB5535
SOX9	R&D Systems	AF3075
Recombinant Anti-Wilms Tumor Protein antibody (Rabbit)	Abcam	ab89901
UTF1 Mouse anti-Human	Millipore/ Fisher Scientific	MAB4337MI
Rabbit IgG	BD Pharmingen	550875
Goat IgG	R&D Systems	AB-108-C
Mouse IgG	BD Pharmingen	557273
Goat anti-rabbit Alexa Fluor™ 488	Invitrogen	A11034
Alexa Fluor™ Donkey anti- rabbit 568	Invitrogen	A10042
Alexa Fluor™ Donkey anti- mouse 488	Invitrogen	A21202
Donkey anti-goat Alexa Fluor™ 647	Invitrogen	A21447
Purified Mouse Anti-Cox2	BD Transduction Laboratories™	610203

APPENDIX B

TABLES ASSOCIATED WITH CHAPTER 5

Table 7.1. Testibow oligonucleotide primers. Oligonucleotide primers used for PCR amplification of DNAs isolated from Testibow 1.0 or Testibow 2.0 hESC cell lines.

Gene	Forward Primer Sequence (5' – 3')	Reverse Primer Sequence (5'-3')
<i>PRM1-tdTomato</i>	CCCCTTTGCCCTCACAATGAC	GGGGAAGGACAGCTTCTTGTAATC
<i>PIWIL2-GFP</i>	GCGGGCAGGTTGGGTTTTTG	TTGTAGTTGCCGTCGTCCTTG
<i>PLZF-CFP</i>	CGTGGGTGCTCTTATGTATGCG	TGCTTCATGTGGTCGGGGTAGC

Table 7.2. Antibodies used for Testibow immunocytochemistry experiments.

Antibodies used for Immunocytochemistry experiments.

Antibody	Company	Catalog Number
Human PLZF Antibody	R&D Systems	MAB2944
Alexa Fluor™ Goat anti-mouse 488	Invitrogen	A11029